ENGINEERING RECOMBINANT, COMPLEX GLYCAN BIOSYNTHESIS IN *ESCHERICHIA COLI* AND INVESTIGATION OF ISOPRENOID-DEPENDENT GLYCAN BIOSYNTHESIS IN *CAULOBACTER CRESCENTUS*

by

Beth Anne Scarbrough

A dissertation submitted to the faculty of
The University of North Carolina at Charlotte
in partial fulfillment of the requirements
for the degree of Doctor of Philosophy in
Nanoscale Science

Charlotte

2024

Approved by:

_____
Dr. Jerry Troutman

_____
Dr. Juan Vivero-Escoto

_____
Dr. Brian Cooper

_____
Dr. Andrew Truman

_____
Dr. Yuri Nesmelov

ABSTRACT

BETH ANNE SCARBROUGH. Engineering Recombinant, Complex Glycan Biosynthesis in *Escherichia coli* and Investigation of Isoprenoid-Dependent Glycan Biosynthesis in *Caulobacter crescentus*.
(Under the direction of DR. JERRY TROUTMAN)

Carbohydrates, or glycans, represent a significant class of cell surface modifications in both eukaryotic and prokaryotic cells. In bacteria, strategic regulation of the display of distinct glycan structures endows cellular fitness and competitive advantages in otherwise uninhabitable or inhospitable environments. These structures have long been known to promote antimicrobial resistance, evasion of host defenses, and potent activation of host immune responses. Moreover, bacteria possess a massive repertoire of unique glycan monomers compared to mammalian cells and, consequently, immensely varied carbohydrate structures between and within species. Together, glycan biosynthesis pathways and unique structures represent advantageous targets for new antimicrobials, attenuation of antimicrobial resistance, and significantly underutilized sources of diverse carbohydrate structures. While potential applications of polysaccharides continue to develop, new tools and techniques to isolate and probe glycan structures and biosynthetic pathways have trailed behind other macromolecules, such as proteins and nucleic acids. This research narrows in on foundational, conserved aspects of bacterial glycan biosynthesis to probe initial stages of lipid-dependent glycan biosynthesis. Specifically, fluorescent analogues of critical lipid precursors were used to probe mechanisms of antimicrobial resistance in *Escherichia coli* and early stages of glycan biosynthesis in *Caulobacter crescentus*, while addressing potential setbacks to current methods of *in vitro* reconstitution of glycan biosynthesis. Finally, a recombinant system for overproduction of capsular polysaccharide A

from *Bacteroides fragilis* was engineered in *E. coli*, effectively modeling a framework for identifying critical bottlenecks that can be broadly applied to other recombinant glycan systems.

ACKNOWLEDGEMENTS

Dr. Jerry Troutman – For fostering a laboratory that inspires great scientific discussion, curiosity, and collaboration. Thank you for continually challenging me and enabling me to pursue my research endeavors.

Dr. Vivero-Escoto, Dr. Truman, Dr. Cooper, and Dr. Nesmelov - Thank you for your expertise, and for encouraging great discourse as your advisee and as your student.

Dr. Richard Jew – Thank you for encouraging me to join a research lab that fits my interests perfectly. I am incredibly grateful for your mentorship and friendship.

Dr. Katelyn Erickson – Thank you for advising me to always ask more questions and providing encouragement and a listening ear in the toughest times.

Dr. Amanda Reid – Thank you for making my time in the laboratory much more enjoyable and for very thoughtful discussions about science and research.

My parents, Andy and Mary Scarbrough – Thank you for supporting me in every step of my academic career and always encouraging me to keep going and pursue what truly makes me happy. Your wisdom and encouragement to help me overcome life's challenges is truly appreciated.

DEDICATION

To my husband, Sheldon, and to my daughters, Ayda and Libby.

TABLE OF CONTENTS

LIST OF FIGURES

LIST OF TABLES

LIST OF ABBREVIATIONS

Ara4FN	L-4-formamido-arabinose
Ara4N	L-4-aminoarabinose
AATGal	2-acetamido-4-amino-2,4,6-trideoxygalactose
BP	Bactoprenyl phosphate
BPP	Bactoprenyl diphosphate
CAMP	Cationic antimicrobial peptides
CPS	Capsular polysaccharides
CPSA	Capsular polysaccharide A
diNAcBac	2,4-diacetamido-2,4,6-trideoxy-d-glucose
EPS	Extracellular polysaccharides
FPP	Farnesyl diphosphate
Gal	Galactose
GalNAc	N-acetylgalactosamine
Glc	Glucose
GlcA	Glucuronic acid
GlcNAc	N-acetyl-glucosamine
GT	Glycosyltransferase
HPLC	High performance liquid chromatography
IM	Inner membrane
IPP	Isopentenyl diphosphate
Kdo	3-deoxy-d-manno-octulosonic acid
LPS	Lipopolysaccharide
LTA	Lipoteichoic acids
L-RhaNAc	L-N-acetylrhamnosamine
Man	Mannose
ManNAc	N-acetylmannosamine
ManNAcA	N-acetylmannosaminuronic acid
NDP	Nucleoside-diphosphate
OM	Outer membrane
PGT	Phospho-glycosyltransferase
UDP	Uridine diphosphate
WTA	Wall teichoic acids
Xyl	Xylose
ZPS	Zwitterionic polysaccharides
2CN-GPP	2-nitrileanilino-geranyl diphosphate
2CN-BP	2-nitrileanilino-bactoprenyl phosphate
2CN-BPP	2-nitrileanilino-bactoprenyl diphosphate

CHAPTER 1: INTRODUCTION

Extracellular modifications are nearly universally exhibited by all phylogenetic kingdoms. These extracellular components are of integral importance as they are the first constituents to encounter other surfaces, both biotic and abiotic, and often define the interactions that occur from then on. Glycans, including mono-, oligo-, and polysaccharides, represent a major class of cell surface modifications. Compared to eukaryotes, prokaryotes display glycans of disproportionately greater structural complexity, often forming a physical barrier between the cell and the environment. In bacteria, this presents notable implications in infectious disease and human health, antibiotic resistance, and cell fitness and survival. Pioneering research in glycomics has been undertaken to advance our understanding of glycan discovery, regulation, structure, and function in prokaryotes.[1-4]

Unlike proteins and nucleic acids, there is no universal code or template in glycan biosynthesis to aid in deciphering constituent monomers or precise polymeric structure. Adding to this challenge, prokaryotes possess an extensive repertoire of sugar monomers. When compared to common carbohydrate monomers composing eukaryotic glycans (e.g., glucose, galactose, mannose, N-acetylglucosamine), bacteria possess at least an order of magnitude greater unique monosaccharides, including rare deoxy-carbohydrates (**Figure 1.1**).[5-7] Due to the vast quantity of distinct monomer building blocks, variation in carbohydrate linkages, and possible substituent modifications, bacterial oligo- and polysaccharides are immensely varied both between and within the same species.[5, 8]

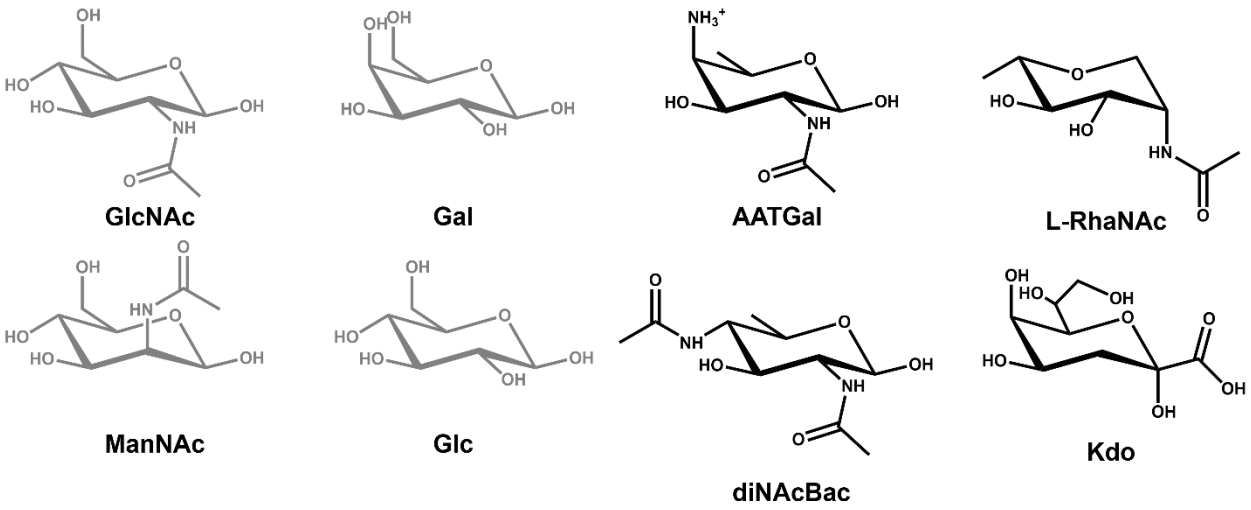

Figure 1.1: Comparison of representative eukaryotic and prokaryotic monosaccharides. Representative monosaccharides from eukaryotes are depicted on the left (grey), while unique representative monosaccharides from bacteria are represented on the right (black). Bacteria utilize all monosaccharides represented here, while the black monosaccharides are not utilized by mammalian cells.[6] N-acetylglucosamine (GlcNAc), galactose (Gal), glucose (Glc), N-acetylmannosamine (ManNAc), 2-acetamido-4-amino-2,4,6-trideoxygalactose (AATGal), L-N-acetylrhamnosamine (L-RhaNAc), 2,4-diacetamido-2,4,6-trideoxy-d-glucose (diNAcBac), 3-deoxy-d-manno-octulosonic acid (Kdo)**.**

Owing to this structural diversity, bacterial glycans serve diverse functions in biological processes that aid in cellular adhesion, biofilm formation, colonization, and cell survival and proliferation despite mammalian host immune responses. On the other hand, specific glycans have significant implications in the health of the human gut microbiome and augmentation of the immune system.[9-12] Free glycans, synthetic and natural, have been shown to alter the prevalence and proportion of symbionts and commensals ("good" bacteria), while polysaccharide-encapsulated symbionts aid in the attenuation of pathogen proliferation via competitive colonization.[9, 10, 13] Pathogen glycans have also been employed in vaccines as glycoconjugates, while others have been studied as a treatment of numerous inflammation-associated diseases and as antibiofilm agents.[14-21] In other taxa, glycans are recognized as an untapped source of

renewable biopolymers for applications as adhesives, thickening agents, and hydrogels.[22-24] Nonetheless, the structures of many natural bacterial glycans remain undetermined.

Bacterial glycopolymers are generally classified into three categories: (1) lipid-linked glycans, (2) protein O- and N-linked glycans, and (3) extracellular polysaccharides (EPS). Current techniques for deciphering the effects of glycan surface modifications in general biological processes and bacterial pathogenicity and virulence have relied on the identification of associated genes and prediction of protein function based on homology.[25-29] While an invaluable tool in the field of glycobiology, without structural characterization, the determination of precise enzyme specificity *in vitro* is still required to infer glycan structures, biosynthetic pathways, physiochemical properties, and glycan-host cell interactions.[30-33] Structural characterization is stymied due to small quantities naturally produced by bacteria, the complexity of branched glycans, and competing expression of other biological polymers. Contrary to nucleic acids, glycan biosynthesis systems are not easily scaled and require the sequential action of multiple, distinct proteins, as well as the availability of unique and often rare nucleotide-linked monosaccharides. Installation of tags for purification is not easily achieved without a template, unlike proteins, or chemically modified precursors, which are hindered by unknown monomer identities.

The research presented here encompasses tools and methods used to probe bacterial glycan biosynthesis and the specificity of glycan biosynthesis machinery. An in-depth analysis of competing systems that hinder *in vitro* characterization of glycan biosynthesis, as well as the production of tagged, varied glycolipid precursors are presented. Ultimately, the information and knowledge gained from these and previous studies were used to develop a recombinant system for the production of a complex glycan, Capsular Polysaccharide A (CPSA) from *Bacteroides*

fragilis. This platform represents a framework for stepwise evaluation of recombinant glycan assembly and reveals new strategies for scaling the production of varied, complex polysaccharides.

BACTERIAL SURFACE GLYCANS AND INFECTIOUS DISEASE

Pathogenic bacteria are often recognized for their display of a dense, extracellular layer of high molecular weight polysaccharides, commonly referred to as a capsule or slime layer. Capsular polysaccharides (CPS) are covalently associated to the cell surface via protein or lipid linkages.[34, 35] A single species can produce many discrete capsules and has thus become the basis for serotyping.[8, 35] The slime layer is a matrix of secreted extracellular polysaccharides (EPS), often including nucleic acids and proteins to form a complex that is loosely associated with the cell surface.[36, 37]

Many important pathogens possess a capsule or slime layer that protects cells from host immune responses or serves as a point of adhesion. This includes Gram-negative *Escherichia coli*, *Neisseria meningitidis*, *Vibrio cholera*, and Gram-positive *Staphylococcus aureus*, and *Streptococcus pneumoniae*.[38-42] This extracellular barrier makes colonization and concomitant infection in otherwise unhabitable conditions possible.[10, 43] For example, Gram-negative *Vibrio vulnificus*, a food-borne pathogen that accounts for a staggering 95 % of seafood-related deaths and a 50 % mortality rate post-infection, evades phagocytosis and other innate immune responses through expression and display of CPS.[44, 45] The CPS of *V. vulnificus* is recognized as one of few virulence factors required for pathogenicity.[44]

On the contrary, *Bacteroides fragilis*, a significant human symbiont and opportunistic pathogen, uniquely regulates the expression of up to eight capsular polysaccharides.[46] Without

CPS, symbiotic *Bacteroides* species are unable to colonize the human gastrointestinal tract, and display of certain polysaccharides is associated with opportunistic infections and subsequent abscess formation.[28, 47-49] More importantly, zwitterionic CPSA from *B. fragilis* has been shown to activate an adaptive, T-cell dependent immune response via a major histocompatibility complex II (MHC II) mechanism.[50-54] Compounding evidence also exists for the induction of anti-inflammatory immune responses, such as IL-10 secreting T regulatory cells, in response to *Bacteroides* species displaying zwitterionic polysaccharides (ZPS).[11, 15, 55, 56]

Antibiotic resistance of many bacterial pathogens is often attributed to the secretion of EPS and the formation of biofilms.[57] Biofilms are a formidable barrier to the treatment of infectious diseases and the development of efficacious antibiotics. They encompass a complex community of microbes adhered to a surface and encased in a matrix of biological polymers.[57] Initiation of biofilms is attributed to cellular adhesion, which is promoted by timely secretion of adhesive glycans or protein.[58-60] Secretion of EPS begins once a bacterium appends itself to a substrate, and eventually establishes a protective, nutrient-rich niche.[57, 58] For example, *Pseudomonas aeruginosa* regulates the production of multiple, structurally distinct EPS.[61] In cystic fibrosis patients, increased morbidity and mortality are associated with *P. aeruginosa* infections and expression of specific EPS, biofilm formation, and consequently, multi-drug resistance.[62, 63] Biofilms are also frequently associated with drug-resistant nosocomial infections in patients with catheters and prostheses.[58, 64, 65] In pathogenic strains of *Escherichia coli*, EPS is associated with resistance to oxidative and osmotic stress and is required for the formation of biofilms.[66, 67]

In Gram-negative bacteria, the outer surface of the cell envelope is composed mostly of lipopolysaccharide (LPS).[68, 69] Phosphate groups present on LPS endow the cell surface with a

negative charge (structure and biosynthesis reviewed by Raetz and Whitfield).[70] A simpler, yet significant modification to the cell surface of *E. coli* and other Gram-negative species requires the strategic appendage of a charged monosaccharide(s) to LPS at the outer surface of the cell envelope (reviewed by Raetz et al., 2007) (**Figure 1.2**).[71] These modifications notably also include the addition of phosphoethanolamine to LPS.[71-73] This ultimately results in electrostatic repulsion of cationic antimicrobials, including those designated as "last resort" antimicrobials such as polymyxins and colistin, and those produced by innate immune responses.[74-77] For example, *E. coli* and *Salmonella* Typhimurium regulate modification of the outer membrane with cationic L-4 aminoarabinose in response to extracellular conditions, such as acidic pH and low concentration of Mg^{2+}.[72, 78] Similar modifications are observed in the pathogens *Bordetella pertussis* with glucosamine, and species of *Francisella* with galactosamine.[79, 80] While these modifications are often tightly controlled, mutations in regulatory genes can confer constitutive expression of LPS modification genes and cationic antimicrobial resistance.[76, 81, 82]

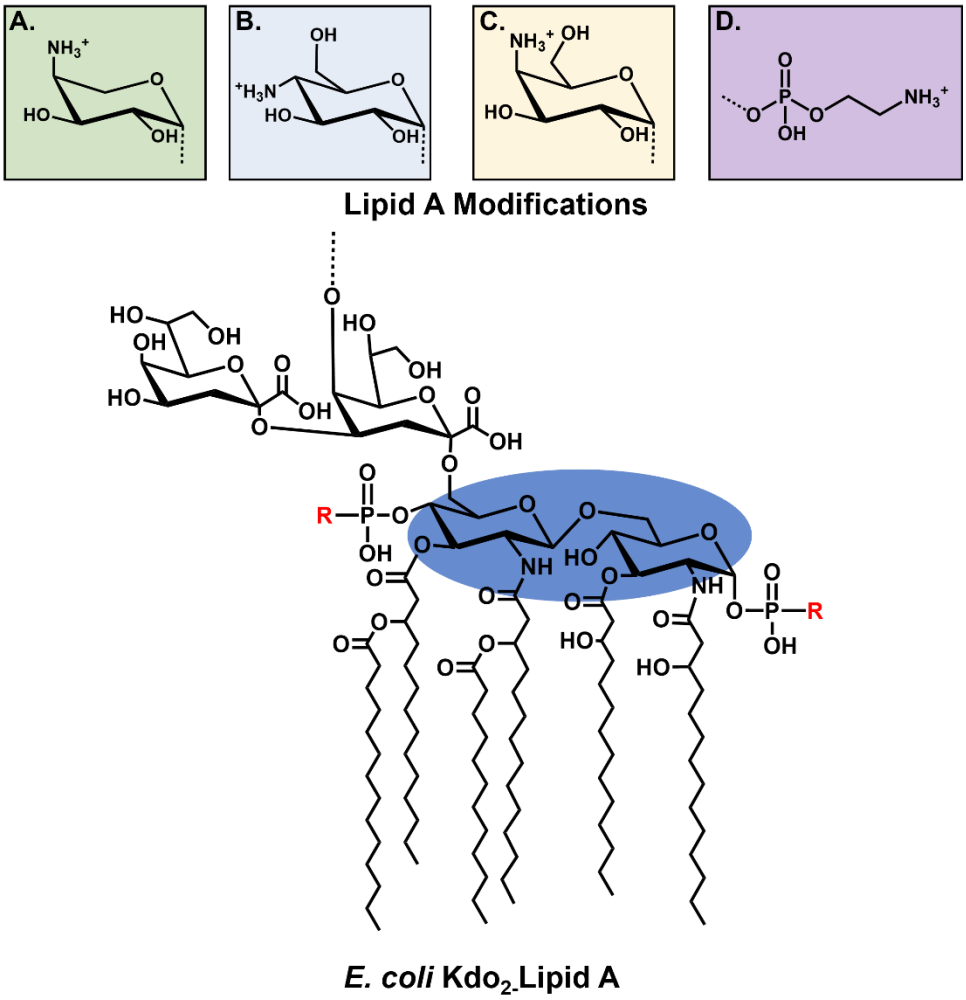

Figure 1.2: Representative LPS modifications that confer antimicrobial resistance in Gram-negative pathogens. Structure of *E. coli* Kdo2-lipid A and covalent modifications to the phosphate groups of lipid A that have been identified in Gram-negative pathogens (A) L-4-aminoarbinose, (B) glucosamine, (C) galactosamine, (D) phosphoethanolamine.

Current broad-spectrum antibiotics targeting common biological processes such as cell wall and protein synthesis often contribute to dysbiosis.[83] The combined presence of rare sugars in pathogen glycans and the absence of these sugars in mammalian cells have illuminated them as attractive targets for narrow-spectrum antibiotics.[84] Targeted delivery of antimicrobials could presumably be designed based on structurally distinct pathogen glycans.[84] Current, broad-spectrum antimicrobials that target bacterial glycan biosynthesis are tunicamycins, inhibitors of

cell wall and early-stage polysaccharide biosynthesis, and bacitracin, a scavenger of a common glycan and cell well precursor.[85-90] Being that pathogenicity is often conferred by expression of polysaccharide capsules or EPS, unique enzyme targets in glycan biosynthesis pathways could serve to attenuate the virulence of pathogenic microbes and prevent opportunistic colonization.

STRUCTURE OF THE BACTERIAL CELL ENVELOPE

The bacterial cell envelope is a complex, layered structure including a bilayer membrane(s) and cell wall (also known as peptidoglycan) that surrounds and protects cytoplasmic components from environmental elements.[69] In general terms, bacteria can be categorized into two groups based on structural characteristics of the cell envelope; Gram-negative or Gram-positive. A traditional Gram-stain developed over a century ago is still one of the most widely used preliminary, diagnostic procedures for assessing bacterial infections, for instance, *E. coli* (Gram-negative) vs. *S. aureus* (Gram-positive) infection. This stain is based on the premise of structural differences between the Gram-negative and Gram-positive cell envelopes.

The peptidoglycan cell wall is common to nearly all bacteria and is a single, crosslinked molecule that encompasses a bacterium in a sac-like structure.[69, 91] It is generally composed of linear strands of alternating N-acetylglucosamine and N-acetyl-muramic acid glycans crosslinked with a short pentapeptide.[91] The basic structure of peptidoglycan is highly conserved but differs in amino acid side chains, length of glycan chains, crosslinking, and nature of chemical modifications.[91, 92] Debate exists on the overall 3D structure of peptidoglycan, for instance, whether it is structured with linear glycans perpendicular to the inner membrane, or whether it possesses a more disorganized structure.[92] Nevertheless, peptidoglycan is essential for cell viability and its biosynthesis is a target of current antimicrobials such as beta-lactams.[92-94]

Gram-negative bacteria possess both an inner membrane (IM) and outer membrane (OM) bilayer (**Figure 1.3**). Sandwiched between these membranes is the aqueous, periplasmic space which also contains a thin layer (< 10 nm) of peptidoglycan.[91] The inner membrane is mainly composed of phospholipids and integral proteins.[69] The type and proportion of phospholipids (e.g., phosphatidylcholine, cardiolipin, phosphatidylethanolamine) differ between species and are altered in terms of ratios, points of saturation, introduction of cycloalkanes, and alkyl chain length in response to environmental cues.[95] On the contrary, the OM contains mostly phospholipids at the inner leaflet and LPS at the outer leaflet.[68] The OM also contains lipoproteins that anchor the OM to peptidoglycan, and porins which enable diffusion of small molecules and ions across the OM.[96, 97] The rigid cell wall, as well as the OM is thought to contribute to cell shape, for example, rod-shaped *E. coli* or comma-shaped *Caulobacter crescentus*.[69, 98]

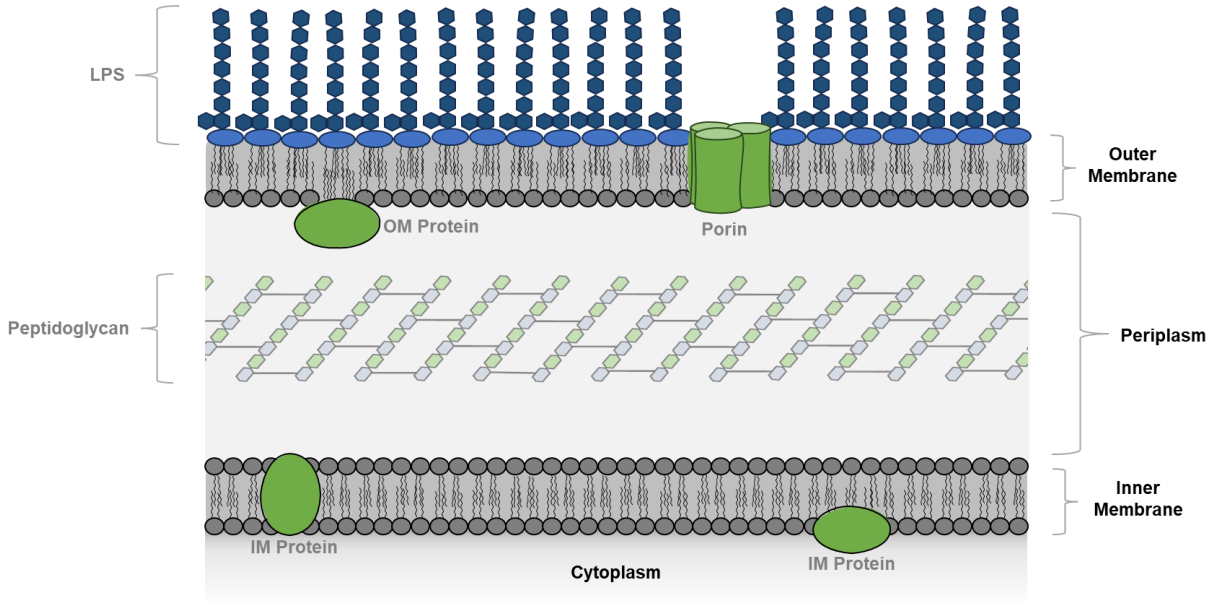

Figure 1.3: Representation of the Gram-negative cell envelope.

LPS, containing endotoxin, is notorious due to its potent activation of innate immune responses and its role in sepsis and septic shock.[70] The structure of LPS is generally classified

into three sections: (1) lipid A, (2) core oligosaccharides, and (3) long-chain polysaccharides, or O-antigen.[70, 71] Lipid A (**Figure 1.2**) is an acylated disaccharide of N-acetylglucosamine and serves as the lipid anchor for LPS.[71] Notably, the 1 and 4' positions of the GlcNAc disaccharide are modified with phosphate groups (**Figure 1.2**). Positioned on the outer leaflet of the OM, divalent cations such as Mg^{2+} and Ca^{2+} crosslink and stabilize these negatively charged groups to fortify the membrane barrier.[99] In the biosynthesis of LPS, lipid A is then modified with inner core sugars, including a 3-deoxy-d-manno-octulosonic acid disaccharide (Kdo) and heptoses, outer core sugars, and finally, O-antigen.[70, 100] The composition of the O-antigen varies within, and between bacterial species, while core sugars are highly conserved.[70, 100, 101] This structural diversity of O-antigen gives rise to Gram-negative O serogroups.[35, 101]

The OM is essential for Gram-negative cell viability and is a critical difference from Gram-positive bacteria.[69] Instead, Gram-positive bacteria possess a single cytoplasmic membrane surrounded by a thick, roughly 30 - 100 nm, layer of peptidoglycan (**Figure 1.4**).[69, 91] Though the general structure of peptidoglycan between Gram-positive and Gram-negatives is similar, Gram-positive peptidoglycan differs most notably in crosslinking with a pentaglycine bridge, rather than direct pentapeptide crossing linking as observed in Gram-negative *E. coli*.[91] Gram-positive bacteria also possess integral membrane-associated proteins, lipoproteins, and teichoic acids.[69] Teichoic acids are typically long polymers of polyglycerol phosphate or polyribitol phosphate, followed by a covalent glycerol phosphate linker and a disaccharide of GlcNAc and ManNAc.[102] Teichoic acid structures differ between Gram-positive species and are characterized as wall teichoic acids (WTA) covalently linked to peptidoglycan, or lipoteichoic acids (LTA).[102] As with Gram-negative species, the display of teichoic acid polymers and

modification with charged or glycan moieties at the cell surface play a significant role in attenuating the efficacy of antibiotics, such as the case for methicillin-resistant *S. aureus*.[102, 103]

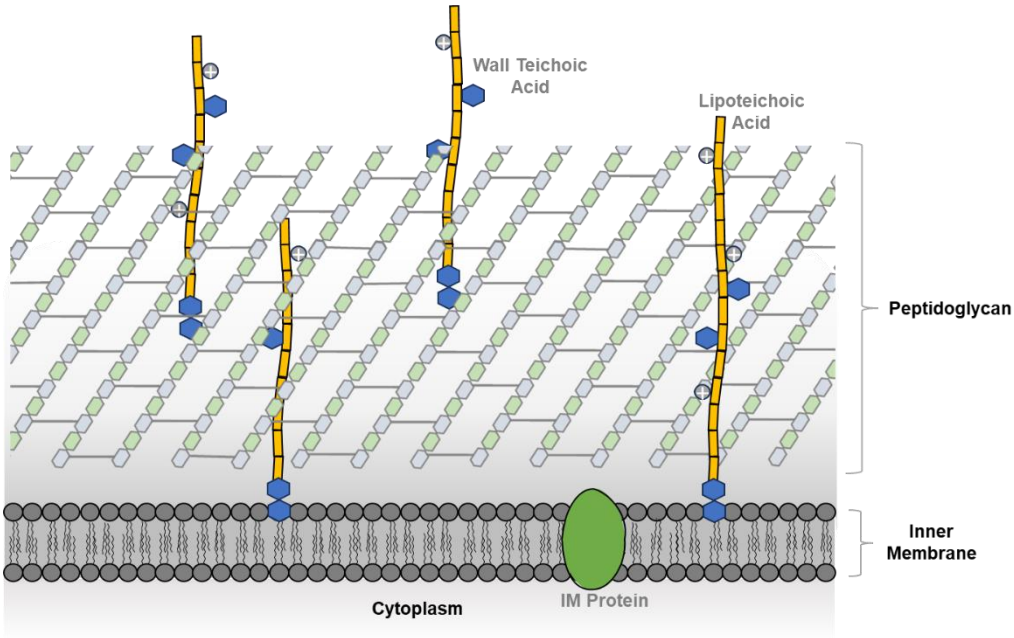

Figure 1.4: Representation of the Gram-positive cell envelope.

WZY/WZX DEPENDENT BACTERIAL GLYCAN BIOSYNTHESIS

Two conserved mechanisms of bacterial glycan biosynthesis have been identified in bacteria. The first mechanism classifies heteropolymeric Group 1 capsular polysaccharides and is characterized by the use of a flippase (Wzx) to transport the polymer from the cytoplasmic face of the inner membrane to the periplasm, and a polymerase (Wzy).[104] A second mechanism, encompasses Group 2 capsular polysaccharides such as poly N-acetyl glucosamine (PNAG), alginate, and sometimes O-antigen, which requires an ATP-dependent ABC transporter protein complex to transport glycans to the outer membrane of a bacterium.[24, 105-107] The presence of proposed *wzx* and *wzy* homologs in glycan biosynthesis operons is a typical, preliminary determinant of the Group 1 mechanism, and is the focus of the research herein.[26, 104, 108]

Bacterial polysaccharides produced through the conserved Group 1 pathway require a polyisoprenoid lipid anchor, bactoprenyl phosphate (BP; also known as undecaprenyl phosphate), that is embedded in the inner membrane of a bacterium at the interface of the cytoplasm (**Figure 1.5**).[35, 109] This includes peptidoglycan, which is essential for cell viability, CPS, EPS, O-antigen, and glycan modifications of LPS. Monophosphorylated BP is produced through the concerted action of undecaprenyl pyrophosphate synthase (UppS) and undecaprenyl pyrophosphate phosphatase (UppP, formerly known as BacA).[110, 111] UppS is a *Z*-prenyl transferase that catalyzes the sequential condensation of isopentenyl phosphate (IPP, C_5) to 2*E*, 6*E*-farnesyl diphosphate (FPP, C_{15}) in the *Z*-configuration to produce *E*,*Z*-mixed bactoprenyl diphosphate (BPP).[112, 113] BPP is subsequently dephosphorylated by UppP. BP can vary in carbon chain length (C_{45}-C_{70}) between species but has more frequently been identified as C_{55} in *E. coli* and other species.[114-116]

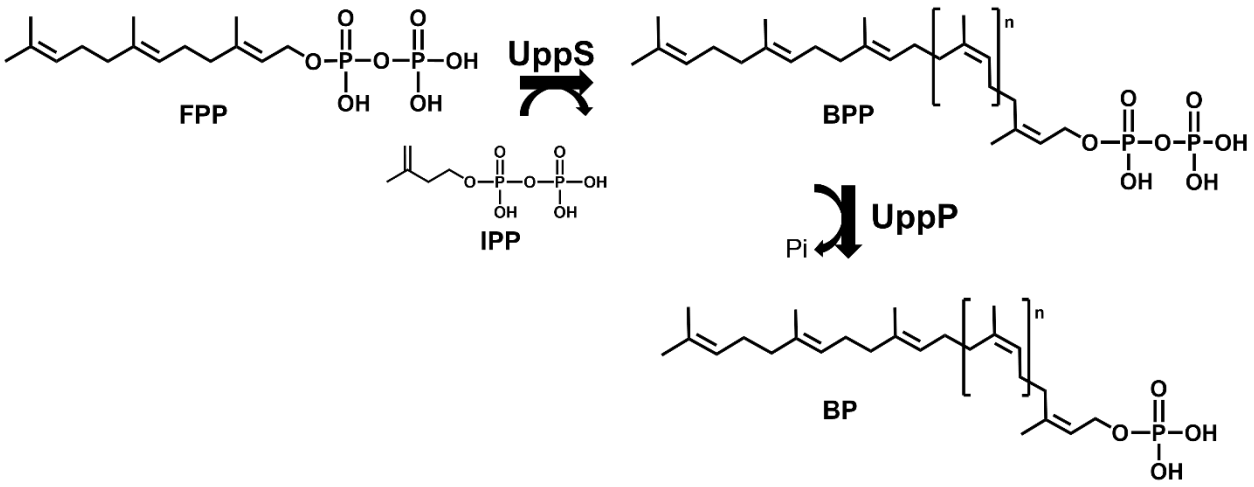

Figure 1.5: Schematic of bactoprenyl phosphate biosynthesis. UppS condenses ~ eight molecules of IPP to FPP in the *Z*-configuration to produce BPP. UppP dephosphorylates BPP to produce BP, the active isoprenoid substrate in group 1 polysaccharide biosynthesis. FPP= farnesyl diphosphate, IPP = isopentenyl diphosphate, BPP = bactoprenyl diphosphate, BP = bactoprenyl monophosphate.

Monophosphorylated BP is the active substrate for downstream glycosyltransferases and is vital for cell wall biosynthesis, thus a target for antimicrobials.[110, 111, 117, 118] Glycosyltransferases also require activated, nucleotide-linked sugars, which tend to include rare deoxy amino or acetamido sugars at the stage of initiation. This includes diNAcBac in N-linked glycosylation in *Campylobacter jejuni* and O-linked glycosylation in *Neisseria gonorrhoeae*, and AATGal in CPSA of *B. fragilis* (**Figure 1.1**).[119-121] Use of rare sugars at the stage of initiation may ostensibly commit BP to a specific glycan pathway. To initiate polysaccharide biosynthesis, a membrane-bound initiating phospho-glycosyltransferase (PGT) enzyme appends a phospho-sugar molecule to BP to form a BPP-linked monosaccharide (**Figure 1.6**).[122, 123] This includes, for example, WecA, a phospho-N-acetylglucosaminyl transferase, and WbaP a phospho-galactosyl transferase.[123-125] WecA initiates biosynthesis of both the enterobacterial common antigen (ECA) and O-antigen biosynthesis in *E. coli*.[124] WbaP initiates O-antigen biosynthesis in *Salmonella enterica*.[125]

Multiple cytosolic glycosyltransferases append additional sugar molecules to the BPP-linked monosaccharide until the final repeat unit is formed (**Figure 1.6**). Modifications to lipid-linked glycan monomers (e.g., acetylation, deacetylation, pyruvylation, alkylation) via sugar modifying enzymes may also occur during or after the biosynthesis of the final repeat unit; however, the precise sequence of these steps has historically been ambiguous until biosynthesis has been reconstituted *in vitro*.[30, 31] Once complete, the repeat unit is translocated into the periplasm by a Wzx flippase and polymerized at the periplasmic face by a Wzy polymerase. The polymer is then transported to the cell surface where it remains anchored or secreted into the environment.[35] Polysaccharide chain length is regulated by a multimeric co-polymerase, Wzz, and genetic inactivation results in a stochastic distribution of polymer length.[126] The precise mechanism of chain length control via the proposed periplasmic complex of Wzy and Wzz is unknown.[127-129] In a typical system, once the preferred chain length or modality of the polysaccharide is achieved, it is exported to the cell surface by an octameric, membrane-spanning transporter, Wza.[130]

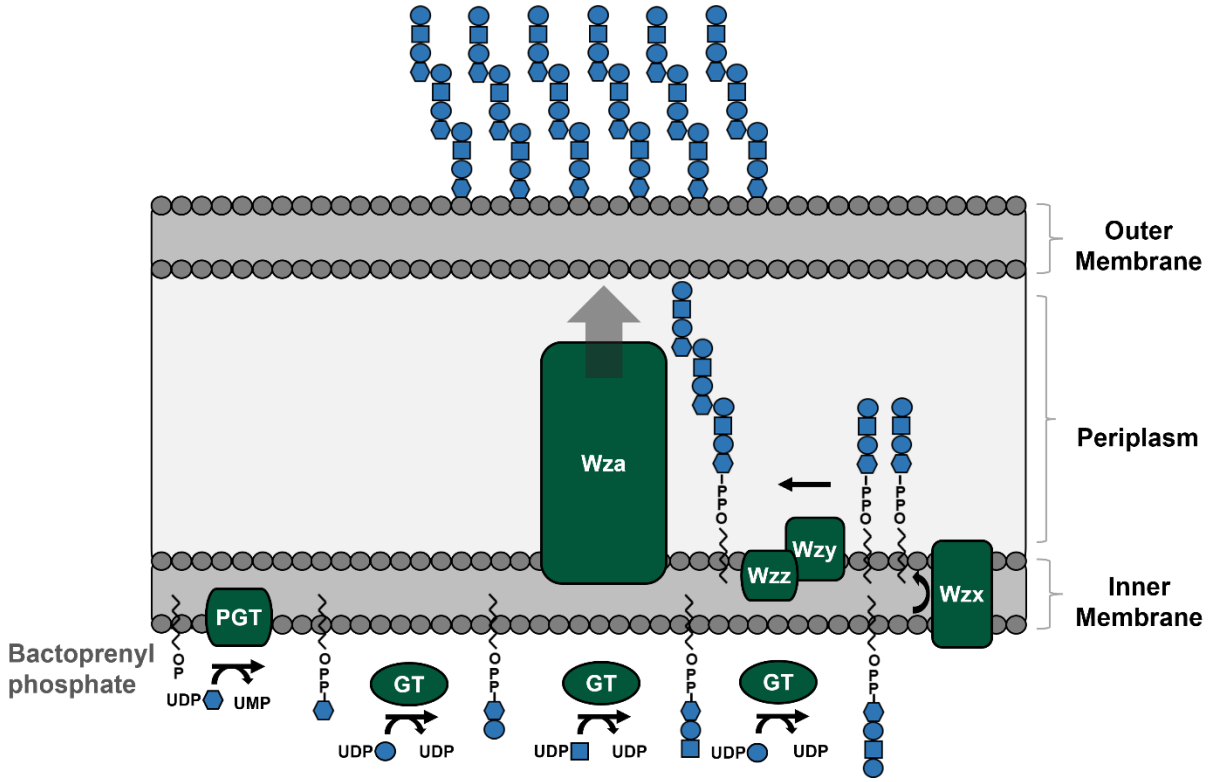

Figure 1.6: Representation of isoprenoid dependent polysaccharide biosynthesis in Gram-negative bacteria. PGT = Initiating phospho-glycosyltransferase, GT = cytosolic or membrane-associated glycosyltransferases, Wzx = flippase, Wzy = polymerase, Wzz = chain length regulator, Wza = polysaccharide exporter. Blue shapes represent monosaccharides either linked to, for example, uridine diphosphate (UDP) or appended to BPP (bactoprenyl diphosphate).

IN VITRO INVESTIGATION OF CAPSULAR AND EXOPOLYSACCHARIDE BIOSYNTHESIS

Precise determination of glycan biosynthesis pathways and structures has been stymied due to a lack of efficient glycosyltransferase screening methods, the presence of unique sugars, and branching in glycan structures. Alternatively, the lack of robust glycan purification procedures from host cells for mass spectrometry or structural characterization with NMR is hindered by time-consuming processes of purification from complex matrices and the presence of structural isomers. Furthermore, these methods do not typically allow for the evaluation and

characterization of precise biosynthetic pathways and identification of unique targets of glycan biosynthesis inhibitors. To this point, previous research has thoroughly demonstrated that selective inactivation of genes midpoint in BP-dependent glycan biosynthesis in *E. coli* induces severe morphological defects via sequestration of the vital BP precursor and cell lysis in BP-limited phenotypes.[131-133] These results provide further evidence that targeting glycan biosynthesis is an effective and selective means to attenuate pathogens.

The lack of a robust chromophore in glycan structures led earlier techniques to depend on radiolabeled NDP-linked sugar precursors to evaluate enzyme specificity.[121, 134, 135]To circumvent this, fluorescent probes of the conserved BP lipid anchor were developed by the Troutman Laboratory.[136] This was achieved by the substitution of a single isoprene of farnesyl diphosphate (FPP) with a fluorescent moiety, such as 2-nitrileaniline (2CN), to form 2CN-geranyl diphosphate (2CN-GPP). 2CN-GPP has been shown to be a successful substrate analogue of FPP which has enabled chemoenzymatic synthesis of fluorescent 2CN-BPP (**Figure 1.7**).[85] Mono-dephosphorylation of BPP to BP, occurs *in vivo* via the activity of membrane-bound UppP or other previously identified phosphatases.[110] Our group has found that it is more efficient to catalyze mono-dephosphorylation of BPP to BP *in vitro* using potato acid phosphatase due to the competing activity of BP-dependent systems, a point that is discussed in depth in **Chapter 2**, and the requirement of UppP purification from the cell membrane.[85] The effectiveness of implementing fluorescent BP analogues has been demonstrated by the successful characterization of each biosynthetic step in colanic acid from *E. coli* and CPSA from *B. fragilis*.[30, 31] This includes elucidation of a required pyruvylation or acetylation of BPP-linked disaccharides before complete oligosaccharide biosynthesis can proceed.[30, 31]

The chemoenzymatic synthesis of 2CN-BP can be monitored using high-performance liquid chromatography (HPLC) and demonstrates a facile method of sensitive and selective detection of BP and BP(P)-linked intermediates of bacterial glycan biosynthesis while eliminating dependence on hazardous, radiolabeled substrates. With this tool, a small library of purified monoglycosylated lipid precursors was generated (**Figure 1.7**).[85, 137, 138] This demonstrates the beginning steps to chemoenzymatic synthesis of a small library of BPP-linked glycan intermediates to characterize elusive bacterial glycan biosynthesis pathways, a point that is discussed in Chapter 4.

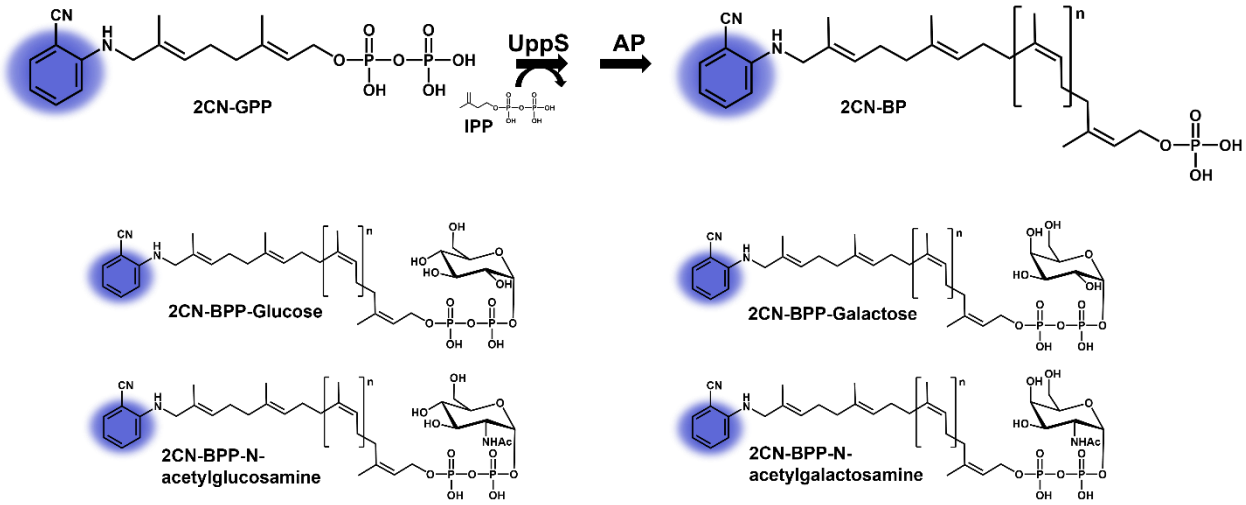

Figure 1.7: Chemoenzymatic synthesis of tagged, fluorescent BP analogues. Fluorescent FPP analogue, 2CN-GPP, is utilized by UppS to form 2CN-BPP, which is then dephosphorylated by acid phosphatase (AP) *in vitro* to produce 2CN-BP.[85] 2CN-BP substrate is successfully used by representative PGTs to produce a small library of fluorescent, BPP-linked monosaccharides.

IN VIVO INVESTIGATION OF BACTERIAL GLYCAN BIOSYNTHESIS

As previously noted, preliminary identification of glycan biosynthesis operons and constituent genes requires extensive genetic manipulations and selective inactivation to determine genes critical for glycan biosynthesis. These techniques frequently employ predictive technologies, including primary sequence and structural homologies, to infer gene product function in glycan

biosynthesis. Naturally, one might suppose that native, co-expressed glycan systems, compensatory mechanisms, or essentiality for survival could convolute the outcome of these determinations, which requires further, rigorous investigations. For example, Gram-negative *C. crescentus* secretes an extremely adhesive polysaccharide (holdfast) on an appendage known as the stalk, which enables the bacterium to adhere to a substrate in aquatic environments permanently. Genetic analyses began in the early 2000s to determine loci required for holdfast-promoted cellular adhesion.[25, 26] Almost 20 years later, Hershey et al. employed saturating transposon mutagenesis to precisely define how inactivation of specific genes contributes to *C. crescentus* adhesion and ultimately identified new gene products involved in holdfast production.[29] Intriguingly, all genetic components required for holdfast biosynthesis are not organized within a single operon, which has likely impeded the definition of required components over the years.

Other techniques have relied on the complete transfer of glycan biosynthesis operons to model organisms, such as *E. coli*, and genetic mutation to delineate glycosyltransferase specificity, biosynthesis pathways, and glycan structure.[139] For example, Linton et al. deployed plasmids encoding the *C. jejuni* N-linked glycosylation (*pgl*) locus with selective mutation of constituent genes to delineate roles of enzymes in the pathway.[140] The structure of the *C. jejuni* N-glycan was inferred based on MS-MS of spectra of purified glycans produced from *E. coli* strains expressing mutant versions of the *C. jejuni pgl* locus.[139] Using a different technique, Reid et. al successfully deployed a successive library of *E. coli* colanic acid mutants combined with colanic acid upregulation to evaluate native BPP-linked colanic acid intermediates.[31] Their results corroborate *in vitro* biosynthesis studies conducted by Scott, Erickson, and Troutman, and define the roles of two previously uncharacterized colanic acid biosynthesis enzymes.[31, 114]

The use of tagged monosaccharide probes and bioorthogonal reactions pioneered by Nobel Laureate, Carolyn Bertozzi, and colleagues for the study of mammalian glycans are now rigorously employed as chemical reporters to identify and visualize bacterial glycans.[4, 141-144] These studies are founded upon the use of monosaccharides chemically modified with a "handle" such as an azide or alkyne, successful uptake and incorporation into native glycan structures, and subsequent "tagging" via biorthogonal reactions with fluorescent reporters or affinity tags.[2, 4] The Dube Laboratory has advanced this strategy to discover bacterial N-linked glycan systems in anaerobic gut pathogens.[145] For example, Moulton et al. utilized azide-sugars to visualize the N-glycan "fingerprint" of wildtype and mutant *H. pylori* to define a new set of glycoproteins, implicate genes associated with N-glycan biosynthesis, and demonstrate evidence of these pathways as being isoprenoid-dependent.[142] This represents a significant advancement in techniques for identifying genes associated with bacterial glycan pathways.

Bioorthogonal cell labeling, for many bacterial glycan pathways, requires intracellular nucleotide-linked (NDP) sugar substrates for successful incorporation into native glycans. Simply feeding cells azide-sugars in some cases does not promote the formation of requisite NDP-sugar azides.[3] Eddenden et al. recently demonstrated successful circumvention of these limitations using recombinant techniques in *E. coli* to promote *in situ* production of UDP-N-azidoacetylglucosamine (GlcNAz) from GlcNAz.[146] GlcNAc is a monomeric constituent of ECA, O-antigen, poly-N-acetylglucosamine (PNAG), and peptidoglycan. The techniques of these authors enabled visualization of GlcNAz incorporation in *E. coli* and discrimination of UDP-GlcNAz utilizing pathways.[146] Another notable challenge is acquiring rare sugars for biorthogonal reactions, such as AAT-Gal or diNAcBac (**Figure 1.1**). GlcNAc is often a precursor in the metabolism of these rare sugars.[120, 147] Intriguingly, Clark et al. found that

GlcNAz uptake and incorporation were not uniform between species, for example, *H. pylori* readily incorporates GlcNAz into glycoproteins, but *C. jejuni*, *B. fragilis*, *P. aeruginosa*, *and Mycobacterium smegmatis* do not.[3] This may be related to the aforementioned limitation in the *in situ* production of NDP-sugar azides.[146] To probe further, the authors synthesized azide-containing analogues of rare bacterial monosaccharides to probe uptake and utilization.[3] While this enabled labeling of most of the pathogenic species the authors probed, the gut commensal *B. fragilis* was not labeled with any of the rare azido-sugars used in their study, representing a potential strategy for targeted antibiotics.[3] While limitations do exist for applying biorthogonal chemistry to bacterial glycans, these and similar strategies have already revealed potential approaches for targeted inhibition of bacterial glycan biosynthesis.[148, 149]

RECOMBINANT BACTERIAL GLYCAN PRODUCTION SYSTEMS

Bacterial glycan biosynthesis is often under the tight regulatory control of a unique operon, in which specific glycan structures are only induced in niche environments or developmental stages to support colonization and proliferation.[29, 43, 59, 150-153] Each gene product is responsible for discrete step(s) in glycan biosynthesis. In some instances, all genetic components, such as those required for metabolism of NDP-monomer requisites, are not located within this operon, which creates a challenge for genetic manipulation and overproduction of complex glycans in their native hosts.[29, 153] The production of these glycans may also come at a metabolic cost that may impede growth and, thus, the quantities of polysaccharides produced.[154] The abovementioned limitations result in a shortage of applications for biomedically or industrially relevant polysaccharides. Thoughtfully designed recombinant systems should enable the de-coupling of

regulatory mechanisms and the inclusion of required machinery for the overproduction of unique glycans in model organisms that are easily genetically manipulated and cultured.

An exemplary model of this was the reconstitution of the *C. jejuni* N-linked glycan in *E. coli*.[16, 155] *C. jejuni* is a well-known gut pathogen, a major cause of gastroenteritis, and the most commonly identified cause of Guillain Barré syndrome.[156] The *C. Jejuni* protein N-glycosylation pathway (Pgl) represents one of the first identified cases of protein N-glycosylation in prokaryotes, and mutations in this pathway impair adherence and invasion of human intestinal epithelial cells.[157-159] Authors of these studies discovered that N-liked glycosylation in *C. jejuni* and other prokaryotic N-linked glycan pathways is a process that shares homology with N-linked glycosylation in eukaryotes.[155, 160] In *C. jejuni*, a heptasaccharide is assembled on an isoprenoid lipid carrier, which is then flipped into the periplasm where an oligosaccharyltransferase, PglB, appends the heptasaccharide en bloc to a periplasmic acceptor protein.[155, 160-164]

Earlier iterations of a recombinant model of this pathway in *E. coli* enabled insights into the N-glycan structure and biosynthesis, and later to the development of an effective, potential chicken vaccine.[16, 155, 165] Remarkably, it was discovered that PglB possesses broad substrate specificity, capable of covalently attaching a broad range of glycopolymers to a protein substrate.[166] The promiscuous PglB oligosaccharyltransferase and the model N-linked glycan pathway underpin recent strategies developed by the Wren laboratory in recombinant glycoconjugate biosynthesis.[167-172]

Currently, techniques for recombinant polysaccharide biosynthesis often rely on the complete, one-step transfer of entire biosynthesis loci into host strains.[173] Polysaccharide biosynthesis loci, which are evidently fine-tuned for transcriptional regulation and expression in host strains, may not be efficiently expressed, or not expressed at all in an *E. coli* host. As

previously noted, *E. coli* and other model hosts may not possess the machinery required to generate requisite NDP-sugars, especially those that are unique and produced by a small number of bacterial species. Unlike *C. jejuni* N-linked glycan, proteins required for rare NDP-sugar biosynthesis may lie outside of the glycan operon, making a successful one-step operon transfer impossible for recombinant production of native structures. Moreover, host strains possess native glycan pathways and processing enzymes, which may either hinder recombinant glycan production by competing for available substrates, or siphon pre-cursors to other, native pathways. Utilizing a one-step cloning method ultimately masks potential bottlenecks in recombinant glycan production and hinders opportunities for overproduction. These points and others are addressed in **Chapter 3**.

The research within utilizes multiple approaches to address fundamental aspects of native glycan assembly, techniques to overcome barriers of *in vitro* investigation of polysaccharide biosynthesis, and comprehensive evaluation of recombinant polysaccharide systems. Instigated by the discovery and identification of a pervasive, non-specific product in reactions containing tagged 2CN-BP and bacterial cell envelope fractions, **Chapter 2** reveals an intriguing reverse reaction attributed to mechanisms of polymyxin resistance in Gram-negative pathogens. Consequently, this led to the development of new methods to probe pathways of polymyxin resistance and strategies to alleviate potential hindrances in the *in vitro* evaluation of glycan biosynthesis. **Chapter 3** successfully demonstrates the development of a recombinant system for overproduction of capsular polysaccharide A from *B. fragilis and* models a practical framework for delineating potential inefficiencies in each step of its biosynthesis. Finally, in **Chapter 4**, the investigation of early stages of *C. crescentus* holdfast biosynthesis resulted in the discovery of

rare, native precursors, insights into the initial stages of holdfast biosynthesis, and characterization of unique glycosyltransferases.

CHAPTER 2: LIPOPOLYSACCHARIDE IS A 4-AMINOARABINOSE DONOR TO EXOGENOUS POLYISOPRENYL PHOSPHATES THROUGH THE REVERSE REACTION OF THE ENZYME ARNT

ABSTRACT

Modification of the lipid A portion of LPS with cationic monosaccharides provides resistance to polymyxins, which are often employed as a last resort to treat multi-drug resistant bacterial infections. Here, we describe the use of fluorescent polyisoprenoids, liquid chromatography-mass spectrometry, and bacterial genetics to probe the activity of membrane-localized proteins that utilize the 55-carbon lipid carrier bactoprenyl phosphate (BP). We have discovered that a substantial background reaction occurs when B-strain *E. coli* cell membrane fractions are supplemented with exogenous BP. This reaction involves proteins associated with the *arn* operon, which is necessary for the covalent modification of lipid A with the cationic 4-aminoarabinose (Ara4N). Using a series of *arn* operon gene deletion mutants, we identified that the modification was dependent on ArnC, which is responsible for forming BP-linked Ara4N, *or* ArnT which transfers Ara4N to lipid A. Surprisingly, we found that the majority of the Ara4N modified isoprenoid was due to the reverse reaction catalyzed by ArnT and demonstrate this using heat-inactivated membrane fractions, isolated lipopolysaccharide fractions, and analyses of a purified ArnT. This work provides methods that will facilitate thorough and rapid investigation of bacterial outer membrane remodeling and the evaluation of polyisoprenoid precursors required for covalent glycan modifications.

INTRODUCTION

Bactoprenyl phosphate (BP, also known as undecaprenyl phosphate) is an essential precursor required to synthesize vital surface polysaccharides including peptidoglycan, capsules, and teichoic acids. BP is also required to glycosylate a variety of outer membrane components. Notably, the 55-carbon BP lipid carrier is necessary for the covalent modification of lipid A with cationic glycoses such as 4-aminoarabinose (Ara4N), glucosamine, and galactosamine in many species of Gram-negative pathogens.[73, 75, 78, 174-176] These outer membrane modifications are frequently associated with resistance to cationic antimicrobial peptides (CAMPs) such as polymyxin B and colistin (polymyxin E) and in certain species are required for cell viability.[75-77] Currently, polymyxin and colistin are being used as last-resort treatments against multi-drug resistant Gram-negative bacterial infections.[74] Consequently, enzymes within lipid A modification pathways are being targeted for the development of inhibitors to resensitize CAMP resistant Gram-negative pathogens.[177, 178]

In *Salmonella enterica* and *Escherichia coli*, CAMP resistance is due to covalent modification of the lipid A portion of LPS with Ara4N (Reviewed by Raetz et al.).[71] In those species, incorporation of Ara4N into the outer membrane begins in the cytosol with the biosynthesis of UDP-L-4-formamido-arabinose (UDP-Ara4FN) from UDP-glucose via the well-characterized enzymes Ugd, ArnA (PmrI), and ArnB (PmrH).[135, 179-182] Membrane-bound ArnC (PmrF) will then append Ara4FN to BP to produce bactoprenyl monophosphate-4-formamido-arabinose (BP-Ara4FN) (**Figure 2.1**).[135] Subsequently, ArnD (PmrJ) will deformylate 4-formamido-arabinose to produce bactoprenyl monophosphate-4-aminoarabinose (BP-Ara4N), which is then flipped into the periplasm by the proposed ArnE/F (PmrM/L) flippase heterodimer.[183, 184] The deformylation of the BP-Ara4FN intermediate likely commits this

pathway to lipid A modification and prevents reversal of the ArnC reaction.[71, 135, 184] In the periplasm, ArnT (PmrK) then transfers Ara4N from BP-Ara4N to lipid A.[185]

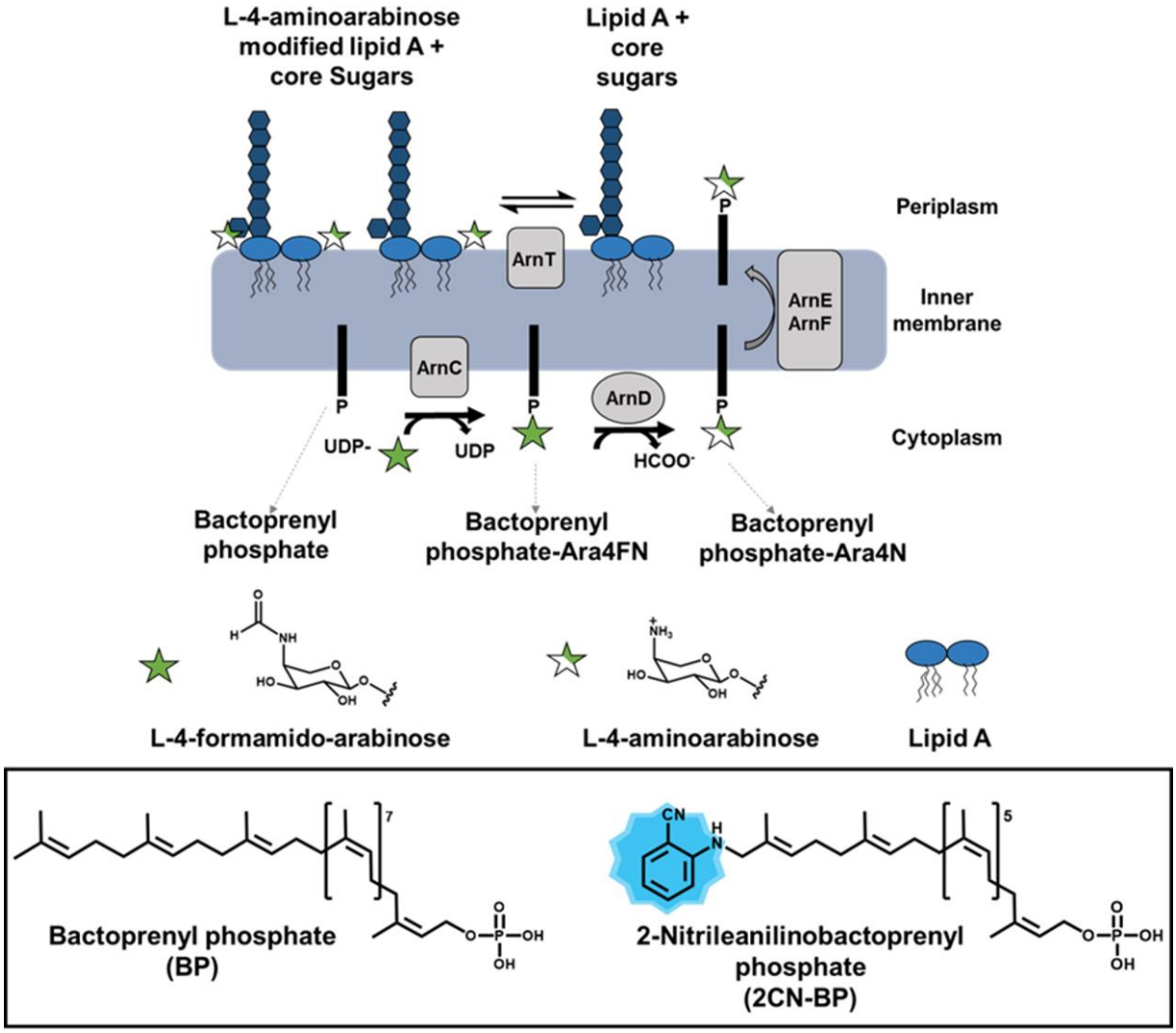

Figure 2.1: Biosynthetic pathway of lipid A modification with L-4-aminoarabinose in *E. coli*. Fluorescently labeled BP (2CN-BP) was used to probe endogenous enzyme activity within *E. coli* membrane fractions.

Limitations in procuring and detecting native BP-linked substrates have hindered characterization of enzymes involved in lipid A modifications. Recently, our group demonstrated the utility of fluorescent bactoprenyl phosphate to rapidly investigate the activity and specificity of bacterial glycosyltransferases including several enzymes within the initiating phospho-

glycosyltransferase (PGT) protein family.[30, 31, 85] Importantly, we found that the initiating PGT WecA from *E. coli*, which is responsible for appending GlcNAc-phosphate (GlcNAc-P) to BP, was present in cell envelope fractions in high enough quantities without overexpression to catalyze exogenous BP modification. In this report, we focused our efforts on determining whether these fluorescent probes could be used to characterize additional important endogenous proteins within the bacterial cell envelope, such as those required for polymyxin resistance.

RESULTS

Utilization of 2CN-BP by *E. coli* cell envelope fractions

In our previous analysis of PGT enzyme activity, we consistently observed that upon incubation of fluorescent 2-nitrileanilinobactoprenyl phosphate (2CN-BP) with membrane fractions prepared from B-strain *E. coli*, an unidentified fluorescent product was formed.[85] The presumed modified 2CN-BP was formed without the addition of nucleotide-linked sugar (NDP-sugar), which suggested that the donor substrate for the reaction was contained within the membrane fraction. In addition, formation of this product was considerably lower, and in some cases undetectable when a PGT (e.g., WecA) and its NDP-sugar substrate were added to the reactions exogenously to compete for available 2CN-BP (**Figure 2.2**).[85] RP-HPLC analysis of C41(DE3) membrane fraction reactions exempt of NDP-sugar demonstrated that 0.5 mg/mL (total protein concentration) of membrane fraction consumed approximately up to 100 pmol of 2CN(*6Z*)BP (six isoprenes in the Z-configuration) (**Supporting Figure 2.1**). As a vehicle control, we found that product formation was not impacted by the presence of DMSO (up to 12%) (**Supporting Figure 2.1**).

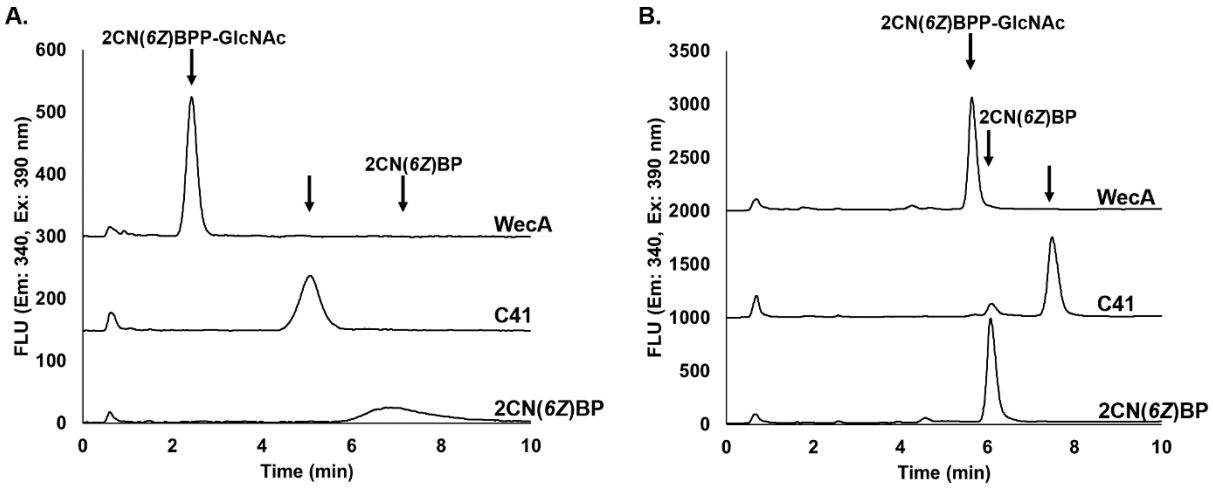

Figure 2.2: Wild-type C41(DE3) cell envelope fraction catalyzes the modification of 2CN(6Z)BP. (A) RP-HPLC (Condition A) analysis of WecA C41(DE3) membrane fraction incubated with 5 µM 2CN(6*Z*)BP and 100 µM UDP-GlcNAc compared to a C41(DE3) membrane fraction incubated with 5µM 2CN(6Z)BP and no nucleotide-linked sugar. Each reaction contained 0.5 mg/mL (total protein) of membrane fraction. The control was 5 µM 2CN(6*Z*)BP input alone. Crude reactions were monitored with fluorescence detection and offset by 150 FLU increments. (B) RP-HPLC (Condition B) analysis of reactions described in Figure A. Crude reactions were monitored with fluorescence detection and offset by 1000 FLU increments.

Notably, the retention time of this product on a conventional C18 column (Agilent Zorbax) with an ammonium bicarbonate/*n*-propanol mobile phase (Condition A) was intermediate to 2CN-BP and 2CN-BPP-GlcNAc, as evidenced by the 2.7 min difference in retention time when compared to the product of WecA (**Figure 2.2A**).[85] However, using a high pH resistant C18 column (Waters XBridge) with an ammonium hydroxide/*n*-propanol mobile phase (Condition B), the retention time of the unidentified product was greater than both 2CN-BP and 2CN-BPP-GlcNAc (**Figure 2.2B**). The chromatographic behavior of the unidentified product under both described conditions was comparable to a 2CN-BP-monosaccharide that we have observed during our investigation of another lipid A modification system (unpublished data), suggesting that the unidentified product too, could be a polyisoprenoid monophosphate-linked sugar.

In support of this, Trent et al. demonstrated that B-strain *E. coli* such as C41(DE3) appear to be inherently resistant to polymyxin and modify lipid A with Ara4N.[186] Since lipid A modification systems are characterized by the requirement of a BP-glycose donor, we viewed this as a possible source of a 2CN-BP-monosaccharide (Reviewed by Mann and Whitfield).[187] Lipid A modification and expression of the *arn* operon (*arnBCADTEF*) in *E. coli* has previously been attributed to the activation of the PmrA/B two-component regulatory system, including constitutively activating mutations in *pmrA* or *pmrB*.[73, 81, 188-190] Unlike B-strains, K-strains do not modify lipid A with Ara4N and are thus sensitive to polymyxin unless induced by various environmental cues such as exposure to Fe^{3+} or metavanadate.[72, 76, 191-193] Therefore, if the unidentified product was associated with Ara4N lipid A modification, no such modification of 2CN-BP should occur with a membrane fraction prepared from a polymyxin-sensitive K-12 strain such as MG1655 grown under standard conditions, but perhaps we could induce this modification by culturing in *arn* inducing conditions.[185]

To test this, we prepared two separate membrane fractions of the *E. coli* K-strain MG1655, the first prepared from cells cultured in LB and the second prepared from cells cultured in LB supplemented with 200 μM Fe^{3+}. When 2CN-BP was incubated with membrane fraction prepared from MG1655 cells cultured in standard conditions, no product was formed (**Figure 2.3A**). However, when compared to the product of C41(DE3) membrane fraction, a new product with an identical retention time was formed only by MG1655 membrane fraction prepared from cells cultured with Fe^{3+} (**Figure 2.3A**). These results indicated that formation of this product could be induced by preparing membrane fractions from cells cultured with Fe^{3+} and that it is likely associated with Ara4N lipid A modification. Additionally, we noted that a new product was formed by MG1655 membrane fraction (cultured without Fe^{3+}) when incubated with

UDP-Glucose (**Figure 2.3A**). This product possessed a similar retention time (6.07 min) to that of the unknown product (6.20 min) and an m/z corresponding to the $[M-H]^-$ ion of a 2CN-BP-Hexose as evidenced by ESI-LC-MS with selected ion monitoring (SIM) in negative ion mode (**Figure 2.3B**). Of the known possible gene products in *E. coli* that may append glucose to 2CN-BP, we attributed this activity to the phage-encoded glucosyltransferase YfdH (GtrB), which is not present in B-strains.[194, 195]

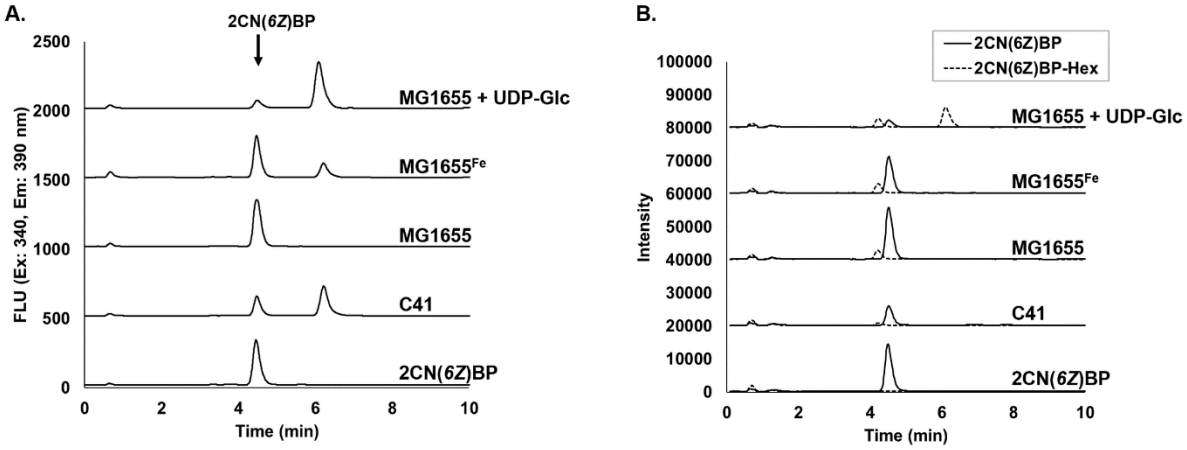

Figure 2.3: MG1655 membrane fraction prepared from cells cultured in the presence of Fe^{3+} utilize 2CN-BP without the addition of nucleotide-linked sugar. (A) RP-HPLC analysis (Condition B) of crude reactions containing 5 µM 2CN(6*Z*)BP and 0.5 mg/mL (total protein) of membrane fractions prepared from *E. coli* C41(DE3) or MG1655. Crude reactions were monitored with fluorescence detection and offset by 500 FLU increments. (B) ESI-LC-MS with SIM in negative ion mode of reactions described in figure A. Chromatograms were offset by 15,000 intensity units. A non-fluorescent peak corresponding to the $[M-H]^-$ ion of 2CN(6*Z*)BP-Glc appears at 4.2 min and is associated with membrane fraction alone (data not shown). Control reactions contained 5 µM 2CN-BP alone.

To aid in the identification of the unknown product from C41(DE3) membrane fraction reactions, we prepared a reaction containing C41(DE3) membrane fraction and 100 nmole 2CN-BP that was subsequently separated and isolated via RP-HPLC. Analysis of the unidentified product with ESI-MS in negative ion mode indicated a predominant ion with an m/z of 888.60 which corresponds to a predicted $[M-H]^-$ m/z of 2CN(*6Z*)BP-Ara4N (888.57) (**Figure 2.4A)**.

Upon collision-induced fragmentation, we observed an m/z of 757.59 which is consistent with the $[M-H]^-$ ion of the fluorescent 2CN(*6Z*)BP (expected m/z 757.51) and a loss of an Ara4N unit (**Figure 2.4B**). We then used ESI-LC-MS with SIM in negative ion mode to evaluate crude membrane fraction reactions for 2CN-BP-Ara4N (2CN-BP-PentN) (**Figure 2.4C**). As expected, the MG1655 membrane fraction produced the purported 2CN-BP-Ara4N product only when cells were cultured in the presence of Fe^{3+}. These results demonstrated that the unidentified product was likely a modification of 2CN-BP with Ara4N or another modification with an identical mass.

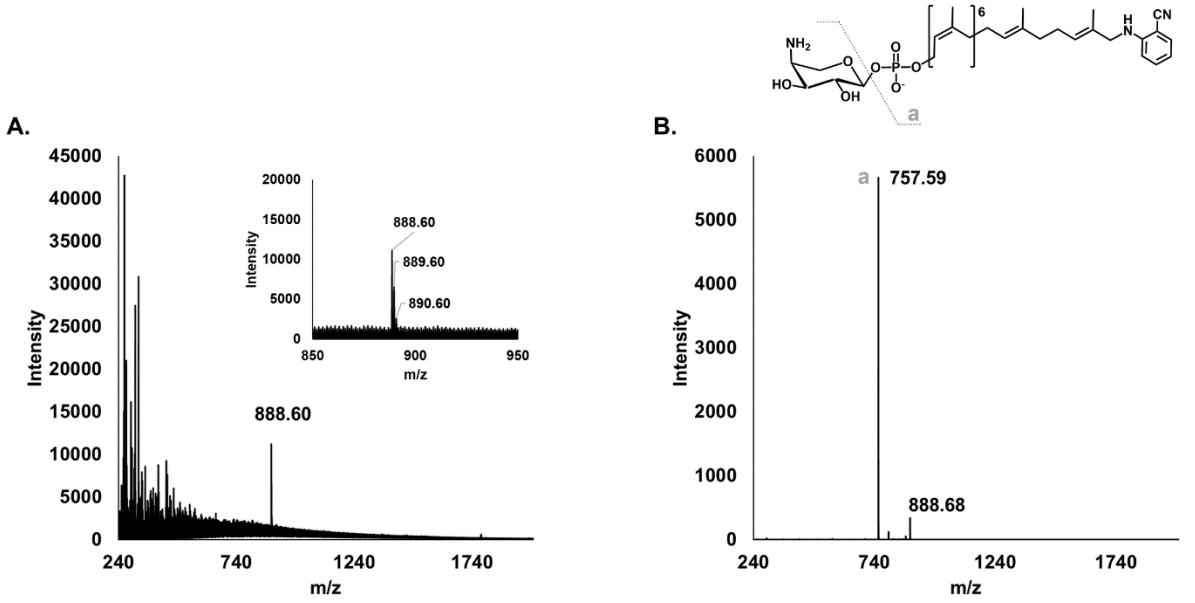

Figure 2.4: MS and MS/MS analysis of the unidentified product indicated an m/z corresponding to 2CN(6Z)BP-Ara4N. (A) ESI-MS of the unidentified product isolated from C41(DE3) membrane fraction reactions with 2CN(6Z)BP. (B) MS/MS analysis of the unidentified product. (C) ESI-LC-MS analysis (Condition B) of crude reactions containing 5 µM 2CN(6Z)BP and 0.5 mg/mL membrane fraction with SIM in negative ion mode. Chromatograms were offset by 20,000 (2CN(6Z)BP) or 5,000 (2CN(6Z)BP-Ara4N) intensity units. Control reactions consisted of 5 µM 2CN-BP alone.

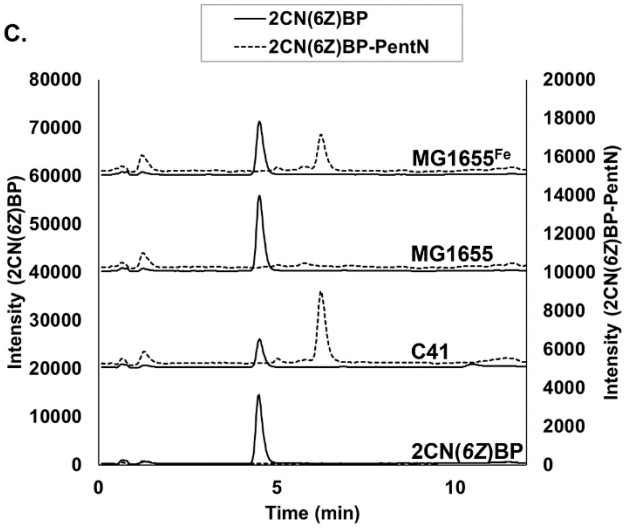

Membrane-bound enzymes in Ara4N lipid A modification pathway contribute to membrane fraction mediated formation of 2CN-BP-Ara4N

We envisioned two possibilities as the source of the membrane fraction mediated Ara4N modification of 2CN-BP: (1) membrane-bound ArnC transfers Ara4FN to 2CN-BP and is subsequently deformylated by membrane-associated ArnD or (2) membrane-bound ArnT transfers Ara4N from either native BP-Ara4N or LPS-Ara4N to 2CN-BP (**Figure 2.5**). To

evaluate each of these possibilities, we created deletions of *arnC* and *arnT* in C41(DE3). We reasoned that a non-polar deletion of *arnC* would not impede the formation of UDP-Ara4FN but would preclude the synthesis of endogenous BP-Ara4N and LPS-Ara4N. Thus, we expected that deleting *arnC* would abolish production of 2CN-BP-Ara4N in membrane fraction reactions by preventing transfer from ArnC *or* ArnT. In the same regard, we anticipated that if ArnCD were responsible for mediating the transfer of Ara4N to 2CN-BP, deletion of *arnT* would not affect the production of 2CN-BP-Ara4N but would preclude the formation of LPS-Ara4N.

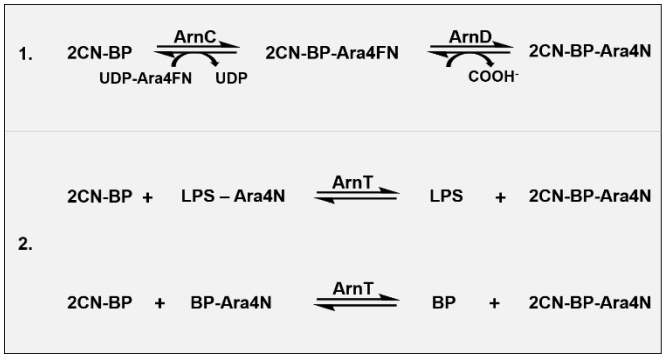

Figure 2.5: Schematic of potential sources of 2CN-BP modification with Ara4N.

To evaluate the activity of Δ*arnT* and Δ*arnC* mutant membrane fraction, we prepared reactions containing either wild type or mutant membrane fraction incubated with 2CN-BP and analyzed the crude reactions for 2CN-BP-Ara4N using RP-HPLC (Condition A) (**Figure 2.6**). As predicted, RP-HPLC analysis of the Δ*arnC* membrane fraction with 2CN-BP did not demonstrate the formation of 2CN-BP-Ara4N. Extrachromosomal complementation of *arnC* with a high copy number plasmid partially restored the activity of Δ*arnC* pArnC membrane fraction compared to wild type. Interestingly, we found that the Δ*arnT* membrane fraction also did not produce 2CN-BP-Ara4N, suggesting that ArnT is required for the modification of exogenous 2CN-BP with Ara4N (**Figure 2.6B**). Complementation of *arnT* restored that activity, while expression of an empty plasmid control in either mutant did not (**Figure 2.6C**). To confirm expression of *arnC* and *arnT* in our complementation analyses, we confirmed the presence of 6XHis-tagged ArnC and ArnT in membrane fractions with an anti-His Western Blot

(**Supporting Figure 2.2**). These results further support our hypothesis that Arn enzymes in membrane fraction are involved in this new product formation and that the modification is indeed Ara4N (i.e., not another modification with an identical mass).

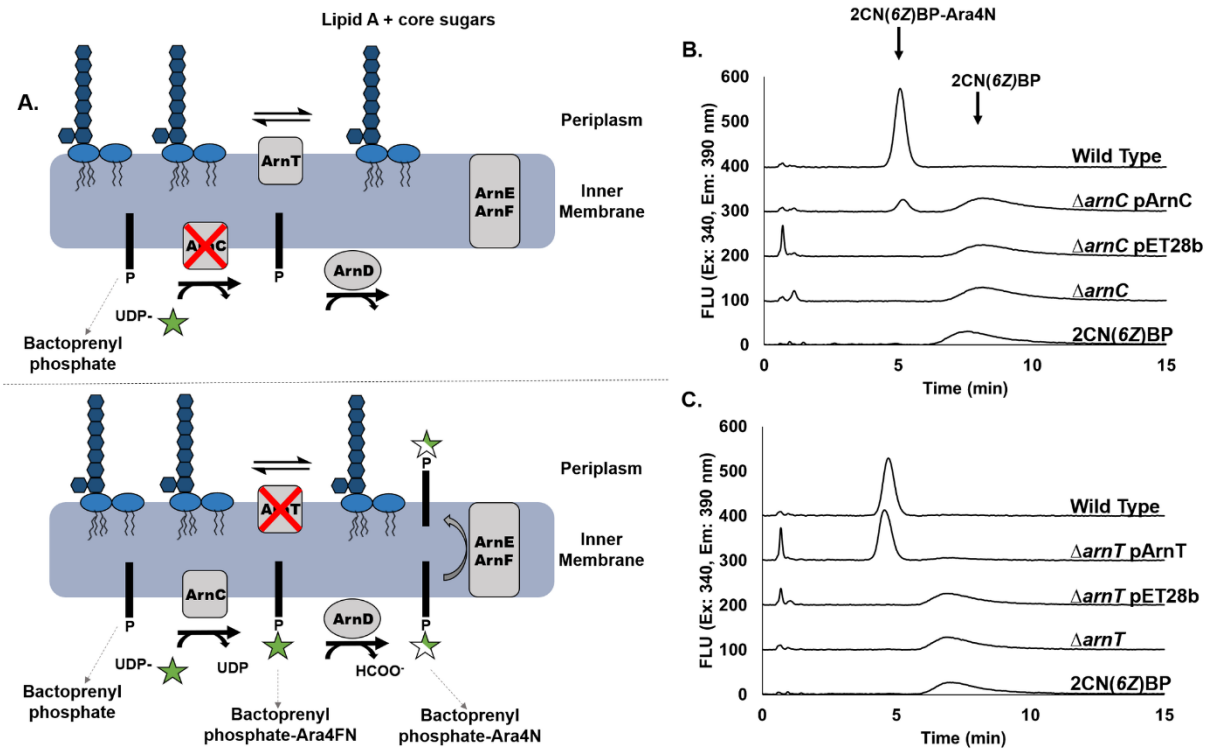

Figure 2.6: Deletion of *arnC* or *arnT* in C41(DE3) abolishes cell envelope production of 2CN-BP-Ara4N. Reactions with 2CN(6*Z*)BP and membrane fractions prepared from wild type or mutant C41(DE3) were separated by RP-HPLC (Condition A) and evaluated for product formation with fluorescence detection. Chromatograms were offset by 100 FLU increments. (A) Schematic of potentially available intermediates in each mutant membrane fraction. (B) Δ*arnC* C41(DE3) membrane fraction compared to wild-type membrane fraction incubated with 2CN(6*Z*)BP. (C) Δ*arnT* C41(DE3) membrane fraction compared to wild-type membrane fraction incubated with 2CN(6*Z*)BP.

Modification of 2CN-BP by ΔarnC membrane fraction is facilitated by the addition of exogenous substrate

We next evaluated potential sources of Ara4N modification by supplying exogenous donor substrate in the form of a heat-inactivated wild-type membrane fraction to either the ΔarnC or ΔarnT mutant membrane fraction (Figure 2.7). The inactivated wild-type membrane fraction

would harbor the donor substrate but the proteins (ArnC or ArnT) are inactive. Supplementation of exogenous substrate to a reaction containing Δ*arnC* membrane fraction would enable us to evaluate the activity of ArnT. Similarly, by using the Δ*arnT* membrane fraction, we could then evaluate the activity of ArnC. To do so, each active membrane fraction was incubated with or without equivalent quantities of inactivated wild-type membrane fraction. Wild-type or inactive wild-type membrane fraction with 2CN-BP were used as controls. When reactions containing 2CN-BP and Δ*arnC* membrane fraction were supplemented with inactive membrane fraction, a new product was formed. The retention time of this new product corresponded to the same retention time as 2CN-BP-Ara4N (4.83 min, Condition A) produced by wild-type membrane fraction. No such product was formed under these conditions with the Δ*arnT* membrane fraction. These results suggest that ArnT is responsible for transferring Ara4N to 2CN-BP.

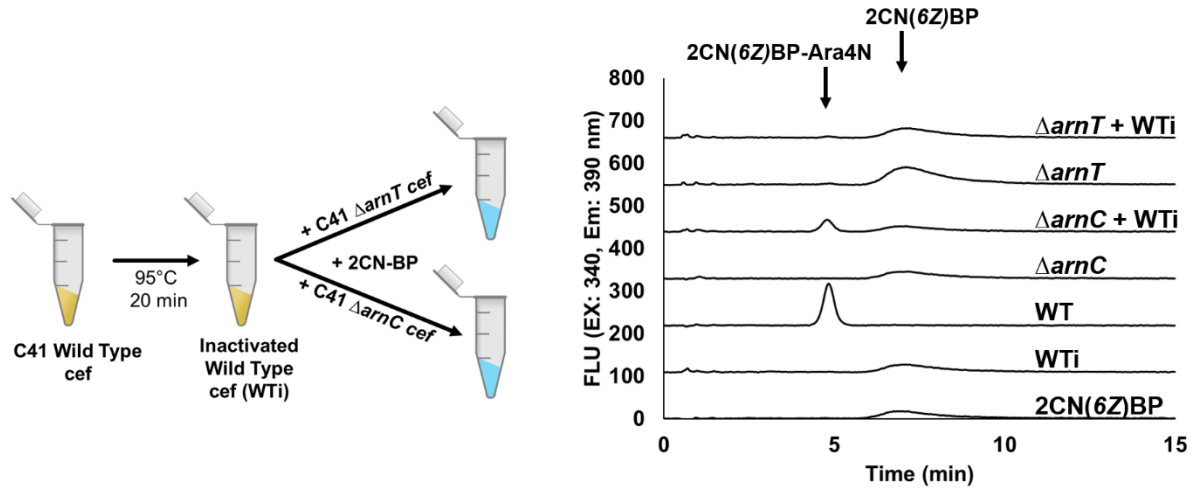

Figure 2.7: *arnT*, but not *arnC* is required for the modification of 2CN-BP in the presence of exogenous substrate. Mutant membrane fractions (0.5 mg/mL) were incubated with 5 μM 2CN(6Z)BP both with and without 0.5 mg/mL of inactivated wild-type membrane fraction (WTi). Crude reactions were separated by RP-HPLC (Condition A) and analyzed with fluorescence detection. Chromatograms are offset by 100 FLU increments.

To address whether native BP-Ara4N could serve as the Ara4N donor substrate for ArnT catalyzed formation of 2CN-BP-Ara4N, we first determined whether native BP-Ara4N would

accumulate in the C41(DE3) strain. Accumulation and detection of BP-Ara4N have been well established in polymyxin resistant *E. coli* and *Salmonella enterica.*[184, 186] These methods typically employ lipid extraction from cell lysates followed by MALDI-MS or ESI-MS.[184, 186, 194] Similarly, we used ESI-LC-MS to detect BP, BP-Ara4FN, and BP-Ara4N in total lipid extracts of *E. coli* cell lysates.[196] Using SIM in negative ion mode, we were able to reliably detect endogenous BP ($[M-H]^-$ m/z 845.7) in wild-type C41(DE3) and mutant lipid extracts. BP-Ara4N (BP-PentN, $[M-H]^-$ m/z 976.7) was detected only in wild-type C41(DE3) and Δ*arnT* C41(DE3), but not in Δ*arnC* C41(DE3) (**Figure 2.8**), a result that is corroborated by previous characterization of BP-Ara4N biosynthesis.[135, 186] Interestingly, triplicate analysis of equally prepared lipids demonstrated a consistent 2.5-fold increase in the abundance of BP in lipids prepared from Δ*arnC* C41(DE3).

Complementation of the Δ*arnC* mutant with a high copy number plasmid restored the accumulation of BP-Ara4N, but only to a minor extent when compared to wild type (**Supporting Figure 2.3**). This result is akin to the previous complementation analysis with RP-HPLC, in which full conversion of 2CN-BP was not achieved by complementation of the Δ*arnC* mutant (**Figure 2.6**). Complementation of the Δ*arnT* mutant did not significantly alter the intensity of either BP or BP-Ara4N relative to wild type. A signal corresponding to BP-Ara4FN was not detected in either wild type or mutant lipid extracts (BP-PentFN, $[M-H]^-$ 1004.71). However, we

were able to detect BP-Ara4FN in lysates prepared from the complemented *arnC* mutant (**Supporting Figure 2.3**).

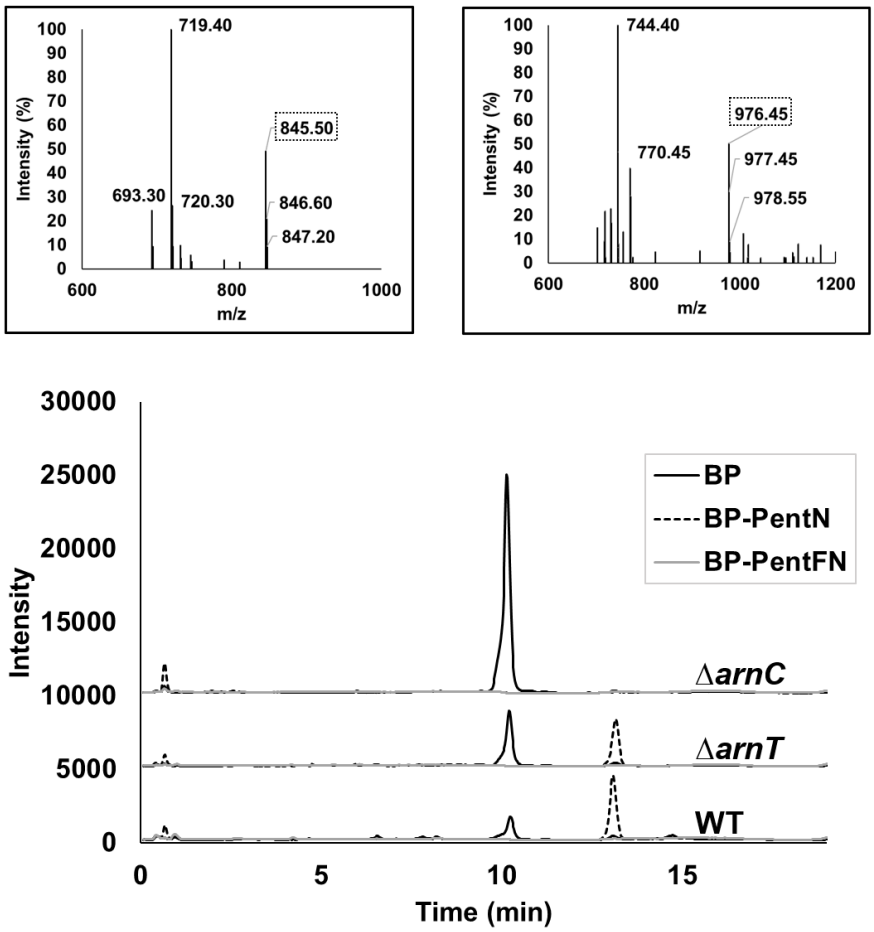

Figure 2.8: ESI-LC-MS with SIM of accumulated BP and BP-Ara4N in wild type and mutant C41(DE3) lipids. Total lipids prepared from wild type, Δ*arnC*, or Δ*arnT* C41(DE3) cells were analyzed with ESI-LC-MS (Condition B) and SIM in negative ion mode. Chromatograms were offset by 5,000 intensity units. Left inset depicts the mass spectrum obtained from the total ion scan from 9.8-10.2 min in lipids prepared from the Δ*arnC* C41(DE3) mutant. Right inset depicts the mass spectrum obtained from the total ion scan from 13.0-13.4 min in lipids prepared from wild-type C41(DE3). Signals observed in the 700-800 m/z range likely correspond to phospholipids.

Based on the analysis of native BP and BP-Ara4N in C41(DE3) lipid extracts, Δ*arnT* membrane fraction would likely harbor both BP and BP-Ara4N, but not lipopolysaccharide (LPS)-Ara4N.[186] To rule out the possibility of native BP-Ara4N as the donor substrate for modification of 2CN-BP, we then prepared inactivated Δ*arnT* membrane fraction and supplied it

to wild type and mutant membrane fraction as a source of BP-Ara4N. HPLC analysis of crude reactions did not indicate the production of 2CN-BP-Ara4N when Δ*arnC* membrane fraction was incubated with inactivated Δ*arnT* membrane fraction (**Supporting Figure 2.4**). These results suggest that endogenous BP-Ara4N does not supply the Ara4N donor for 2CN-BP modification, and collectively indicate that the aberrant production of 2CN-BP-Ara4N is mediated through the reverse reaction of ArnT, in which Ara4N is transferred from LPS-Ara4N to exogenously supplied 2CN-BP.

ArnT catalyzed reverse transfer of Ara4N occurs with fluorescent and native BP

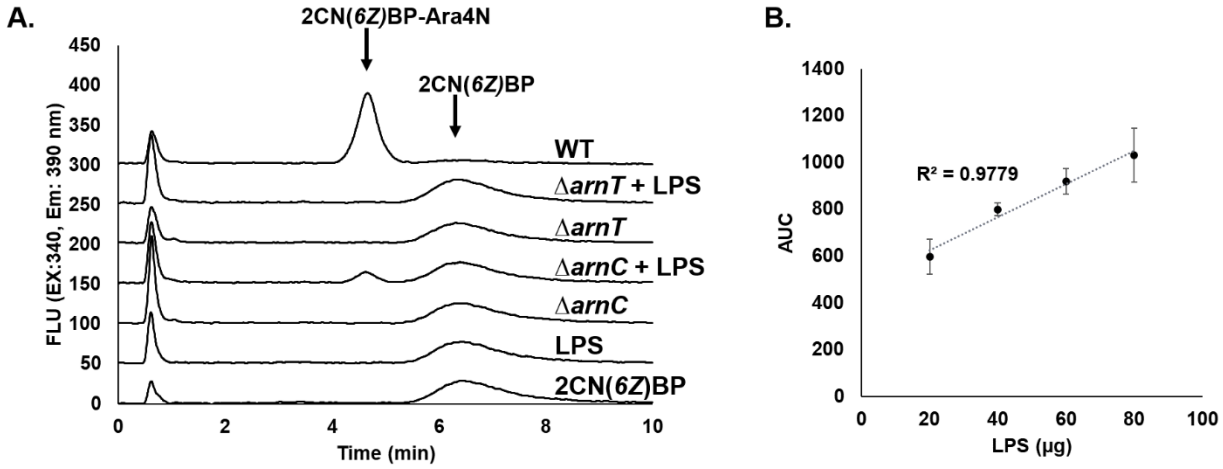

Figure 2.9: Δ*arnC* C41(DE3) membrane fraction catalyzes the conversion of 2CN-BP in the presence of wild-type LPS. (A) Mutant membrane fractions (0.5 mg/mL total protein) were incubated with 5 μM 2CN(6*Z*)BP both with and without 20 μg of isolated wild-type LPS and analyzed by RP-HPLC (Condition A). Chromatograms were offset by 50 FLU increments. (B) Reactions were supplemented with incremental amounts of LPS (20 – 80 μg) which increased the turnover of 2CN(6*Z*)BP linearly. Turnover of 2CN(6Z)BP was determined by measuring the peak area associated with 2CN(6*Z*)BP-Ara4N (4.8 min). Error bars represent the standard deviation of triplicate experiments.

To evaluate whether LPS could serve as an Ara4N donor substrate, a fraction of LPS was prepared from wild-type C41(DE3) that was expected to contain Ara4N modified LPS. Using a shortened procedure for lipid A isolation, C41(DE3) cells were lysed in a single-phase Bligh and

Dyer solution and crude LPS was collected as an insoluble precipitate.[196, 197] Samples prepared using this method are expected to be relatively free of any BP and BP-linked intermediates, as phospholipids and prenyl lipids are extracted in the soluble fraction (see methods).[197] A sample of isolated material was visualized with SDS-PAGE which showed minimal contamination and a banding pattern consistent with the anticipated truncated LPS of B-strain *E. coli* (**Supporting Figure 2.5**).[198, 199] Isolated material was then added to reactions containing 2CN-BP and wild-type or mutant membrane fraction (**Figure 2.9A**). In this analysis, we found that only the Δ*arnC* membrane fraction produced 2CN-BP-Ara4N when incubated with isolated LPS fractions. Additionally, a consistent, linear increase in the turnover of 2CN-BP was observed in reactions containing Δ*arnC* membrane fraction when the amount of LPS (approximately 20 μg) was increased up to 4-fold (**Figure 2.9B and Supporting Figure 2.6**).

Based on our analysis of BP and BP-Ara4N levels in wild type and mutant C41(DE3) cell lysates (**Figure 2.8**), we determined that Δ*arnC* cells have an abundance of available BP. To ensure that transfer of Ara4N from LPS-Ara4N also occurred with native BP and not just 2CN-BP, we prepared reactions containing Δ*arnC* membrane fraction supplemented with LPS, in which the Δ*arnC* membrane fraction would serve as a source of both BP and ArnT (**Figure 2.10A**). Lipids were then extracted with *n*-butanol, dried under vacuum, and resuspended in *n*-propanol/10 mM ammonium hydroxide prior to ESI-LC-MS analysis. As anticipated, BP-Ara4N was observed only when Δ*arnC* membrane fraction was incubated with LPS but not in Δ*arnC* membrane fraction or LPS alone.

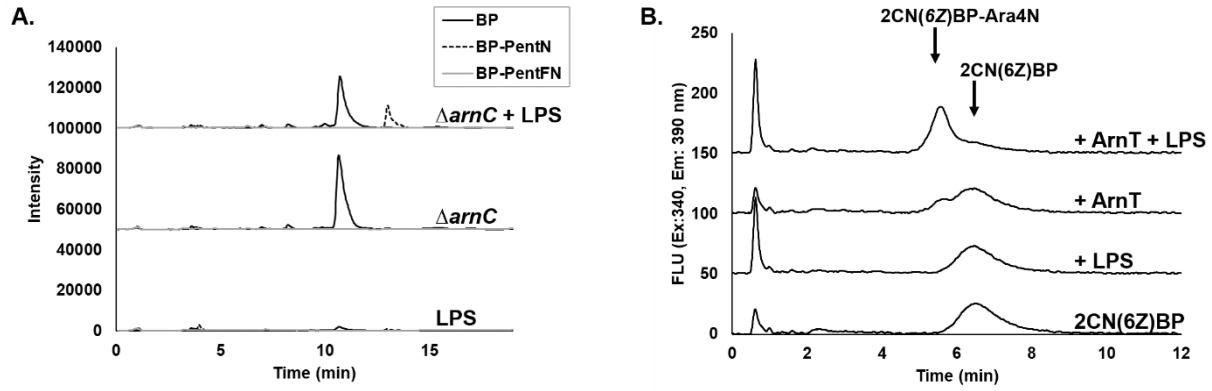

Figure 2.10: Cell envelope fraction prepared from ΔarnC C41(DE3) produces BP-Ara4N when incubated with LPS. (A) Δ*arnC* C41(DE3) membrane fraction (0.5 mg/mL total protein) was incubated in buffered reaction conditions with approximately 50 µg of purified LPS prepared from wild-type C41(DE3) cells. The Δ*arnC* membrane fraction or LPS alone were used as controls. Crude reactions were monitored for the presence of BP-Ara4N with ESI-LC-MS and SIM (Condition B). Chromatograms were offset by 50,000 intensity units. (B) Purified ArnT was incubated with 2CN(6*Z*)BP both with and without 20 µg LPS. Crude reactions were monitored with RP-HPLC (Condition A) and fluorescence detection. Chromatograms were offset by 50 FLU increments.

To demonstrate that reverse transfer is catalyzed by ArnT and not another enzyme within the membrane fraction, ArnT bearing a 6xHis-tag was overproduced in C41(DE3), and solubilized as described in the materials and methods (**Supporting Figure 2.7**).[200] To evaluate the activity of purified ArnT, we incubated ArnT and 2CN-BP both with and without LPS and monitored for 2CN-BP-Ara4N (**Figure 2.10B**). RP-HPLC analysis of these reactions indicated that purified ArnT without added LPS catalyzed the conversion of 2CN-BP, albeit full-turnover was not achieved. This result was not surprising since isolated proteins are typically contaminated with LPS.[201] When purified LPS from C41(DE3) was added to ArnT reactions, 2CN-BP was nearly consumed as indicated by the increase in 2CN-BP-Ara4N and reduction in 2CN-BP.

Characterization of *E. coli* ArnD with native BP-Ara4FN substrate

Based on the utility of ESI-LC-MS methods described above to detect native BP-linked intermediates, we next sought to apply these methods to characterize the function of ArnD with its native substrate, BP-Ara4FN. In similar lipid A modification pathways, deacetylation or deformylation is required to finalize the transfer of cationic glycoses to lipid A (Reviewed by Mann and Whitfield).[187] Recent analysis of an ArnD homolog from *Burkholderia cenocepacia* with a synthetic analogue of BP-Ara4FN demonstrated ArnD deformylase activity.[183] To bypass the need for syntheses of BP-Ara4FN or UDP-Ara4FN, we used a genetic approach to promote the accumulation of native BP-Ara4FN in *E. coli* which could then be collected and used for functional assays *in vitro*. To do so, we created a Δ*arnD* mutation in the K-12 MG1655 background and tested whether the accumulation of BP-Ara4FN could be promoted by culturing these cells in the presence of Fe^{3+}. ESI-LC-MS analysis of total lipid extracts from wild-type MG1655 demonstrated a minor accumulation of BP-Ara4N when cells were cultured in the presence of Fe^{3+} (**Figure 2.11A)**. Accordingly, analysis of lipid extracts from Δ*arnD* MG1655 cells demonstrated that BP-Ara4FN was only detected when cells were grown in the presence of Fe^{3+} (**Figure 2.11A and 2.11B**).

Using lipid extracts of Δ*arnD* MG1655 cells containing BP-Ara4FN, we then assessed the deformylase activity of *E. coli* ArnD. To express and purify ArnD, we used a purification procedure recently reported by Adak et al.[183] The presence of ArnD was confirmed with SDS-PAGE and anti-His Western blotting (**Supporting Figure 2.8**). Purified ArnD was then incubated in buffered reactions with lipids prepared from MG1655 Δ*arnD* cells cultured with Fe^{3+}. Deformylase activity was monitored with ESI-LC-MS using SIM in negative ion mode and evidenced by the formation of BP-Ara4N (**Figure 2.11**).

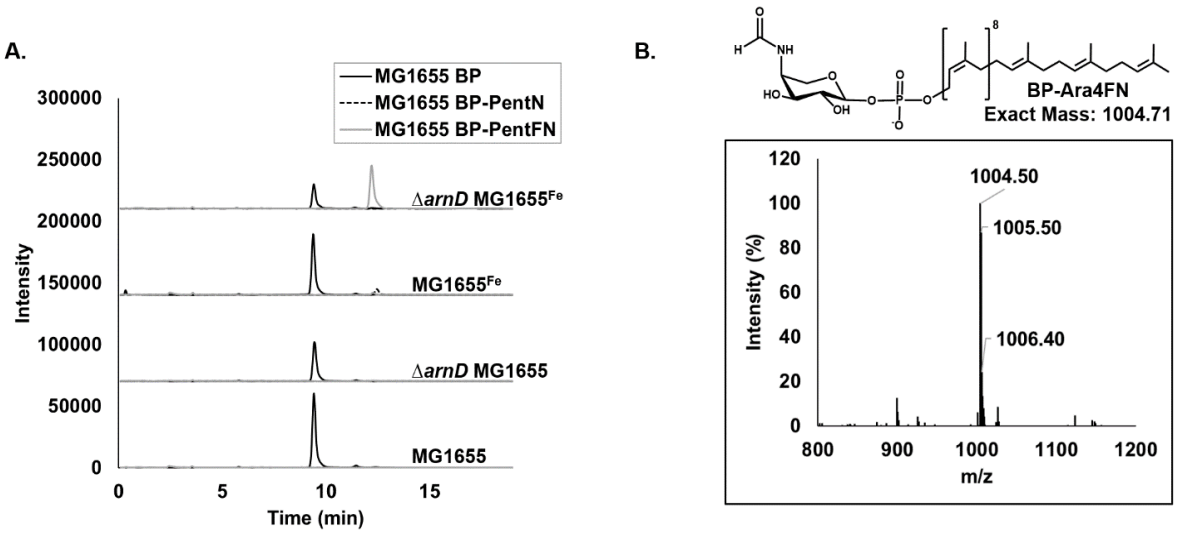

Figure 2.11: Induced accumulation of native BP-Ara4FN and deformylation of BP-Ara4FN by *E. coli* ArnD. (A) Lipids prepared from MG1655 and Δ*arnD* MG1655 cells cultured in LB with or without Fe^{3+} were analyzed with ESI-LC-MS (Condition B) with SIM in negative ion mode for BP, BP-PentN, and BP-PentFN ([M-H]$^-$ m/z 1004.7). (B) Mass spectrum obtained from total ion scan of ΔarnD MG1655^{Fe} from 12.0 – 12.6 min (C) Reactions containing lipids prepared from MG1655 Δ*arnD* cultured with Fe^{3+} and 0.05 mg/mL ArnD were monitored for BP-Ara4N (BP-PentN) with SIM. Control reactions contained lipids in reaction buffer with no ArnD.

DISCUSSION

Previously established methods for evaluating polyprenyl-phosphate glycosyltransferases have relied on the specific detection of radiolabeled glycoses. Here, we have highlighted additional polyisoprenoid-linked products that are formed due to the reversibility of these reactions and likely go undetected. In events of poor recombinant protein production or function, exogenously added isoprenoid substrate may be consumed by these reactions, significantly reducing the availability of BP, and preventing glycosylation or detection of the intended product. On the other hand, we also note that the availability of BP glycose substrates is limited, and that reverse reactions demonstrated here may be used to generate these substrates *in vitro*. As noted by Olagnon et al., new strategies for acquiring and evaluating polyisoprenyl-phosphate intermediates will address the lack of available substrates required for the rational design of inhibitors, as well as limitations associated with clarifying the function of enzymes involved in lipid A modifications with cationic glycoses.[202]

Accordingly, this research directly addresses the deficit of polyisoprenoid substrates by demonstrating the utility of two efficient methods used to obtain both native and tagged BP-glycoses. Specifically, we demonstrate the unique advantage of 2CN-BP used to selectively probe the activity of endogenous BP utilizing proteins within membrane fractions of both K- and B-strains of *E. coli*. This method may also prove effective for the evaluation of other Gram-negative pathogens, particularly, without the need for gene overexpression and protein purification. Previously, such findings have enabled the characterization of early stages of bacterial glycan biosynthesis such as the enterobacterial common antigen in *E. coli*.[203]

Similarly, our methods revealed an unestablished activity of ArnT, for which prior characterization of the forward reaction has required the isolation of small quantities of native BP-

Ara4N or the use of shorter, synthetically prepared Ara4N-linked isoprenoids.[186, 202] Reverse catalysis of PGT enzymes, where UDP-sugar is formed from BPP-sugar in the presence of UMP, has been demonstrated *in vitro* with various initiating PGT and glycosyltransferase enzymes.[204, 205] Research has also been directed at harnessing these reactions to obtain complex NDP-linked sugars, akin to our generation of fluorescent BP-linked Ara4N here.[206] We show that the reverse transfer of ArnT may be harnessed to provide ample fluorescent BP-Ara4N donor substrate for further analysis of ArnT activity *in vitro*.

It is interesting to consider whether reverse transfer of Ara4N from LPS to BP may occur in the cell. LPS transport from the inner membrane to the outer membrane requires an ATP-binding cassette (ABC) transporter and a protein bridge to shuttle the large glycolipid through the periplasmic space to the outer leaflet of the outer membrane.[100, 207, 208] Recently, Owens et al. demonstrated that ATP hydrolysis promotes LPS movement onto the protein bridge and prevents the backward transport of LPS, providing substantial evidence of unidirectional LPS transport.[209] With the exception of reaction equilibriums at the periplasmic inner membrane, the ArnT catalyzed reverse transfer of Ara4N to BP would require LPS to be translocated back to the periplasmic face of the inner membrane where ArnT is situated.[185] We conclude that reverse transfer of Ara4N to BP after LPS has been modified and translocated to the outer membrane is unlikely. Additionally, in the cell, the rapid translocation of modified LPS to the outer membrane likely pushes the reaction forward. It is more likely that reverse transfer is an artifact of cell membrane fractionation. Nonetheless, this report reveals considerations that must be made during *in vitro* analyses of glycosyltransferases and substrate utilization, where this unfavored reaction may consume, as evidenced by our analyses, a large portion of exogenously added isoprenoid.

In addition to analyses with fluorescent BP, our methods enabled the rapid detection of native BP and BP intermediates in lipids collected from constitutive and Fe^{3+} induced polymyxin resistant *E. coli*. Considering the unlikely reversibility of the BP-Ara4N intermediate, we noted a consistent increase in the abundance of BP in C41(DE3) cells lacking *arnC*, which is likely the result of BP being relinquished from the lipid A modification pathway.[135, 210] We also note that the sequestration of BP through other pathways is associated with deformed cell shape, cell membrane permeability, and increased sensitivity to bile salts.[131, 133, 210] Presumably, deleterious effects of an accumulated intermediate in the Arn pathway and the resultant sequestration of the vital BP precursor would make ArnT an ideal candidate for the development of inhibitors.[178, 211] ArnT inhibition could result in BP sequestration as BP-Ara4N, and simultaneously eliminate polymyxin resistance and sensitize CAMP resistant bacteria to environmental or host-mediated stressors. Ultimately, the methods presented here will facilitate a more quantitative assessment of accumulated BP intermediates, BP expenditure, and sequestration in various culturing conditions and amongst various genotypes. Future research should be directed at characterizing and quantifying the effects of BP sequestration as an Arn intermediate.

EXPERIMENTAL METHODS

Materials and bacterial strains

The fluorescent 2CN(*6Z*)BP substrate was prepared as previously described (Ex: 340, Em: 390 nm).[85, 212] *E. coli* MG1655 was generously provided by the Young/Jorgenson Laboratory at the University of Arkansas for Medical Sciences. C41(DE3) was purchased from Novagen.

Cell envelope fractionation

To evaluate the activity of *E. coli* membrane proteins with the 2CN(*6Z*)BP, we prepared membrane fractions from wild-type and mutant *E. coli* in both C41(DE3) and MG1655. Starter cultures were prepared from isolated colonies and incubated overnight at 37 °C. Cultures containing 250 mL of LB Miller Broth were inoculated with a 1:1000 dilution of starter culture and incubated at 37 °C at 220 rpm until an OD_{595} of 0.8-1.0. Cells were then pelleted at 5,000 RCF for 15 min. Cell pellets were resuspended in 0.8% NaCl, pelleted at 5,000 RCF for 15 min and stored at -80 °C for about one week prior to preparation of membrane fraction. To prepare membrane fractions, cells were resuspended in Buffer A (50 mM Tris pH 8.0, 300 mM NaCl) and lysed with sonication (Fisher Sonic Dismembrator). Lysates were centrifuged at 5,000 RCF for 20 min to remove unlysed cells and cellular debris. The supernatant was then spun at 100,000 RCF for 1 hr. The resulting pellets were resuspended in Buffer B (50 mM Tris, 200 mM NaCl) and stored at -80 °C until use. Total protein content of membrane fractions was determined with a Bradford Assay at 595 nm using bovine serum albumin (BSA) as a standard.

RP-HPLC

All RP-HPLC (Condition A) was performed with an Agilent 1100 HPLC system equipped with a variable wavelength and fluorescence detector (FLD) using an Agilent Zorbax XBD-C18 column (4.6 mm x 50 mm, 3 μm, 80 Å). The mobile phase was comprised of *n*-propanol (Solvent A) and

100 mM ammonium bicarbonate (Solvent B). Analysis occurred with an isocratic mobile phase consisting of 50% Solvent A/50% Solvent B at a flow rate of 1 mL/min. Injection quantities of starting material (2CN(*6Z*)BP) were kept consistent at 100 pmol unless noted otherwise.

ESI-LC-MS

All ESI-LC-MS analysis (Condition B) was performed with an Agilent 1260 Infinity II system equipped with a single quadrupole and fluorescence detector using a Waters XBridge Peptide BEH C18 column (4.6 mm x 50 mm, 3.5 μm, 300 Å). The mobile phase was comprised of *n*-propanol (Solvent C) and 10 mM ammonium hydroxide (Solvent D) with a flow rate of 1 mL/min. For all analyses, the column temperature was set to 30°C. MS parameters for each analysis included a nebulizer pressure of 50 psi, drying gas flow of 12.0 L/min, drying gas temperature of 350°C, and a capillary voltage of 4000 V. All analyses were performed in negative ion mode.

For analysis of native BP, BP-Ara4N, and BP-Ara4FN with ESI-LC-MS, each of four channels analyzed three SIM ions and one scan from 400 – 1500 m/z. Scan parameters included: fragmentation voltage 350 V, gain 1.0, threshold 150, step size 0.1, and a scan speed of 2600 u/sec. SIM parameters included: fragmentation voltage 350 V, gain 1.0, dwell time 215 msec. The predicted m/z value for the [M-H]- ion of each analyte used for SIM are as follows: bactoprenyl phosphate (BP) 845.66, bactoprenyl phosphate-4-aminoarabinose (BP-Ara4N) 976.72, bactoprenyl phosphate-4-formamido-arabinose (BP-Ara4FN) 1004.71. For each analysis, 5 – 10 μL of total lipids were analyzed with a linear gradient starting with 15% Solvent C and 85% Solvent D, raising to 75% Solvent C over 15 min, then raising to 95% Solvent C over 1 min and holding for 1 min, and finally decreasing to 15% Solvent C over 3 min with a post run of 2 min. Each analysis included a 3 s needle wash.

For analysis of fluorescent 2CN-BP and enzyme products with LC-MS, a TEE connector was used to split the solvent through both the MSD and FLD. Each of four channels analyzed three SIM ions and one scan from 500-2000 m/z. MS parameters were the same as described above except the fragmentation voltage was set to 50V. The predicted m/z value for the $[M-H]^-$ ion of each analyte used for SIM are as follows: 2CN(*6Z*)BP 757.51, 2CN(*6Z*)BP-PentN 888.57, 2CN(*6Z*)BP-Hex 919.56. For each analysis, 100 - 200 pmol of starting material (2CN(*6Z*)BP) was analyzed with a linear gradient method starting with 25% Solvent C/75% Solvent D, raising to 65% Solvent C over 10 min then decreasing back to 25% Solvent C over 2 min with a 2 min post run.

ESI-MS-MS

To obtain purified C41(DE3) membrane fraction product, a reaction containing 10 nmol 2CN(*6Z*)BP and 0.5 mg/mL C41(DE3) membrane fraction were incubated in buffered reaction conditions (100 mM Bicine pH 8.0, 200 mM KCl, 15 mM cholate, and 5 mM $MgCl_2$) overnight at 37 °C. The unidentified product was then purified from the reaction mixture with RP-HPLC (condition A) using an Agilent Zorbax XBD-C18 column (9.4 mm x 250 mm, 5µm, 80 Å), dried under vacuum, and resuspended in *n*-propanol and 25 mM ammonium bicarbonate (1:1). The isolated product was then analyzed by MS using a VELOS Pro Dual-Pressure Linear Ion Trap with direct infusion (100 µL/min) in negative ion mode. MS was performed with a capillary voltage of 4 kV, capillary temperature of 200°C, and in a range of 240 – 2,000 m/z. MS/MS was performed by CID of the parent ion with an m/z of 888.60.

Cell envelope fraction assays with 2CN-BP

To assess transferase activity of *E. coli* C41(DE3) and MG1655 membrane fraction with 2CN(*6Z*)BP, membrane fraction (0.5 mg/mL total protein) were incubated with 2CN(*6Z)*BP in

reaction buffer at 37°C for 2 hr. Reactions contained 5 μM 2CN(*6Z)*BP unless otherwise indicated. Turnover of 2CN-BP was monitored by RP-HPLC and fluorescence detection. Inactivated wild-type C41(DE3) membrane fraction was prepared by heating wild-type membrane fraction to 95°C for 20 min. In experiments with inactivated membrane fraction, equivalent amounts (0.5 mg/mL total protein) of inactive and active membrane fraction were used.

Preparation of total lipids

To identify accumulated BP and BP-linked intermediates in wild-type and mutant *E. coli* MG1655 or C41(DE3), samples of total lipids were separated and analyzed by ESI-LC-MS. To prepare samples of total lipids, cultures consisting of 100 mL of Miller LB were prepared from a 1:1,000 dilution of an overnight starter culture and grown to an OD_{595} of 1.0. In experiments with MG1655 and MG1655 Δ*arnD*, cells were cultured with or without 100 μM $FeSO_4$. Cells were then pelleted at 15,000 RCF for 15 min, resuspended in 1.6 mL of deionized water and transferred to glass centrifuge tubes. To aid in cell lysis and solubilization of prenyl and phospholipids each cell suspension was mixed with 2 mL of chloroform and 4 mL of methanol to form a single-phase Bligh and Dyer solution (chloroform, methanol, water; 1:2:0.8 v/v)).[196] Cell suspensions were then vortexed and incubated at room temperature for 20 min. Cell lysates were clarified of LPS and other contaminants by centrifugation at 2,500 x RCF for 20 min. The supernatant of each lysate was transferred to a glass culture tube and then dried under vacuum overnight. Dried samples were resuspended using 1 mL of BP uptake solution (hexanes, acetone, DMSO; 10:10:0.5) and vortexed. Soluble material was partitioned into a new glass culture tube and dried under vacuum. Dried samples were then resuspended in 200 μL of a solution of *n*-

propanol and 10 mM ammonium hydroxide (1:1). Total lipids (5 – 10 µL) were then analyzed by ESI-LC-MS in negative ion mode.

Preparation of purified LPS from wild-type C41(DE3) cells

Crude LPS from polymyxin resistant *E. coli* C41(DE3) cells was obtained using a modified lipid A isolation procedure developed by Hankins et al.[213] A 50 mL culture of C41(DE3) cells was grown in Miller LB broth at 37°C on a rotary shaker at 220 rpm until reaching an OD_{595} of 1.0. Cells were pelleted for 15 min at 5,000 RCF and washed with 25 mL of 10 mM phosphate buffered saline (PBS) pH 7.4. The cells were then resuspended in 3.2 mL PBS and divided equally between two 15 mL glass centrifuge tubes (1.6 mL of cell resuspension in each tube). To each glass centrifuge tube, 2 mL of chloroform and 4 mL of methanol was added to create a single-phase Bligh and Dyer solution.[196] Tubes were vortexed and incubated for 20 min at room temperature. LPS along with insoluble proteins and nucleic acids were precipitated from the single-phase solution by centrifugation at 2,000 RCF for 20 min. The supernatant was discarded and the crude LPS pellet was washed with a second single-phase Bligh and Dyer solution (see above). The supernatant was discarded and the crude LPS pellet was dried under vacuum to remove any remaining solvent. The LPS pellet was then resuspended in 15 mL of 10 mM Tris-HCl pH 7.5 and 15 mM NaCl with vigorous vortexing and sonication. The LPS pellet was then treated with 100 µg/mL of RNase A and incubated at 65°C for 30 min. Once the solution cooled to room temperature, 1.5 mM $MgCl_2$, 0.5 mM $CaCl_2$, and 50 U of DNase I was added and the solution was incubated at 37°C for 30 min. After 30 min, 100 µg/mL of proteinase K was added and the solution was incubated at 37°C for 60 min. Digested proteins and nucleic acids were removed from the LPS samples by converting the solution to a single-phase Bligh and Dyer solution and centrifugation at 5,000 RCF for 10 min. The supernatant containing the digested

proteins and nucleic acids was discarded and the insoluble LPS precipitate was dried under vacuum. Finally, the dried LPS was resuspended in 1X PBS to a concentration of approximately 10 mg/mL. Protein and nucleic acid contamination was evaluated by SDS-PAGE and staining with either Coomassie Blue, ethidium bromide, or silver stain.[214]

Testing purified LPS as a donor substrate for ArnT

Reactions to test LPS as a Ara4N donor substrate contained 200 mM Bicine pH 8.0, 100 mM KCl, 5 mM $MgCl_2$, 15 mM sodium cholate, 5.0 µM 2CN(*6Z*)BP, 0.5 mg/mL (total protein) of membrane fraction, and approximately 20 µg of LPS unless otherwise specified. Reactions were incubated for 2 hr at 37 °C and monitored by fluorescence using RP-HPLC as previously described for the presence of 2CN(*6Z*)BP-Ara4N. In a second experiment, incremental amounts of purified LPS (20-80 µg) were added to reactions consisting of the same buffering conditions and incubated for 2 hr prior to RP-HPLC analysis. To evaluate the activity of purified ArnT, 0.005 mg/mL of protein was incubated with 5 µM 2CN(*6Z*)BP in reaction buffer (described above) both with and without approximately 20 µg of LPS. The reactions were monitored by fluorescence using RP-HPLC (condition A) as previously described.

Transferase assays with native BP

To assess transferase activity of Δ*arnC* membrane fraction with native BP using wild-type LPS as a donor substrate, Δ*arnC* membrane fraction (0.5 mg/mL) was incubated in buffered reaction conditions (described above) with 500 µg of LPS in a total volume of 500 µL. Reactions were then incubated for 2 hr at 37 °C and extracted twice with 500 µL of *n*-butanol. The upper phase was collected, dried under vacuum, and resuspended in 50 µL of *n*-propanol/10 mM ammonium hydroxide (1:1). The reactions were monitored for the formation of BP-Ara4N using ESI-LC-MS with SIM in negative ion mode.

Bacterial strain construction

Bacterial mutants **(Table S1)** were constructed by using the lambda red recombineering method of Datsenko and Wanner.[215] In brief, parent strains MG1655 or C41 (DE3) were transformed with the plasmid pKD46. Transformants were grown to log phase at 30 °C in LB supplemented with 50 µg/mL carbenicillin, then induced by the addition of 100 mM arabinose. After 1 hr induction, bacteria were made electrocompetent by washing 3-6 times with ice-cold 0.3 M sucrose, then resuspending in 0.3 M sucrose at apx. 1/50th original culture volume. This preparation was either transformed immediately or aliquoted and stored at -80°C. To transform electrocompetent cells, 50 µL cells were combined with purified PCR amplicon (apx 2 µg), generated as described below. This mixture was electroporated at 2500 V, followed by the immediate addition of LB media. After overnight recovery at 30°C, cells were plated on LB agar with the appropriate selective media (chloramphenicol at 10-20 µg/mL for Δ*arnC::cam*^{R}, and Δ*arnT::cam*^{R}; kanamycin at 50 µg/mL for Δ*arnD::kan*^{R}). Resistant colonies were evaluated by colony PCR to confirm the desired insertion. Primers for these reactions are listed in supporting information **(Table S2)**. To remove antibiotic resistance genes, strain CE356 or CE391 was transformed with pCP20, and streaked on LB agar with 50 µg/mL carbenicillin for 2 successive single colony purifications, maintaining plates at 30 °C. pCP20 was cured by restreaking each strain on plain LB agar and incubating plates at 37°C until sampled isolates exhibited sensitivity to carbenicillin and chloramphenicol/kanamycin (typically 3 days).

Molecular cloning

Vector, restriction enzyme, and epitope tags used for each plasmid construct are listed in Supporting Information **(Table S3)**. Gene inserts were amplified from *E. coli* MG1655 using Phusion High-Fidelity DNA polymerase (ThermoFisher Scientific). Purified inserts and vector

were ligated using T4 DNA Ligase (Invitrogen) at room temperature for 30 min. Cloning efficiency of *arnT* in pET-28b was very poor and required incubation with T4 DNA Ligase at 16°C for 16 hrs. Ligation reactions were chemically transformed into *E. coli* DH5α cells. Positive clones were confirmed with sequencing (Eurofins). For complementation assays, plasmids were transformed into chemically competent mutants. Cultures were supplemented with 0.1 mM IPTG and 50 μg/mL of Kanamycin from the time of inoculation.

Purification of ArnT

To solubilize the ArnT protein from the membrane fraction, we followed a previously reported procedure for extraction of ArnT from *Salmonella* typhimurium expressed in *E. coli*.[200] All steps of this protein purification occurred at 4 °C unless otherwise noted. A 5 mL culture of Miller LB broth supplemented with 50 μg/mL of Kanamycin was inoculated from a single colony of C41(DE3) cells harboring the pArnT plasmid. Starter cultures were incubated overnight at 37 °C with shaking at 220 rpm. Terrific Broth (24 g yeast extract, 20 g tryptone, 0.4% glycerol, and 10 mM PBS in a total volume of 1 L) containing 50 μg/mL of Kanamycin were inoculated with a 1:1,000 dilution of the starter culture and incubated at 37 °C with shaking at 220 rpm. Protein expression was induced at an OD_{595} of 1.0 with 1 mM IPTG. Cultures were then incubated overnight at 16°C with shaking at 220 rpm. Cells were pelleted at 5,000 RCF for 15 min and resuspended in Buffer A containing 0.1% *n*-dodecyl-maltoside (DDM). Resuspended cells were lysed with sonication (Fisher Sonic Dismembrator). Lysates were clarified with centrifugation at 5,000 RCF for 30 min. The supernatant was then spun at 100,000 RCF for 60 min. Insoluble fractions were resuspended and homogenized in Buffer A with 1.0% DDM and placed on a spinner overnight at 4 °C. Homogenate was clarified with ultracentrifugation at 100,000 RCF for

60 min. The resulting supernatant was purified using 1 mL of Ni-NTA (Thermo Scientific). The fractions were then analyzed by SDS-PAGE and Anti-His (GenScript) Western Blotting.

Purification of ArnD

To overproduce and isolate ArnD, a 5 mL culture of Miller LB supplemented with 50 µg/mL of kanamycin was inoculated with a single colony of C41(DE3) cells harboring pArnD and grown overnight. Terrific broth (1L) supplemented with 50µg/mL of kanamycin was inoculated with a 1:1000 dilution of the overnight culture and incubated at 37 °C with shaking at 220 rpm. Protein expression was induced with 1 mM IPTG at an OD_{595} of 0.6. Cells were then incubated at 30 °C with shaking at 300 rpm overnight. Cells were harvested at 15,000 RCF for 15 min and resuspended in lysis buffer containing 1% Triton X-100.[183] Resuspended cells were lysed by sonication (Fisher Sonic Dismembrator). Lysates were clarified with centrifugation at 5000 RCF for 20 min. The supernatant was then spun for 1 hr at 150,000 RCF. ArnD was isolated from the supernatant with Ni-NTA affinity chromatography and assessed for protein content with SDS-PAGE and Anti-His Western Blotting. Fractions containing ArnD were dialyzed in buffer B and stored at -80°C until use.

ArnD activity analyses with native BP-Ara4FN

To enable the characterization of *E. coli* ArnD, we used crude lipids prepared from MG1655 Δ*arnD* cultured with 100 µM FeSO4 as a source of native BP-Ara4FN substrate. To prepare lipids from MG1655 Δ*arnD*, single colonies cultured on LB/agar supplemented with 50 µg/mL of Kanamycin were used to prepare 5 mL overnight cultures. Total lipids were prepared from 100 mL of cells at an OD_{595} of 1.0 as described above. To evaluate the activity of ArnD, 0.20 mg/mL of protein was added to reactions consisting of 50 mM Hepes pH 7.0, 100 mM NaCl, 5 mM $MnCl_2$, 20 mM DTT, and 2 µL of MG1655 Δ*arnD* lipids in a total volume of 40 µL.

Reactions were incubated at 30 °C for 2 hr and evaluated for the formation of BP-Ara4N using ESI-LC-MS with 20 µL injections as previously described.

Acknowledgements

We thank Matthew Jorgenson (University of Arkansas for Medical Sciences) for providing *E. coli* MG1655 and for discussions about the project.

APPENDIX A: CHAPTER 2 SUPPORTING INFORMATION

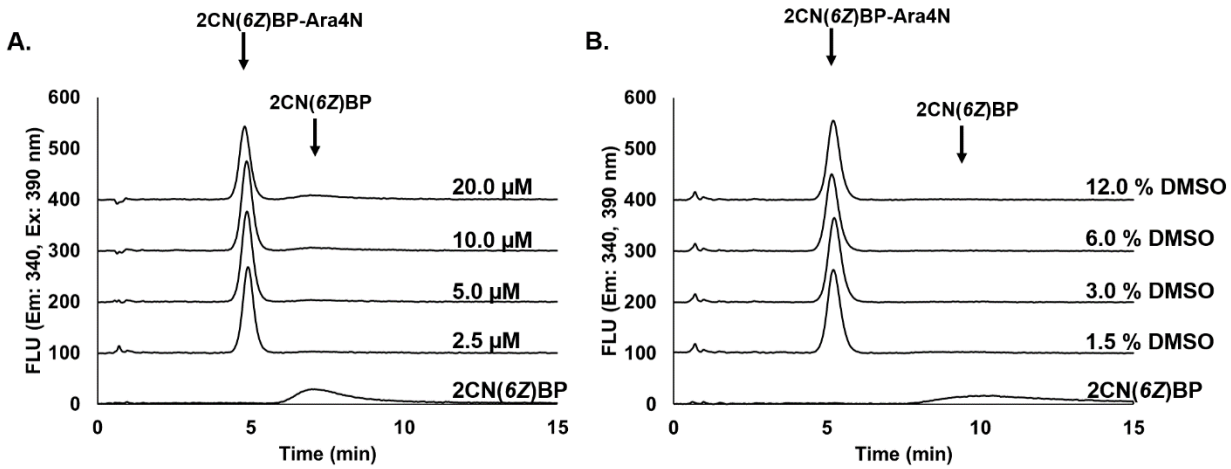

Supporting Figure 2.1: Wild type C41(DE3) membrane fraction turnover of 2CN(6*Z*)BP. Wild type C41(DE3) membrane fraction was incubated with (A) increasing concentrations 2CN(6*Z*)BP (up to 20 µM) and (B) with 5 µM 2CN(6*Z*)BP and increasing concentrations of DMSO (up 12% of the total reaction volume). 2CN(6*Z*)BP alone was used as a control. Reactions were analyzed by RP-HPLC with fluorescence detection. Injections consisted of 50 pmol of starting material (2CN(6*Z*)BP). Chromatograms were offset by 100 FLU increments.

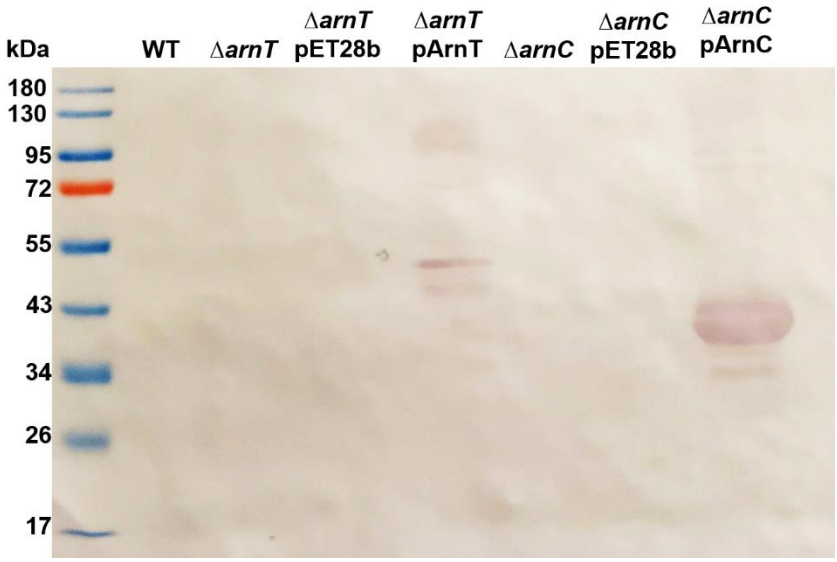

Supporting Figure 2.2: Anti-His Western Blot of C41(DE3) and complemented C41(DE3) mutants.

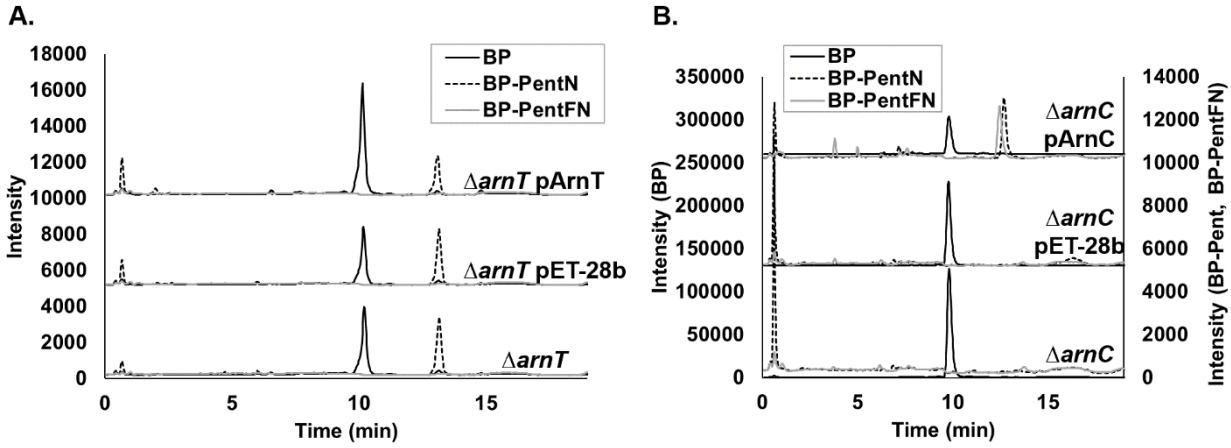

Supporting Figure 2.3: ESI-LC-MS SIM of BP, BP-Ara4N, BP-Ara4FN in complemented C41(DE3) mutants. Analysis of lipids prepared from (A) complemented *arnT* or (B) *arnC* mutants and empty plasmid controls.

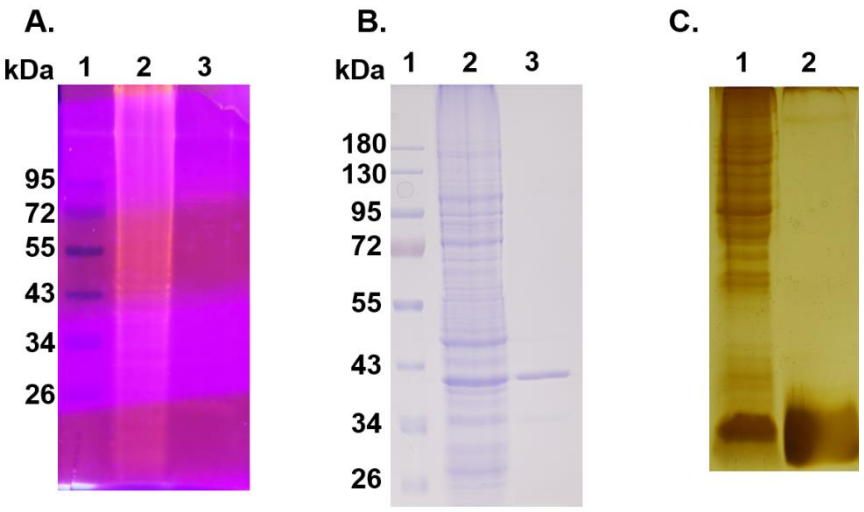

Supporting Figure 2.5: SDS-PAGE analysis of crude and purified LPS. 10% SDS-PAGE of (A) MW markers (lane 1) crude (lane 2) and purified LPS (lane 3) stained with EtBr, (B) MW markers (lane 1) crude (lane 2) and purified LPS (lane 3) stained with Coomassie blue. (C) 14% SDS-PAGE of crude (lane 1) and purified LPS (lane 2) silver stain.

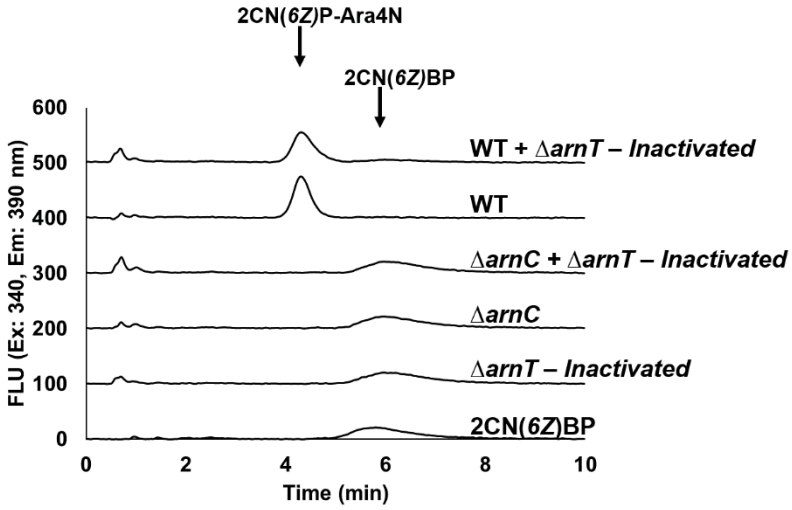

Supporting Figure 2.4: BP-Ara4N supplied as Ara4N donor substrate does not promote 2CN-BP-Ara4N production by C41(DE3) membrane fraction. RP-HPLC analysis (Condition A) of reactions containing 2CN-BP and wild-type or mutant C41(DE3) membrane fraction supplemented either with or without equivalent amounts of heat inactivated Δ*arnT* membrane fraction.

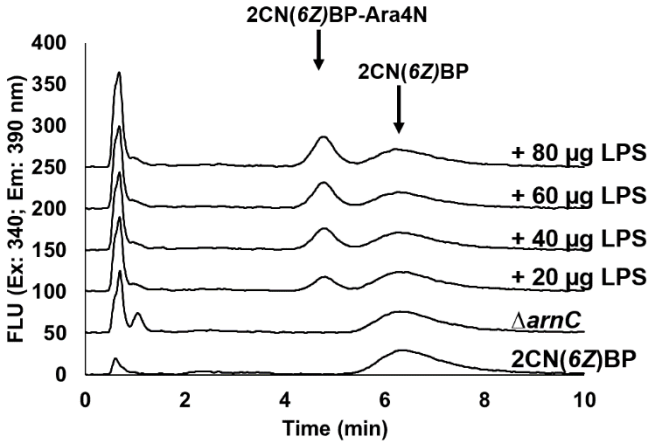

Supporting Figure 2.7: Incremental additions of LPS increases the amount of 2CN-BP-Ara4N formed in reactions with 2CN(6*Z*)BP and Δ*arnC* membrane fraction. RP-HPLC analysis (Condition A) of reactions containing 2CN(6*Z*)BP and Δ*arnC* C41(DE3) membrane fraction with increasing amounts of LPS. Quantification based on peak integrals is provided in **Figure 2.5** of the results.

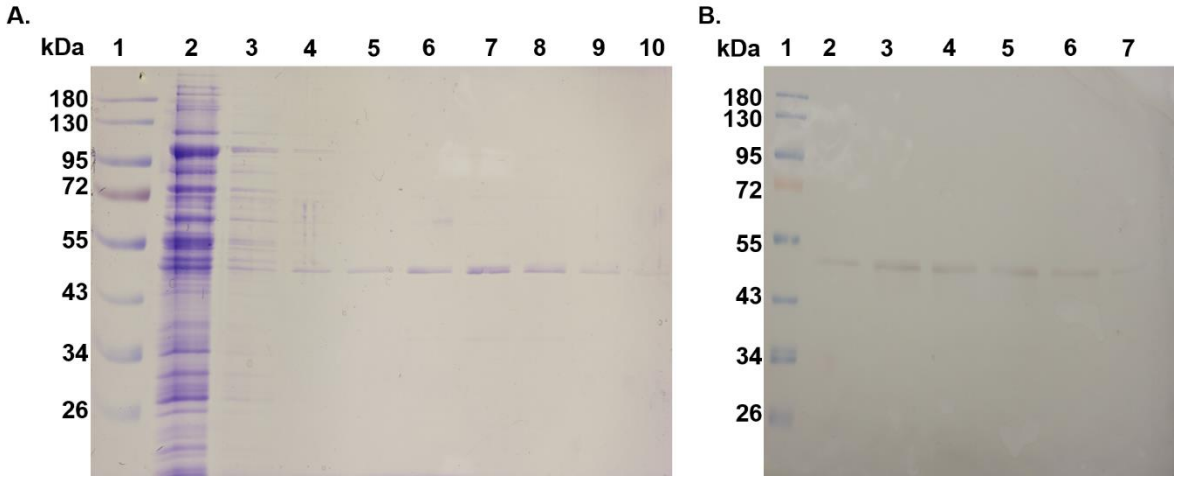

Supporting Figure 2.6: Purification of *E. coli* ArnT. (A) SDS-PAGE of Ni-NTA purified N-terminal 6xHis-tagged ArnT. MW markers (lane 1), flow through (lane 2), first wash (lane 3), second wash (lane 4), elution 1-6 (lane 5-10). (B) Anti-His Western Blot of purified 6xHis-tagged ArnT. MW markers (lane 1), elutions 1-6 (lane 2-7).

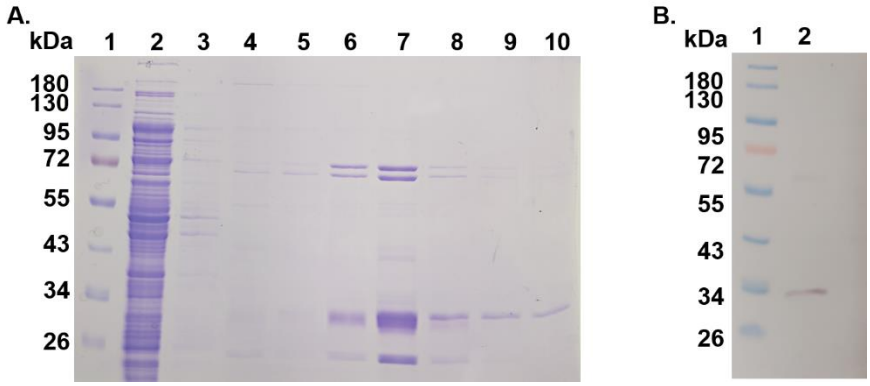

Supporting Figure 2.8: Purification of *E. coli* ArnD. (A) SDS-PAGE and Coomassie stain of Ni-NTA purified C-terminal 6xHis-tagged ArnD. MW markers (lane 1), flow through (lane 2), first wash (lane 3), second wash (lane 4) elution 1-6 (lane 5-10). (B) Anti-His western blot of purified ArnD. MW markers (lane 1), ArnD (lane 2).

Supporting Table 2.1: Bacterial mutants used in this study.

Designation	Strain Background	Genotype	Description of Strain
CE356	*E. coli* C41 (DE3)	*ΔarnC::cam*^{R}	Insertion of *frt*-flanked *cam*^{R} from pKD3 in place of *arnC*
CE368	*E. coli* C41 (DE3)	*ΔarnC::frt*	Generated by pCP20 transformation of CE391
CE391	*E. coli* C41 (DE3)	*ΔarnT::cam*^{R}	Insertion of *frt*-flanked *cam*^{R} from pKD3 in place of *arnD*
JT218	*E. coli* C41 (DE3)	*ΔarnT::frt*	Generated by pCP20 transformation of CE391
CE457	*E. coli* MG1655	*ΔarnD::kan*^{R}	Insertion of *frt*-flanked *kan*^{R} from pKD4 in place of *arnT*

Supporting Table 2.2: Primers used for mutant construction and confirmation.

Designation	Gene	Accession Code	Vector	Restriction Enzymes	Epitope Tag	Primers
pArnT	*arnT*	P76473	pET-28b	NdeI XhoI	N-term 6xHis	CTCTCCATATGATGAAAT CGGTACGTTACC
						GAGAGCTCGAGTCATTT GGGACGATACTGAATC
pArnC	*arnC*	P77757	pET-28b	NheI XhoI	N-term 6xHis	CTCTCGCTAGCATGTTTG AAATCCACCCTG
						GAGAGCTCGAGTTATTCA TTTTCCTTGCTGG
pArnD	*arnD*	P76472	pET-28b	NcoI XhoI	C-term 6xHis	CTCTCCCATGGATGACCA AAGTAGGCTTACGC
						GAGAGCTCGAGGCGACT ACCCGCAATTTGTTGG

Supporting Table 2.3: Primers and restriction enzymes used to prepare plasmid constructs.

To Make Strain:	Primers to Generate Linear Amplicon Used for Transformation	Template	Primers to Confirm Insertion
CE356	TGTCATCACAGCCCTTCAGCAACTCGCAGGACAATAAGCCCCATGGTCCATATGAATATCCTCCTTAGTTC	pKD3	TTCTTGCCCGCCTGATGAAT
	GGCATCCCATATCGTGGTAGGCAAAAACGACGGTTTTCATGATTGTGTAGGCTGGAGCTGCTTCG		AGACGAGCCACCGAACCATA
CE391	CCGGACGTGAAGGCTGGCTGGGTTGCCAACAAATTGCGGGTAGTCGCTGAGATTGTGTAGGCTGGAGCTGCTTCG	pKD3	TTCTTGCCCGCCTGATGAAT
	TGCCCGGCAACGCTAAGCAAGCTGGCAAAGACTAATGTTAGCCAGATCATCCATGGTCCATATGAATATCCTCCTTAGTTC		GGGATGAAGTGATTGGTCG
CE457	CTTCCTGCGCACCGTTGATCTTACGGATAAACCATCATGAGATTGTGTAGGCTGGAGCTGCTTCG	pKD4	TGGCTGCTATTGGGCGAA
	TAAACGCGAAGAGGCCGATAAGGTAACGTACCGATTTCATCCATGGTCCATATGAATATCCTCCTTAGTTC		GCGTTTCATCGGGTTGCC

CHAPTER 3: RECOMBINANT PRODUCTION OF BACTEROIDES FRAGILIS CAPSULAR POLYSACCHARIDE A IN *ESCHERICHIA COLI*

INTRODUCTION

Polysaccharides have drawn considerable attention as potent and renewable sources of biological polymers. These polymers are ubiquitous among prokaryotes, and many possess unique chemical structures that bestow distinct physical and chemical attributes. Diverse physicochemical properties present advantages of applying these polymers in various settings such as wound healing, pharmaceuticals, cosmetics, and food industries.[216]

A major hindrance to the application of many bacterial polysaccharides is the inability to isolate or synthesize them in large quantities. This is due to complex growth requirements of bacterial hosts, complicated and laborious isolation procedures, and the difficulty of genetic manipulation of hosts to improve the yield of isolation. Thus, recombinant polysaccharide production in model strains of *E. coli* has been underway, including multiple *Streptococcus pneumoniae* capsule serotypes, and the N-linked glycan from *Campylobacter jejuni*.[16, 32, 167, 171] In both instances, these recombinant polysaccharides were used for the development of glycoconjugate vaccines.

The goal of this study was to devise a recombinant system for the overproduction of capsular polysaccharide A (CPSA) from *Bacteroides fragilis* NTCT 9343. CPSA belongs to a unique class of zwitterionic polysaccharides that possess a distinct charge motif of alternating positive and negative charges. In contrast to neutral carbohydrates, zwitterionic polysaccharides elicit a potent, T-cell dependent immune response.[51, 217] These distinctive and potent immunomodulatory properties of CPSA and other zwitterionic polysaccharides are modulated by both positively and negatively charged substituents, as well as their helical structure.[51-53, 218] Akin

to an immune response elicited by a proteinaceous antigen, CPSA is processed by antigen-presenting cells and presented to $CD4^+$ T-cells via the major histocompatibility complex II (MHCII).[51, 54, 219] As such, CPSA has been employed in the development of carbohydrate-based vaccines.[220] Paradoxically, CPSA also activates anti-inflammatory innate immune responses by stimulating the production of anti-inflammatory cytokines, such as IL-10.[15, 56] The activation of anti-inflammatory cytokines has advanced CPSA as a potential therapeutic for inflammation-associated diseases such as multiple sclerosis, ulcerative colitis, viral encephalitis, and irritable bowel syndrome.[14, 15, 19, 221]

CPSA is composed of a repeating tetrasaccharide consisting of [→3)-β-d-pyrGalp-(1→3)-α-d-AATGalp-(1→4)[β-d-Galf-(1→3)]-α-d-GalpNAc-(1→], where AAT-Gal is 2-acetamido-4-amino-2,4,6-trideoxygalactopyranose, and pyrGal is 4,6-O-pyruvate-galactopyranose (**Figure 3.1**).[222] It is assembled on a common lipid anchor, bactoprenyl phosphate (BP; also known as undecaprenyl phosphate), at the cytoplasmic face of the inner membrane. Biosynthesis begins with the addition of phospho-AATGal to BP by the initiating phospho-glycosyltransferase WcfS to produce BPP-AATGal (**Figure 3.1**).[147, 222] The remaining sugars, galactose (Gal), N-acetylgalactosamine(GalNAc), and galactofuranose (Galf) are sequentially appended to BPP-AATGal by the glycosyltransferases WcfQ, WcfP, and WcfN, respectively.[30] The pyruvyltransferase, WcfO, pyruvylates galactose after the formation of BPP-AATGal-Gal, and before the addition of GalNAc.[30] WcfM is a UDP-galactopyranose mutase that produces UDP-galactofuranose, the final sugar in CPSA repeat unit biosynthesis.

Current techniques for recombinant polysaccharide overproduction heavily rely on en bloc cloning of biosynthesis loci into expression hosts.[155, 167, 173, 223] Cloning of such large fragments (~ 10 – 20 kbp) is prone to error and does not take into consideration intergenic

regions or the utility and strength of interspecies ribosome binding sites in host strains.[224] In many instances, sugar-nucleotide modifying enzymes are not included in glycan biosynthesis loci, thus requiring a multistep cloning procedure[29].[43] An exception to this is presence of genes required for UDP-diNAcBac biosynthesis located within the *C. jejuni* N-glycan (Pgl) operon.[120, 139, 157] Moreover, recombinantly produced glycans and glycan intermediates are prone to utilization by *E. coli* native glycan processing enzymes.

In this study, we devised a recombinant system for CPSA production in *E. coli* by implementing a stepwise method and strategic incorporation of robust glycan modification enzymes. In doing so, we confirmed the production of each lipid-linked intermediate and finally, CPSA polymers of biologically relevant length. Ultimately, we model an effective approach to evaluate recombinant polysaccharide production, which may be applied to other glycan biosynthesis systems that are not confined within a single operon. These results could aid in the identification of potential targets to increase recombinant polymer quantity and increase the availability of biologically relevant glycans.

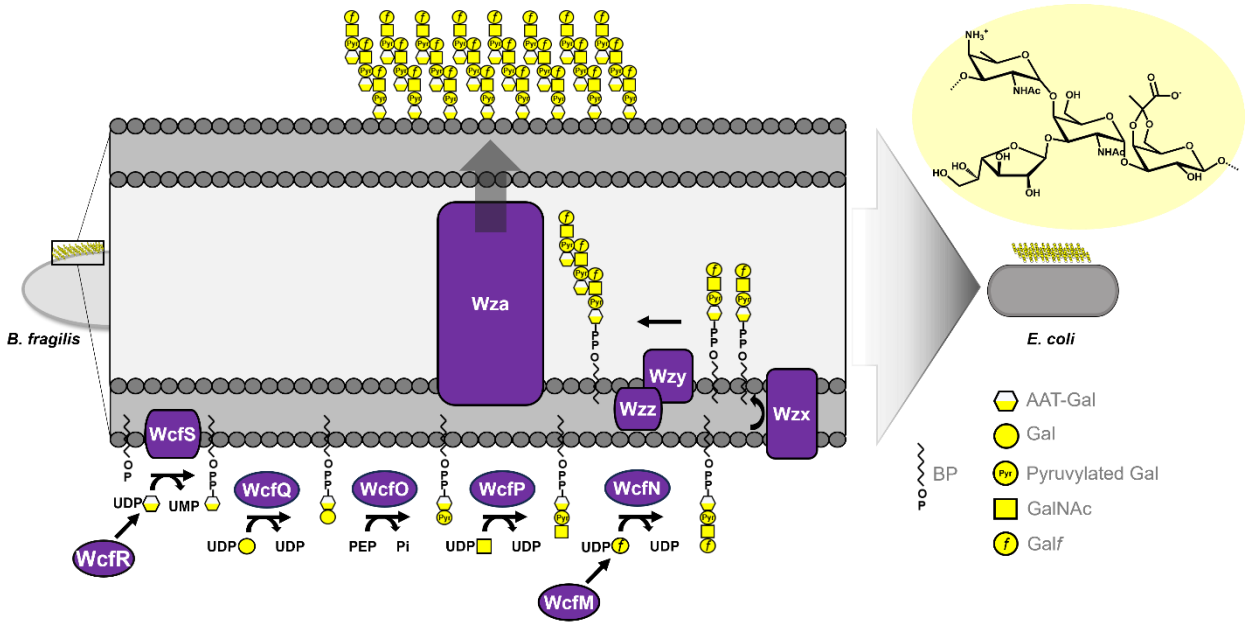

Figure 3.1: Representation of CPSA biosynthesis pathway and structure in *Bacteroides fragilis* and reconstitution of its biosynthesis in *E. coli*. The structure of the CPSA unit oligosaccharide is highlighted in yellow.

RESULTS

Construction of a CPSA expression plasmids

To produce CPSA in *E. coli*, we first sought to assemble the CPSA locus from *B. fragilis* into a plasmid. However, the CPSA locus does not contain all genes required for the assembly of UDP-AATGal and UDP-GalNAc, which are also not native to our *E. coli* K12 host strains. In *B. fragilis*, UDP-AATGal is formed through the activity of a dehydrogenase that produces a 4-keto sugar, and an aminotransferase that covalently appends an amine to the 4-position to produce a 4-aminogalactose configured sugar-nucleotide. UDP-GalNAc could be readily formed through the epimerization of the *E. coli* abundant NDP-sugar UDP-GlcNAc. To ensure all NDP-sugars required for CPSA biosynthesis were available, Gibson assembly was used to incorporate *pglF*, a dehydrogenase from *Campylobacter jejuni*, which catalyzes dehydration of the 6-position of

UDP-GlcNAc and oxidation of the 4-position to give UDP-2-acetamido-2,6-dideoxy-α-d-xylo-hexos-4-ulose, a precursor of UDP-AATGal.[120, 147, 225] UDP-AATGal is formed from the 4-keto sugar by the aminotransferase WcfR, a gene product from the CPSA locus (**Figure 3.2A**).[147] We also incorporated *wbpP* from *Vibrio vulnificus* M0-624, a UDP-GlcNAc C4 epimerase that produces UDP-GalNAc (**Figure 3.2B**).[226, 227] Previous work from our laboratory and others have shown that PglF and WbpP are readily overproduced and functional after purification from *E. coli*.[228, 229]

Implementation of recombinant glycan production in *E. coli* has been demonstrated through the complete transfer of biosynthesis loci into a plasmid for expression.[155, 167, 173] While this can be robust, it does not allow for evaluation of individual steps in the biosynthetic pathway, and bottlenecks in production can be challenging to delineate. To evaluate potential bottlenecks that may hinder CPSA biosynthesis in *E. coli*, we generated an incremental set of plasmids designed to produce each individual BPP-linked CPSA intermediate in a stepwise manner (**Figure 3.1, Table 3.1**). It is important to note that each gene in Gibson assembled plasmids was preceded by a strong *E. coli* ribosomal binding site (RBS) often used for over production of gene products. Assembly of each plasmid was confirmed by PCR (data not shown).

Table 3.1: Description of plasmids used to generate individual CPSA intermediates in *E. coli* and the exact mass of each intermediate.

Plasmid designation	Genes incorporated	Predicted CPSA Intermediate
pQE	-	BP
pBAS8	$pglF_{Cj}$, *wcfRS*	BPP-AATGal
pBAS9	$pglF_{Cj}$, *wcfRSQ*	BPP-AATGal-Gal
pBAS10	$pglF_{Cj}$, *wcfRSQO*	BPP-AATGal-PyrGal
pBAS11	$pglF_{Cj}$, *wcfRSQOP*	BPP-AATGal-PyrGal
pBAS12	$pglF_{Cj}$, *wcfRSQOPMN*	BPP-AATGal-PyrGal
pBAS15	$pglF_{Cj}$, $wbpP_{Vv}$ *wcfRSQOP*	BPP-AATGal-PyrGal-GalNAc
pBAS16	$pglF_{Cj}$, $wbpP_{Vv}$ *wcfRSQOPMN*	BPP-AATGal-PyrGal-GalNAc-Gal*f*

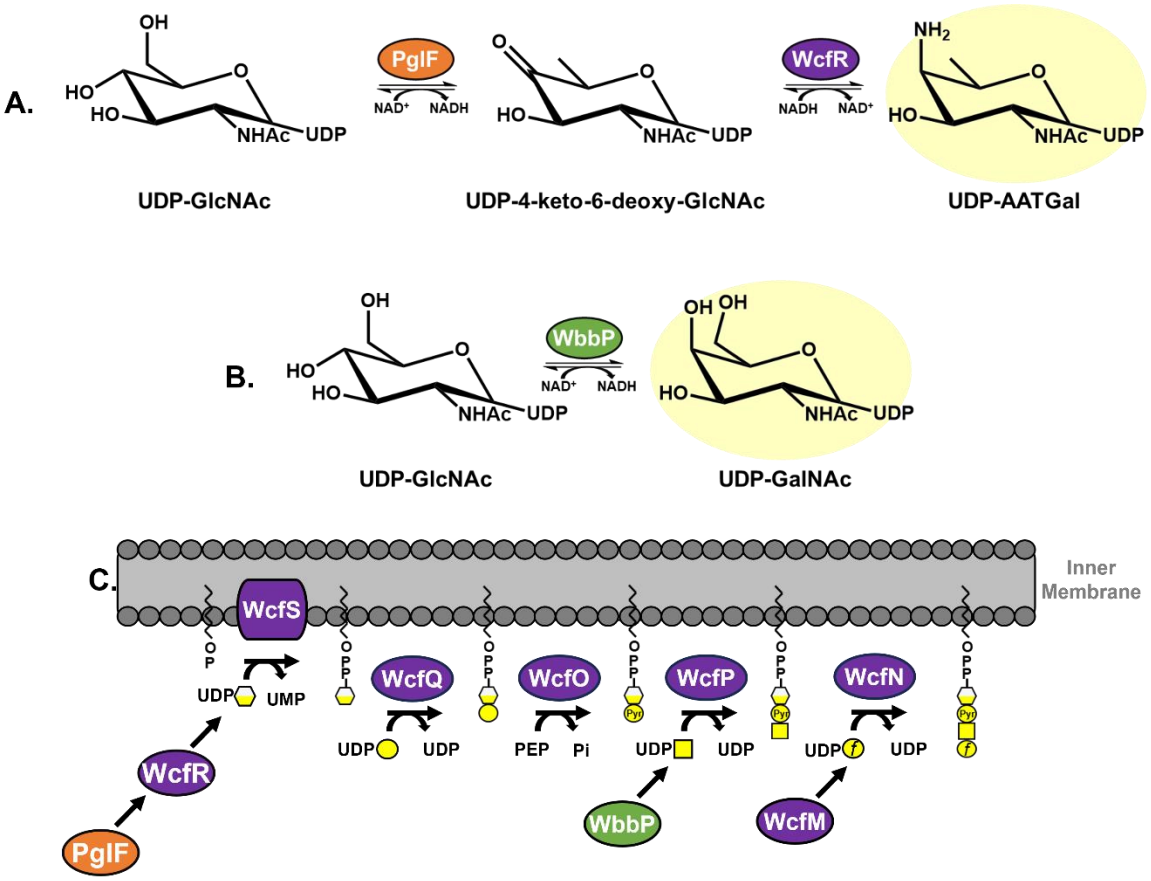

Figure 3.2: Recombinant UDP-AATGal and UDP-GalNAc biosynthesis in *E. coli*. (A) UDP-AATGal is produced from UDP-GlcNAc by PglF from Campylobacter jejuni and WcfR from B. fragilis. (B) UDP-GalNAc is produced from UDP-GlcNAc by WbpP from Vibrio vulnificus. (C) Schematic of CPSA biosynthesis in *E. coli* utilizing PglF and WbpP.

Stepwise analysis of CPSA repeat unit biosynthesis by ESI-LC-MS

To investigate production of lipid-linked CPSA intermediates, we utilized an established ESI-LC-MS based method for tracking glycan intermediates in *E. coli*.[114] Previously, we showed the precise order and function of enzymes involved in CPSA production *in vitro*, which enabled us to predict the *m/z* of BPP-linked CPSA intermediates based on which genes were expressed (**Table 3.1**).[30] To ensure that each intermediate corresponded to the inclusion of the appropriate Wcf glycosyltransferase(s), we used selected ion monitoring (SIM) to analyze each cell lysate for the $[M-H]^-$ and/or $[M-H]^{2-}$ ion of (1) BP, (2) the expected BPP-linked intermediate, and (3) the

subsequent predicted intermediate (**Figure 3.3**). We chose to monitor for later intermediates in the pathway to confirm that CPSA intermediates were not produced without the incorporation of the appropriate genes (i.e., intermediates were not utilized by *E. coli* native proteins). Spectra were collected from the total ion chromatogram (TIC) of each injection (**Supporting Figure 3.1, Supporting Table 3.1**). Intermediates only corresponding to what was predicted were identified in cell lysates. Additionally, we did not observe isobaric compounds with identical or similar retention times of CPSA intermediates in cells harboring an empty vector (**Supporting Figure 3.2**). BPP-linked pyruvylated trisaccharide was not produced until $wbpP_{Vv}$ was co-expressed with *wcfP* and preceding glycosyltransferases (**Supporting Figure 3.3**), confirming that the C4 epimerase was critical for CPSA oligosaccharide production in *E. coli*.[227]

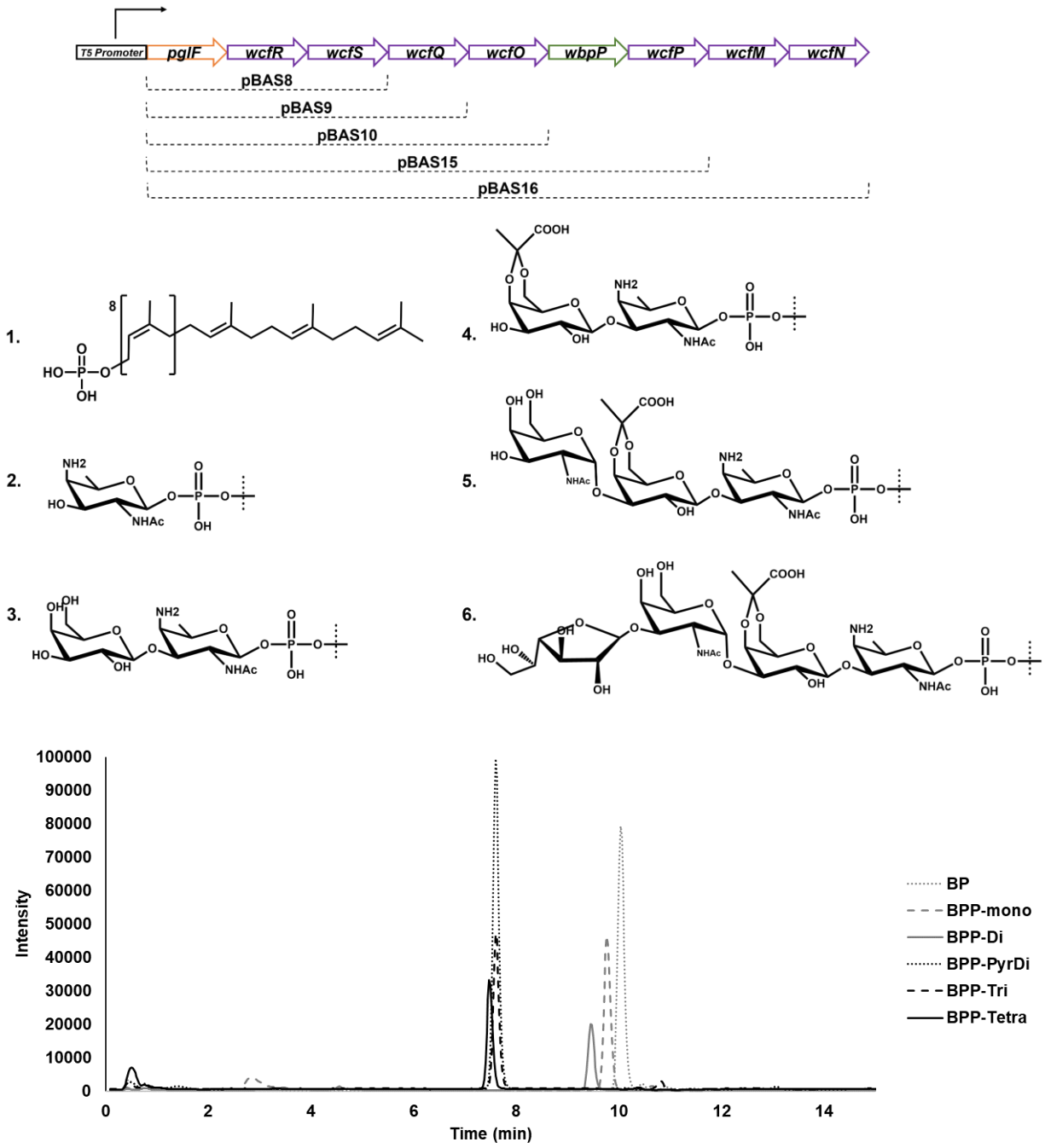

Figure 3.3: LC-MS identification of individual BPP-linked CPSA intermediates recombinantly produced in *E. coli*. Each BPP-linked CPSA intermediate was identified in lysates of *E. coli* DH5α cells recombinantly expressing genes from the CPSA biosynthesis operon using ESI-LC-MS and SIM. Schematic representation of plasmids used to generate intermediates (top). Descriptions of plasmids and the predicted *m/z* used for SIM can be found in **Supporting Table 3.1**. Only chromatograms generated from SIM of the anticipated intermediates were overlayed in this figure (see **Supporting Figure 3.3**).

Co-expression of *wzx* and *wzy* from *B. fragilis* produce CPSA polymers in *E. coli*

Once we confirmed production of the CPSA repeat unit by our recombinant *E. coli* strain, we evaluated whether an *E. coli* flippase or polymerase could catalyze polymer formation or whether the CPSA specific flippase or polymerase from *B. fragilis* was required. To determine if both Wzx and Wzy were necessary for CPSA polymerization, we constructed plasmids containing only *B. fragilis* flippase *wzx* (pBAS18) or polymerase *wzy* (pBAS19), and *B. fragilis wzx and wzy* together (pBAS17), along with all other genes required for oligosaccharide biosynthesis (**Table 3.2**). To determine whether CPSA polymers were formed, we evaluated cell lysates using SDS-PAGE and Western blotting with an anti-CPSA antibody serum (**Figure 3.4**).[230]

Table 3.2: Plasmids used to determine if co-expression of wzx_{Bf} and wzy_{Bf} is needed for recombinant production of CPSA polymers in *E. coli.*

Plasmid designation	Genes included
pQE-80L (Empty Vector)	-
pBAS16	$pglF_{Cj}$, $wbpP_{Vv}$ *wcfRSQOPMN*
pBAS17	$pglF_{Cj}$, $wbpP_{Vv}$ *wcfRSQOPMN,wzx,wzy*
pBAS18	$pglF_{Cj}$, $wbpP_{Vv}$ *wcfRSQOPMN,wzx*
pBAS19	$pglF_{Cj}$, $wbpP_{Vv}$ *wcfRSQOPMN,wzy*

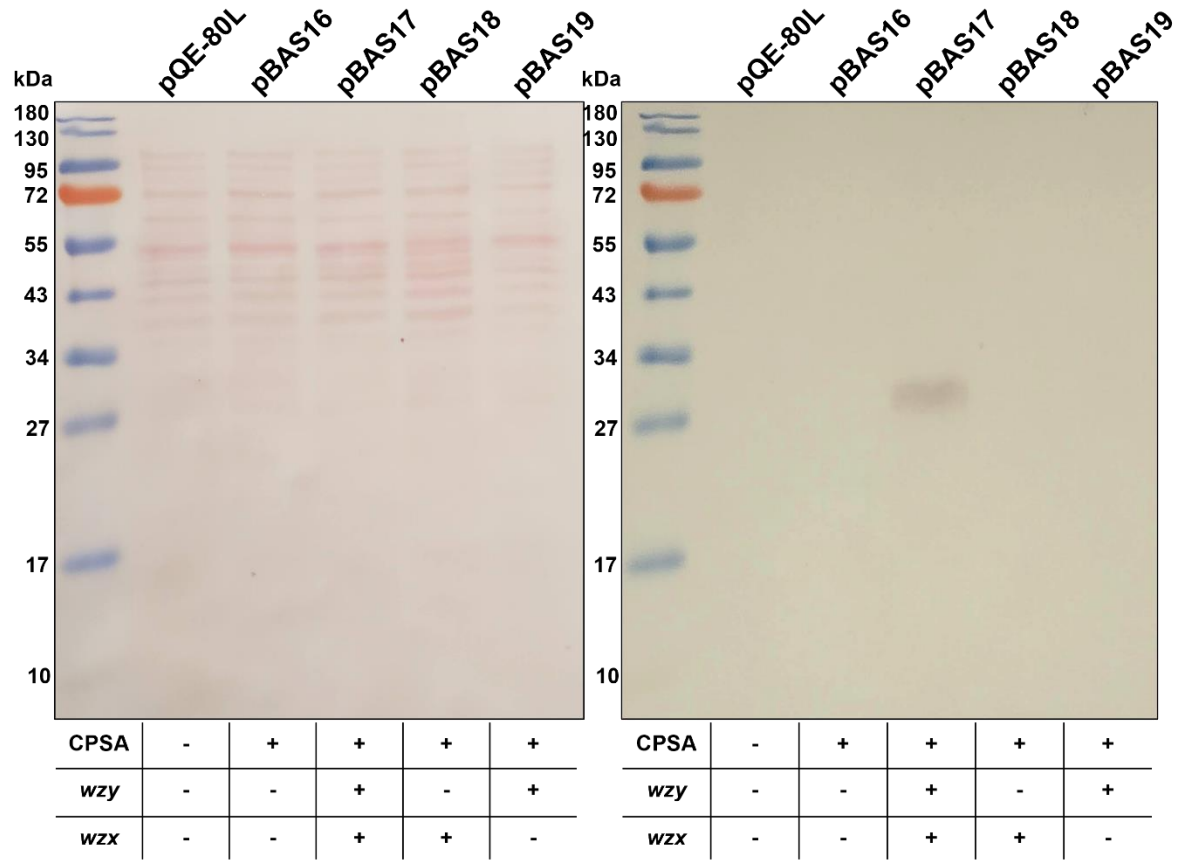

Figure 3.4: Both flippase, Wzy, and polymerase, WzX, from *B. fragilis* may be required for polymerization of CPSA oligomers in *E. coli*. SDS-PAGE and anti-CPSA western blot of *E. coli* DH5α cell lysates expressing an empty vector control (pQE-80L), pBAS16(- wzx_{Bf}, -wzy_{Bf}), pBAS17(+ wzx_{Bf}, +wzy_{Bf}), pBAS18 (+wzx_{Bf}), or pBAS19 (+wzy_{Bf}). (Left) Ponceau stain of normalized cell lysates. (Right) Anti-CPSA western blot of cell lysates. Genes assembled in plasmids are listed in **Table 3.3**. CPSA positive indicates that all genes are present to produce CPSA oligosaccharide.

Polymerized CPSA with a molecular weight around 30 kDa was only observed in cells expressing pBAS17 (+wzx_{Bf}, +wzy_{Bf}), and not in cells expressing pBAS16 (-wzx_{Bf}, -wzy_{Bf}), pBAS18 (+wzx_{Bf}), or pBAS19 (+wzy_{Bf}) (**Figure 3.3**). We conclude that CPSA is polymerized in *E. coli* only when wzx_{Bf} and wzy_{Bf} are co-expressed, or that polymers produced in other strains were below the detection limits of this assay.

CPSA oligo- and polymers are likely ligated to lipid A core

We next sought to determine if CPSA could be detected on the surface of *E. coli* expressing pBAS17 (+ wzx_{Bf}, +wzy_{Bf}) **(Table 3.1)**. For this and remaining experiments, we transitioned to *E. coli* MG1655 as the host due to the availability of a small library of relevant mutants. Expression of CPSA in *E. coli* MG1655 did not qualitatively differ from CPSA expression in DH5α (**Supporting Figure 3.4**). Using confocal microscopy, we confirmed that intact cells expressing pBAS17 reacted with anti-CPSA antiserum and FITC conjugated secondary antibodies, while cells expressing an empty plasmid did not (**Figure 3.5**). Using a whole-cell dot blot, we confirmed that pBAS8-15 did not react with anti-CPSA antiserum, but it was surprising to find that cells expressing pBAS16 did (**Supporting Figure 3.4, Table 3.1**).

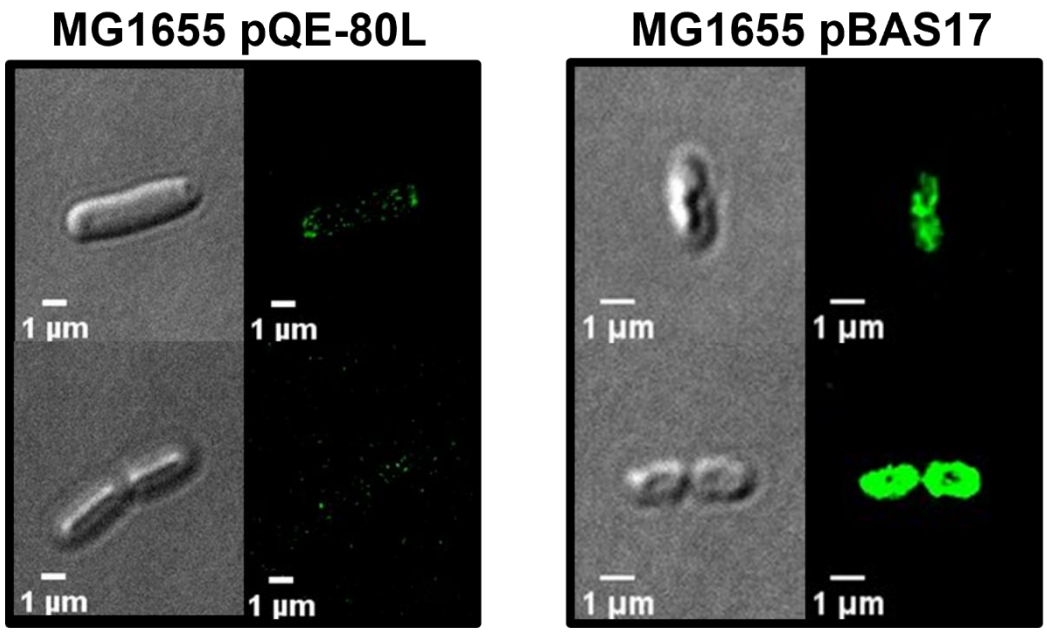

Figure 3.5: Confocal microscopy of *E. coli* expressing CPSA compared to an empty vector control. Credit: Dr. James Grissom, Dr. Shreya Goyal, and Dr. Richard Chi for expertise and assistance with collecting confocal micrographs. Micrographs were chosen from a heterogeneous population.

To better understand CPSA glycoforms present in wild-type MG1655, cell lysates were partitioned into organic, aqueous, and insoluble fractions using the Bligh and Dyer method of lipid extraction.[196, 197] For cells harboring pBAS17, the aqueous fraction was expected to contain water-soluble polysaccharides, potentially including lipid-linked CPSA intermediates.[114] The organic fraction, typically used for phospholipid isolation, might also contain early BPP-linked CPSA intermediates.[114] The insoluble phase, largely consisting of LPS would contain LPS-CPSA conjugates.[197] Each of these fractions were analyzed by SDS-PAGE and western blotting (**Figure 3.6**). Intriguingly, polymerized CPSA was observed in both the aqueous and insoluble cell fractions in wild-type MG1655 pBAS17, with lower molecular weight polymers observed in the aqueous fraction (~30 kDa) than the organic fraction (~ 40 kDa). Combined with the previous results of surface expressed CPSA (**Figure 3.5**, **Supporting Figure 3.4**), this strongly suggested to us that CPSA may be ligated to LPS.

In *E. coli*, it has been shown that oligo- and polysaccharides other than O-antigens (O-Ag) can be ligated to the lipid A core of LPS, including colanic acid, enterobacterial common antigen (ECA), and peptidoglycan repeat units.[231-233] Additionally, recent developments in recombinant bacterial glycan production demonstrate that non-native glycans may be ligated to the lipid A core.[16, 171] These glycan modifications of LPS are primarily attributed to the promiscuity of the *E. coli* O-antigen ligase, WaaL, which appends O-antigen to the heptose residue of the lipid A core.[234, 235]

To evaluate whether WaaL contributes to the production of higher molecular weight CPSA in the insoluble fraction of cell lysates, pBAS17 was overexpressed in an MG1655 Δ*waaL* mutant. Analysis of MG1655 Δ*waaL* pBAS17 cell lysate fractions revealed CPSA only in the

aqueous fraction of cell lysates (**Figure 3.6**) indicating that a Δ*waaL* mutant is needed to procure solely aqueous CPSA polymer.

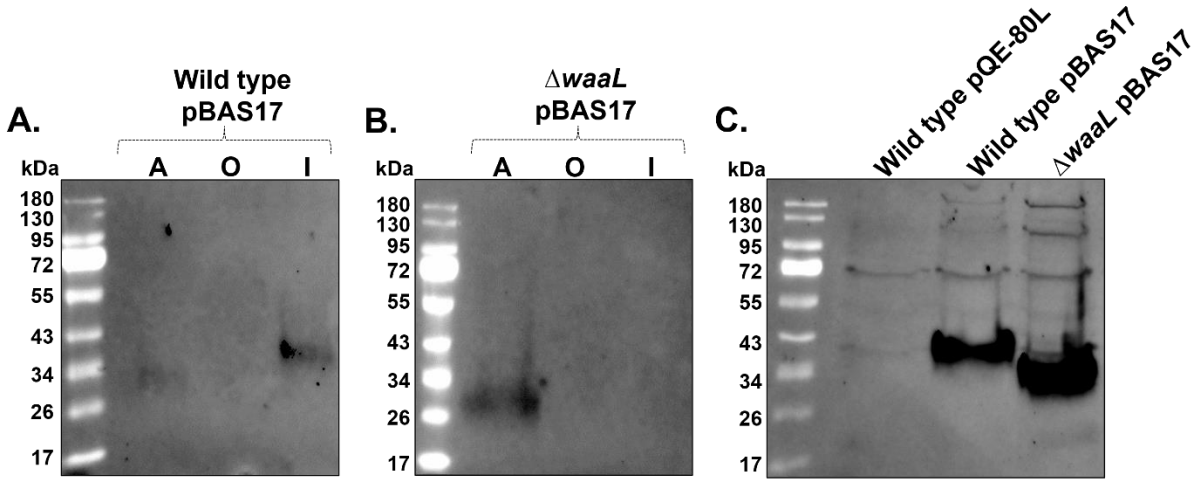

Figure 3.6: CPSA polymers are detected in both aqueous and organic fractions of *E. coli* pBAS17 lysates. Wild-type (A) and a Δ*waaL* mutant (B) of *E. coli* MG1655 pBAS17 were evaluated for the presence of CPSA polymers in aqueous, organic, and insoluble cell fractions. Cell fractions were separated using SDS-PAGE and anti-CPSA antiserum. Lanes designated with an "A" are aqueous fractions, lanes "O" are organic fractions, and lanes "I" are insoluble cell fractions. (C) SDS-PAGE and anti-CPSA western blot of whole cell lysates.

In consideration of these previous findings, we thought it possible that CPSA oligomer or polymer may be ligated to lipid A of *E. coli* cells expressing pBAS16 (-wzx_{Bf}, -wzy_{Bf}) or pBAS17 (+wzx, +wzy_{Bf}), respectively. As demonstrated by a whole-cell dot blot, CPSA surface expression appears to be disrupted in *waaL* mutant expressing pBAS16 (**Figure 3.7**). Based on this finding, we proposed that CPSA may be ligated in oligomeric form to LPS and requires WaaL for ligation to the lipid A core. To confirm this, LPS profiles of pronase treated cell lysates were evaluated using SDS-PAGE and the Pro-Q™ Emerald 300 Lipopolysaccharide Gel Stain Kit stain (Pierce). In MG1655, O-antigen production is disrupted by an IS5 insertion into the *wbbL* region of the O-antigen operon.[236] Therefore, LPS profiles of this strain would contain only lipid A core. Fluorescence imaging of Pro-Q™ Emerald 300 stained gels revealed an additional band

of a higher molecular weight than lipid A core in pronase treated lysates of cells expressing pBAS16, but not in a *waaL* mutant or those expressing a plasmid control (**Figure 3.7**). We were unable to detect these species with anti-CPSA antiserum, which may be due to levels below our detection limit. We also tested whether inactivation of *wzxB,* the O-antigen flippase in *E. coli* disrupted surface expression of CPSA or altered LPS profiles in cells expressing pBAS16. Western blot signals for Δ*wzxB* MG1655 pBAS16 were attenuated compared to wild type cells, but still present, indicating that WzxB may, in part, have a role in CPSA oligomer transport and surface expression (**Figure 3.7**). Deletion of *E. coli* polysaccharide export protein, *wza,* had no effect on surface expression or LPS profiles of cells expressing pBAS16 compared to wild type.

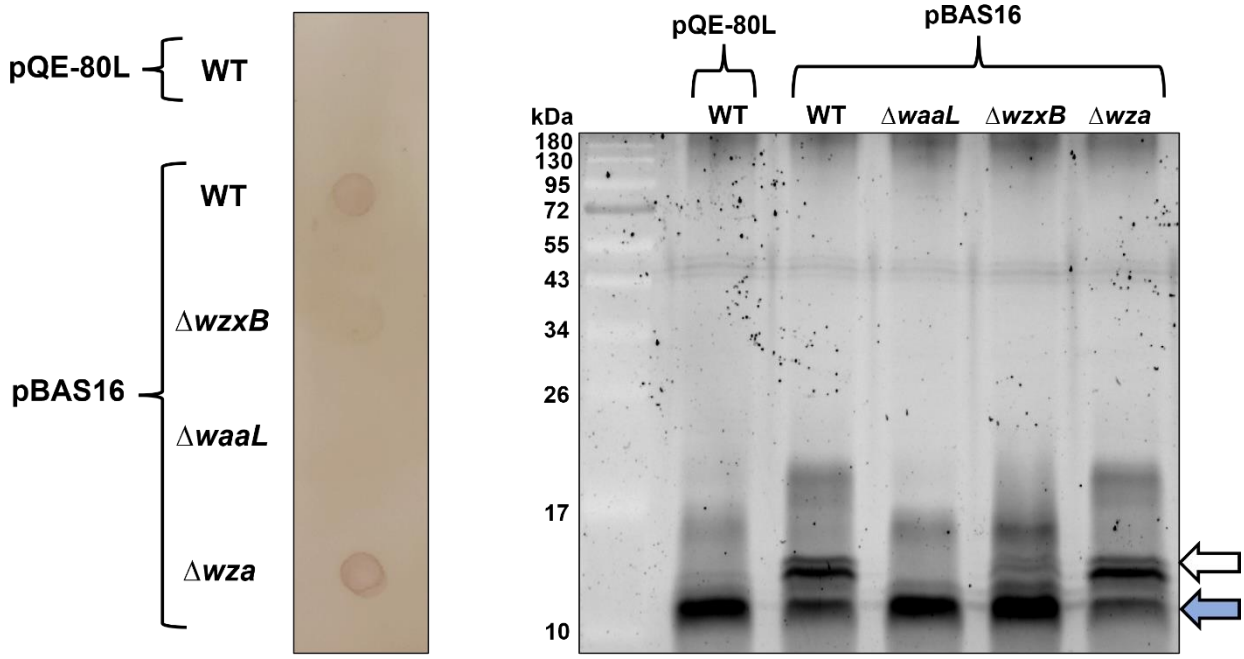

Figure 3.7: Whole cell western blot of *E. coli* MG1655 expressing pBAS16 or an empty vector control. (Left) Whole-cell dot blot of wild-type (WT) and mutant MG1655 expressing pBAS16 (-wzx_{Bf}, -wzy_{Bf}). (Right) Pro-Q™ Emerald staining of LPS in normalized, pronase treated lysates. The blue arrow indicates lipid A core. The white arrow likely indicates CPSA oligomer(s) ligated to lipid A core.

Evaluation of potential mechanisms of CPSA polymer export

Polysaccharide assembly and export typically occurs via a Wzx/Wzy dependent pathway and its cognate Wza transporter, or via an ATP-binding cassette (ABC) transporter such as observed with LPS transport.[35] Since our evidence suggests that CPSA may be ligated to LPS and that *B. fragilis* Wza was not included in our constructs, we considered both of these pathways in *E. coli* as possible means of CPSA polymer export. We also considered that CPSA oligomers are still present in cells expressing pBAS17 (**Supporting Figure 3.5**), even though CPSA polymers are produced. Like cells expressing pBAS16, if CPSA polymers or oligomers are ligated to Lipid A core and transported across the membrane via the well-defined Lpt transport pathway, a *waaL* mutant would abolish CPSA surface expression. Conversely, if CPSA expression was dependent on Wza_{Ec} for export across the outer membrane in cells expressing pBAS17, a wza_{Ec} mutant would no longer exhibit surface expression of CPSA.

To test whether CPSA polymer export is dependent on *E. coli* Wza and/or WaaL, we transformed pBAS17 into MG1655 lacking either *wza* or *waaL* and evaluated CPSA surface expression using a whole-cell dot blot. Surprisingly, a positive, but not as robust signal for CPSA was observed in a Δ*wza* and a Δ*waaL* mutant, indicating that neither may be essential for CPSA export (**Figure 3.8**). To assess whether CPSA polymers are appended to Lipid A core in MG1655 pBAS17, we performed an analysis of LPS profiles (**Figure 3.8**). SDS-PAGE of pronase treated lysates and staining with Pro-Q™ Emerald 300 revealed the presence of glycoforms of much higher molecular weights (~ 30 kDa), like those observed with anti-CPSA western blotting, and with a ladder-like banding pattern (**Figure 3.4 and Figure 3.6**). Polymers of slightly lower average molecular weight were observed in the *waaL* mutant compared to the *wza* mutant or wild type, suggesting that the polymer is no longer associated with lipid A core

when *waaL* is inactivated (**Figure 3.8**). Consistent with our findings in cells expressing pBAS16 (-*wzx*, -*wzy*), a low molecular weight band consistent with an oligomer of CPSA appended to lipid A core is no longer apparent in the *waaL* mutant. Notably, this low molecular weight band is fully present in Δ*wzxB* mutant. No differences in CPSA modality or signal intensity were noted between the Δ*waaL* mutant, and a Δ*wza*Δ*waaL* double mutant.

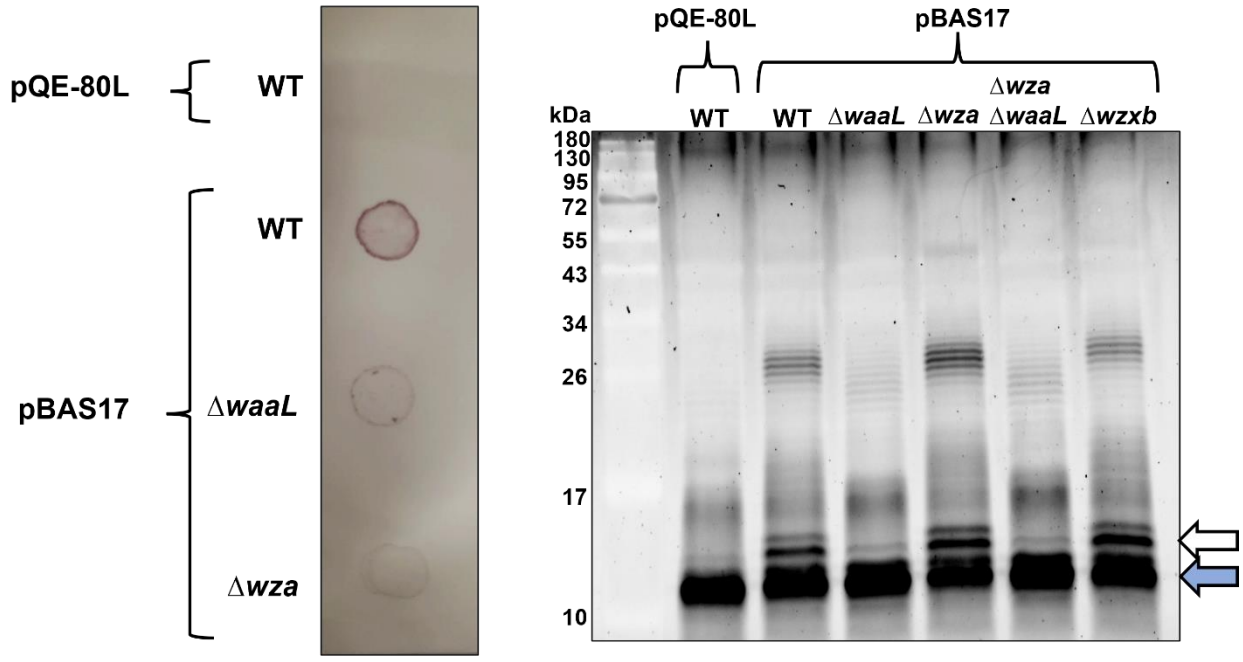

Figure 3.8: CPSA surface expression is not abolished in a Δ*waaL* or Δ*wza* mutant expressing pBAS17. (Left) Whole cell western blot of *E. coli* MG1655 expressing pBAS17 (+wzx_{Bf}, + wzy_{Bf}) or an empty vector control (EV). (Right) Pro-Q™ Emerald 300 stain of LPS from pronase treated cell lysates. The blue arrow indicates lipid A core. The white arrow likely indicates CPSA oligomer(s) ligated to lipid A core.

DISCUSSION

A thorough understanding of recombinant polysaccharide biosynthesis in *E. coli* and hindrances in production at early stages could bolster production and isolation of rare polysaccharides. Our method demonstrates a systematic approach for evaluating individual steps of recombinant Wzx/Wzy dependent polysaccharide systems.[155, 173] The efficacy of this method was

demonstrated by production of complete polysaccharide of biologically relevant length, and used as a model to address missing or poorly expressed requisites, such as the UDP-GlcNAc C4 epimerase and 4,6-dehydratase not present in the CPSA operon.[147, 237]

Stepwise reconstruction of CPSA biosynthesis in *E. coli* also provided the opportunity to evaluate whether co-expression of wzx_{Bf} and wzy_{Bf} was necessary for detectable levels of polymerization of the CPSA unit oligosaccharide in *E. coli*. We were surprised to find CPSA polymers could not be detected without the expression of both wzx_{Bf} and wzy_{Bf}.[238] This supports a previously proposed model that Wzx, Wzy, and Wza form a multi-protein complex wherein the translocase flips the unit oligosaccharide into the periplasm where it is then immediately "passed off" to the cognate polymerase and transporter or ligase (e. g. WaaL).[108, 232, 239] Nevertheless, it would be interesting to determine whether Wzx_{Bf} and Wzy_{Bf} colocalize and function as a unit in *E. coli* to ultimately enhance polymer quantity.

In the same regard, we found that deletion of *wzxB* resulted in a significant attenuation of surface expressed CPSA in cells expressing pBAS16 (-*wzx*, -*wzy*), with a simultaneous decrease in a signal in SDS-PAGE gels that we propose is lipid A core-linked CPSA oligomer (**Figure 3.7**). Perhaps, introduction of wzx_{Bf} in this strain (pBAS19, $+wzx_{Bf}$) could reverse this effect. The fact that a Δ*wzxB* mutant did not appear to affect LPS/CPSA profiles in size distribution or signal intensity in cells expressing pBAS17 ($+wzx_{Bf,} + wzy_{Bf}$) suggests both Wzx_{Bf} functionality in *E. coli* and its ability to compensate for the lack of *wzxB* in the WaaL-CPSA pathway (**Figure 3.8**). This also implies promiscuous specificity of *E. coli* WzxB since it can accept CPSA oligomers, which could prove useful in the design of complex polysaccharide production systems.[240]

Noting the potential activity of both flippases, $WzxB_{Ec}$ and Wzx_{Bf}, we were surprised to find that BPP-tetrasaccharide could still be detected in cells expressing pBAS17 (+*wzx*, +*wzy*),

albeit at a much lower intensity (**Figure 3.5**). This points toward a potential inefficiency in the activity of Wzy_{Bf} polymerase in *E. coli* and will be a future point of focus for improving CPSA output. Perhaps, this is due to a lack of the *B. fragilis* CPS transporter and chain length regulators, Wza and Wzz, in our construct which are suspected to form an active transporting complex (Reviewed by Cuthbertson et al.).[109]

Irregular cell shapes were also noted in strains expressing CPSA plasmids (**Figure 3.5**), as well as anomalous growth curves upon plasmid induction (data not shown). To this point, previous research has demonstrated that underutilized BPP-linked intermediates of glycan biosynthesis distort cell shape and result in cell lysis in BP constrained phenotypes.[131-133, 210, 241] Noting detectable levels of BPP-tetrasaccharide in cells expressing pBAS17, together, suggests a point of improvement of recombinant CPSA production. Additionally, we show that a Δ*waaL* mutant is likely required to procure aqueous, non-LPS associated CPSA, which has been demonstrated elsewhere in recombinant polysaccharide production systems.[167] This could also include the use of various genotypes to determine which gene products in *E. coli* hinder production *and* isolation of recombinant polysaccharides, specifically those that utilize the same nucleotide sugars and BP lipid precursor.[171, 242]

Complete, en bloc transfer of biosynthesis loci into expression hosts does not always result in robust expression of non-native glycans, including our own attempts to clone the entire CPSA operon. To address some of the aforementioned challenges in recombinant polysaccharide production, the Wren Laboratory has recently designed strains of *E. coli* to enhance recombinant polysaccharide biosynthesis, control chain length, and circumvent utilization of recombinant polysaccharides by *E. coli* native glycan pathways.[171] The strategy presented here enables a fundamental evaluation of recombinant polysaccharide overproduction, and systematic

evaluation of bottlenecks in recombinant systems. The combination of these strategies could dramatically improve glycopolymer production and reveal targeted opportunities to increase polymer quantity.

MATERIALS AND METHODS

General

Polyclonal anti-CPSA antibodies were generously provided by Dr. Laurie Comstock. All bacterial cultures were grown in Miller Lysogeny Broth unless otherwise specified. *E. coli* mutants and pQE-80L plasmid were generously provided by Dr. Matthew Jorgensen of the University of Arkansas Medical Center. LC-MS analysis was performed on an Agilent 1260 Infinity II equipped with a quaternary pump and MSD. All mobile phases were prepared from LC-MS grade reagents.

Construction of CPSA plasmids

CPSA plasmids were constructed using the primers listed **Supporting Table 3.3**. Briefly, pQE80L vector was isolated from *E. coli* DH5α cells. The vector was digested with restriction enzymes BamHI and HindII and purified with gel electrophoresis. Gene inserts with amplified with Phusion DNA polymerase (New England Biolabs). Amplicons were purified using the Wizard® SV Gel and PCR Clean-Up System (Promega). Purified, digested vector and inserts were incubated with NEBuilder HiFi DNA Assembly Mix (New England Biolabs) according to the manufacturer's instructions and incubated at 50 °C, or overnight for constructs with more than 4 fragments. *E. coli* DH5α cells were then chemically transformed with 5 µL of assembly reaction mixture and plated on selective media (LB/Carb^{100}). Successful transformants were confirmed by colony PCR.

An artificial SacI site was incorporated into pBAS8 immediately following *wcfS*. For construction of pBAS9-19, SacI digested pBAS8 was used as the vector backbone. For construction of pBAS16, *wcfO* and *wcfQ* were amplified as a single insert using pBAS10 as a template. For construction of pBAS 17-19, six genes (*wcfOQP*$_{Bf}$, *wbpP*$_{Vv}$, *wcfMN*) were amplified as a single fragment using pBAS16 as a template.

Extraction of BPP-linked CPSA intermediates

Cultures for glycolipid extraction were prepared by inoculating a single colony into 5 mL of LB/Carb^{100} and 2% glucose. Cultures were grown overnight for 16 hr at 37 °C, 220 rpm. Cell cultures were then diluted 1:1000 into 5 mL of LB/Carb^{100} and grown at 37 °C, 220 rpm until reaching an OD_{600} of approximately 0.6 before induction with 0.1 mM IPTG. After overnight induction, liquid cultures were transferred to falcon tubes and centrifugated at 5,000 x g for 15 min at 4 °C. The supernatant was discarded, and the cell pellet was resuspended in 10 mM PBS. The cell suspension was then transferred to a 15 mL glass centrifuge tube. To the cell suspension, 1 mL of chloroform and 2 mL of methanol were added to create a single-phase solution of water:chloroform:methanol (0.8:1:2.0). Each sample was vortexed and incubated at room temperature for 20 min to ensure cell lysis. Resulting insoluble materials were clarified from the cell lysate solution by centrifugation at 2,500 x g for 20 min at room temperature. The supernatant was then transferred to a clean glass culture tube, frozen at -80 °C, then dried under vacuum. Dried samples were resuspended in a solution of 1 mM ammonium hydroxide:n-propanol (1:1).

LC-MS analysis of BPP-linked CPSA intermediates

To evaluate the presence of CPSA intermediates in *E. coli*, 10 µL of cell extract was injected and separated using Waters XBridge BEH C18 column (5 µm, 4.6 x 100 mm, 300 Å). For LC-MS

analysis, mobile phase A consisted of 0.1% ammonium hydroxide and mobile phase B was n-propanol. BPP-linked intermediates were separated using a 5 – 75% gradient of mobile phase B over 15 min, then 75 – 95% B for 1 min, and an isocratic hold at 95% B for 5 min at 1 mL/min for a total run time of 21 min. A 3 s needle wash was performed between injections. The column was equilibrated for 4 min at 5 % B prior to the next injection. Intermediates were detected using SIM of the predicted $[M-H]^-$ and/or $[M-H]^{-2}$ ion of each intermediate. Total ion chromatograms were collected for each injection. Controls were prepared from parent strains expressing empty plasmids and evaluated for CPSA intermediates or isobaric compounds (**Supporting Figure 2**).

Whole-cell dot blots

Cultures were prepared from single colonies, induced with 0.1 mM IPTG at OD600nm, and grown overnight at 37 °C at 220 rpm. Whole-cell dot blots were prepared using 5 µL of liquid culture dried on nitrocellulose. After drying, the nitrocellulose was blocked with a 5 % milk solution for 30 min. The nitrocellulose was then rinsed gently with deionized water (x3) and incubated at room temperature for 1 hr with 1 mL of an adsorbed CPSA antiserum diluted 1:30 in sterile 10 mM PBS. CPSA antiserum was provided by Dr. Laurie Comstock.[230] After incubation with anti-CPSA, the nitrocellulose was washed twice for 5 min in 0.3 % PBST, then placed in alkaline phosphatase conjugated anti-rabbit goat secondary antibody (1:10,000) for 1 hr at room temperature. The nitrocellulose was then washed 3X for 1 min with 0.3 % PBST and developed with NBT-BCIP.

Cell fractionation and SDS PAGE

To evaluate CPSA glycoforms in *E. coli*, overnight cultures (5 mL) were prepared from single colonies, induced with 1 mM IPTG after reaching an OD_{600} of 0.8, and incubated overnight at 37C with shaking at 220 rpm. Cell were pelleted at 5,000 x g, resuspended in 0.8 mL PBS, and

transferred to a glass culture tube. To the cell suspensions, 3 mL of a 1:2 solution of chloroform:methanol was added and incubated at room temperature for 20 min. Insoluble material containing LPS was removed from cell suspensions by centrifugation at 2,500 x g for 20 min.[197] The insoluble fraction was washed with a second, single phase solution of water:chloroform:methanol (0.8:1:2) and dried under vacuum to remove any remaining solvent. The soluble fraction was converted to a two-phase Bligh and Dyer solution by the addition of water and chloroform.[196] The aqueous and organic phases were separated into two glass tubes and then dried under vacuum. Dried samples were resuspended in PBS and evaluated with 10% SDS-PAGE and anti-PSA western blotting.

SDS-PAGE and LPS staining

To evaluate LPS and CPS profiles of *E. coli* expressing either pBAS16 or pBAS17, overnight cultures were diluted 1:100 in LB and incubated at 37 °C with shaking until reaching an OD of ~ 0.6. Cell cultures were then induced with 0.01 mM IPTG and incubated overnight at 37 °C. Cell cultures were normalized to an OD_{600} of 1.0, and a 0.5 mL volume of each sample was pelleted and resuspended in 100 µL of 1X SDS dye. Cell samples were then lysed at 95 °C for 10 min and cooled to room temperature before 20 µg of pronase (Sigma) was added. The samples were incubated at room temperature for 20 min prior to 14 % SDS-PAGE. A 5 µL sample of each lysate was added to individual wells and separated at 40 mA for 60 min. Gels were then stained with the Pro-Q™ Emerald 300 kit (Thermo Fisher Scientific) according to the manufacturer's instructions.

Generation of *E. coli* mutants

E. coli mutants (**Supporting Table 3.3**) were either generously provided by the Jorgenson laboratory or prepared using the lambda red recombinase method of Datsenko and Wanner.[215]

Briefly, parent strains of *E. coli* were transformed with pKD46. Single colonies of transformants were used to inoculate 5 mL cultures containing LB/Carb^{100} and incubated at 30 °C. Cultures were induced with 100 mM L-arabinose and returned to the incubator for 1 hr at 30 °C. Cells were then pelleted at 5,000 RCF at 4 °C and washed six times with ice-cold 10 % glycerol. These cells were used immediately for transformation or stored as aliquots at -80 °C. For transformation, approximately 1-2 µg of purified amplicon was added to cell suspensions. Cells were then electroporated at 2,500 V and immediately recovered in LB at 30 °C overnight. Recovered cells were plated on LB/Cam^{20} to select for *waaL* mutants. Colony PCR was used to confirm the correct insertion of antibiotic resistance cassettes. Primers used to generate and confirm mutants are listed in **Supporting Table 3.4**. BAS13 was prepared by transforming DR35, a strain provided by the Young Laboratory, with pCP20 to remove the Kan resistance cassette.[243] To ensure that the Kan resistance cassette was successfully removed, cells were tested for sensitivity against Kan^{50}. To cure the cells of the pCP20 plasmid, cells were cultured on LB agar and incubated at 37 °C and colony purified twice more at 37 °C. Plasmid curing was confirmed by testing cells for sensitivity to Carb^{100}.

Confocal Microscopy

Cultures of *E. coli* MG1655 pQE-80L and MG1655 pBAS17 were prepared from single colonies. Once cultures reached an OD_{600nm} of 0.6, they were induced with 0.1 mM IPTG for 2 hr. Cells were pelleted at 5,000 x g for 15 min at 4 °C and washed twice with 5 mL of 10 mM PBS. Cells were then resuspended 100 µL of 10 mM PBS. Primary anti-CPSA antiserum was added to cell suspensions at a final concentration of 1:25, to make a final cell suspension of 100 µL. Cells were incubated with CPSA-antiserum at room temperature with rocking for 30 min. Cells were then pelleted at 10,000 x g for 5 min and washed twice with 1 mL of PBS. Cells were

resuspended in a 1:2,500 dilution of FITC conjugated secondary antibody and incubated at room temperature with rocking for 30 mins. Cells were again pelleted at 10,000 x g for 5 min and washed once with 10 mM PBS. Cells were resuspended in 100 µL of 10 mM PBS and 10 µL were dropped onto 0.7 % agar pads prepared on a clean glass slide. Once cells were dried, a cover slip was added. Confocal microscopy was performed by Dr. Shreya Goyal and Dr. James Grissom.

ACKNOWLEDGEMENTS

Dr. James Grissom, Dr. Shreya Goyal, and Dr. Richard Chi for assistance and expertise in confocal microscopy. Dr. Laurie E. Comstock (University of Chicago) for providing adsorbed anti-CPSA antiserum. Dr. Matthew Jorgenson (University of Arkansas for Medical Sciences) for providing *E. coli* mutants. Claire Moneghan for assistance with SDS-PAGE and western blotting of pBAS16-pBAS19.

APPENDIX B: CHAPTER 3 SUPPORTING INFORMATION

Supporting Table 3.1: CPSA plasmids and *m/z* of predicted intermediates.

Plasmid	Predicted CPSA Intermediate	Monoisotopic mass (Da)	$[M-H]^-$	$[M-2H]^{-2}$
1. Empty Vector	BP	846.67	846	
2. pBAS8	BPP-AATGal	1112.73	1112	555
3. pBAS9	BPP-AATGal-Gal	1274.76	1274	636
4. pBAS10	BPP-AATGal-PyrGal	1344.79	1344	671
5. pBAS15	BPP-AATGal-PyrGal-GalNAc	1547.87	1547	773
6. pBAS16	BPP-AATGal-PyrGal-GalNAc-Gal*f*	1709.92	1709	854

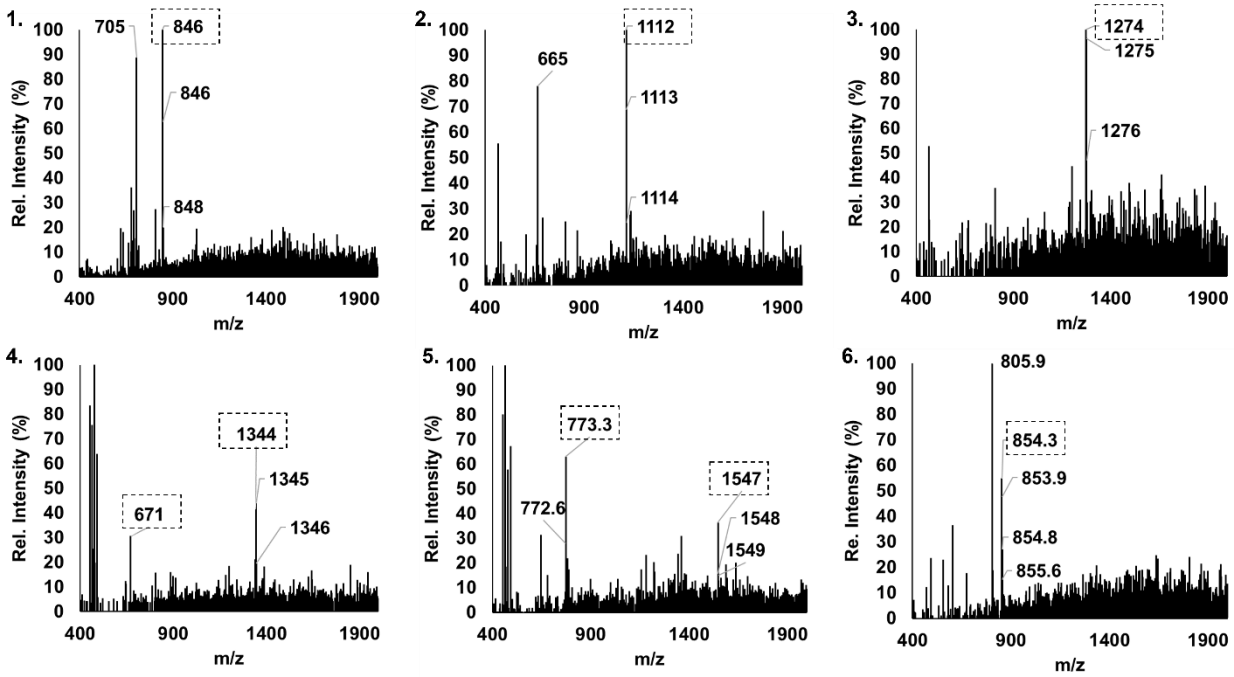

Supporting Figure 3.1: Spectra of recombinantly produced BPP-linked CPSA intermediates identified within *E. coli* cell lysates. Plasmids, CPSA intermediate, and $[M-H]^-$ or $[M-2H]^{-2}$ ion of each intermediate described in **Supporting Table 3.1** correspond to each numbered spectrum.

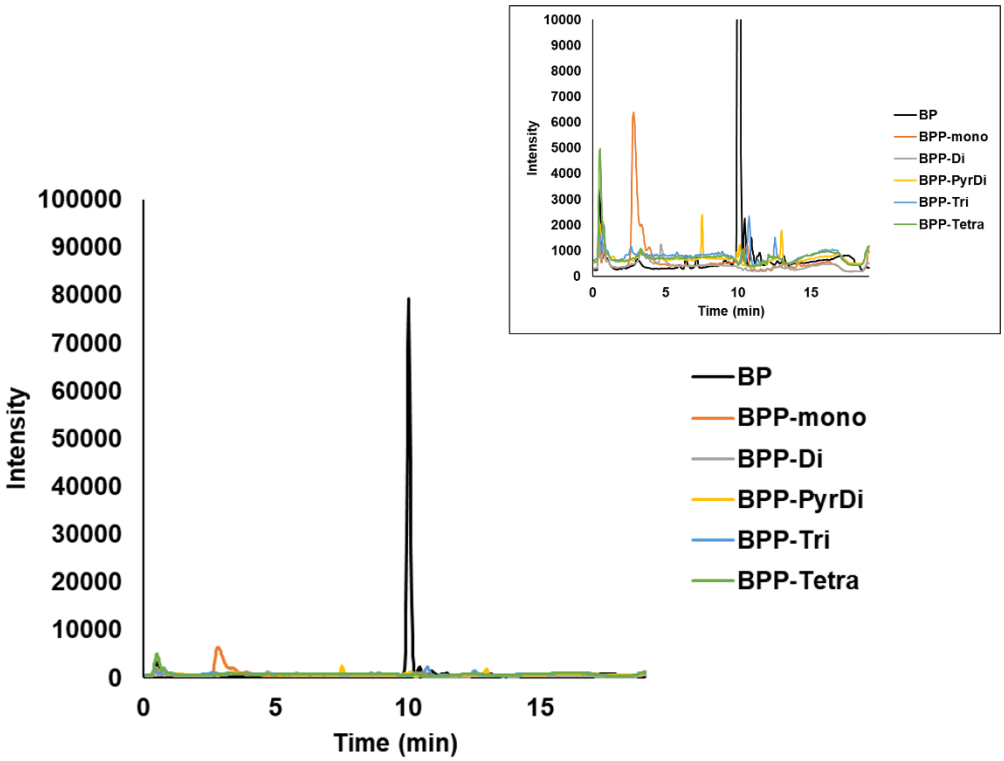

Supporting Figure 3.2: CPSA intermediates are not detected in *E. coli* expressing an empty vector control. Lysates of *E. coli* expressing an empty vector control were evaluated with ESI-LC-MS and SIM for all BPP-linked CPSA intermediates. A contaminant with a *m/z* identical to the first CPSA intermediate (BPP-mono) is observed at 2.84 min which is inconsistent with the retention time for a BPP-linked monosaccharide. Inset depicts a zoomed in region of the chromatogram to depict less abundant contaminants.

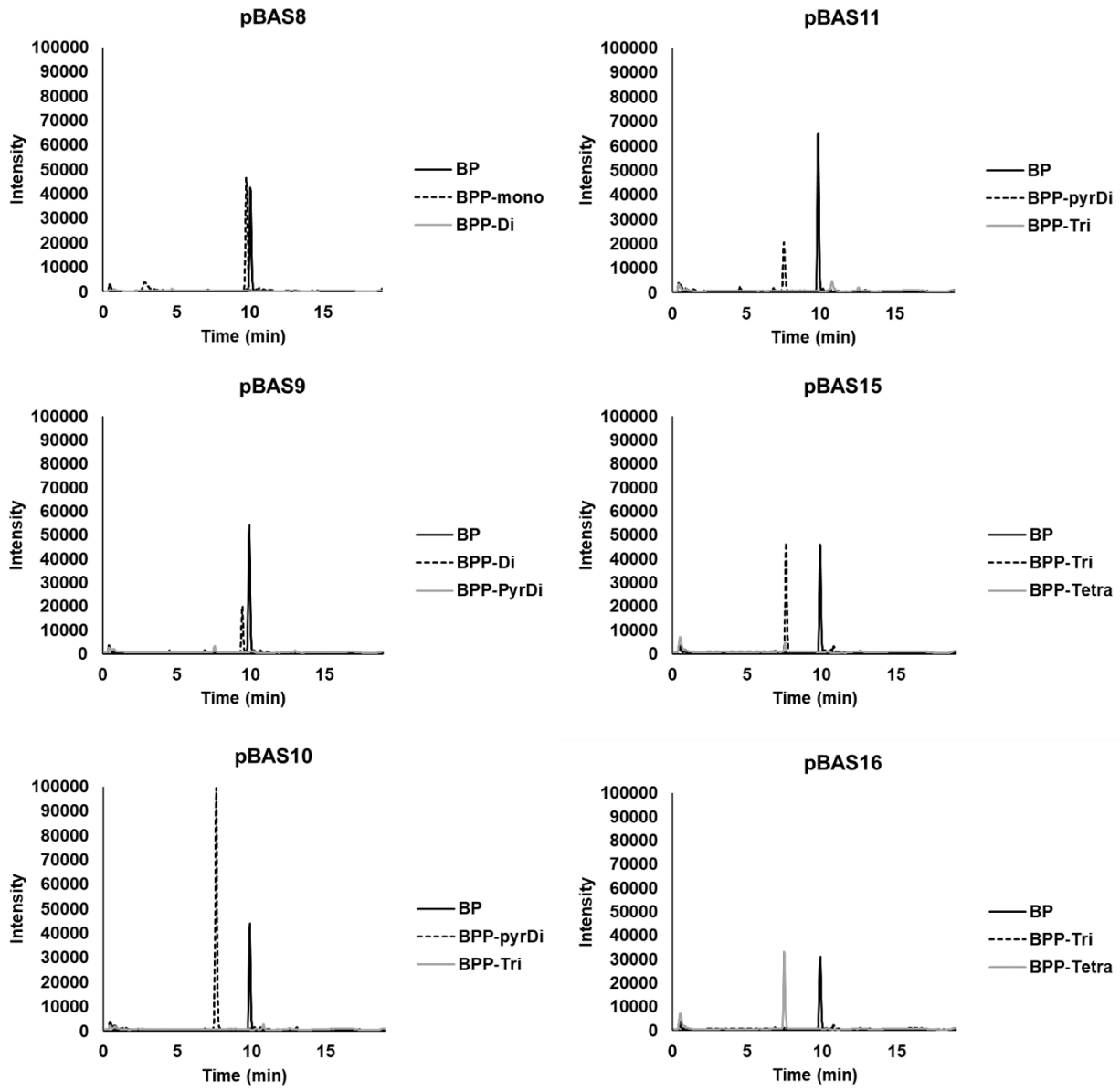

Supporting Figure 3.3: LC-MS with SIM of recombinant *E. coli* cell lysates with overexpressed CPSA plasmids. Each *E. coli* lysate was evaluated for the presence of (1) BP, (2) the expected CPSA intermediate, and (3) the subsequent intermediate, with the exception of pBAS11. Cells expressing pBAS11, lacking the C4 epimerase, *wbpP*, do not produce the CPSA BPP-linked trisaccharide. Only BPP-linked pyruvylated disaccharide (BPP-pyrDi) could be detected in cell expressing pBAS11. pBAS15 does include *wbpP*, and BPP-linked trisaccharide was detected in these lysates. Plasmids are described in **Table 3.1**.

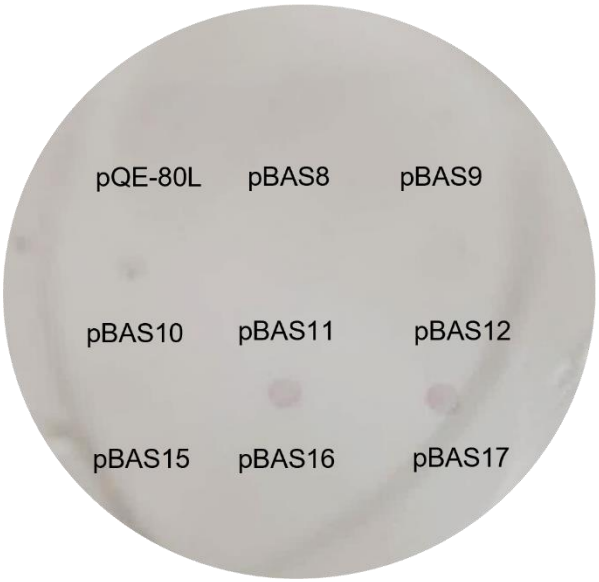

Supporting Figure 3.4: *E. coli* DH5α expressing pBAS16 and pBAS17 react with anti-CPSA antiserum. Whole-cell dot blot of *E. coli* DH5α expressing CPSA plasmids. Descriptions of plasmids used in this dot blot are described in Table 1. A positive signal for CPSA is only observed with cells expressing pBAS16 and pBAS17 plasmids.

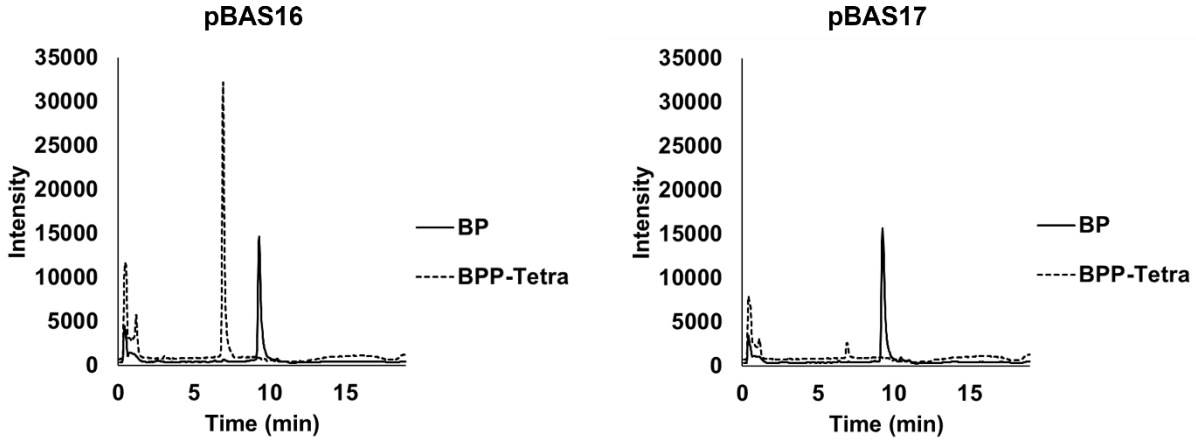

Supporting Figure 3.5: LC-MS analysis of BPP-linked CPSA tetrasaccharide in *E. coli* cell lysates. Normalized cell lysates expressing pBAS16 (-*wzx*$_{Bf}$, -*wzy*$_{Bf}$) or pBAS17 (+*wzx*$_{Bf}$, +*wzy*$_{Bf}$) were evaluated for the presence of BP and BPP-linked CPSA tetrasaccharide using ESI-LC-MS with SIM. BPP-tetrasaccharide is still present in pBAS17 cell lysates but appears to be much less abundant compared to cells expressing pBAS16.

Supporting Table 3.2: Primers used to generate CPSA plasmids.

Plasmid	Genes	Organism/ template	Primers
pBAS1	*pglF*$_{Cj}$	*C. jejuni* ATCC 700819	5'CATCACCATCACCATCACGACATGATTTTTTATA AAAGCAAAAGATTAGC 5'GGATTTGTTGGTATTTGGTCATATGTATATCCTC CTTTATACACCTTCTTTATTGTGTTTAAATTC
	wbpP$_{Vv}$	*V. vulnificus* M06-24	5'ATGACCAAATACCAACAAATCC 5'GTTATTCTTTATTGATTGTCCCATATGTATATCC TCCTCTATTTTATAAATCGCACATACC
	CPSA operon	*B. fragilis* ATCC 9343	5'ATGGGACAATCAATAAAGAATAAC 5'GAGTCCAAGCTCAGCTAATTACTAACGAATGAT GCTCCAAAATG
pBAS8	*pglF*$_{Cj}$	*C. jejuni* ATCC 700819	5'GGATCGCATCACCATCACCATCACGgaATGATT TTTTATAAAAGCAAAAGATTAGC 5'GGTATTTTCATATGTATATCCTCCTTTATACACC TTCTTTATTGTG
	wcfR$_{Bf}$	*B. fragilis ATCC 9343*	5'AGGAGGATATACATATGAAAATACCTTTTTCAC CACC 5'CAAATGTATATCCTCCTCTAGTGGTGGTGGTG GTGGTGTCGGTTTTCTGCAATTACG
	wcfS$_{Bf}$	*B. fragilis ATCC 9343*	5'CCACTAGAGGAGGATATACATTTGATCCGTTTT TTTGATATCG 5'GAGTCCAAGCTCAGCTAATTAGAGCTCCTAAC GAATGATGCTCC
Plasmids below were constructed using SacI digested pBAS8 as vector backbone. See Materials and Methods.			
pBAS9	*wcfQ*$_{Bf}$	*B. fragilis ATCC 9343*	5'GCATCATTCGTTAGGAGCTCAGGAGGATATAC ATATGAAATTGGCTGTCATTTC 5'CAAGCTCAGCTAATTAGAGCTTCACTTGTCGT CATCGTCTTTGTAGTCACGTACTGTTTTATAGATT ATG
pBAS10	*wcfQ*$_{Bf}$	*B. fragilis* ATCC 9343	5'GCATCATTCGTTAGGAGCTCAGGAGGATATAC ATATGAAATTGGCTGTCATTTC 5'CCTTCAACGTACTGTTTTATAGATT
	wcfO$_{Bf}$	*B. fragilis* ATCC 9343	5'AATCTATAAAACAGTACGTTGAAGGAGGATATA CATATGAGGAAGATATTATTAACATATGG 5'CAAGCTCAGCTAATTAGAGCTTCACTTGTCGT CATCGTCTTTGTAGTCTGACATCATAAATTTATTA CATATATTAATTAATC
pBAS11	*wcfQ*$_{Bf}$	*B. fragilis* ATCC 9343	5'GCATCATTCGTTAGGAGCTCAGGAGGATATAC ATATGAAATTGGCTGTCATTTC 5'CCTTCAACGTACTGTTTTATAGATT

Supporting Table 3.3: Primers used to generate CPSA plasmids (continued).

pBAS12	*wcfQ*$_{Bf}$	*B. fragilis* ATCC 9343	5’GCATCATTCGTTAGGAGCTCAGGAGGATATAC ATATGAAATTGGCTGTCATTTC 5’CCTTCAACGTACTGTTTTATAGATT
	wcfO$_{Bf}$	*B. fragilis* ATCC 9343	5’AATCTATAAAACAGTACGTTGAAGGAGGATATA CATATGAGGAAGATATTATTAACATATGG 5’CTCATATGTATATCCTCCTTCATGACATCATAAA TTTATTACATATATTAATTAATC
	wcfP$_{Bf}$	*B. fragilis* ATCC 9343	5’CATGAAGGAGGATATACATATGAGGGATGGAA AGCC 5’CCTCCTTCATTTATGTAAAAGATTTAAATATATT CTTTCGAG
	wcfM$_{Bf}$	*B. fragilis* ATCC 9343	5’AAATCTTTTACATAAATGAAGGAGGATATACATA TGAAAAAAAAATATGACTATCTAATTG 5’CAACTACAGCAAATATCTTCATATGTATATCCTC CTTCATAAGTCACTATTTATAACTTTTTCCAC
	wcfN$_{Bf}$	*B. fragilis* ATCC 9343	5’ATGAAGATATTTGCTGTAGTTG 5’CAAGCTCAGCTAATTAGAGCTTTACTTGTCGTC ATCGTCTTTGTAGTCATAGGTAGCTCCATTTTTTT TACG
pBAS15	*wcfQ*$_{Bf}$	*B. fragilis* ATCC 9343	5’GCATCATTCGTTAGGAGCTCAGGAGGATATAC ATATGAAATTGGCTGTCATTTC 5’CCTTCAACGTACTGTTTTATAGATT
	wcfO$_{Bf}$	*B. fragilis* ATCC 9343	5’AATCTATAAAACAGTACGTTGAAGGAGGATATA CATATGAGGAAGATATTATTAACATATGG 5’CTCATATGTATATCCTCCTTCATGACATCATAAA TTTATTACATATATTAATTAATC
	wcfP$_{Bf}$	*B. fragilis* ATCC 9343	5’CATGAAGGAGGATATACATATGAGGGATGGAA AGCC 5’GTAAAAGATTTAAATATATTCTTTCGAG
	wbpP$_{Vv}$	*V. vulnificus* M06-24	5’CTCGAAAGAATATATTTAAATCTTTTACATAAAT GAAGGAGGATATACATATGACCAAATACGAAAAA ATCC 5’CAAGCTCAGCTAATTAGAGCTTTATTTTTTATCA TTTATAAAGCTTATATACC

Supporting Table 3.4: Primers used to generate CPSA plasmids (continued).

pBAS16	*wcfQO*$_{Bf}$	pBAS10	5’GCATCATTCGTTAGGAGCTCAGGAGGATATAC ATATGAAATTGGCTGTCATTTC 5’CTCATATGTATATCCTCCTTCATGACATCATAAA TTTATTACATATATTAATTAATC
	wcfP$_{Bf}$	*B. fragilis* ATCC 9343	5’CATGAAGGAGGATATACATATGAGGGATGGAA AGCC 5’GTAAAAGATTTAAATATATTCTTTCGAG
	wbpP$_{Vv}$	*V. vulnificus* M06-24	5’CTCGAAAGAATATATTTAAATCTTTTACATAAAT GAAGGAGGATATACATATGACCAAATACGAAAAA ATCC 5’CAAGCTCAGCTAATTAGAGCTTTATTTTTTATCA TTTATAAAGCTTATATACC
	wcfM$_{Bf}$	*B. fragilis* ATCC 9343	5’GCTTTATAAATGATAAAAAATAAAGGAGGATATA CATATGAAAAAAAAATATGACTATCTAATTG 5’CAACTACAGCAAATATCTTCATATGTATATCCTC CTTCATAAGTCACTATTTATAACTTTTTCCAC
	wcfN$_{Bf}$	*B. fragilis* ATCC 9343	5’ATGAAGATATTTGCTGTAGTTG 5’CAAGCTCAGCTAATTAGAGCTTTAATAGGTAGC TCCATTTTTTTTACG
pBAS17	*wcfQOP_ wbpP_ wcfMN*	pBAS16	5’GCATCATTCGTTAGGAGCTCAGGAGGATATAC ATATGAAATTGGCTGTCATTTC 5’CCTCCTTTAATAGGTAGCTCCATTTTTTTTACG
	wxz$_{Bf}$	*B. fragilis* ATCC 9343	5’TGGAGCTACCTATTAAAGGAGGATATACATATG GGACAATCAATAAAGAATAAC 5’CCTCCTTCATTGTTTAAATATTGAAAGTAATAAT TTC
	wzx$_{Bf}$	*B. fragilis* ATCC 9343	5’CAATATTTAAACAATGAAGGAGGATATACATATG ACTAGTACTTCTTTCTTTATTATTAAG 5’AAGCTCAGCTAATTAGAGCTTTAAAATTTGATT TTGGCATTAAAC
pBAS18	*wcfQOP_ wbpP_ wcfMN*	pBAS16	5’GCATCATTCGTTAGGAGCTCAGGAGGATATAC ATATGAAATTGGCTGTCATTTC 5’CCTCCTTTAATAGGTAGCTCCATTTTTTTTACG
	wzx$_{Bf}$	*B. fragilis* ATCC 9343	5’TGGAGCTACCTATTAAAGGAGGATATACATATG GGACAATCAATAAAGAATAAC 5’CAAGCTCAGCTAATTAGAGCTTCATTGTTTAAA TATTGAAAGTAATAATTTC
pBAS19	*wcfQOP_ wbpP_ wcfMN*	pBAS16	5’GCATCATTCGTTAGGAGCTCAGGAGGATATAC ATATGAAATTGGCTGTCATTTC 5’CCTCCTTTAATAGGTAGCTCCATTTTTTTTACG
	wzy$_{Bf}$	*B. fragilis* ATCC 9343	5’TGGAGCTACCTATTAAAGGAGGATATACATATG GGACAATCAATAAAGAATAAC 5’CAAGCTCAGCTAATTAGAGCTTCATTGTTTAAA TATTGAAAGTAATAATTTC

Supporting Table 3.5: *E. coli* strains used in this study.

Strain	Genotype
DH5α	F– φ80lacZΔM15 Δ(lacZYA-argF)U169 recA1 endA1 hsdR17(rK–, mK+) phoA supE44 λ–thi-1 gyrA96 relA1
MG1655	K-12 F^- λ^- *ilvG*$^-$ *rfb-50 rph-1*
DR35	MG1655 Δ*wza::Kan*^{243}
BAS5	MG1655 Δ*wzxB*::frt
BAS13	MG1655 Δ*wza*::frt
MAJ975	MG1655 Δ*waaL*::frt
BAS24	MG1655 Δ*wza*::frtΔ*waaL*::cam

Supporting Table 3.6: Primers used for *E. coli* mutants.

Strain Designation	Primers	Template	Check Primers
BAS5	5’GAAAGGCTCTTTACGTTAGATG AGCTTATCAGATTAAAATTAATTGC ATGACATTACACGTCTTGAGCGAT 5’GCACAAACGGCACCAAACAAAC CAGAACCAACAATGATATAATCGT ACATATGAATATCCTCCTTAGTTCC	pKD4	5’TGGCTGCTATTG GGCGAA 5’TCCACCGATATG ATTTCTTTTC
BAS24	5’TCAACAGTCAAGCAGTTTTGGA AAAGTTATCATCATTATAAAGGTAA AACTGAATATCCTCCTTAGTTCC 5’TTGTATAGATAAGAAGTGAGTTT TAACTCACTTCTTAAACTTGTTTAT TCATTGTGTAGGCTGGAGC	pKD3	5’TATCCCAATGGC ATCG 5’ACCCTAATTCAC GTACTCC

CHAPTER 4. ANALYSIS OF *C. CRESCENTUS* HOLDFAST BIOSYNTHESIS

INTRODUCTION

Caulobacter crescentus holdfast polysaccharide

C. crescentus exhibits a unique dimorphic life cycle, in which a non-replicating motile swarmer cell will shed its pili and flagellum to become a stalked, sessile cell capable of cell division.[244, 245] The stalk is a thin, polar extension of the cell membrane. Interestingly, once the stalk is formed the bacterium will produce an adhesive substance, known as the holdfast, that is composed of repeating units of oligosaccharides.[59, 245, 246] This adhesive substance is localized only at the end of the stalk and promotes the permanent, polar attachment of *C. crescentus* cells to exogenous surfaces. The *C. crescentus* holdfast is unique in that it is one of the strongest adhesive glycopolymers known to date, and retains its adhesive properties in aqueous environments.[22, 247] Past research has been devoted to understanding the mechanisms that tightly regulate holdfast production, such as holdfast inhibiting enzymes, pleiotropic cell cycle regulators, transcriptional regulators, and enzymes associated with flagellar and pili assembly.[29, 59, 152, 153, 248, 249]

Early investigation of the holdfast from *C. crescentus* provided evidence that the holdfast is composed of carbohydrates. This includes sensitivity to glycosidases, lectin binding, and homology of genes involved in bacterial glycan assembly.[26, 250, 251] Holdfast composition has been surmised using wheat germ agglutinin (WGA), a lectin that is specific for polymers containing N-acetylglucosamine (GlcNAc). WGA appears to be specific for the holdfast polysaccharide, and, when co-incubated with *C. crescentus* becomes localized at the end of stalked cells where holdfast is secreted.[250, 251] This evidence suggests that the holdfast is a glycopolymer that contains oligomers of GlcNAc. These findings were corroborated based on the reduction of *C. crescentus* cellular adhesion in the presence of lysozyme and chitinase,

glycohydrolases that catalyze the hydrolysis of oligomers of GlcNAc.[251] While other polymers such as proteins and DNA have been implicated in the physical, adhesive properties of holdfast, the main contributing factor appears to be cooperation between discrete oligosaccharide units, as determined by atomic force microscopy (AFM).[22]

Previous research has also shown that mutation of key genes thought to be involved in holdfast biosynthesis may abolish or disrupt holdfast production and cellular adhesion, confirming their role in the production of native holdfast structures.[22, 25, 26, 29, 246, 252] These genes have been annotated based on identity or similarity to genes from other organisms involved in bacterial glycan biosynthesis, such as WecG, an enzyme involved in the biosynthesis of enterobacterial common antigen in *E. coli* (28% identity; 44% similarity), and WbaP, an enzyme that initiates the biosynthesis of O-antigen in *Salmonella enterica* (29% identity; 46% similarity).[253] Hershey et al. employed saturating transposon mutagenesis coupled with cell adhesion assays to identify key genes involved in holdfast biosynthesis.[29] This extensive genetic analysis of *C. crescentus* determined the genes that are required for holdfast-dependent cellular adhesion (**Figure 4.1**). Additionally, these results provide unambiguity toward defining the roles of flagellar, pili, and lipopolysaccharide biosynthesis enzymes in holdfast-dependent adhesion.[25, 26, 29, 254]

The holdfast, roughly 100 nm in diameter, has previously been characterized as a hydrogel with similar properties to other biological gels such as collagen and gelatin.[251] Tsang et al. investigated the adhesive properties of the *C. crescentus* holdfast using micromanipulation of single cells.[247] The authors characterized the holdfast as the strongest biological adhesive known to date with a force adhesion of 68 N/mm^2 on a borosilicate substrate. For comparison, the strongest commercial adhesive provides a bond strength of up to 30 N/mm^2, and the strongest

biological adhesives of up to 10 N/mm^2. Based on this research, 1 cm^2 of *C. crescentus* holdfast could potentially hold up to 680 kg of weight on a wet surface.[247]

Additional investigations of holdfast adhesion strength were carried out using a *C. crescentus* mutant that sheds the holdfast from the stalk. Using shed holdfast recovered from the culture medium, Berne et al. employed dynamic force microscopy to measure holdfast adhesion to a variety of substrates.[22] These researchers concluded that the holdfast enables attachment to a broad range of substrates and facilitates adhesion in aqueous environments, in addition to providing sustainability and biodegradability.[22] Glycopolymers such as cellulose, alginate, and hyaluronate have already been established as sustainable, biodegradable biopolymers.[216] Determining the precise function of holdfast synthesizing (Hfs) enzymes will reveal the structures that govern the adhesive nature of this polymer that make it a promising biopolymer for future applications in biomedicine as a wound adhesive and in industry as an adhesive that maintains its properties in aqueous environments.

Holdfast Biosynthesis

In holdfast biosynthesis, there appears to be genetic redundancy in enzymes responsible for the initial addition of a phospho-sugar to BP. This was evidenced by the identification of three genes, *hfsE,* and two paralogs, *pssY,* and *pssZ,* which share significant amino acid identity to HfsE (51% and 41%, respectively) (**Figure 4.1, Table 4.1**).[26] Toh et al. demonstrated that single deletions of each of these genes only result in a slight decrease in *C. crescentus* adhesion; however, a triple deletion is required to completely abolish adhesion and holdfast production.[26] It has been proposed by other researchers that PssY and PssZ are part of other BPP utilizing pathways in *C. crescentus*.[26, 29] To determine if all three of the genetically identified initiating phospho-glycosyltransferases (HfsE, PssY, and PssZ) contribute to the production of holdfast,

our collaborator conducted complementation analyses of a holdfast mutant (*ΔhfsEΔpssYΔpssZ*) using xylose inducible plasmid constructs of *hfsE*, *pssY*, or *pssZ*. The results indicated that holdfast production, cellular adhesion, and consequently biofilm formation, can be rescued by complementation with *hfsE* and *pssY*, but not *pssZ* (data not shown). These results indicate that *pssZ* likely does not contribute to the final structure of the holdfast polysaccharide, and thus, is not included in this study.

Table 4.1: Proposed holdfast oligosaccharide biosynthesis enzymes and functions.

Protein	Proposed function	Reference
HfsE	Initiating phospho-glycosyltransferase (PGT)	26
PssY	Initiating phospho-glycosyltransferase (PGT)	26
HfsJ	WecG/TagA-family glycosyltransferase	153
HfsG	GT2 Family Glycosyltransferase	26
HfsL	GT2 Family Glycosyltransferase	29
HfsH	Polysaccharide Deacetylase	26, 255, 257
HfsK	CelD Family Acyltransferase	152

Three cytosolic glycosyltransferases (HfsJGL), one deacetylase (HfsH), and one acyltransferase (HfsK) involved in holdfast biosynthesis have also been identified (**Figure 4.1, Table 4.1**); however, the precise succession of these enzymes in holdfast biosynthesis is currently unknown.[26, 29, 152, 255-257] The proposed enzyme functions were established through analysis of protein sequence homology, but the majority of Hfs enzymes have yet to be functionally characterized, with the exception of HfsH.[257] The order of glycan biosynthesis enzymes is increasingly important for precise characterization of intermediates, characterization of glycosyltransferase specificity, and development of synthetic bioproduction systems.[30, 31]

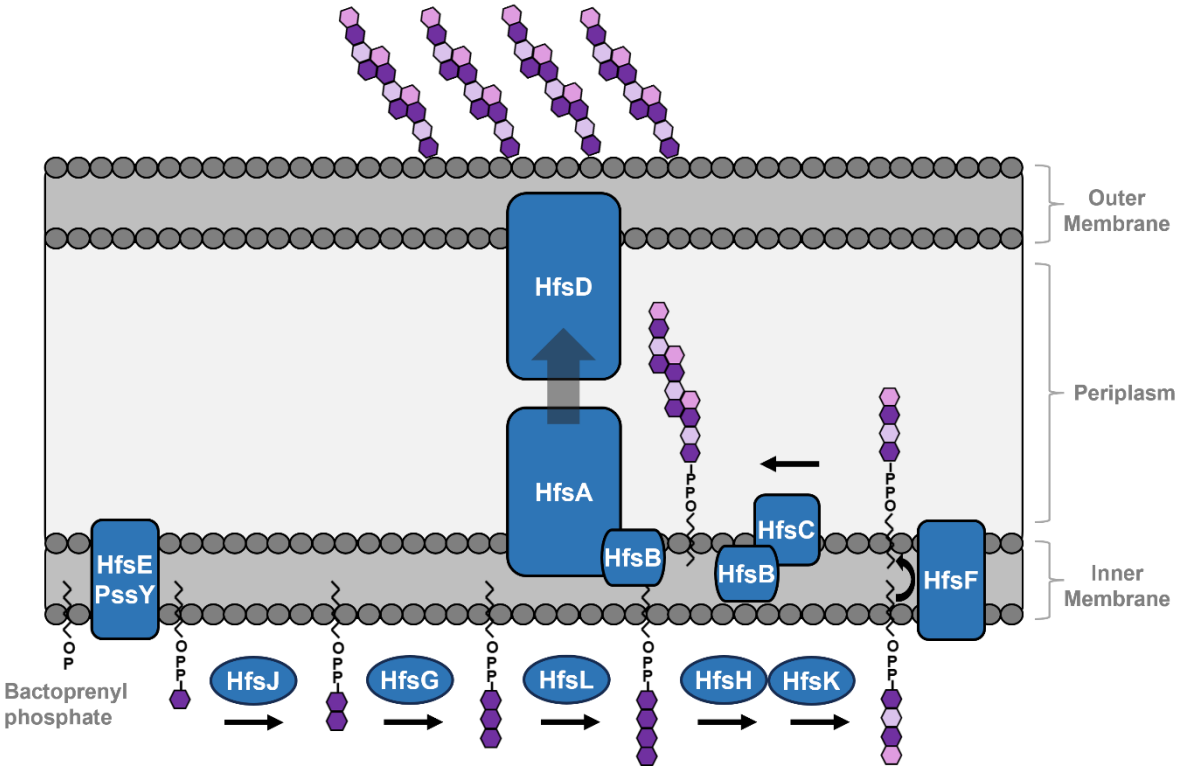

Figure 4.1: Representation of proposed Holdfast biosynthesis pathway. An initial phospho-sugar is appended to BP by HfsE or PssY. Cytosolic glycosyltransferases HfsJ, HfsG, and HfsL transfer additional sugar molecules to the growing polymer, however the sequence of these steps is unknown. HfsH and HfsK catalyze sugar modifications to form the final repeat unit which is flipped to the periplasm and polymerized by HfsF and HfsCB enzymes, respectively. Holdfast polymers are transported to the cell surface by a complex of HfsA, HfsB, and HfsD. Secreted holdfast anchor proteins, HfaABDE, secure holdfast to the cell surface (not pictured).

Once the complete holdfast oligosaccharide is produced, it is proposed that a flippase, HfsF, flips the BPP-linked oligo from the cytoplasmic face of the inner membrane to the periplasmic face.[26] Here, a polymerase and proposed chain length regulator, HfsC and HfsB respectively, elongate the BPP-glycan to form holdfast polymers.[26, 109] A transporter protein complex composed of HfsA, HfsB, and HfsD, facilitate passage of holdfast across the periplasm to the outer leaflet of the outer membrane. Outer membrane-associated adhesion proteins, HfaABDE, form a complex that secures holdfast polymers to the tip of the *C. crescentus* stalk.[29, 246, 252, 258] HfaABDC are located within a single operon separate from the holdfast biosynthesis

operon.[258] However, HfaC is not involved in mediating attachment of holdfast to the stalk.[246, 258] Essential holdfast components such as *hfsEFGH* are organized in an operon with transporter proteins immediately adjacent. Genes *hfsJ* and *hfsK* are not included in either operon.

Evidence thus far suggests that holdfast is composed of "housekeeping" sugars that are involved in other cellular processes. During their extensive genetic analyses of *C. crescentus* of holdfast biosynthesis, Hershey et al. concluded that enzymes involved in the production of rare sugars in *C. crescentus* do not contribute to or affect the production of holdfast.[29] However, the results do suggest that the adhesive nature of holdfast may be correlated to sugar modifications that occur during holdfastbiosynthesis.[29] This conclusion was corroborated by the identification of proposed sugar modifying enzymes (enzymes that append or modify key carbohydrate functional groups) HfsH and HfsK, as well as AFM analysis of holdfast adhesion in Δ*hfsH* mutants.[29, 152, 255]

Based on the identification of four glycosyltransferases, the structure of holdfast is proposed to be a repeating tetrasaccharide unit harboring an appended acyl group with possible branching.[29] Analysis of the carbohydrate composition of *C. crescentus* holdfast suggests that this polymer likely contains a 1'-4' linked backbone of glucose, mannose, N-acetylglucosamine, and xylose.[33] Nonstoichiometric amounts of 3-O-methylglucose were also detected, which is likely present as a branched terminal carbohydrate.[33] Trace amounts of galactose were also present in these samples.

Gaps in knowledge of holdfast biosynthesis

While the essential genetic components of holdfast biosynthesis have been determined, the precise function of holdfast synthesizing (Hfs) enzymes and the structure of the holdfast

polysaccharide have yet to be established. Genetic analyses typically rely on mutations to identify genes that are essential for polysaccharide production and characterize structural intermediates; however, these methods are hindered by the build-up of intermediates that may be lethal or toxic to bacterial cells.[133, 243] Genetic complementation with plasmid constructs of similar genes with known functions has also been employed to elucidate holdfast biosynthesis. This method provides insight into the function of proposed genes but demonstrates little about their specificity. Holdfast sensitivity to glycolytic enzymes such as lysozyme and chitinase provides supporting evidence for GlcNAc polymers in the holdfast structure but does not reveal information regarding glycosidic linkages and the specific structure of oligosaccharides.[250] These techniques can be important for distinguishing specific glycan motifs, such as GlcNAc dimers and trimers, but cannot distinguish other structural characteristics unique to different bacterial glycans such as acetylation, pyruvylation, and acylation.

Current techniques for investigating initiating phospho-glycosyltransferase and glycosyltransferase specificity *in vitro* necessitate costly and hazardous materials such as radiolabeled substrates. Thin layer chromatography (TLC) analysis of enzyme products may lack the sensitivity and selectivity required for the detection and identification of various sugar modifications that are often present in unique bacterial glycan structures, including holdfast. This research addresses key questions regarding the biosynthesis of the holdfast polysaccharide such as enzyme activity and specificity using fluorescent, tagged holdfast precursors, as well as LC-MS detection of native BPP-linked intermediates. Advancements in determining the *C. crescentus* holdfast composition and structure will facilitate its use within our communities and promote the investigation of complex bacterial glycans as sustainable, biodegradable, and renewable biopolymers.

RESULTS AND DISCUSSION

LC-MS detection of BP and BPP-linked intermediates in holdfast biosynthesis mutants

Detection of BP-linked glycan intermediates presents a challenge due to the lack of a selective chromophore in natural bactoprenyl phosphate (BP) structures. To circumvent this, our laboratory developed a protocol for crude extraction and analysis of endogenous BP- and BPP-linked glycan intermediates from whole cell lysates using LC-MS.[114, 115] Differing lengths of BP have been identified between bacterial species, therefore, to identify BP(P)-glycans in *C. crescentus*, BP must first be identified.[259, 260] To this end, lysates of wild type (WT) *C. crescentus* were prepared using the established method of Bligh and Dyer for crude extraction of phospholipids, including BP.[196] Crude extracts were then analyzed using LC-MS with selected ion monitoring (SIM) for sequential lengths of BP (**Table 4.2**).

Table 4.2: Monoisotopic and $[M-H]^-$ SIM masses used to probe for BP species in *E. coli* overexpressing uppS plasmids.

Bactoprenyl phosphate	Monoisotopic Mass	$[M-H]^-$
C_{35}-BP	574.42	573
C_{40}-BP	642.48	642
C_{45}-BP	710.54	710
C_{50}-BP	778.6	778
C_{55}-BP	846.67	846
C_{60}-BP	914.73	914
C_{65}-BP	982.79	982
C_{70}-BP	1050.85	1050
C_{75}-BP	1118.92	1118

Interestingly, it was discovered that *C. crescentus* produces longer phospho-isoprenoids, likely in the form of C_{65} and C_{70} BP, with the major product being C_{65} BP **(Figure 4.2)**. For

comparison, our laboratory and others have found that *E. coli* and many other bacterial species produce a major product of C_{55} BP.[114, 115] Shorter versions of prenyl phosphates, C_{40} and C_{50}, have been identified in *Paracoccus denitrificans* and *Mycobacterium tuberculosis*, respectively.[259, 260] The *Z* or *E* configuration of *C. crescentus* C_{65} and C_{70} prenyl phosphate has yet to be determined; however, sequence alignment suggests that *C. crescentus* UppS is a *Z*-prenyl transferase, as opposed to an *E*-prenyl transferase.[113] It was also confirmed that WecA transfers P-GlcNAc to C_{65} BP in *C. crescentus* lipid extracts (**Figure 4.2**).

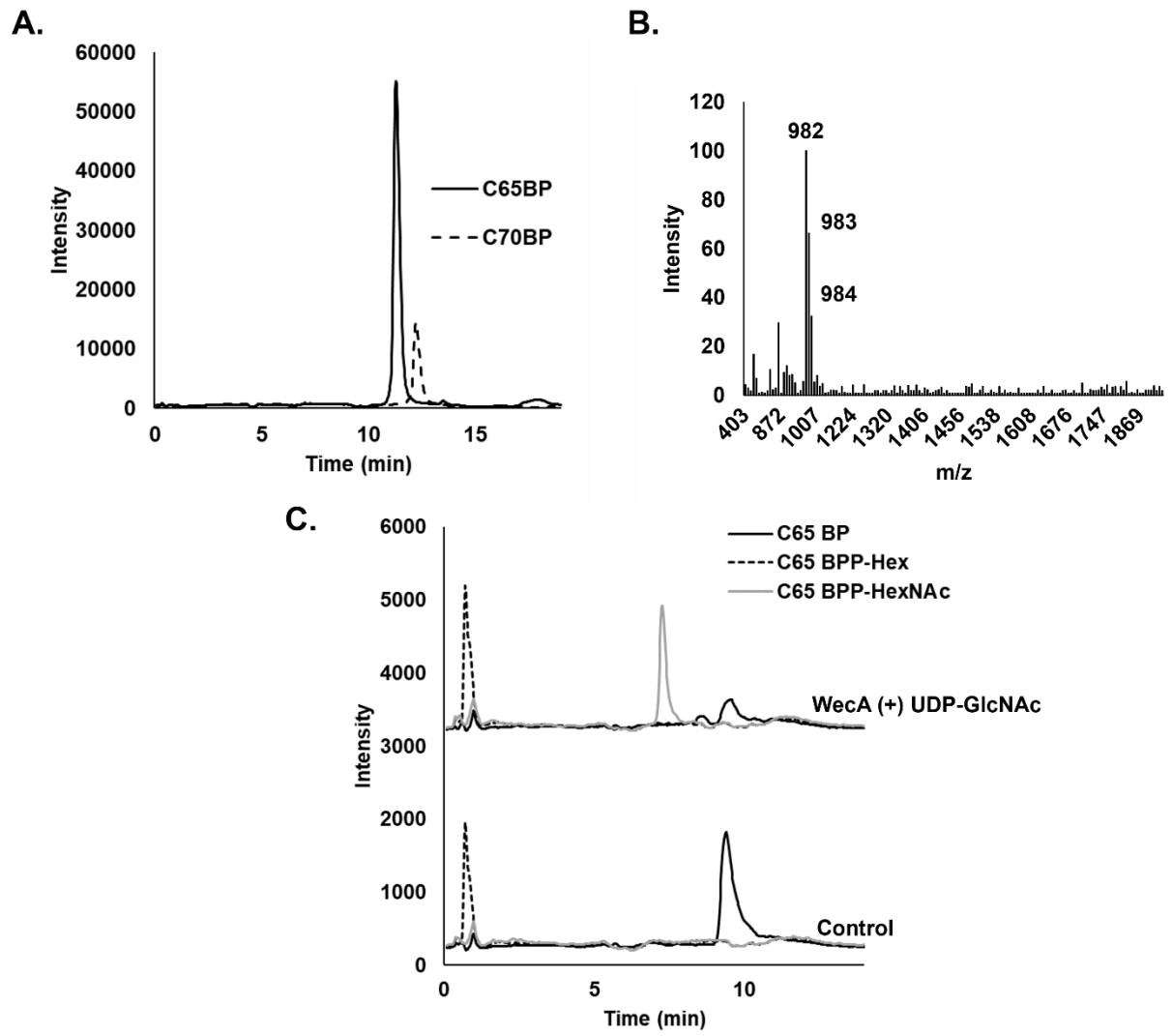

Figure 4.2: LC-MS analysis of phospholipids from *C. crescentus* indicates C_{65} BP as the major form of BP. (A) Sequential isoprenoid lengths of BP ($C_{35} – C_{75}$) were scanned for in *C. crescentus* phospholipid extracts using SIM. (B) The major form of BP detected in wild type lysates was the $[M-H]^-$ ion of C_{65} BP with a m/z of 981.8. (C) C_{65}BP in *C. crescentus* lipid extract is utilized by WecA to form a new product consistent with the $[M-H]^-$ ion of C_{65}BPP-GlcNac (*m/z* 1264.83). Control reaction does not contain UDP-GlcNAc or WecA.

Overproduction of *C. crescentus* UppS in *E. coli* produces longer chain, C_{65} and C_{70} bactoprenyl phosphate

After the discovery of C_{65} BP, a new objective emerged to disentangle whether production of longer chain BP in *C. crescentus* is influenced by local cellular conditions, such as the

composition of the cell envelope (known to differ in type and proportions of phospholipids between bacterial species), availability of precursors (e.g., FPP, IPP), or attributed to differences in protein structure of undecaprenyl pyrophosphate synthase (UppS).[112, 261-263] For example, Allen and Muth demonstrated that UppS from *Lactobacillus plantarum*, a Gram-positive bacterium, was stimulated by anionic surfactants and phospholipids, including those naturally present in *L. plantarum* and *E. coli*.[264] Additionally, our laboratory demonstrated that the length of chemoenzymatically synthesized bactoprenyl phosphate analogues can be tuned based on the type and concentration of surfactant.[212] We have also confirmed that increasing or decreasing concentrations of the IPP substrate *in vitro* result in shorter or longer BPP analogues, respectively.[114] Temperature of *in vitro* reactions may also play a role in the length of BP.[265]

To evaluate whether the length of BP differs between UppS enzymes, multiple non-native *uppS* genes were overexpressed separately in a single *E. coli* host strain. This experiment included *uppS* from *Caulobacter crescentus*, *Staphylococcus aureus*, *Bacteroides fragilis*, and *Helicobacter pylori*, as well as *E. coli's* native UppS (**Table 4.3**). *E. coli* harboring *uppS* plasmids were cultured, overexpressed, and the cells were harvested. Lipids extracts were prepared using chloroform, methanol, and water, as previously described, to allow for qualitative evaluation of BP species after *uppS* overexpression.[115] Cell extracts were evaluated for prenyl phosphate species of consecutive lengths using LC-MS with SIM (**Table 4.2**). Total ion chromatograms were collected for each injection.

Table 4.3: References and Accessions of non-native uppS overexpressed in *E. coli*

Organism	NCBI Reference	Accession	Plasmid	Designation
C. crescentus CB15	AAK23894.1	Q9A707	pET-24a	$pUppS_{Cc}$
S. aureus N315	WP_000473699.1	P60477		$pUppS_{Sa}$
H. pylori UMB_G1	EMR55920.1	M7SME2		$pUppS_{Hp}$
B. fragilis NCTC 9343	CAH06211.1	Q5LI17		$pUppS_{Bf}$
E. coli K12	AAC73285.1	P60472		$pUppS_{Ec}$

Evaluation of BP species showed that *E. coli* expressing an empty plasmid produced a narrow range of BP lengths including C_{50} and C_{55} BP, with an obvious majority of C_{55} (**Figure 4.3**). These results are comparable to previous evaluations of BP chain length in wild-type *E. coli*.[114-116, 266] *E. coli* cells overexpressing its native *uppS* produced a broader distribution of different length BPs, ranging from C_{45} to C_{55}, with C_{50} as the most abundant form. Overexpression of *C. crescentus uppS* in *E. coli* altered this distribution to favor longer chain isoprenoids of C_{50} – C_{65} length, with the most abundant forms as C_{55} and C_{60}. These results suggest that longer chain BP produced by *C. crescentus* UppS are likely attributed to both protein structure and host cell conditions.

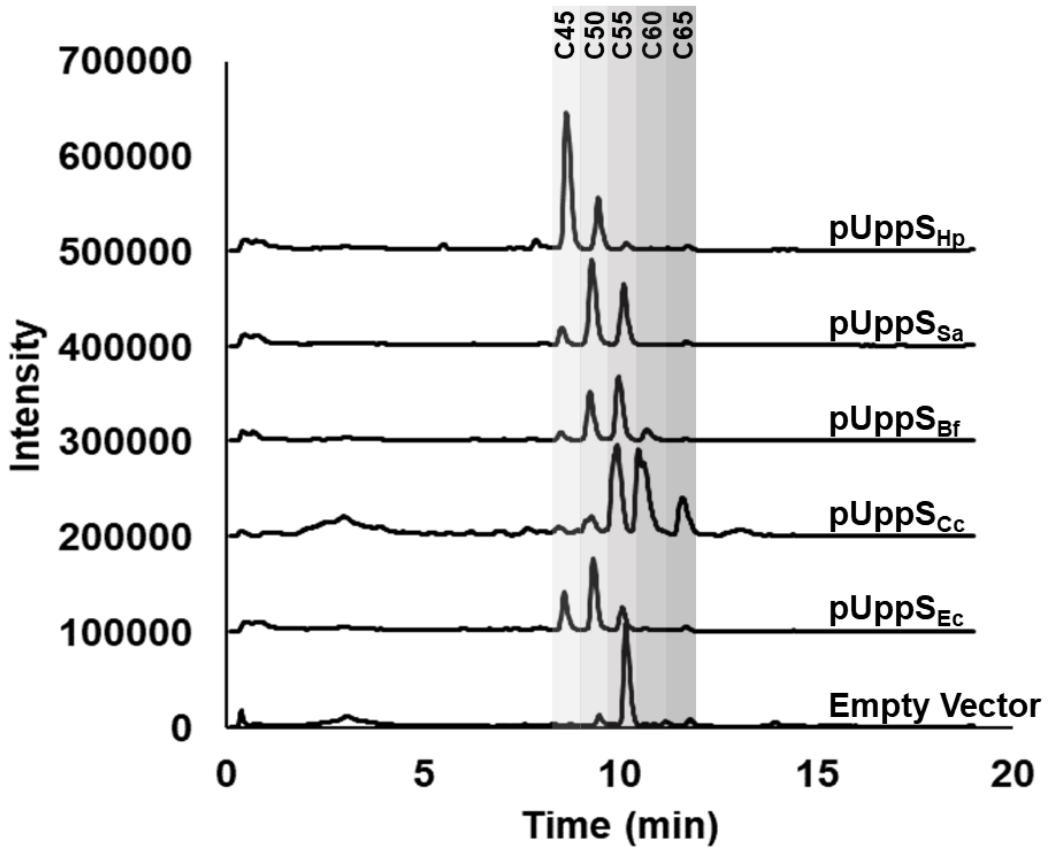

Figure 4.3: *E. coli* cells overexpressing non-native *uppS* produce varying lengths of BP. Lipid extracts of *E. coli* cells overproducing non-native UppS were evaluated for BP species using LC-MS with SIM and compared to an empty vector control. For each injection, multiple ions were monitored within a single SIM channel. Signals were offset by 100,000 intensity units.

Crystallographic studies of *E. coli* UppS structure and catalytic mechanism depict an elongated, tunnel-like active site surrounded by two α-helices (α2 and α3) and four β-strands (βA, βB, βC, βD) (**Figure 4.3**).[263, 267] Structural analyses of bound substrates and site directed mutagenesis strongly suggest that FPP and IPP substrates are initially bound at the top of the tunnel.[266, 268, 269] As the product chain length elongates by consecutive condensations of IPP and FPP in the *Z*-configuration, the FPP moiety migrates toward the bottom of the tunnel before the

elongated prenyl phosphate product it is released. Product release is stimulated by the presence of a surfactant such as Triton.[269] In several cases, it has been proposed that amino acid residues located at the bottom of this tunnel are implicated in the control of product chain length. This is consistent with previous evaluation of product elongation in *E*-prenyl transferases, which share no sequence homology to *Z*-prenyl transferases.[113, 270, 271] Other groups have considered the physical size of the hydrophobic cavity in determining product chain length.[272]

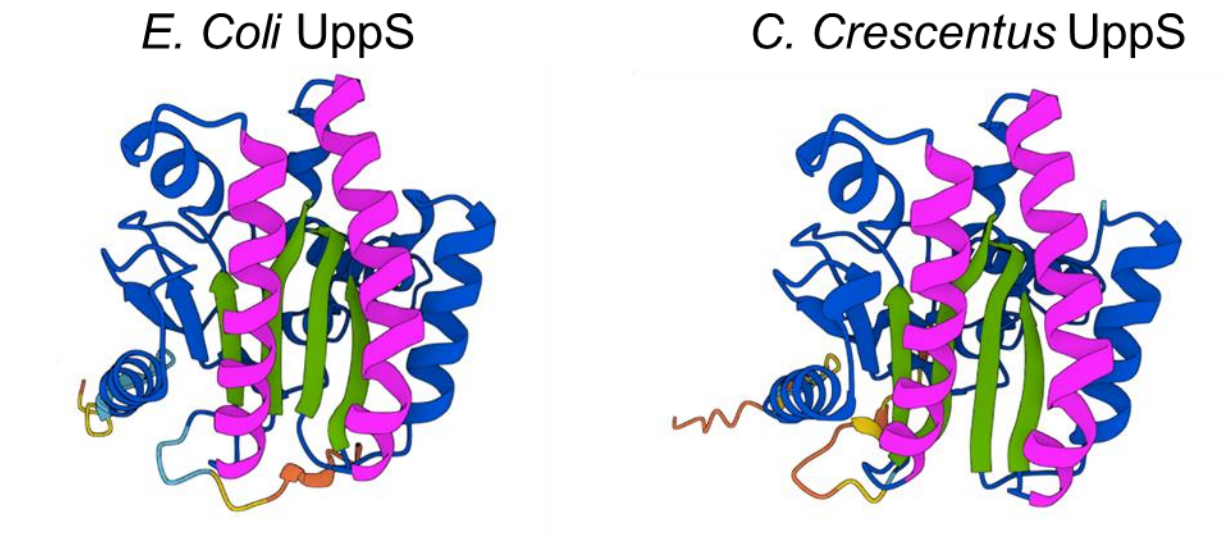

Figure 4.4: Structure of *E. coli* UppS and proposed structure of *C. crescentus* UppS. 3D Image was generated with AlphaFold.[267, 284, 285] Helices (α2 and α3) and strands (βA, βB, βC, βD) constituting the hydrophobic tunnel are colored pink and green, respectively.

To this end, several groups have identified amino acid residues in *Z*-prenyl transferases that are implicated in regulating chain length of prenyl diphosphate. For instance, during investigation of prenyl transferases from *Mycobacterium tuberculosis,* Wang et al. identified a double point mutation in Rv1086, a short chain (C_{15}) *Z*-prenyl transferase, at positions L84A and L85F that resulted in the production of longer chain prenyl phosphates up to C_{50} (**Figure 4.5**).[273] Similarly, in an extensive evaluation of BP chain length regulation in *E. coli*, Ko et al. proposed that the presence of bulky residues, such as Val, at positions occupying the top of the

hydrophobic tunnel would prevent formation of longer isoprenes.[263] Previous studies suggest that this position directly interacts with FPP and shorter, elongated products. Supporting this, a single point mutation in $UppS_{Ec}$ A69L, located at the top of the hydrophobic tunnel, formed a shorter C_{50} product, with notable levels of C_{30} intermediates. This site (A69) is analogous to L84 in *M. tuberculosis* Rv1086 (**Figure 4.5**).[273-275] These findings are corroborated by an additional study by Kharel et al., in which mutagenesis of *Micrococcus luteus* UppS (accession O82827) residues A72L, F73L, and W78L (to mimic those of *M. tuberculosis* Rv1086) resulted in the production of much shorter products (C_{25} – C_{35}).[272] These sites are analogous to G73, F74, and W79 in *C. crescentus*. In consideration of these findings, the absence of a side chain on G73 of $UppS_{Cc}$ could potentially be involved in regulation of longer BP.

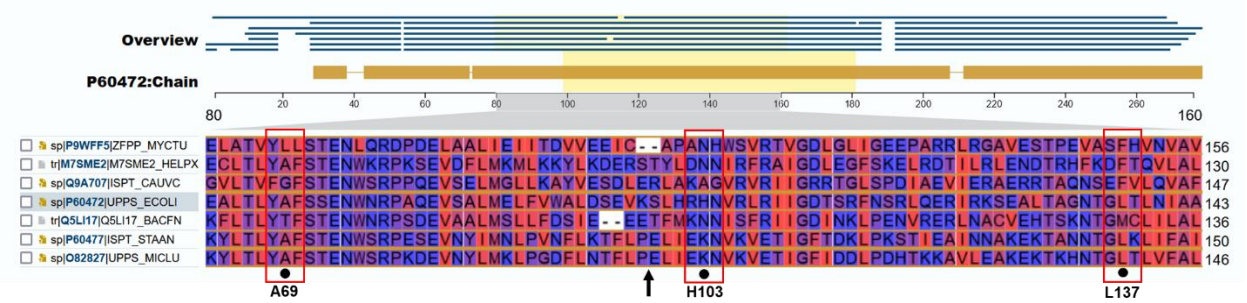

Figure 4.5: Alignment of *Z*-prenyl transferases. Sequence alignment was generated using the UniProt Knowledgebase. Sites of mutagenesis in *E. coli* UppS are indicated by a black circle (●), with the position indicated beneath. Amino acids are color coded based on hydrophobicity from red (hydrophobic) to blue (hydrophilic). A69 is analogous to position L84 in *M. tuberculosis*, A72 in *M. luteus*, and G73 in *C. crescentus*. H103 in *E. coli* UppS is analogous to A107 in *C. crescentus* UppS. The black arrow (↑) indicates the site of insertion of three to six charged residues in *M. luteus* UppS.

As for sites potentially involved in increasing BP chain length, Ko et al. found that a single point mutation at L137A, resulted in predominantly C_{70} prenyl phosphate in the absence of Triton X-100.[263] This residue, amongst others, was chosen as a point of mutation due to its position toward the bottom of the hydrophobic tunnel occupied by the elongated isoprene

chain.[276] In *C. crescentus* UppS, this position is occupied by a Phe residue (F141) (**Figure 4.5**). The bulkiness and hydrophobicity of Leu and Phe residues are comparable; thus, it is not likely that F141 is a significant contributing factor to increased lengths of BP in *C. crescentus* (**Figure 4.6**).[267]

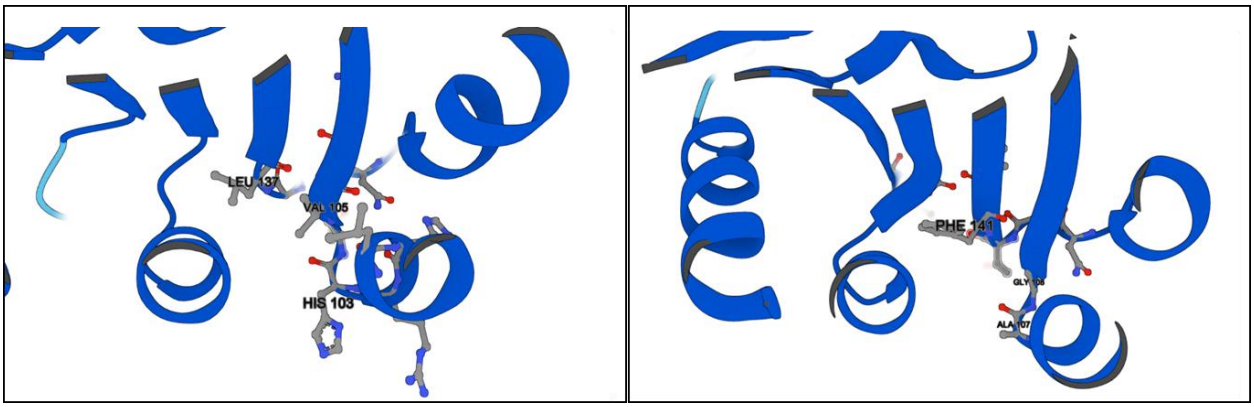

Figure 4.6: Comparison of residues within the hydrophobic tunnel between *E. coli* and *C. crescentus* UppS. Ribbon models were generated using AlphaFold. Images are a close-up of the bottom portion of the hydrophobic tunnel in each protein to provide a spatial comparison of residues implicated in controlling prenyl phosphate chain length. L137 and H103 in $UppS_{Ec}$ are analogous to F141 and A107 in $UppS_{Cc}$, respectively.

In the same study, Ko et al. evaluated H103 and V105 in $UppS_{Ec}$ as a potential regulators of BP chain length as these residues are located at the bottom of the hydrophobic tunnel in helix α3 and strand βC.[263] Similar to the aforementioned mutagenesis studies, the authors proposed that replacing these large residues with Ala would alter BP chain length. In the absence of surfactant, the H103A mutant did not reveal any significant differences in product distribution or major BP products compared to wild-type $UppS_{Ec}$. However, considerably higher ratios of C_{60}, C_{65}, and C_{70} were observed with the V105 mutant compared to wild type. At these positions, $UppS_{Cc}$ possesses an Ala residue (A107) followed by Gly and Val (G108 and V109). For comparison, in other model UppS sequences, A107 and G108 positions are typically occupied by

charged, bulky residues (N, H, or K) (**Figure 4.5**). Perhaps, the presence of neutral, less bulky residues at the bottom of the tunnel in UppS$_{Cc}$ facilitates elongation of BP before release based on the absence of steric or electrostatic repulsions.

In their evaluation of long-chain prenyl transferases (> C_{55}), Kharel et al. also demonstrated that insertion of 3 – 6 charged amino acids in UppS$_{Ml}$ helix α3, which constitutes a portion of the hydrophobic tunnel, resulted in increased product length (C_{60} – C_{75}) (**Figure 4.5**).[272] This portion of the sequence was chosen based on multiple sequence alignment of *Z*-prenyl transferases which revealed that long-chain *Z*-prenyl transferases possess an extra three to seven charged residues at this position. Interestingly, a mutant possessing an extra five Ala residues at this position did not show the same effect. As noted by the authors, this model does not support that sheer expansion of the hydrophobic cavity increases the length of BP. Instead, it implies the significance of polar or charged residues at these positions for increasing chain length.[272] None of the UppS constructs evaluated in this study present additional polar or charged residues at this site, therefore, it is unlikely that this model applies to elongated products found in *C. crescentus*.

Based on the results presented here, it is likely that local cellular environment, lipid composition, or other cell conditions impart some significance in regulating BP length in *C. crescentus* (C_{65} and C_{70}). This is evidenced by slightly shorter main products identified in *E. coli* pUppS$_{Cc}$ lipid extracts (C_{50} to C_{65}). Ultimately, site-directed mutagenesis of UppS$_{Cc}$ will lead to a more defined role of individual amino acid residues in regulating BP length, including F141, G73, A107, and G108. *In vitro* analyses with BP analogues could provide insight into what other factors, including phospholipids or surfactants, promote longer-chain isoprenoids. Intriguingly, amino acid residues mentioned here that are associated with short BP products are not found in

H. pylori UppS, which produced mainly C_{45} and C_{50} BP in *E. coli*; however, the results of recombinant $UppS_{Hp}$ could indicate the presence of slightly shorter, C_{50} or C_{45}, BP in *H. pylori*.

Evaluation of native holdfast intermediates in *C. crescentus* mutants

The discovery of C_{65} and C_{70} BP in *C. crescentus* enabled the selective evaluation of BP(P)-linked glycan profiles in *C. crescentus* holdfast mutants. All *C. crescentus* mutants were generously provided by Dr. David Hershey (**Table 4.4**). HfiA is a small, 8.3 kDa protein that inhibits holdfast production by direct interaction with the HfsJ glycosyltransferase (**Figure 4.7**).[153, 277] Thus, inactivated *hfiA* mutants were also included in this study.

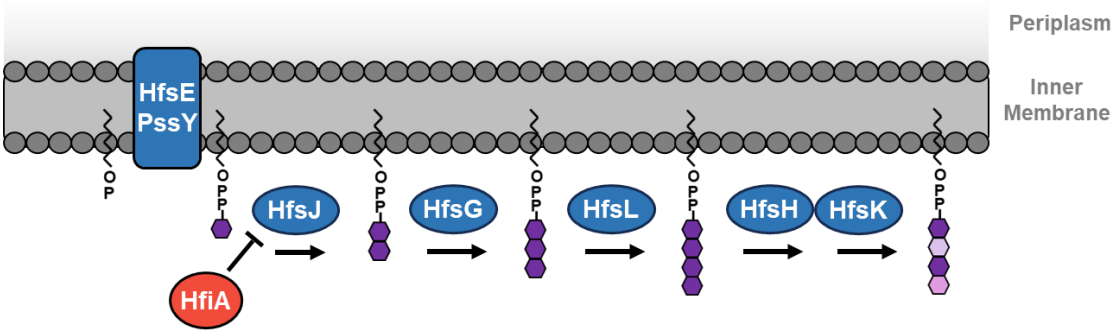

Figure 4.7: Proposed pathway of holdfast oligosaccharide biosynthesis. Sugar modifying enzymes, HfsH and HfsK, are not essential for holdfast biosynthesis but play a significant role in modulating the adhesive properties of holdfast. The precise sequence of enzyme activity is unknown. Sequence alignment and gene annotation strongly suggest HfsE and PssY are initiating transferases. HfsJ may be the next step in the pathway that commits BPP-monosaccharide to the holdfast pathway. HfsJ is directly regulated by the small holdfast inhibitor, HfiA.

Table 4.4: *C. crescentus* strains used to evaluate native, accumulated holdfast intermediates. All strains were provided by Dr. David Hershey.

Organism	Strain Designation	Genotype
C. crescentus CB15	DH103	Wild type
	DH105	Δ*hfsJ*
	DH211	Δ*hfsG*
	DH303	Δ*hfsC*Δ*hfsI*
	DH251	Δ*hfiA*Δ*hfsJ*
	DH247	Δ*hfiA*Δ*hfsG*
	DH1017	Δ*hfiA*Δ*hfsL*
	DH1042	Δ*hfiA*Δ*hfsC*Δ*hfsI*

Based on previous research, it was predicted that accumulation of holdfast intermediates may occur in holdfast mutants, enabling increased sensitivity and detection of such intermediates.[114, 116, 133] To evaluate this, *C. crescentus* cultures were prepared from single colonies and incubated in PYE medium as described by Hershey et al.[33] Concentrated cell extracts were evaluated using LC-MS with SIM for anticipated holdfast intermediates. Total ion chromatograms were evaluated for both BP- and BPP-glycan intermediates based on the previously proposed carbohydrate content of holdfast.[33] For example, DH105 (*C. crescentus* Δ*hfsJ*) was evaluated for a BPP-monosaccharide as anticipated in the proposed model of holdfast biosynthesis (**Figure 4.7**), including C_{65} BPP-GlcNAc, -Glc, -Gal, -GalNAc, and -Xyl. Time course studies were also employed to determine a potential timepoint of detectable levels of BPP intermediates. Density centrifugation, used to isolate swarmer and stalked cells, was also performed to separate holdfast-producing stalked cells from swarmer cells.[278]

To date, native C_{65} BP(P) linked glycan intermediates in *C. crescentus* holdfast mutants have not been identified. A plausible explanation for no discernable glycan intermediates is that mutations in this pathway halt transcription as the result of complex, compensatory feedback

signals. These feedback signals have been the focus of much research concerning *C. crescentus* and its unique lifecycle, including the identification of multiple two-component systems involved in regulating cell adhesion and activation of holdfast.[22, 153, 249, 279] In addition to providing checkpoints for cellular adhesion and proliferation in nutritionally appropriate environments, tight regulation of holdfast biosynthesis could prevent potentially deleterious effects of appropriating BP to holdfast biosynthesis at underutilized and inappropriate segments of the cell cycle.[131, 133, 153] One might also hypothesize that BPP-linked intermediates from other pathways might exist at detectable levels; however, previous investigations of bacterial polysaccharide biosynthesis have shown that native intermediates (BPP-monosaccharide, -disaccharide, etc.) are not detected in wild-type cells.[114, 116]

Substrate specificity of initiating glycosyltransferases, HfsE and PssY: PssY is an initiating phospho-glucosyltransferase

The two proposed initiating glycosyl transferases of holdfast, HfsE and PssY, share transmembrane domain homology with established PGTs WbaP, WcaJ, and WecP, but not WecA (**Figure 4.8**).[**280**] WecA is a phospho-glycosyltransferase found in *E.coli* that initiates O-antigen and ECA biosynthesis.[124] It transfers GlcNac-1-P from UDP-GlcNAc to BP, but can also utilize UDP-GalNAc to a limited extent.[85, 124] WecA contains 11 transmembrane domains, 5 periplasmic loops, and 5 cytosolic loops.[124] WbaP, WecP, WcaJ, and HfsE contain four predicted

membrane domains at the N-terminus and an additional transmembrane domain near the C-terminus. In contrast, PssY contains two predicted membrane domains.

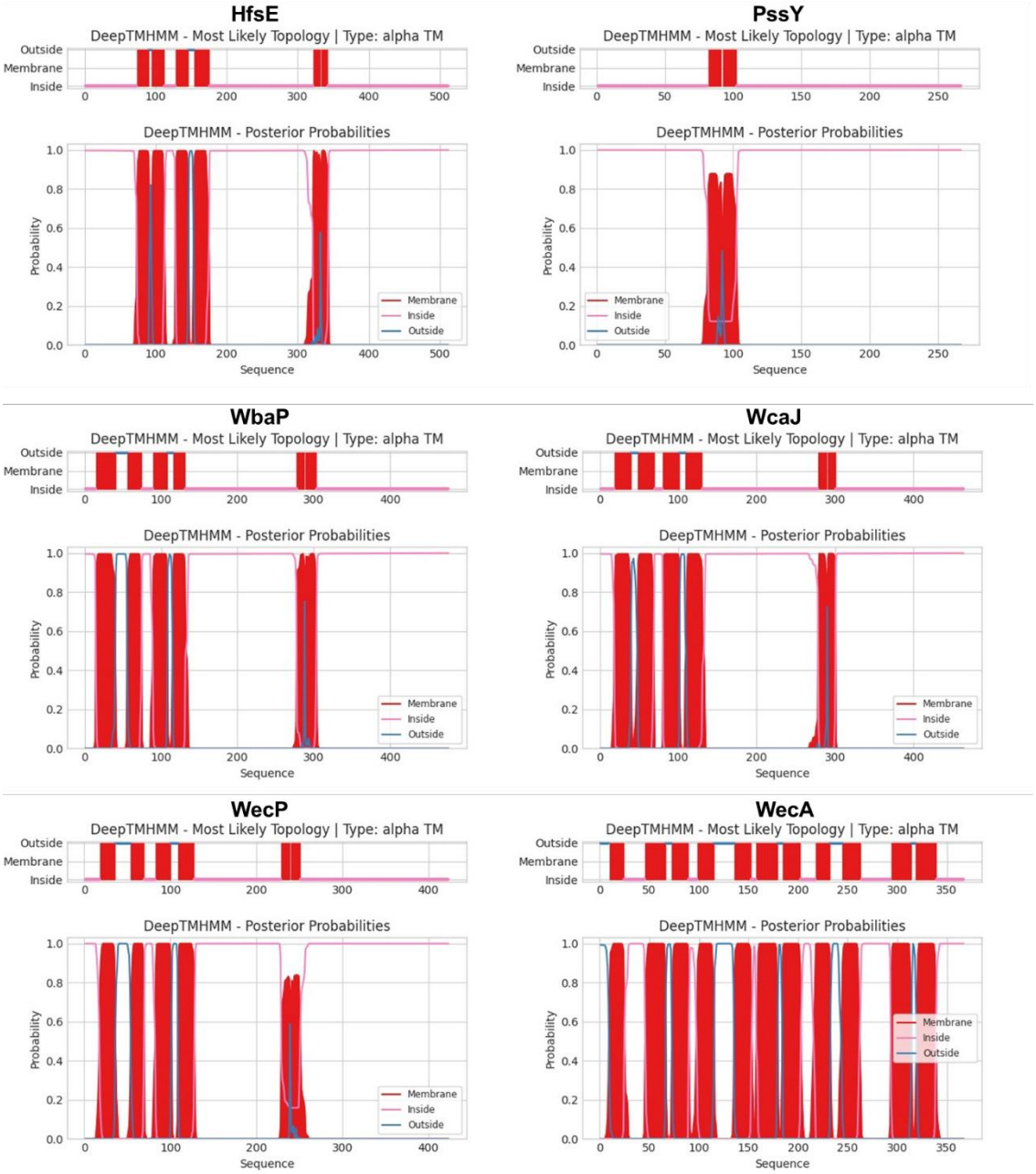

Figure 4.8: Predicted topological models of representative PGTs, including HfsE and HfsY. Transmembrane domain prediction was generated using Deep TMHMM prediction software.[280]

To determine the specificity of the proposed initiating phospho-glycosyltransferase, *hfsE* was overexpressed in *E. coli* RP(DE3) (**Figure 4.9**). Cell envelope fractions harboring HfsE were evaluated *in vitro* using fluorescent 2CN-BP with UDP-Glc, -Gal, -GlcNAc, -GalNAc, and -Xyl donor substrates. However, investigation of initiating glycosyltransferases within cell envelope fractions has presented a few challenges, mainly including the activity of endogenous membrane-bound proteins within *E. coli* cell envelope fractions which obfuscates evidence of recombinant enzyme activity.[85, 115] From repeated evaluation of HfsE cell envelope fractions, it appears that HfsE may transfer P-GlcNAc to 2CN-BP, but attempts to conclusively discern this activity from the activity of endogenous *E. coli* WecA were unsuccessful (**Figure 4.9**). Additionally, another non-specific product was consistently formed in these reactions (5.9 min). This product is attributed to the activity of ArnT, a glycosyltransferase involved in the modification of Lipid A.[115] Transfer of P-Glc to 2CN-BP was not observed in any of these experiments.

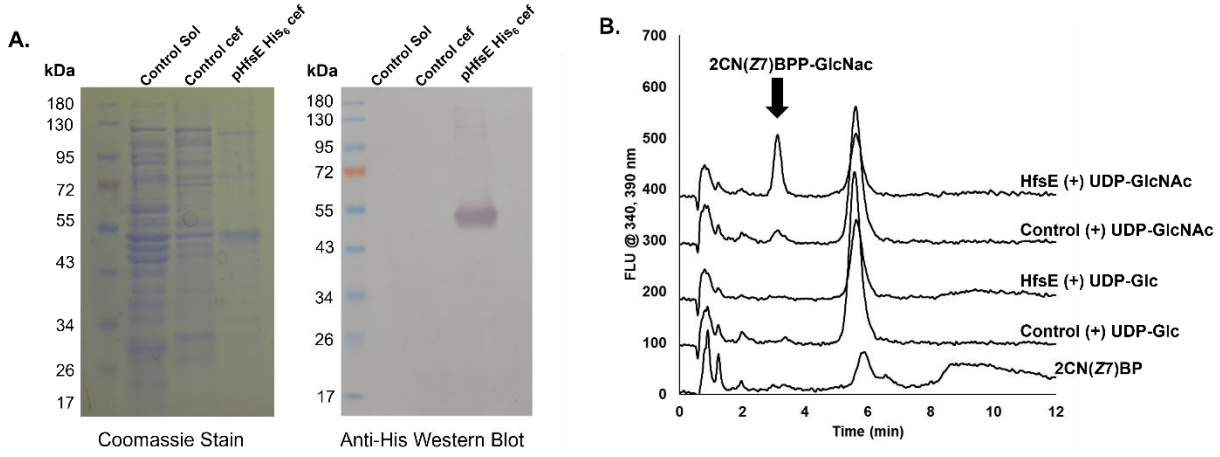

Figure 4.9: Evaluation of HfsE activity *in vitro* with BP analogue substrate. (A) Coomassie stain and Western blot of overproduced His_6-tagged HfsE in *E. coli* BL21(DE3)-RP. (B) RP-HPLC analysis of cell envelope fractions harboring HfsE. HfsE and control reactions with UDP-GlcNAc produce 2CN-BPP-GlcNAc (3.2 min). A new product is also formed at 3.2 min with a cell envelope fraction expressing an empty plasmid. In each reaction containing cell envelope fraction, an additional, non-specific product with an intermediate retention time is also produced at 5.6 min. This product has been attributed to a lipid A modification system in *E. coli* described in Chapter 2.

To circumvent interfering endogenous membrane enzymes (WecA and ArnT), a truncated, soluble mutant, $HfsE_{298}$, was utilized. The ability of $HfsE_{298}$ to complement an Δ*hfsE* mutant was confirmed by Dr. David Hershey (data not shown). Attempts to establish transferase activity of $HfsE_{298}$ with UDP-GlcNAc were not successful. $HfsE_{298}$ was tested *in vitro* with varied lengths of 2CN-BP (*Z*4-*Z*8), varied types and concentrations of surfactants (Triton X-100, n-octyl β-D-thioglucopyranoside, n-dodecyl β-D-maltoside), buffers (pH 6-10), divalent cations (Mn^{2+}, Mg^{2+}, Ca^{2+}, and Zn^{2+}), in the presence or absence of organic alcohols, in the presence or absence of lipids isolated from *C. crescentus*, and in the presence or absence of *C. crescentus* cell lysate. Curiously, a previous study conducted by Patel et al. was also not able to establish substrate specificity of HfsE.[134] They also found that *hfsE* could not complement an *E. coli*

Δ*wcaJ* mutant, but that *E. coli wcaJ* complements a *C. crescentus* Δ*hfsE*Δ*pssY*Δ*pssZ* mutant. WcaJ is an initiating phospho-glucosyltransferase in colanic acid biosynthesis. Nevertheless, the specificity of HfsE unfortunately remains elusive. In future studies, it would be very interesting to see if *hfsE* complements a Δ*wecA* mutant in ECA biosynthesis, where GlcNAc is the first sugar in the ECA oligosaccharide unit.[116, 281]

Previous research has proposed that PssY contributes to holdfast biosynthesis either simultaneously or in the absence of HfsE by adding the first phospho-sugar to BP.[26] It should be noted that PssY is not located in the *hfs* operon[26] In the above-mentioned study, Patel et al. evaluated the specificity of PssY with radiolabeled UDP-Glc, -Gal, and -GlcNAc.[134] These authors found that PssY was specific for UDP-Glc and that *pssY* complements a Δ*wcaJ* mutant in colanic acid biosynthesis.[134] In this study, to produce the first intermediate of holdfast, the activity of PssY was evaluated with 2CN(*Z6*)BP and various UDP-linked sugar substrates, including UDP-Glc, -GlcNAc, -Gal, -GalNAc, -GlcA, - Xyl, and GDP-Man. RP-HPLC analysis of these reactions with fluorescence detection demonstrated that PssY is specific for the UDP-Glc donor substrate and catalyzes the formation of 2CN-BPP-Glc, which is consistent with previous literature (**Figure 10)**. This analysis corroborates evidence that the first sugar of the holdfast oligosaccharide unit could be glucose, or that downstream Hfs glycosyltransferases can utilize more than one monoglycosylated acceptor substrate.

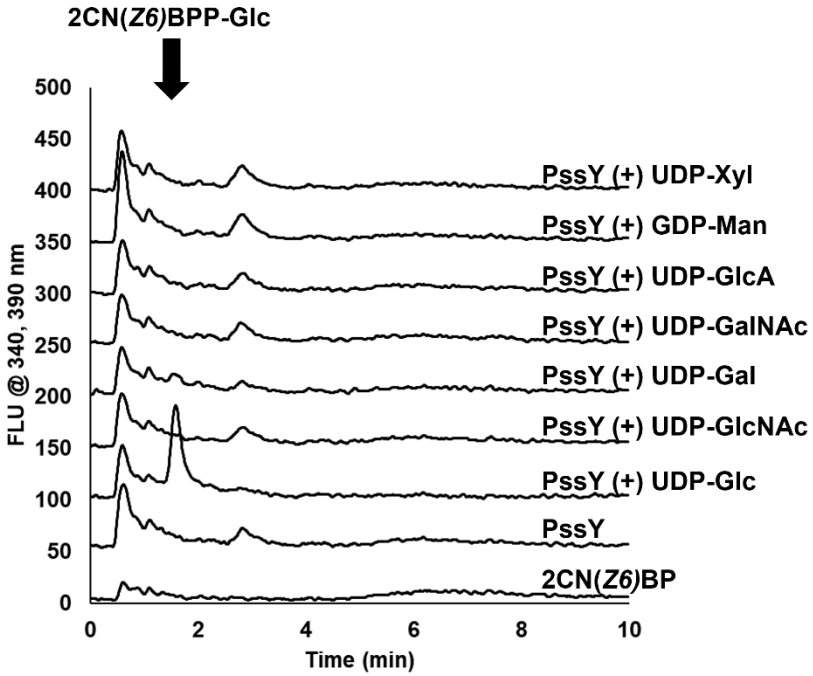

Figure 4.10: PssY is an initiating phospho-glucosyltransferase. PGT activity of PssY was evaluated with fluorescent 2CN(Z6)BP acceptor substrate and various UDP-linked sugar donor substrates using RP-HPLC. The formation of a peak at 1.8 min indicates the addition of a phospho-sugar to BP only in the presence of the UDP-Glc donor substrate.

HfsJ may be specific for uronic acid substrates in the absence of cyclic-di-GMP

HfsJ, a predicted member of the WecG/TagA glycosyltransferase family, is the second proposed glycosyltransferase that commits BPP-monosaccharide to holdfast biosynthesis. HfsJ is heavily regulated at both transcriptional and post-translational levels, including direct inhibition by HfiA post-translationally (**Figure 4.7**), and transcriptionally by cell cycle regulators.[153] Evidence also suggests that HfsJ is allosterically activated by cyclic-di-GMP.[282] To assess HfsJ glycosyltransferase activity *in vitro*, HfsJ was overexpressed, extracted from cell lysates with cholate and partially purified with Ni-NTA affinity chromatography (**Figure 4.11**). As with other members of the WecG/TagA family, extraction with detergent was necessary to procure soluble

protein as it was determined through cell fractionation that HfsJ is membrane-associated. HfsJ does not contain any predicted transmembrane domains.

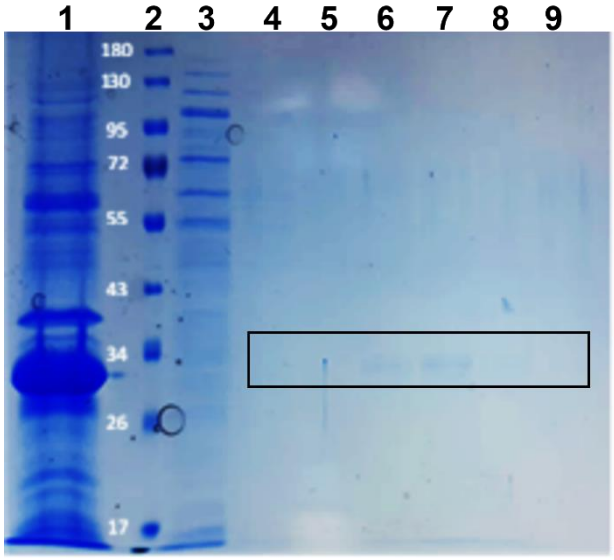

Figure 4.11: SDS-PAGE of HfsJ overproduction and purification. HfsJ is observed in cell envelope fractions of *E. coli* C41(DE3). Cell envelope fractions were solubilized with 20 mM cholate, and HfsJ was purified with affinity chromatography. Lane 1: cell envelope fraction, Lane 2: ladder, Lane 3: flow through, Lane 4: wash, Lane 5-9: elutions. HfsJ is approximately 35 kDa.

To evaluate HfsJ and other Hfs glycosyltransferase specificity for BPP-monosaccharides, initiating phospho-glycosyltransferases WecA, WecP, Cps2E, and WbaP were used to produce tagged, 2CN-BPP-GlcNAc, -GalNAc, -Glc, and -Gal, respectively (**Figure 4.12**). Monoglycosylated products of these reactions were purified by HPLC. To evaluate enzyme specificity, HfsJ was incubated with monoglycosylated 2CN-BPP-Glc and 2CN-BPP-GlcNAc acceptor substrate and various sugar nucleotides. In these experiments, UDP-N-acetyl-mannosaminuronic acid (UDP-ManNAcA) was included due to HfsJ similarity to *E. coli* WecG (28% identity; 44% similarity). WecG is a glycosyltransferase that transfers ManNAcA to BPP-GlcNAc in the biosynthesis of *E. coli* enterobacterial common antigen (ECA). UDP-ManNAcA

is challenging to procure in terms of both cost and availability, therefore, WecB and WecC enzymes from the enterobacterial common antigen pathway of *E. coli* were cloned, overexpressed, and used to produce UDP-ManNAcA from UDP-GlcNAc (**Figure 4.13A**).[116, 283] WecB is a UDP-GlcNAc 2-epimerase, that produces UDP-ManNAc. WecC is a dehydrogenase that produces UDP-ManNAcA from UDP-ManNAc.[116] In HfsJ reactions, unpurified WecBC **r**eactions were used as the source of UDP-ManNAcA substrate.

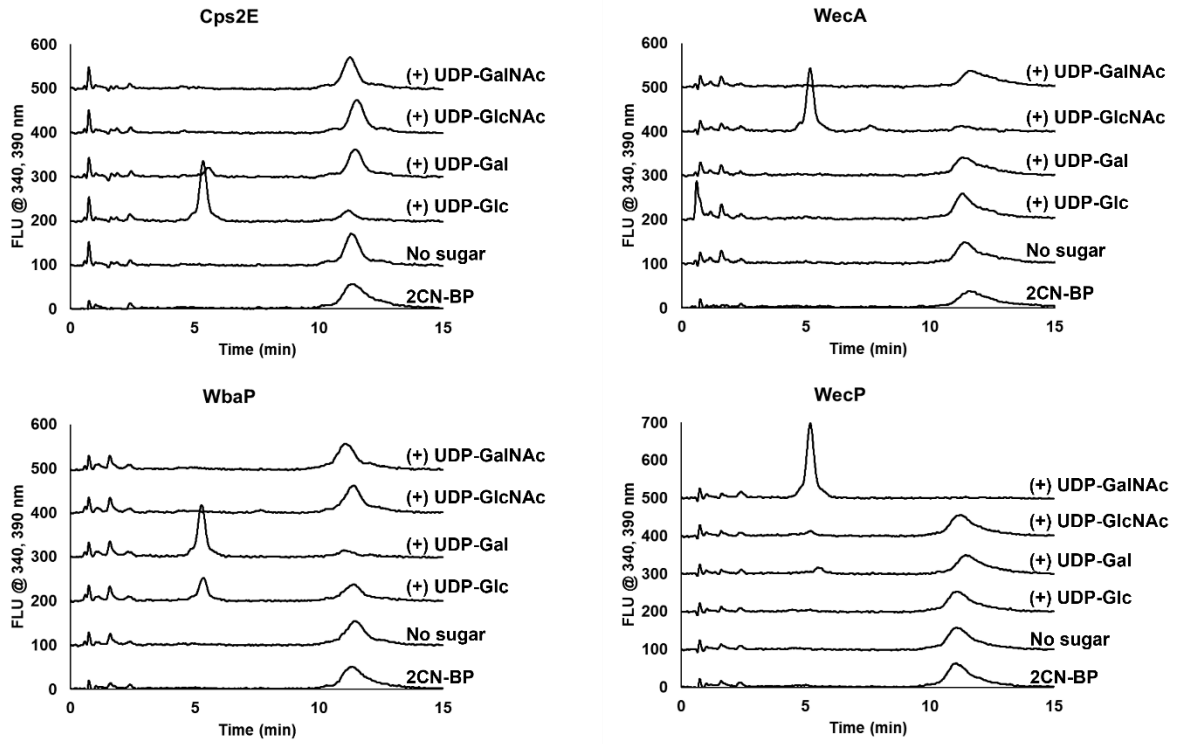

Figure 4.12: Chemoenzymatic synthesis of fluorescent BPP-linked monosaccharides. Initiating phospho-glycosyltransferases WecA, Cps2E, WbaP, and WecP were probed for specificity with sugar-nucleotides using fluorescent 2CN-BPP, as previously reported. These initiating phospho-glycosyltransferases were used to procure HPLC purified fluorescent BPP-linked monosaccharides, 2CN-BPP-Glc, 2CN-BPP-Gal, 2CN-BPP-GlcNAc, and 2CN-BPP-GalNAc.

Interestingly, HPLC analysis of reactions containing HfsJ and 2CN-BPP-Glc acceptor revealed new product only with UDP-ManNAcA as the donor substrate (**Figure 4.13A**). This is noted by the reduction in area of the 2CN-BPP-Glc peak (4.5 – 5.1 min) and new product (2.7

min) with a nearly two-minute less retention time, indicative of the addition of a more polar, uronic acid compared to a neutral sugar. Analysis of reactions containing HfsJ and 2CN-BPP-GlcNAc acceptor (4.2 – 4.4 min) indicated transferase activity with two different uronic acid donor substrates, UDP-GlcA and UDP-ManNAcA (**Figure 4.13B)**. A new product is formed with UDP-GlcA as the donor substrate at 2.5 min, and with UDP-ManNAcA also at 2.5 min. Notably, the utilization of multiple acceptor substrates added to the challenge of determining whether Glc or GlcNAc is the first sugar in the holdfast oligosaccharide. However, this analysis could suggest that the second proposed sugar in the holdfast oligosaccharide is a uronic acid.

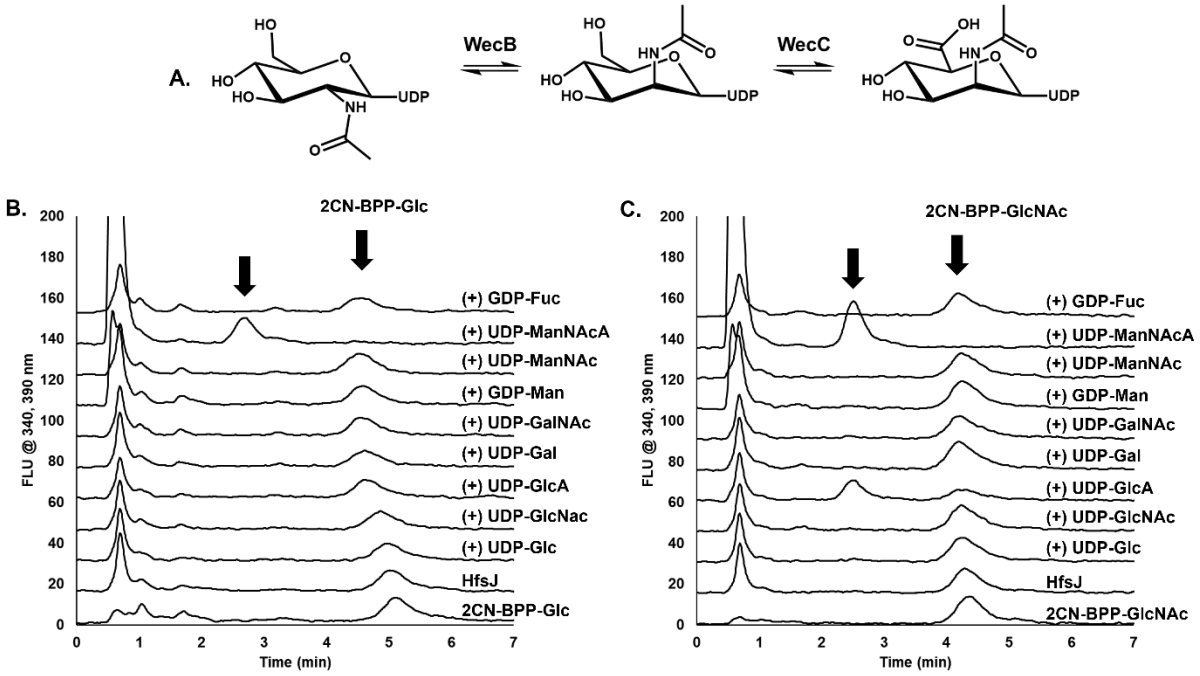

Figure 4.13: HfsJ may be specific for uronic acid substrates. (A) Schematic of UDP-ManNAcA production by WecB and WecC from *E. coli*. (B) HfsJ was evaluated with 2CN(*Z*8)BPP-Glc as the acceptor substrate, and various NDP-sugars. A new product is observed at 2.7 min only when UDP-ManNAcA is present. (C) HfsJ activity was evaluated with 2CN(*Z*8)BPP-GlcNAc as the acceptor substrate. New products were observed at 2.5 min with UDP-ManNAcA and -GlcA present.

Contrary to this evidence, Fiebig et al. found that *E. coli wecG*, encoding an N-acetyl mannosaminuronic acid (ManNAcA) transferase, and *Bacillus subtilis tagA*, encoding an N-

acetylmannosaminyl (ManNAc) transferase, do not complement a Δ*hfsJ* adhesion defects.[10] Compositional analysis of holdfast carbohydrate content also did not reveal a uronic acid sugar.[33] If HfsJ does indeed transfer GlcA, a UDP-GlcA decarboxylase could be a potential explanation for the existence of xylose in the holdfast carbohydrate content. Such a factor has not been identified in genetic analyses of holdfast biosynthesis and *C. crescentus* adhesion but does exist as a predicted protein in the *C. crescentus* CB15 proteome (gene cc_1146). A BLAST of proteins similar to WecC in *C. crescentus* CB15 does reveal a potential dehydrogenase, which is annotated as a UDP-glucose 6-dehydrogenase (E value 1.4 e^{-42}), but there were no significant hits for a WecB homolog.

BoWecG from *Brucella ovis*, complements an *hfsJ* holdfast mutant and is a robust glucosyltransferase

Evidence from our collaborator indicates that a WecG homologue from *Brucella ovis* (BoWecG) restores holdfast production in a *C. crescentus* Δ*hfsJ* mutant (data not shown) (**Figure 4.14**). Based on this, it was proposed that the specificity of HfsJ may be inferred by that of BoWecG. BoWecG (GenBank WP_006015053.1) is 32 % identical and 48 % similar to *E. coli* WecG.

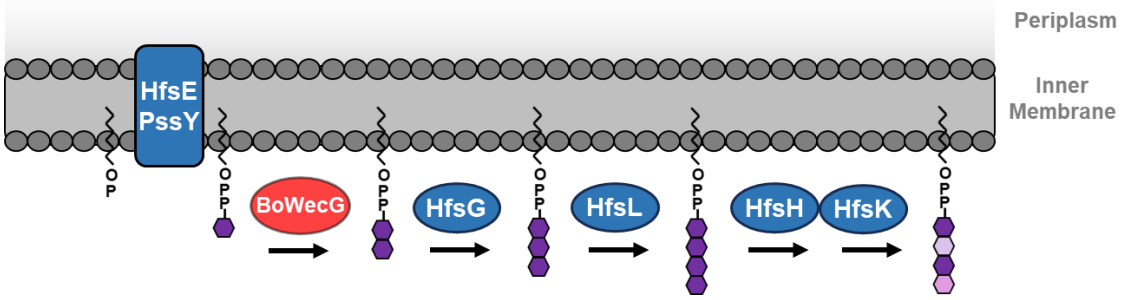

Figure 4.14: BoWecG from *B. ovis* complements a Δ*hfsJ* mutant in cell adhesion and holdfast production.

To determine the preferred acceptor and donor substrates of BoWecG, reactions containing monoglycosylated 2CN-BPP-Glc, 2CN-BPP-GlcNAc, 2CN-BPP-Gal, or 2CN-BPP-

GalNAc acceptor substrates and NDP-sugars were incubated with BoWecG. Reactions were analyzed with HPLC to confirm the extent of transfer. Like HfsJ, BoWecG utilized both the 2CN-BPP-Glc and 2CN-BPP-GlcNAc acceptor substrates, but not 2CN-BPP-Gal or 2CN-BPP-GalNAc (**Figure 4.15**). With 2CN-BPP-Glc as the acceptor substrate (3 min), transfer was observed with multiple donor substrates, including UDP-Glc, UDP-GlcNAc, UDP-Gal, and GDP-Man (2.6 min) (**Figure 4.15A**). Curiously, two products are observed in reactions containing UDP-GlcNAc (2.6 and 2.2 min). The most reasonable explanation for this is that BoWecG appends two neutral sugars to 2CN-BPP-Glc. With 2CN-BPP-GlcNAc as the acceptor (3.9 min), a new product is formed in the presence of UDP-Glc at 3.3 min (**Figure 4.15C**). This small shift in retention time is indicative of the addition of a neutral sugar to 2CN-BPP-GlcNAc. A new, albeit much less abundant product at 2.4 min is observed in the presence of UDP-GlcA.

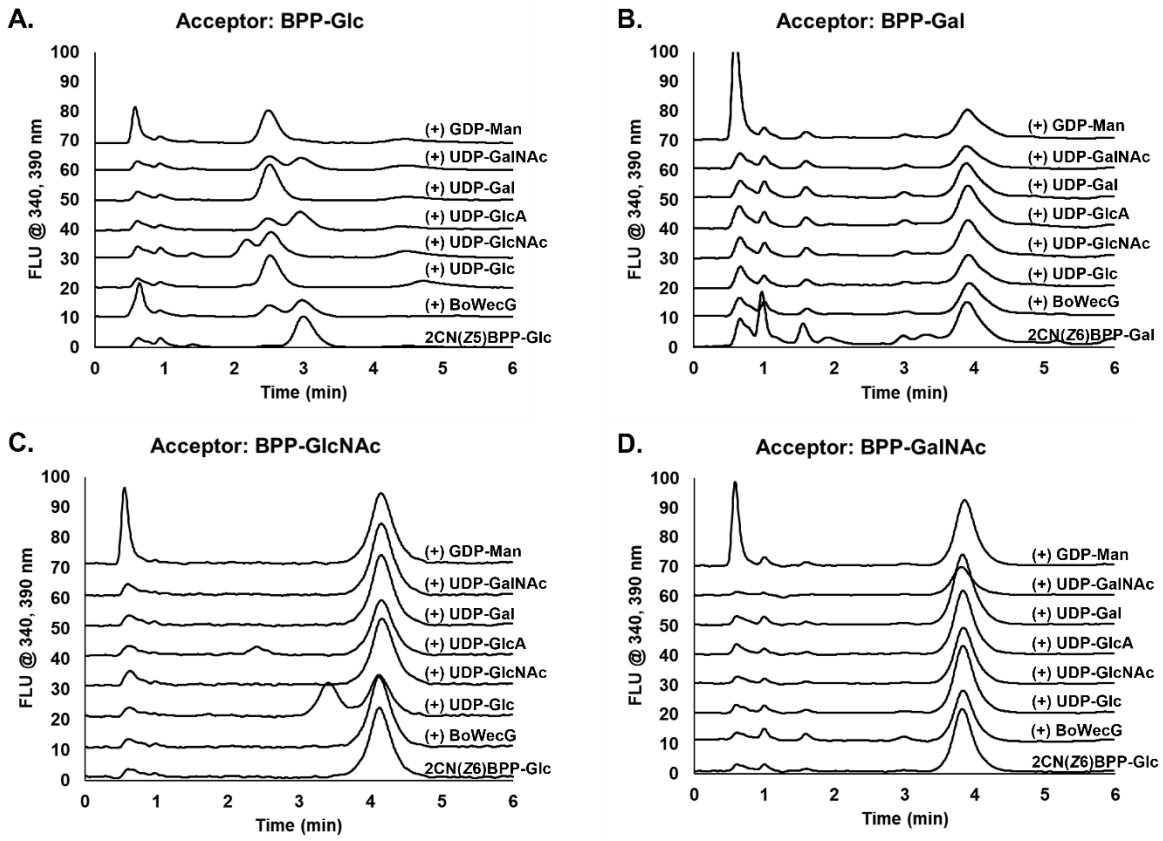

Figure 4.15: BoWecG utilizes both 2CN-BPP-Glc and -GlcNAc as an acceptor substrate. (A) BoWecG specificity evaluated with 2CN-BPP-Glc acceptor substrate and NDP-sugars. A new product is observed at 2.6 min in all reactions that contain BoWecG. A second product is observed at 2.2 min only in the presence of UDP-GlcNAc. (B) BoWecG specificity evaluated with 2CN-BPP-Gal acceptor substrate. (C) BoWecG specificity evaluated with 2CN-BPP-GlcNAc acceptor substrate. New products are only observed in the presence of UDP-Glc (3.3 min) and UDP-GlcA (2.4 min). (D) BoWecG specificity evaluated with 2CN-BPP-GalNAc acceptor substrate. Reactions were not quenched.

Upon further investigation, it was discovered that with 2CN-BPP-Glc as the acceptor substrate, the presence of BoWecG alone (no NDP-sugar) was enough to form a new product of a lesser retention time (**Figure 16A**). A closer investigation of BoWecG activity revealed that concentrations as low as 150 nM resulted in almost half the turnover of 2CN-BPP-Glc substrate after 10 min (**Figure 16A**). In fact, this product was evaluated with LC-MS and SIM, and it was

discovered that BoWecG, without the addition of NDP-sugar, appends a hexose (or molecule of similar mass that results in similar retention characteristics) to 2CN-BPP-Glc (**Figure 16C**). Recognizing the stoichiometry of this reaction, as it contains 5 µM 2CN-BPP-Glc and 150 nM BoWecG, it is speculated that UDP-hexose either remained with the HPLC purified 2CN-BPP-Glc substrate, or that non-stoichiometric levels of UDP-Hexose are present in purified preparations of BoWecG. It should be noted that BoWecG was not purified in the presence of UDP-sugar. Revisiting BoWecG specificity with this in mind, reactions containing 5 nM BoWecG and 1 mM NDP-sugar were quenched after 20 min and evaluated by HPLC (**Figure 16B**). In this instance, HPLC analysis of crude reactions showed that transfer only occurred with UDP-Glc as the donor substrate.

Overall, these results indicate that BoWecG is a robust glucosyltransferase, but may be capable of transferring other UDP-sugars, particularly those that are neutral, to a BPP-Glc acceptor. Further analyses are required to determine the precise NDP-sugar specificity of BoWecG. BoWecG could prove to be a useful enzyme in the design and implementation of complex polysaccharide biosynthesis systems. Combined with complementation analyses and comprehensive genetic probes of holdfast biosynthesis, these results also suggest that HfsJ may transfer a neutral sugar in holdfast assembly.

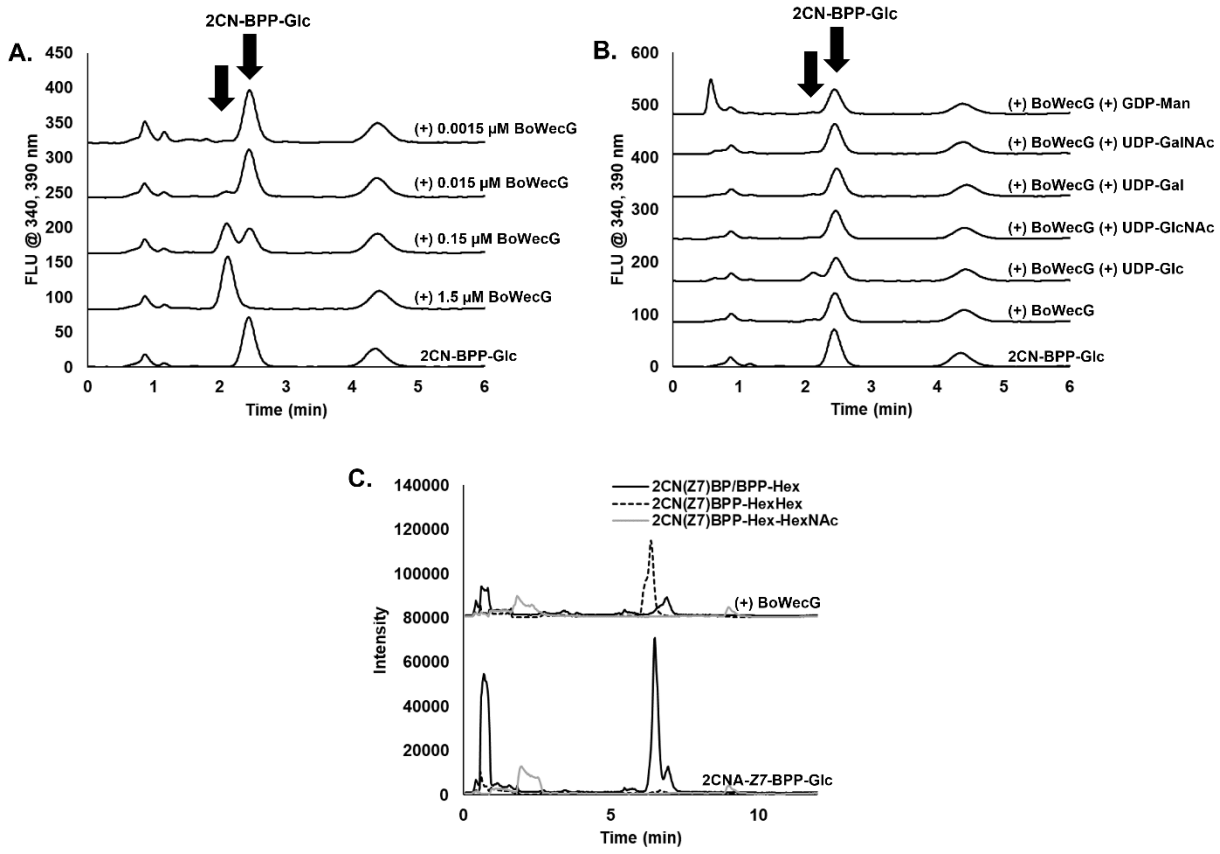

Figure 4.16: Purified BoWecG forms new product without exogenous NDP-sugar. Transferase activity of BoWecG was evaluated with 2CN(Z7)BPP-Glc acceptor substrate. (A) Quenched reactions (20 min) containing serial dilutions of BoWecG without surfactant. (B) Quenched reactions (20 min) containing 5 nM BoWecG and 200 µM NDP-sugar. (C) Unquenched BoWecG reaction (no NDP-sugar) evaluated with LC-MS and SIM. Reactions were monitored for neutral hexose and N-acetylhexosamine additions. 2CN(Z7)BP $[M-H]^-$ and 2CN(Z7)BPP-Hex $[M-H]^-$ 1067.59 were monitored on the same channel; 2CN(Z7)BPP-Hex-Hex $[M-H]^-$ 1229.64; 2CN(Z7)BPP-Hex-HexNAc $[M-H]^-$ 1270.67.

HfsG is a glycosyltransferase that transfers two glucose or two galactose molecules to BPP-Glc

To determine substrate specificity of HfsG, purified enzyme was first evaluated with 2CN-BPP-Glc and -GlcNAc and various UDP-sugar donor substrates. HPLC analysis of crude reactions containing the 2CN-BPP-Glc acceptor indicated new products with UDP-Glc and -Gal present (**Figure 4.17**). More interestingly, it was noted that this new product's retention time was

reduced by >1 min, which in these studies, is not indicative of the addition of a single, neutral sugar. To investigate further, similar reactions were prepared, but quenched after 10 min and evaluated by HPLC. Surprisingly, this analysis showed two distinct products, indicating the transfer of two Glc molecules. Based on these results, one may hypothesize whether HfsG may append branching units to holdfast oligosaccharide. These branching units have been proposed in the most recent model of holdfast carbohydrate composition.[33] This hypothesis is based on evidence provided by Hershey et al., that terminal galactose is detected as minor components suggesting that it may be an occasional branching unit displayed on the holdfast polysaccharide.[33]

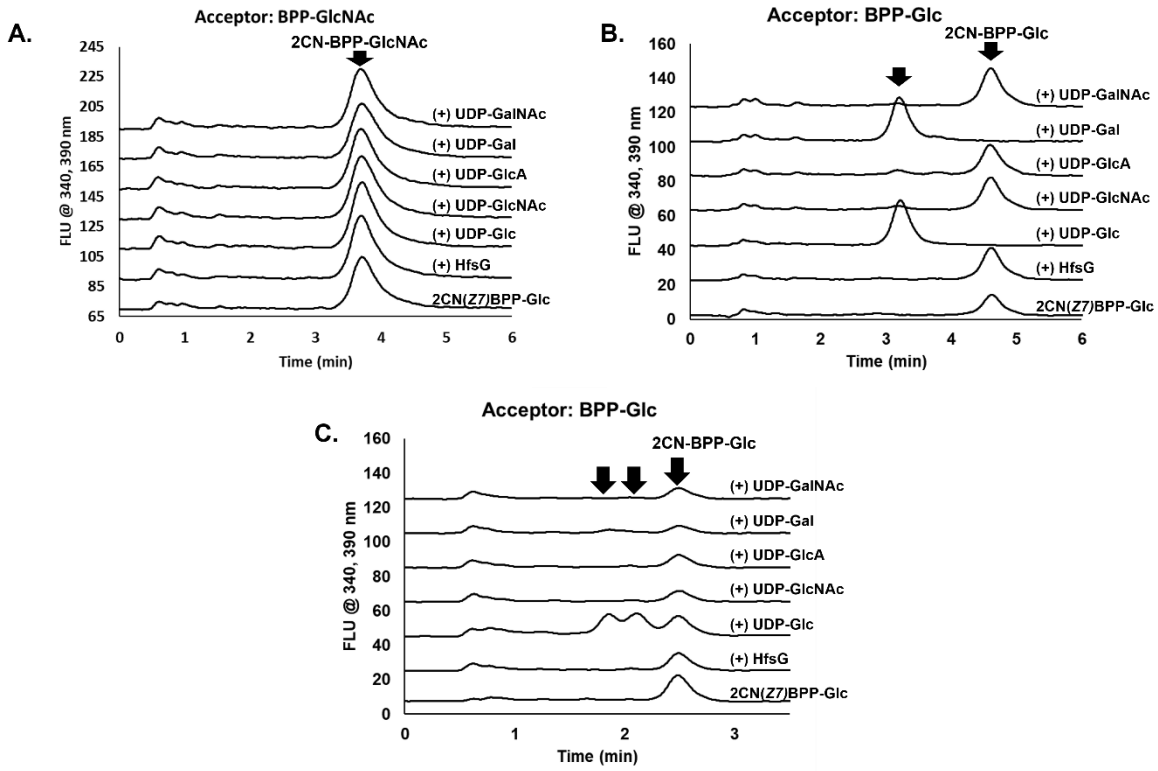

Figure 4.17: HfsG transfers two Glc or two Gal molecules to 2CN(*Z*7)BPP-Glc acceptor substrate. HPLC analysis of HfsG glycosyltransferase activity revealed the addition of multiple sugar substrates. (A) HfsG with 2CN-BPP-GlcNAc acceptor substrate and various UDP-sugar donor substrates. No new products are observed. (B)HfsG with 2CN-BPP-Glc (4.6 min) as the acceptor substrate. A new peak is observed when HfsG is incubated with UDP-Glc or Gal (3.2 min). (C) Quenched reactions with HfsG, 2CN-BPP-Glc acceptor substrate and UDP-Glc donor substrate reveal the likely addition of two Glc molecules.

MATERIALS AND METHODS

General

All *C. crescentus* strains and plasmids used for overproduction of Hfs enzymes were provided by Dr. David Hershey at the University of Wisconsin-Madison (**Table 4**). Preparations of purified HfsJ, HfsH, BoWecG, soluble $HfsE_{298}$, and cell envelope fractions of HfsE and PssY were also kindly provided by Dr. David Hershey. All UppS plasmids were purchased from GenScript. Accession numbers of UppS enzymes are provided in **Table 3**. All sequence alignments were

performed with the Uniprot Knowledgebase, and all protein structures were generated with using the AlphaFold Protein Structure Database.[267, 274, 284, 285] Predicted transmembrane domains and topological models were generated using the Deep TMHMM prediction software.[280] 2CN-BP and -BPP (Ex: 340, Em: 390 nm) substrates was prepared as previously described.[85, 212]

ESI-LC-MS of cell extracts

LC-MS was performed on an Agilent 1260 Infinity II LC system equipped with a fluorescence detector and single quadrupole mass spectrometer. All analyses were performed with LC-MS grade solvents using a Waters Xbridge Peptide BEH C18 column (3.5 µm, 4.6 x 50 mm, 300 Å) at a flow rate of 1 mL/min in negative ion mode. For all analyses, the column temperature was 30 °C. Mobile phase A was 0.1% ammonium hydroxide and mobile phase B was n-propanol. Cell extracts and reactions were evaluated with a 15-minute linear gradient of 15 – 75 % B, then raising to 95 % B in 1 min, with an isocratic hold at 95 % C for 1 min. Solvent B was then decreased to 15% over 3 min, with a post run at 15 % B for 2 min. MS parameters for each injection were set to a nebulizer pressure of 50 psi, drying gas temperature of 350 °C, and capillary voltage of 4000 V. Only LC-MS grade solvents and reagents were used for ESI-LC-MS.

To evaluate length of BP in *E. coli* cells overexpressing UppS, separate 5 mL cultures of *E. coli* C41 (DE3) harboring UppS plasmids were prepared in Lysogeny Broth. Once cultures reached an OD_{600nm} of ~0.6, they were induced with 1 mM IPTG and incubated overnight at 30 °C with shaking at 220 rpm. Cells were then pelleted at 5,000 x g for 15 min in glass centrifuge tubes. The supernatant was discarded, and cell pellets were resuspended in a single-phase Bligh and Dyer solution (0.8:1.0:2:0 water:chloroform:methanol).[196] Cell suspensions were incubated

for 20 min at room temperature before centrifugation at 5,000 x g for 15 min to remove insoluble materials. The supernatant was moved to a clean, glass culture tube and dried under vacuum. Samples were then resuspended in 200 µL of a 1:1 solution of 0.1 % ammonium hydroxide and n-propanol. Injection volumes were 5 µL.

To evaluate native BP and BP(P)-linked glycans in *C. crescentus*, 5 mL cultures were prepared in PYE broth and incubated overnight at 30 °C for 48 hr with shaking at 200 rpm. Cells were then pelleted at 10,000 x g and lysed with a single-phase Bligh and Dyer Solution (0.8:1.0:2.0 water:chloroform:methanol).[196] The supernatant was moved to a clean glass culture tube and dried under vacuum overnight. The clarified lysate was resuspended in 200 µL of a 1:1 solution of 0.1 % ammonium hydroxide and n-propanol. Total ion chromatograms were collected from 400 – 2000 *m/z*. Injection volumes of *C. crescentus* extracts were 20 µL.

WecA reactions with *C. crescentus* lipid extracts

WecA, from *E. coli* was used to evaluate whether proposed C_{65} BP from *C. crescentus* cell extracts could be utilized by an initiating glycosyltransferase. Cell envelope fractions harboring overproduced WecA were prepared from *E. coli* C43(DE3) cells as previously described.[85] *C. crescentus* cell extracts (50 µL) were mixed with 25 µL of DMSO, and dried under a stream of air until approximately 25 µL total remained. Reactions with WecA contained 200 mM Bicine pH 8, 5 mM $MgCl_2$, 100 mM KCl, 15 mM cholate, 1 mM UDP-GlcNAc, 0.05 mg/mL cell envelope fraction, and 2 µL of *C. crescentus* extract in DMSO. Reactions (20 µL) were incubated at 37 °C for 1 hr prior to LC-MS analysis. Control reactions contained only cell extracts (no WecA). To evaluate whether WecA utilized proposed C_{65} BP as a substrate, 10 µL

of these reactions were injected and evaluated by LC-MS as described above using SIM for C_{65}BP ($[M-H]^-$ 981.78), C_{65}BPP-GlcNAc ($[M-H]^-$ 1264.83), and C_{65}BPP-Glc ($[M-H]^-$ 1223.80).

Overproduction of HfsE and preparation of cell envelope fractions

To overproduce full-length HfsE, a 250 mL cell culture of *E. coli* BL21(DE3)-RP was grown to an OD_{600} 0.6 and induced with 0.5 mM IPTG. The culture was incubated at 16°C overnight and cells were harvested by centrifugation at 5000 x g for 15 min. Cells were then lysed in lysis buffer (50 mM Tris pH 8.0, 300 mM NaCl, 20 mM Imidazole) with sonication. Lysates were clarified by centrifugation at 2500 x g for 20 min prior to ultracentrifugation at 150,000 x g for 60 min. The supernatant was discarded, and cell envelope fractions were homogenized in 50 mM Tris pH 8.0, 300 mM NaCl, and a 10 % glycerol solution and stored at -80 °C. Overproduction of 6X His-tagged HfsE was confirmed by 10 % SDS-PAGE and anti-His Western blotting.

Overproduction and purification of HfsJ

To obtain purified HfsJ, 1 L of *E. coli* C41(DE3) pHfsJ grown to an OD_{600} of 1.0 at 37 °C with shaking at 220 rpm before induction with 1 mM IPTG. Cultures were then incubated overnight at 37°C with shaking at 220 rpm. Cells were pelleted at 5000 x g for 10 min and resuspended in 20 mL of lysis buffer (50 mM Tris-HCl pH 7.4, 300 mM NaCl, 15 mM cholate, 20 mM Imidazole). Cells were lysed twice with sonication and centrifuged at 200,000 x g for 1 hr. Aliquots from resulting soluble and membrane fractions were reserved for SDS-PAGE analysis. Membrane fractions were resuspended and homogenized in lysis buffer containing 20 mM cholate, agitated at 4°C for overnight, and then centrifuged at 150,000 x g for 30 min. Solubilized HfsJ was purified using Ni-NTA. Elutions were stored in 20% glycerol at -80°C.

Production of UDP-N-acetylmannosaminuronic acid

Conditions for WecB and WecC were used as previously reported.[283] Reactions consisted of 4 mM UDP-GlcNAc, 100 mM Tris pH 9.0, 20 mM DTT, 8 mM NAD^+, 12 μM WecB, and 2 μM WecC and were incubated at 37°C for 1 hr before storage at -20°C. Crude WecB/WecC reactions were used for HfsJ glycosyltransferase assays and were not confirmed for UDP-ManNAcA production prior to use. Control reactions did not contain WecB or WecC.

Monitoring glycosyltransferase reactions with RP-HPLC

All fluorescence-based HPLC analyses of glycosyltransferase reactions were performed on an Agilent 1100 LC system equipped with a VWD and FLD using an Agilent Zorbax XBD-C18 column (3 μm, 4.6 x 100 mm, 80 Å). Mobile phase A was 100 mM ammonium bicarbonate, and mobile phase B was n-propanol. The column temperature was maintained at 30 °C and the flow rate was 1 mL/min.

HfsE reactions contained 2 μM 2CN-*Z*7-BP, 50 mM Tris-acetate (pH 7.5), 5 mM $MgCl_2$, 15 mM sodium cholate, 100 mM KCl, and 1 mM UDP-Glc or 1 mM UDP-GlcNAc. Control reactions contained cell envelope fractions of *E. coli* BL21(DE3)-RP expressing an empty vector. PssY reactions contained 1 μM 2CN-*Z*7-BP, 200 mM Bicine pH 8, 5 mM $MgCl_2$, 100 mM KCl, 15 mM cholate, 100 μM NDP-sugar, 0.10 mg/mL cell envelope fraction. PssY control reactions did not contain NDP-sugar.

BoWecG was screened for glycosyltransferase activity with each of the isolated products from initiating phospho-transferases WecA, WecP, WbaP, and Cps2E, 2CN-BPP-GlcNAc, 2CN-BPP-GalNAc, 2CN-BPP-Gal, and 2CN-BPP-Glc, respectively. Reactions contained 200 mM Bicine pH 8.0, 5 mM $MgCl_2$, 100 mM KCl, 20 mM DTT, 15 mM cholate, 5 μM 2CN-BPP-

monosaccharide, 1 mM NDP-sugar, and 300 nM BoWecG. Reactions were incubated at 30°C. Equal volumes of isopropanol were added to quenched reactions.

HfsG was also screened for glycosyltransferase activity with 2CN-BPP-monosaccharides. Reactions contained 200 mM Bicine pH 8.0, 100 mM NaCl, 5 mM $MgCl_2$, 20 mM DTT, 15 mM sodium cholate, 5 μM 2CN-BPP-Glc or 2CN-BPP-GlcNAc, 1 mM sugar, and 250 nM HfsG. Reactions were incubated overnight at 25°C prior RP-HPLC analysis. Equal volumes of isopropanol were added to quenched HfsG reactions.

CHAPTER 5: CONCLUSIONS

Bacterial surface glycans have been recognized for decades as critical factors affecting pathogenicity and have been significantly implicated in human health as potent activators of innate and adaptive immune responses.[286-288] Moreover, they represent a vast, untapped source of renewable biopolymers. While the implications and applications of bacterial glycans continue to expand, the tools to investigate these structures have undoubtedly lagged behind that of proteins and nucleic acids. One might imagine how remarkably fast the field of glycobiology would advance if we could remodel the glycan code to enable capture and isolation, like proteins, or encode unique glycan structures that can be reconstituted and amplified in a single-pot reaction. As demonstrated here, using *E. coli* as a vessel, analogous processes can be achieved and is also evidenced by new, burgeoning technologies in recombinant polysaccharide biosynthesis.[168] These models are underpinned by glycan detection strategies, strategic investigations of precise biosynthesis mechanisms, and structural characterization. All-encompassing, these tools will advance unique carbohydrate structures as advantageous biopolymers in medicine and industry, and illuminate targeted opportunities for combating antimicrobial resistance.[216, 289]

NEW STRATEGIES FOR EVALUATING PATHWAYS OF POLYMYXIN RESISTANCE IN GRAM-NEGATIVE PATHOGENS

Modification of the lipid A of LPS with cationic monosaccharides is a significant contributor to antibiotic resistance in many recognized pathogens such as *E. coli*, *P. aeruginosa*, *Yersinia pestis, Salmonella* Typhimurium, and *Bordetella pertussis*.[79, 176, 185, 290] The strategies described in Chapter 2 firstly provided opportunities to directly evaluate key enzymes involved in intrinsic cationic antimicrobial resistance in *E. coli*, including the characterization of ArnD. These

methods provide an advantage in both speed and efficacy and can be broadly applied to other polymyxin-resistant pathogens. Serendipitously, screening for polymyxin resistance (lipid A modification with Ara4N) in *E. coli*, in our case, was as simple as supplying exogenous labeled BP to cell envelope fractions and measuring the retention time and *m/z* of the output. Moreover, treatment of cells with excess Fe^{3+} and its effect on induction of lipid A modification could be observed in only cell envelope fractions treated with 2CN-BP, presenting a rather simple approach to qualitatively evaluate external stimuli and lipid A modification with cationic monosaccharides (**Figure 2.4**). These techniques enabled us to procure tagged BP-intermediates in each step of the Ara4N LPS modification pathway, bypassing the need for complete synthesis of substrates.[202] A simpler approach to procuring each Arn pathway intermediate and monitoring enzyme activity could prove advantageous in the design and development of Arn enzyme inhibitors.

Additionally, we were able to evaluate the accumulation of precursors linked to the vital BP substrate in mutants of this pathway (**Figure 2.8**). Although the implications of accumulated BP-Ara4N weren't fully evaluated in this study, previous research provides significant evidence of the deleterious effects of BPP-glycan intermediate accumulation on cell fitness and morphology.[116, 131-133, 210, 241] Based on those studies, it is proposed that a common pool of BP is utilized for simultaneous processes, including cell wall, O-antigen, and polysaccharide biosynthesis.[133] Thus, inactivation or inhibition of ArnT would render BPP-Ara4N unusable and incapable of being recycled back into the pool of usable BP for cell wall biosynthesis. In consideration of potential Arn pathway inhibitors, this is a significant point that should be considered, particularly for pathogens that exhibit constitutive expression of LPS modification with cationic monosaccharides.

Secondly, this study enabled a thorough investigation of interferences in current practices of *in vitro* construction of bacterial polysaccharides. Early glycan biosynthesis in bacteria relies on initiating phospho-glycosyltransferases that are embedded within the cell envelope membrane (**Figure 1.2**). These membrane-bound enzymes, with numerous transmembrane domains, are notoriously difficult to procure in pure, soluble forms, often requiring liters of bacterial cultures and days-long procedures of extraction, solubilization, purification, and optimization, which may or may not result in active or stable preparations. Often, to circumvent this, simple preparations of cell envelope fractions are utilized to evaluate the activity of recombinantly expressed initiating glycosyltransferases.[85, 124, 134] In experiments utilizing isotopically labeled sugars and radiography, non-specific products of endogenous cell envelope proteins would remain undetected. Thus, simultaneous, competing utilization of BP by endogenous enzymes, like ArnT, has the potential to thwart functional characterization and determination of kinetic parameters.

In these studies, non-specific products in reactions containing cell envelope fractions became evident during the evaluation of *E. coli* undecaprenyl pyrophosphate phosphatase (UppP; **Figure 2.5**). UppP, containing 11 transmembrane domains, was evaluated for utility in preparing fluorescent, monophosphorylated 2CN-BP from 2CN-BPP products of UppS. While UppP functioned as a successful tool to produce activated, monophosphorylated 2CN-BP, it was abundantly evident in these experiments that co-eluting contaminants were present in UppP membrane fraction reactions with 2CN-BPP. Unbeknownst at the time, this was likely due to the simultaneous activity of ArnT, which utilizes the 2CN-BP substrate to form 2CN-BP-Ara4N without the addition of exogenous NDP-sugar.[115] Since this is the initial substrate in recapitulating glycan biosynthesis *in vitro*, this co-eluting product remained a contaminant throughout downstream analysis of glycosyltransferases. This contaminant (2CN-BP-Ara4N)

was effectively avoided by using a mutant strain of *E. coli*, which furthermore highlights the significance of tailoring expression strains specifically for overproduction of polysaccharide biosynthesis enzymes.

EFFECTIVE STRATEGIES FOR IMPROVING NON-NATIVE POLYSACCHARIDE BIOSYNTHESIS IN *E. COLI*

To the best of this author's knowledge, this is the first report of recombinant CPSA expression in *E. coli.* Foundational studies in structural characterization, biosynthesis, and development of adsorbed antiserum supported its success.[30, 222, 230, 291] Overall, a sequential, multi-step cloning procedure yielded a robust approach to evaluating individual intermediates in recombinant CPSA biosynthesis, providing a framework methodology for the evaluation of future, recombinant polysaccharide systems.

Initially, traditional strategies of cloning the CPSA locus en bloc, along with sugar-modifying enzymes WbpP and PglF were attempted, but not successful. The precise reasons have not yet been determined but likely pertain to challenges associated with cloning large fragments of DNA. The CPSA locus itself contains nine genes and is approximately 9.3 kb. Nevertheless, a step-by-step approach was applied for two main reasons: 1) to circumvent potential interference of intergenic regions and inefficiencies of *B. fragilis* ribosome binding sites in the CPSA locus, and 2) to evaluate Wcf enzyme robustness at each stage of CPSA production and delineate potential bottlenecks. To this first point, CPSA plasmids (pBAS8 – 19) were designed to include a strong ribosome binding site (RBS) preceding each gene. While RBS sequences differ between *B. fragilis* and *E. coli*, it is not yet known to what extent CPSA production in *E. coli* is affected by these differences.[224] To address such unknowns, the Wren

Laboratory recently investigated the effect of various RBS and promoter sequences in model systems of recombinant glycoconjugate vaccines.[172] Pairing this stepwise approach of evaluating individual intermediates with strategic incorporation of these elements will undoubtedly bolster polysaccharide production systems.

Moreover, the evaluation of individual intermediates revealed underutilized CPSA BPP-tetrasaccharide (**Supporting Figure 3.5**). As demonstrated in ECA and colanic acid biosynthesis in *E. coli*, optimized glycan systems are characterized by a lack of detectable levels of BPP-oligosaccharide intermediates.[114, 116] Without recombinant intervention and upregulation, or selective inactivation of genes, pathway-specific lipid intermediates are scarcely abundant, or undetectable with LC-MS.[114, 116] Additional evidence of defects in cell morphology points toward growth defects in CPSA-producing cells and reveals a significant opportunity for improvement in CPSA production (**Figure 3.5**). Currently, it is unclear whether this is due to poor activity of the *B. fragilis* flippase (Wzx_{Bf}) and/or polymerase (Wzy_{Bf}), or other factors in *E. coli*. More importantly, this demonstrates an advantageous approach for speedier identification of critical bottlenecks, such as underutilized intermediates, in recombinant glycan production.

Since this evaluation focused on developing a framework for the detection of individual intermediates, it is important to note factors that were not included yet significant to improving the robustness of CPSA polysaccharide production in *E. coli*. For one, *B. fragilis* produces high molecular weight polymers of CPSA (~110 kDa).[292] Polysaccharide chain length regulators (Wzz) work synergistically with a cognate Wzy polymerase in Wzx/Wzy dependent pathways to regulate the molecular weight and modality of polysaccharides.[108, 127, 293] The recombinant model demonstrated here does not include a Wzz chain length regulator from *B. fragilis* and may plausibly result in underperforming Wzy, as evidenced by underutilized BPP-tetrasaccharide.

Since colanic acid production is heavily regulated and induced only in opportune conditions, it is more reasonable that ECA biosynthesis machinery (WzzE) of *E. coli* may intervene in recombinant CPSA polymerization and chain length regulation.[114, 150, 294] Future iterations of this model that include a proposed Wzz from *B. fragilis* could afford higher molecular weight polymers and bolster the activity of Wzy to increase the yield of CPSA.[295]

Current models of polysaccharide systems employ oligosaccharyltransferases, such as PglB from *Campylobacter jejuni*, for purification.[168] This study instead focused on the evaluation of two potential mechanisms of polysaccharide export in *E. coli*, Wza (polysaccharide exporter) and WaaL (O-antigen ligase). Inactivation of *wza* and *waaL* in cells expressing CPSA provides evidence for enabling the procurement of water-soluble, free CPSA polymers, bypassing the need for oligosaccharyltransferases. Inclusion of a native *B. fragilis* polysaccharide transporter, Wza, while not yet identified, could improve the yield of lipid-free CPSA in a Δ*waaL* background. Overall, the sequential investigation of each step, including polymerization and export, revealed key opportunities to improve CPSA yield.

DISCOVERY OF C_{65} AND C_{70} BACTOPRENYL PHOSPHATE IN *C. CRESCENTUS* AND INVESTIGATION OF EARLY STEPS IN HOLDFAST BIOSYNTHESIS

Two distinct methods were employed to define the biosynthetic steps of *C. crescentus* holdfast. First, cell lysates were probed for native glycan biosynthesis precursors (BP) and lipid-glycan intermediates. Second, early steps of holdfast biosynthesis were evaluated *in vitro* with tagged BP substrates. These findings led to the discovery of rare precursors that will enable future evaluation of native *C. crescentus* glycan biosynthesis, as well as characterization of unique

glycosyltransferases that, upon further investigation, could enable production of custom oligo- and polysaccharides.

Early evaluations of *C. crescentus* lysates were focused on the usual C_{55} BP precursor, which can be readily detected in glycan-free form in wild-type cell lysates of *E. coli* using LC-MS.[85, 114-116] However, the C_{55} BP species could not be detected in wild-type or mutant lysates of *C. crescentus*. Therefore, attention was drawn to the potential that *C. crescentus* does not utilize the typical C_{55} length BP, and lysates were scanned for various lengths of BP species. This led to the discovery of longer-chain isoprenoids in *C. crescentus* (C_{65} and C_{70}) and has significant implications regarding the application of LC-MS-based detection of glycan intermediates in other bacterial species. Furthermore, evaluation of recombinant cell lysates overexpressing *uppS* demonstrated that the length of BP in *E. coli* can be adjusted to favor longer (C_{60}) or shorter (C_{45}) BP based on the species of origin of UppS and corroborates longer chain lengths identified in *C. crescentus* (**Figure 4.3**). This suggests that the C_{55} BP species may be less ubiquitous than previously suggested.

In consideration of glycan studies of *E. coli*, it was speculated that C_{65}BPP- and C_{70}BPP-glycan intermediates would be detectable by LC-MS.[114, 116] However, analysis of wild type, single Δ*hfs* mutants, and double Δ*hfiA*Δ*hfs* mutants did not reveal anticipated intermediates, which were based on the carbohydrate content of holdfast.[33] Previous models of this approach have been applied to *E. coli* enterobacterial common antigen (ECA) and colanic acid glycan pathways. In *E. coli*, ECA is constitutively expressed, while colanic acid production is induced by environmental stimuli or by overexpression of a positive transcriptional regulator.[66, 150, 296-298] To this point, upregulation of colanic acid biosynthesis was necessary to evaluate individually accumulated intermediates in colanic acid mutants.[114] Noting the precisely timed transcriptional

and post-translational regulation of holdfast biosynthesis, it is evident that techniques outside of inactivation of the holdfast inhibitor, HfiA, are needed to evaluate native, accumulated holdfast intermediates in the same fashion.[152, 153, 277, 282]

During *in vitro* studies with tagged 2CN-BPP substrates, it was intriguing to note that both BPP-GlcNAc and BPP-Glc were utilized as acceptor substrates by multiple Hfs glycosyltransferases. The evidence thus far, including PssY specificity for UDP-Glc and its ability to compensate for a lack of HfsE in holdfast production, precludes GlcNAc as the first sugar in holdfast, leaving Glc as the probable candidate.[134] While questions remain about the precise sequence of Hfs glycosyltransferase activity, evidence for multiple sugar transfers performed by HfsG is supported by previous characterization of holdfast composition containing up to six to seven sugars with only four identified glycosyltransferases.[33] However, with HfsJ as the second proposed glycosyltransferase in the pathway, based on homology and regulatory factors, questions remain as to how utilization of BPP-Glc by HfsG is regulated. Perhaps HfsG precedes the activity of HfsJ or acts upon BPP-monosaccharide while HfsJ is inhibited to yield a BPP-di, or -trisaccharide of Glc.

Overall, the studies herein encompass the evaluation of foundational components of bacterial glycan biosynthesis pathways, mechanisms of glycan-associated antimicrobial resistance, and characterization of pertinent glycosyltransferases and sugar-modifying enzymes. Characterization of early steps in glycan biosynthesis, including the identification of critical, native precursors, represents the first steps toward defining precise chemical structures and biosynthetic pathways. Taking the results of these and previous studies together, a strategic framework for recombinant overproduction of bacterial glycans was developed.

REFERENCES

1. Keppler, O. T.; Horstkorte, R.; Pawlita, M.; Schmidt, C.; Reutter, W., Biochemical engineering of the N-acyl side chain of sialic acid: biological implications. *Glycobiology* **2001,** *11* (2), 11R-18R.
2. Agard, N. J.; Prescher, J. A.; Bertozzi, C. R., A strain-promoted [3 + 2] azide−alkyne cycloaddition for covalent modification of biomolecules in living systems. *Journal of the American Chemical Society* **2004,** *126* (46), 15046-15047.
3. Clark, E. L.; Emmadi, M.; Krupp, K. L.; Podilapu, A. R.; Helble, J. D.; Kulkarni, S. S.; Dube, D. H., Development of rare bacterial monosaccharide analogs for metabolic glycan labeling in pathogenic bacteria. *ACS Chemical Biology* **2016,** *11* (12), 3365-3373.
4. Prescher, J. A.; Dube, D. H.; Bertozzi, C. R., Chemical remodelling of cell surfaces in living animals. *Nature* **2004,** *340* (7002), 873-877.
5. Herget, S.; Toukach, P. V.; Ranzinger, R.; Hull, W. E.; Knirel, Y. A.; von der Lieth, C.-W., Statistical analysis of the Bacterial Carbohydrate Structure Data Base (BCSDB): Characteristics and diversity of bacterial carbohydrates in comparison with mammalian glycans. *BMC Structural Biology* **2008,** *8* (1), 35.
6. Toukach, P. V.; Egorova, K. S., Carbohydrate structure database merged from bacterial, archaeal, plant and fungal parts. *Nucleic Acids Research* **2016,** *44* (D1), D1229-D1236.
7. Werz, D. B.; Ranzinger, R.; Herget, S.; Adibekian, A.; von der Lieth, C.-W.; Seeberger, P. H., Exploring the Structural Diversity of Mammalian Carbohydrates ("Glycospace") by Statistical Databank Analysis. *ACS Chemical Biology* **2007,** *2* (10), 685-691.
8. Bentley, S. D.; Aanensen, D. M.; Mavroidi, A.; Saunders, D.; Rabbinowitsch, E.; Collins, M.; Donohoe, K.; Harris, D.; Murphy, L.; Quail, M. A.; Samuel, G.; Skovsted, I. C.; Kaltoft, M. S.; Barrell, B.; Reeves, P. R.; Parkhill, J.; Spratt, B. G., Genetic analysis of the capsular biosynthetic locus from all 90 Pneumococcal serotypes. *PLOS Genetics* **2006,** *2* (3), e31.
9. Surana, N. K.; Kasper, D. L., The yin yang of bacterial polysaccharides: lessons learned from *B. fragilis* PSA. *Immunological reviews* **2012,** *245* (1), 13-26.
10. Porter, N. T.; Martens, E. C., The critical roles of polysaccharides in gut microbial ecology and physiology. *Annual Review of Microbiology* **2017,** *71* (Volume 71, 2017), 349-369.
11. Troy, E. B.; Kasper, D. L., Beneficial effects of *Bacteroides fragilis* polysaccharides on the immune system. *Frontiers in Bioscience-Landmark* **2010,** *15*, 25-34.
12. Eribo, O. A.; du Plessis, N.; Chegou, N. N., The intestinal commensal, *Bacteroides fragilis*, modulates host responses to viral infection and therapy: Lessons for exploration during *Mycobacterium tuberculosis* infection. *Infection and Immunity* **2021**, Iai0032121.
13. Tolonen, A. C.; Beauchemin, N.; Bayne, C.; Li, L.; Tan, J.; Lee, J.; Meehan, B. M.; Meisner, J.; Millet, Y.; LeBlanc, G.; Kottler, R.; Rapp, E.; Murphy, C.; Turnbaugh, P. J.; von Maltzahn, G.; Liu, C. M.; van Hylckama Vlieg, J. E. T., Synthetic glycans control gut microbiome structure and mitigate colitis in mice. *Nature Communications* **2022,** *13* (1), 1244.
14. Zheng, L.; Luo, M.; Kuang, G.; Liu, Y.; Liang, D.; Huang, H.; Yi, X.; Wang, C.; Wang, Y.; Xie, Q.; Zhi, F., Capsular Polysaccharide From *Bacteroides fragilis* Protects Against Ulcerative Colitis in an Undegraded Form. *Frontiers in Pharmacology* **2020,** *11* (1835).

15. Ramakrishna, C.; Kujawski, M.; Chu, H.; Li, L.; Mazmanian, S. K.; Cantin, E. M., *Bacteroides fragilis* polysaccharide A induces IL-10 secreting B and T cells that prevent viral encephalitis. *Nature Communications* **2019,** *10* (1), 2153.
16. Nothaft, H.; Davis, B.; Lock, Y. Y.; Perez-Munoz, M. E.; Vinogradov, E.; Walter, J.; Coros, C.; Szymanski, C. M., Engineering the *Campylobacter jejuni* N-glycan to create an effective chicken vaccine. *Scientific Reports* **2016,** *6* (1), 26511.
17. Schneerson, R.; Barrera, O.; Sutton, A.; Robbins, J. B., Preparation, characterization, and immunogenicity of Haemophilus influenzae type b polysaccharide-protein conjugates. *Journal of Experimental Medicine* **1980,** *152* (2), 361-376.
18. Gasparini, R.; Panatto, D., Meningococcal glycoconjugate vaccines. *Human Vaccines* **2011,** *7* (2), 170-182.
19. Ochoa-Repáraz, J.; Mielcarz, D. W.; Wang, Y.; Begum-Haque, S.; Dasgupta, S.; Kasper, D. L.; Kasper, L. H., A polysaccharide from the human commensal *Bacteroides fragilis* protects against CNS demyelinating disease. *Mucosal Immunology* **2010,** *3* (5), 487-95.
20. Bernal-Bayard, J.; Thiebaud, J.; Brossaud, M.; Beaussart, A.; Caillet, C.; Waldvogel, Y.; Travier, L.; Létoffé, S.; Fontaine, T.; Rokbi, B.; Talaga, P.; Beloin, C.; Mistretta, N.; Duval, J. F. L.; Ghigo, J.-M., Bacterial capsular polysaccharides with antibiofilm activity share common biophysical and electrokinetic properties. *Nature Communications* **2023,** *14* (1), 2553.
21. Powell, L. C.; Pritchard, M. F.; Ferguson, E. L.; Powell, K. A.; Patel, S. U.; Rye, P. D.; Sakellakou, S.-M.; Buurma, N. J.; Brilliant, C. D.; Copping, J. M.; Menzies, G. E.; Lewis, P. D.; Hill, K. E.; Thomas, D. W., Targeted disruption of the extracellular polymeric network of *Pseudomonas aeruginosa* biofilms by alginate oligosaccharides. *npj Biofilms and Microbiomes* **2018,** *4* (1), 13.
22. Berne, C.; Ma, X.; Licata, N. A.; Neves, B. R.; Setayeshgar, S.; Brun, Y. V.; Dragnea, B., Physiochemical properties of *Caulobacter crescentus* holdfast: a localized bacterial adhesive. *The Journal of Physical Chemistry B* **2013,** *117* (36), 10492-503.
23. Mohammed, A. S. A.; Naveed, M.; Jost, N., Polysaccharides; Classification, Chemical Properties, and Future Perspective Applications in Fields of Pharmacology and Biological Medicine (A Review of Current Applications and Upcoming Potentialities). *Journal of Polymers and the Environment* **2021,** *29* (8), 2359-2371.
24. Remminghorst, U.; Rehm, B. H. A., Bacterial alginates: from biosynthesis to applications. *Biotechnology Letters* **2006,** *28* (21), 1701-1712.
25. Smith, C. S.; Hinz, A.; Bodenmiller, D.; Larson, D. E.; Brun, Y. V., Identification of genes required for synthesis of the adhesive holdfast in *Caulobacter crescentus*. *Journal of Bacteriology* **2003,** *185* (4), 1432-42.
26. Toh, E.; Kurtz, H. D., Jr.; Brun, Y. V., Characterization of the *Caulobacter crescentus* holdfast polysaccharide biosynthesis pathway reveals significant redundancy in the initiating glycosyltransferase and polymerase steps. *Journal of Bacteriology* **2008,** *190* (21), 7219-31.
27. Coyne, M. J.; Kalka-Moll, W.; Tzianabos, A. O.; Kasper, D. L.; Comstock, L. E., *Bacteroides fragilis* NCTC9343 produces at least three distinct capsular polysaccharides: Cloning, characterization, and reassignment of polysaccharide B and C biosynthesis loci. *Infection and Immunity* **2000,** *68* (11), 6176.
28. Coyne, M. J.; Tzianabos, A. O.; Mallory, B. C.; Carey, V. J.; Kasper, D. L.; Comstock, L. E., Polysaccharide biosynthesis locus required for virulence of *Bacteroides fragilis*. *Infection and Immunity* **2001,** *69* (7), 4342-50.

29. Hershey, D. M.; Fiebig, A.; Crosson, S., A genome-wide analysis of adhesion in *Caulobacter crescentus* identifies new regulatory and biosynthetic components for holdfast assembly. *mBio* **2019,** *10* (1).
30. Sharma, S.; Erickson, K. M.; Troutman, J. M., Complete Tetrasaccharide Repeat Unit Biosynthesis of the Immunomodulatory Bacteroides fragilis Capsular Polysaccharide A. *ACS Chemical Biology* **2017,** *12* (1), 92-101.
31. Scott, P. M.; Erickson, K. M.; Troutman, J. M., Identification of the Functional Roles of Six Key Proteins in the Biosynthesis of Enterobacteriaceae Colanic Acid. *Biochemistry* **2019,** *58* (13), 1818-1830.
32. Feldman Mario, F.; Wacker, M.; Hernandez, M.; Hitchen Paul, G.; Marolda Cristina, L.; Kowarik, M.; Morris Howard, R.; Dell, A.; Valvano Miguel, A.; Aebi, M., Engineering N-linked protein glycosylation with diverse O antigen lipopolysaccharide structures in *Escherichia coli*. *Proceedings of the National Academy of Sciences* **2005,** *102* (8), 3016-3021.
33. Hershey, D. M.; Porfírio, S.; Black, I.; Jaehrig, B.; Heiss, C.; Azadi, P.; Fiebig, A.; Crosson, S., Composition of the holdfast polysaccharide from *Caulobacter crescentus*. *Journal of Bacteriology* **2019,** *201* (17), e00276-19.
34. Bushell, S. R.; Mainprize, I. L.; Wear, M. A.; Lou, H.; Whitfield, C.; Naismith, J. H., Wzi is an outer membrane lectin that underpins group 1 capsule assembly in *Escherichia coli*. *Structure* **2013,** *21* (5), 844-53.
35. Whitfield, C., Biosynthesis and assembly of capsular polysaccharides in Escherichia coli. *Annual Review of Biochemistry* **2006,** *75*, 39-68.
36. Roberts, I. S., The biochemistry and genetics of capsular polysaccharide production in bacteria. *Annual Review of Microbiology* **1996,** *50* (Volume 50, 1996), 285-315.
37. Flemming, H.-C.; Neu Thomas, R.; Wozniak Daniel, J., The EPS Matrix: The "House of Biofilm Cells". *Journal of Bacteriology* **2007,** *189* (22), 7945-7947.
38. Attridge, S. R.; Holmgren, J., *Vibrio cholerae* O139 capsular polysaccharide confers complement resistance in the absence or presence of antibody yet presents a productive target for cell lysis: implications for detection of bactericidal antibodies. *Microbial Pathogenesis* **2009,** *47* (6), 314-320.
39. Thomassin, J.-L.; Lee, M. J.; Brannon, J. R.; Sheppard, D. C.; Gruenheid, S.; Le Moual, H., Both Group 4 Capsule and Lipopolysaccharide O-Antigen Contribute to Enteropathogenic Escherichia coli Resistance to Human α-Defensin 5. *PLOS One* **2013,** *8* (12), e82475.
40. Spinosa Maria, R.; Progida, C.; Talà, A.; Cogli, L.; Alifano, P.; Bucci, C., The Neisseria meningitidis Capsule Is Important for Intracellular Survival in Human Cells. *Infection and Immunity* **2007,** *75* (7), 3594-3603.
41. Kuipers, A.; Stapels, D. A. C.; Weerwind, L. T.; Ko, Y.-P.; Ruyken, M.; Lee, J. C.; van Kessel, K. P. M.; Rooijakkers, S. H. M., The Staphylococcus aureus polysaccharide capsule and Efb-dependent fibrinogen shield act in concert to protect against phagocytosis. *Microbiology* **2016,** *162* (7), 1185-1194.
42. Hyams, C.; Camberlein, E.; Cohen Jonathan, M.; Bax, K.; Brown Jeremy, S., The *Streptococcus pneumoniae* capsule inhibits complement activity and neutrophil phagocytosis by multiple mechanisms. *Infection and Immunity* **2010,** *78* (2), 704-715.

43. Coyne, M. J.; Chatzidaki-Livanis, M.; Paoletti, L. C.; Comstock, L. E., Role of glycan synthesis in colonization of the mammalian gut by the bacterial symbiont *Bacteroides fragilis*. *Proceedings of the National Academy of Sciences* **2008,** *105* (35), 13099-13104.
44. Jones Melissa, K.; Oliver James, D., Vibrio vulnificus: Disease and Pathogenesis. *Infection and Immunity* **2009,** *77* (5), 1723-1733.
45. Oliver, J. D., Vibrio vulnificus: Death on the Half Shell. A Personal Journey with the Pathogen and its Ecology. *Microbial Ecology* **2013,** *65* (4), 793-799.
46. Krinos, C. M.; Coyne, M. J.; Weinacht, K. G.; Tzianabos, A. O.; Kasper, D. L.; Comstock, L. E., Extensive surface diversity of a commensal microorganism by multiple DNA inversions. *Nature* **2001,** *414* (6863), 555-558.
47. Liu, C. H.; Lee, S. M.; VanLare, J. M.; Kasper, D. L.; Mazmanian, S. K., Regulation of surface architecture by symbiotic bacteria mediates host colonization. *Proceedings of the National Academy of Sciences* **2008,** *105* (10), 3951-3956.
48. Gibson, F. C., III; Onderdonk, A. B.; Kasper, D. L.; Tzianabos, A. O., Cellular mechanism of intraabdominal abscess formation by *Bacteroides fragilis*. *The Journal of Immunology* **1998,** *160* (10), 5000-5006.
49. Onderdonk, A. B.; Kasper, D. L.; Cisneros, R. L.; Bartlett, J. G., The Capsular Polysaccharide of Bacteroides fragilis as a Virulence Factor: Comparison of the Pathogenic Potential of Encapsulated and Unencapsulated Strains. *The Journal of Infectious Diseases* **1977,** *136* (1), 82-89.
50. Tzianabos, A. O.; Onderdonk, A. B.; Smith, R. S.; Kasper, D. L., Structure-function relationships for polysaccharide-induced intra-abdominal abscesses. *Infection and Immunity* **1994,** *62* (8), 3590-3593.
51. Tzianabos, A. O.; Finberg, R. W.; Wang, Y.; Chan, M.; Onderdonk, A. B.; Jennings, H. J.; Kasper, D. L., T Cells Activated by Zwitterionic Molecules Prevent Abscesses Induced by Pathogenic Bacteria *. *Journal of Biological Chemistry* **2000,** *275* (10), 6733-6740.
52. Wang, Y.; Kalka-Moll, W. M.; Roehrl, M. H.; Kasper, D. L., Structural basis of the abscess-modulating polysaccharide A2 from *Bacteroides fragilis*. *Proceedings of the National Academy of Sciences* **2000,** *97* (25), 13478.
53. Choi, Y.-H.; Roehrl, M. H.; Kasper, D. L.; Wang, J. Y., A unique structural pattern shared by T-cell-activating and abscess-regulating zwitterionic polysaccharides. *Biochemistry* **2002,** *41* (51), 15144-15151.
54. Cobb, B. A.; Wang, Q.; Tzianabos, A. O.; Kasper, D. L., Polysaccharide processing and presentation by the MHCII pathway. *Cell* **2004,** *117* (5), 677-687.
55. Arnolds, K. L.; Yamada, E.; Neff, C. P.; Schneider, J. M.; Palmer, B. E.; Lozupone, C. A., Disruption of genes encoding putative zwitterionic capsular polysaccharides of diverse intestinal *Bacteroides* reduces the induction of host anti-inflammatory factors. *Microbial Ecology* **2023,** *85* (4), 1620-1629.
56. Zhou, J. Y.; Zhou, D.; Telfer, K.; Reynero, K.; Jones, M. B.; Hambor, J.; Cobb, B. A., Antigen presenting cell response to polysaccharide A is characterized by the generation of anti-inflammatory macrophages. *Glycobiology* **2022,** *32* (2), 136-147.
57. Donlan, R., Biofilms: Microbial life on surfaces. *Emerging Infectious Disease journal* **2002,** *8* (9), 881.
58. Lewis, K., Multidrug Tolerance of Biofilms and Persister Cells. In *Bacterial Biofilms*, Romeo, T., Ed. Springer Berlin Heidelberg: Berlin, Heidelberg, 2008; pp 107-131.

59. Bodenmiller, D.; Toh, E.; Brun, Y. V., Development of surface adhesion in *Caulobacter crescentus*. *Journal of Bacteriology* **2004,** *186* (5), 1438-47.
60. Götz, F., *Staphylococcus* and biofilms. *Molecular Microbiology* **2002,** *43* (6), 1367-1378.
61. Billings, N.; Ramirez Millan, M.; Caldara, M.; Rusconi, R.; Tarasova, Y.; Stocker, R.; Ribbeck, K., The extracellular matrix component Psl provides fast-acting antibiotic defense in *Pseudomonas aeruginosa* biofilms. *PLOS Pathogens* **2013,** *9* (8), e1003526.
62. Ma, L.; Wang, S.; Wang, D.; Parsek, M. R.; Wozniak, D. J., The roles of biofilm matrix polysaccharide Psl in mucoid Pseudomonas aeruginosa biofilms. *FEMS Immunology & Medical Microbiology* **2012,** *65* (2), 377-380.
63. Ciofu, O.; Tolker-Nielsen, T.; Jensen, P. Ø.; Wang, H.; Høiby, N., Antimicrobial resistance, respiratory tract infections and role of biofilms in lung infections in cystic fibrosis patients. *Advanced Drug Delivery Reviews* **2015,** *85*, 7-23.
64. Assefa, M.; Amare, A., Biofilm-associated multi-drug resistance in hospital-acquired infections: A review. *Infection and Drug Resistance* **2022,** *15* (15), 5061-5068.
65. Hanna, A.; Berg, M.; Stout, V.; Razatos, A., Role of capsular colanic acid in adhesion of uropathogenic *Escherichia coli*. *Applied and Environmental Microbiology* **2003,** *69* (8), 4474-4481.
66. Chen, J.; Lee, S. M.; Mao, Y., Protective effect of exopolysaccharide colanic acid of *Escherichia coli* O157:H7 to osmotic and oxidative stress. *International Journal of Food Microbiology* **2004,** *93* (3), 281-286.
67. Danese, P. N.; Pratt, L. A.; Kolter, R., Exopolysaccharide production is required for development of *Escherichia coli* K-12 biofilm architecture. *Journal of bacteriology* **2000,** *182* (12), 3593-3596.
68. Fau, K. Y.; Nikaido, H., Outer membrane of *Salmonella typhimurium*: accessibility of phospholipid head groups to phospholipase c and cyanogen bromide activated dextran in the external medium. *Biochemistry* **1976,** *15(12)* (2561–2570).
69. Silhavy, T. J.; Fau, K. D.; Walker, S., The bacterial cell envelope. *Cold Spring Harbor Perspectives in Biology* **2010,** *2(5)* (a000414).
70. Raetz, C. R. H.; Whitfield, C., Lipopolysaccharide Endotoxins. *Annual Review of Biochemistry* **2002,** *71* (1), 635-700.
71. Raetz, C. R.; Reynolds, C. M.; Trent, M. S.; Bishop, R. E., Lipid A modification systems in gram-negative bacteria. *Annual Review of Biochemistry* **2007,** *76*, 295-329.
72. Gibbons, H. S.; Kalb, S. R.; Cotter, R. J.; Raetz, C. R. H., Role of Mg2+ and pH in the modification of *Salmonella* lipid A after endocytosis by macrophage tumour cells. *Molecular Microbiology* **2005,** *55* (2), 425-440.
73. Nummila, K.; Kilpeläinen, I.; Zähringer, U.; Vaara, M.; Helander, I. M., Lipopolysaccharides of polymyxin B-resistant mutants of Escherichia coli are extensively substituted by 2-aminoethyl pyrophosphate and contain aminoarabinose in lipid A. *Molecular Microbiology* **1995,** *16* (2), 271-8.
74. Nation, R. L.; Li, J.; Cars, O.; Couet, W.; Dudley, M. N.; Kaye, K. S.; Mouton, J. W.; Paterson, D. L.; Tam, V. H.; Theuretzbacher, U.; Tsuji, B. T.; Turnidge, J. D., Framework for optimisation of the clinical use of colistin and polymyxin B: the Prato polymyxin consensus. *The Lancet. Infectious Diseases* **2015,** *15* (2), 225-34.

75. Hamad, M. A.; Di Lorenzo, F.; Molinaro, A.; Valvano, M. A., Aminoarabinose is essential for lipopolysaccharide export and intrinsic antimicrobial peptide resistance in *Burkholderia cenocepacia*†. *Molecular Microbiology* **2012,** *85* (5), 962-974.
76. Gunn, J. S.; Lim, K. B.; Krueger, J.; Kim, K.; Guo, L.; Hackett, M.; Miller, S. I., PmrA-PmrB-regulated genes necessary for 4-aminoarabinose lipid A modification and polymyxin resistance. *Molecular Microbiology* **1998,** *27* (6), 1171-82.
77. Jayol, A.; Poirel, L.; Brink, A.; Villegas, M.-V.; Yilmaz, M.; Nordmann, P., Resistance to Colistin Associated with a Single Amino Acid Change in Protein PmrB among *Klebsiella pneumoniae* Isolates of Worldwide Origin. *Antimicrobial Agents and Chemotherapy* **2014,** *58* (8), 4762.
78. Zhou, Z.; Ribeiro, A. A.; Lin, S.; Cotter, R. J.; Miller, S. I.; Raetz, C. R., Lipid A modifications in polymyxin-resistant Salmonella typhimurium: PMRA-dependent 4-amino-4-deoxy-L-arabinose, and phosphoethanolamine incorporation. *Journal of Biological Chemistry* **2001,** *276* (46), 43111-21.
79. Shah, N. R.; Hancock, R. E. W.; Fernandez, R. C., Bordetella pertussis lipid A glucosamine modification confers resistance to cationic antimicrobial peptides and increases resistance to outer membrane perturbation. *Antimicrobial agents and chemotherapy* **2014,** *58* (8), 4931-4934.
80. Wang, X.; Ribeiro, A. A.; Guan, Z.; Raetz, C. R. H., Identification of undecaprenyl phosphate-β-d-galactosamine in Francisella novicida and its function in lipid A modification. *Biochemistry* **2009,** *48* (6), 1162-1172.
81. Froelich, J. M.; Tran, K.; Wall, D., A pmrA constitutive mutant sensitizes *Escherichia coli* to deoxycholic acid. *Journal of Bacteriology* **2006,** *188* (3), 1180-3.
82. Gunn, J. S.; Miller, S. I., PhoP-PhoQ activates transcription of pmrAB, encoding a two-component regulatory system involved in *Salmonella typhimurium* antimicrobial peptide resistance. *Journal of Bacteriology* **1996,** *178* (23), 6857.
83. Kesavelu, D.; Jog, P., Current understanding of antibiotic-associated dysbiosis and approaches for its management. *Therapeutic Advances in Infectious Disease* **2023,** *10*.
84. Tra, V. N.; Dube, D. H., Glycans in pathogenic bacteria – potential for targeted covalent therapeutics and imaging agents. *Chemical Communications* **2014,** *50* (36), 4659-4673.
85. Reid, A. J.; Scarbrough, B. A.; Williams, T. C.; Gates, C. E.; Eade, C. R.; Troutman, J. M., General Utilization of Fluorescent Polyisoprenoids with Sugar Selective Phosphoglycosyltransferases. *Biochemistry* **2020,** *59* (4), 615-626.
86. Price, N. P. J.; Labeda, D. P.; Naumann, T. A.; Vermillion, K. E.; Bowman, M. J.; Berhow, M. A.; Metcalf, W. W.; Bischoff, K. M., Quinovosamycins: new tunicamycin-type antibiotics in which the α, β-1″,11′-linked N-acetylglucosamine residue is replaced by N-acetylquinovosamine. *The Journal of Antibiotics* **2016,** *69* (8), 637-646.
87. Economou, N. J.; Cocklin, S.; Loll, P. J., High-resolution crystal structure reveals molecular details of target recognition by bacitracin. *Proceedings of the National Academy of Sciences* **2013,** *110* (35), 14207-14212.
88. Storm, D. R., Mechanism of bacitracin action: A specific lipid-peptide interaction. *Annals of the New York Academy of Sciences* **1974,** *235* (1), 387-398.
89. Huszár, S.; Singh, V.; Polčicová, A.; Baráth, P.; Barrio María, B.; Lagrange, S.; Leblanc, V.; Nacy Carol, A.; Mizrahi, V.; Mikušová, K., N-Acetylglucosamine-1-Phosphate

transferase, WecA, as a validated drug target in *Mycobacterium tuberculosis*. *Antimicrobial Agents and Chemotherapy* **2017,** *61* (11), 10.1128/aac.01310-17.
90. Hakulinen, J. K.; Hering, J.; Brändén, G.; Chen, H.; Snijder, A.; Ek, M.; Johansson, P., MraY–antibiotic complex reveals details of tunicamycin mode of action. *Nature Chemical Biology* **2017,** *13* (3), 265-267.
91. Vollmer, W.; Blanot, D.; De Pedro, M. A., Peptidoglycan structure and architecture. *FEMS Microbiology Reviews* **2008,** *32* (2), 149-167.
92. Turner, R. D.; Vollmer, W.; Foster, S. J., Different walls for rods and balls: the diversity of peptidoglycan. *Molecular Microbiology* **2014,** *91* (5), 862-874.
93. Lebar, M. D.; Lupoli, T. J.; Tsukamoto, H.; May, J. M.; Walker, S.; Kahne, D., Forming cross-linked peptidoglycan from synthetic gram-negative Lipid II. *Journal of the American Chemical Society* **2013,** *135* (12), 4632-5.
94. Qiao, Y.; Srisuknimit, V.; Rubino, F.; Schaefer, K.; Ruiz, N.; Walker, S.; Kahne, D., Lipid II overproduction allows direct assay of transpeptidase inhibition by beta-lactams. *Nature Chemical Biology* **2017,** *13* (7), 793-798.
95. Zhang, Y.-M.; Rock, C. O., Membrane lipid homeostasis in bacteria. *Nature reviews. Microbiology* **2008,** *6* (3), 222-233.
96. Braun, V., Covalent lipoprotein from the outer membrane of *Escherichia coli*. *Biochimica et Biophysica Acta (BBA) - Reviews on Biomembranes* **1975,** *415* (3), 335-377.
97. Cowan, S. W.; Schirmer, T.; Rummel, G.; Steiert, M.; Ghosh, R.; Pauptit, R. A.; Jansonius, J. N.; Rosenbusch, J. P., Crystal structures explain functional properties of two *E. coli* porins. *Nature* **1992,** *358* (6389), 727-733.
98. Fivenson, E. M.; Rohs, P. D. A.; Vettiger, A.; Sardis, M. F.; Torres, G.; Forchoh, A.; Bernhardt, T. G., A role for the Gram-negative outer membrane in bacterial shape determination. *Proceedings of the National Academy of Sciences* **2023,** *120* (35), e2301987120.
99. Leive, L., Release of lipopolysaccharide by EDTA treatment of *E. coli*. *Biochemical and Biophysical Research Communications* **1965,** *21* (4), 290-296.
100. Whitfield, C.; Trent, M. S., Biosynthesis and Export of Bacterial Lipopolysaccharides. *Annual Review of Biochemistry* **2014,** *83* (1), 99-128.
101. Wang, L.; Wang, Q.; Reeves, P. R., The Variation of O Antigens in Gram-Negative Bacteria. In *Endotoxins: Structure, Function and Recognition*, Wang, X.; Quinn, P. J., Eds. Springer Netherlands: Dordrecht, 2010; pp 123-152.
102. Swoboda, J. G.; Campbell, J.; Meredith, T. C.; Walker, S., Wall Teichoic Acid Function, Biosynthesis, and Inhibition. *ChemBioChem* **2010,** *11* (1), 35-45.
103. Lu, Y.; Chen, F.; Zhao, Q.; Cao, Q.; Chen, R.; Pan, H.; Wang, Y.; Huang, H.; Huang, R.; Liu, Q.; Li, M.; Bae, T.; Liang, H.; Lan, L., Modulation of MRSA virulence gene expression by the wall teichoic acid enzyme TarO. *Nature Communications* **2023,** *14* (1), 1594.
104. Whitfield, C.; Paiment, A., Biosynthesis and assembly of Group 1 capsular polysaccharides in Escherichia coli and related extracellular polysaccharides in other bacteria. *Carbohydrate Research* **2003,** *338* (23), 2491-2502.
105. Willis, L. M.; Whitfield, C., Structure, biosynthesis, and function of bacterial capsular polysaccharides synthesized by ABC transporter-dependent pathways. *Carbohydrate Research* **2013,** *378*, 35-44.
106. Itoh, Y.; Rice John, D.; Goller, C.; Pannuri, A.; Taylor, J.; Meisner, J.; Beveridge Terry, J.; Preston James, F.; Romeo, T., Roles of pgaABCD genes in synthesis, modification,

and export of the *Escherichia coli* biofilm adhesin poly-β-1,6-N-acetyl-d-glucosamine. *Journal of Bacteriology* **2008,** *190* (10), 3670-3680.
107. Liston, S. D.; McMahon, S. A.; Le Bas, A.; Suits, M. D. L.; Naismith, J. H.; Whitfield, C., Periplasmic depolymerase provides insight into ABC transporter-dependent secretion of bacterial capsular polysaccharides. *Proceedings of the National Academy of Sciences* **2018,** *115* (21), E4870-E4879.
108. Islam, S. T.; Lam, J. S., Synthesis of bacterial polysaccharides via the Wzx/Wzy-dependent pathway. *Canadian Journal of Microbiology* **2014,** *60* (11), 697-716.
109. Cuthbertson, L.; Mainprize, I. L.; Naismith, J. H.; Whitfield, C., Pivotal roles of the outer membrane polysaccharide export and polysaccharide copolymerase protein families in export of extracellular polysaccharides in gram-negative bacteria. *Microbiology and Molecular Biology Reviews* **2009,** *73* (1), 155-177.
110. El Ghachi, M.; Bouhss, A.; Blanot, D.; Mengin-Lecreulx, D., The bacA gene of *Escherichia coli* encodes an undecaprenyl pyrophosphate phosphatase activity. *Journal of Biological Chemistry* **2004,** *279* (29), 30106-13.
111. Teng, K.-H.; Liang, P.-H., Undecaprenyl diphosphate synthase, a cis-prenyltransferase synthesizing lipid carrier for bacterial cell wall biosynthesis. *Molecular Membrane Biology* **2012,** *29* (7), 267-273.
112. Baba, T.; Allen, C. M., Prenyl transferases from *Micrococcus luteus*: Characterization of undecaprenyl pyrophosphate synthetase. *Archives of Biochemistry and Biophysics : ABB.* **1980,** *200* (2), 474-484.
113. Shimizu, N.; Koyama, T.; Ogura, K., Molecular cloning, expression, and purification of undecaprenyl diphosphate synthase: No sequence similarity between *E* and *Z* prenyl diphosphate synthases *. *Journal of Biological Chemistry* **1998,** *273* (31), 19476-19481.
114. Reid, A. J.; Eade, C. R.; Jones, K. J.; Jorgenson, M. A.; Troutman, J. M., Tracking Colanic Acid Repeat Unit Formation from Stepwise Biosynthesis Inactivation in Escherichia coli. *Biochemistry* **2021,** *60* (27), 2221-2230.
115. Scarbrough, B. A.; Eade, C. R.; Reid, A. J.; Williams, T. C.; Troutman, J. M., Lipopolysaccharide Is a 4-Aminoarabinose Donor to Exogenous Polyisoprenyl Phosphates through the Reverse Reaction of the Enzyme ArnT. *ACS Omega* **2021,** *6(39)*, 25729-25741.
116. Eade, C. R.; Wallen, T. W.; Gates, C. E.; Oliverio, C. L.; Scarbrough, B. A.; Reid, A. J.; Jorgenson, M. A.; Young, K. D.; Troutman, J. M., Making the enterobacterial common antigen glycan and measuring its substrate sequestration. *ACS Chemical Biology* **2021,** *16* (4), 691-700.
117. Farha, M. A.; Czarny, T. L.; Myers, C. L.; Worrall, L. J.; French, S.; Conrady, D. G.; Wang, Y.; Oldfield, E.; Strynadka, N. C.; Brown, E. D., Antagonism screen for inhibitors of bacterial cell wall biogenesis uncovers an inhibitor of undecaprenyl diphosphate synthase. *Proceedings of the National Academy of Sciences* **2015,** *112* (35), 11048-53.
118. El Ghachi, M.; Howe, N.; Huang, C. Y.; Olieric, V.; Warshamanage, R.; Touze, T.; Weichert, D.; Stansfeld, P. J.; Wang, M.; Kerff, F.; Caffrey, M., Crystal structure of undecaprenyl-pyrophosphate phosphatase and its role in peptidoglycan biosynthesis. *Nature Communications* **2018,** *9* (1), 1078.
119. Morrison, M. J.; Imperiali, B., Biosynthesis of UDP-N,N′-diacetylbacillosamine in Acinetobacter baumannii: Biochemical characterization and correlation to existing pathways. *Archives of Biochemistry and Biophysics* **2013,** *536* (1), 72-80.

120. Olivier, N. B.; Chen, M. M.; Behr, J. R.; Imperiali, B., In vitro biosynthesis of UDP-N,N'-diacetylbacillosamine by enzymes of the Campylobacter jejuni general protein glycosylation system. *Biochemistry* **2006,** *45* (45), 13659-69.
121. Hartley, M. D.; Morrison, M. J.; Aas, F. E.; Børud, B.; Koomey, M.; Imperiali, B., Biochemical characterization of the O-linked glycosylation pathway in *Neisseria gonorrhoeae* responsible for biosynthesis of protein glycans containing N,N′-diacetylbacillosamine. *Biochemistry* **2011,** *50* (22), 4936-4948.
122. Lukose, V.; Walvoort, M. T.; Imperiali, B., Bacterial phosphoglycosyl transferases: initiators of glycan biosynthesis at the membrane interface. *Glycobiology* **2017,** *27* (9), 820-833.
123. Al-Dabbagh, B.; Olatunji, S.; Crouvoisier, M.; El Ghachi, M.; Blanot, D.; Mengin-Lecreulx, D.; Bouhss, A., Catalytic mechanism of MraY and WecA, two paralogues of the polyprenyl-phosphate N-acetylhexosamine 1-phosphate transferase superfamily. *Biochimie* **2016,** *127*, 249-57.
124. Lehrer, J.; Vigeant, K. A.; Tatar, L. D.; Valvano, M. A., Functional characterization and membrane topology of Escherichia coli WecA, a sugar-phosphate transferase initiating the biosynthesis of enterobacterial common antigen and O-antigen lipopolysaccharide. *Journal of Bacteriology* **2007,** *189* (7), 2618-28.
125. Saldías, M. S.; Patel, K.; Marolda, C. L.; Bittner, M.; Contreras, I.; Valvano, M. A., Distinct functional domains of the Salmonella enterica WbaP transferase that is involved in the initiation reaction for synthesis of the O antigen subunit. *Microbiology* **2008,** *154* (2), 440-453.
126. Batchelor, R. A.; Haraguchi, G. E.; Hull, R. A.; Hull, S. I., Regulation by a novel protein of the bimodal distribution of lipopolysaccharide in the outer membrane of *Escherichia coli*. *Journal of Bacteriology* **1991,** *173* (18), 5699-5704.
127. Collins, R. F.; Kargas, V.; Clarke, B. R.; Siebert, C. A.; Clare, D. K.; Bond, P. J.; Whitfield, C.; Ford, R. C., Full-length, oligomeric structure of Wzz determined by cryoelectron microscopy reveals insights into membrane-bound states. *Structure* **2017,** *25* (5), 806-815.e3.
128. Wiseman, B.; Nitharwal, R. G.; Widmalm, G.; Högbom, M., Structure of a full-length bacterial polysaccharide co-polymerase. *Nature Communications* **2021,** *12* (1), 369.
129. Weckener, M.; Woodward, L. S.; Clarke, B. R.; Liu, H.; Ward, P. N.; Le Bas, A.; Bhella, D.; Whitfield, C.; Naismith, J. H., The lipid linked oligosaccharide polymerase Wzy and its regulating co-polymerase, Wzz, from enterobacterial common antigen biosynthesis form a complex. *Open Biology* **2023,** *13* (3), 220373.
130. Dong, C.; Beis, K.; Nesper, J.; Brunkan-LaMontagne, A. L.; Clarke, B. R.; Whitfield, C.; Naismith, J. H., Wza the translocon for *E. coli* capsular polysaccharides defines a new class of membrane protein. *Nature* **2006,** *444* (7116), 226-229.
131. Jorgenson, M. A.; Young, K. D., Interrupting Biosynthesis of O Antigen or the Lipopolysaccharide Core Produces Morphological Defects in Escherichia coli by Sequestering Undecaprenyl Phosphate. *Journal of Bacteriology* **2016,** *198* (22), 3070-3079.
132. Jorgenson, M. A.; MacCain, W. J.; Meberg, B. M.; Kannan, S.; Bryant, J. C.; Young, K. D., Simultaneously inhibiting undecaprenyl phosphate production and peptidoglycan synthases promotes rapid lysis in *Escherichia coli*. *Molecular Microbiology* **2019,** *112* (1), 233-248.
133. Jorgenson, M. A.; Kannan, S.; Laubacher, M. E.; Young, K. D., Dead-end intermediates in the enterobacterial common antigen pathway induce morphological defects in *Escherichia coli* by competing for undecaprenyl phosphate. *Molecular Microbiology* **2016,** *100* (1), 1-14.

134. Patel, K. B.; Toh, E.; Fernandez, X. B.; Hanuszkiewicz, A.; Hardy, G. G.; Brun, Y. V.; Bernards, M. A.; Valvano, M. A., Functional characterization of UDP-glucose:undecaprenyl-phosphate glucose-1-phosphate transferases of *Escherichia coli* and *Caulobacter crescentus*. *Journal of Bacteriology* **2012,** *194* (10), 2646-57.
135. Breazeale, S. D.; Ribeiro, A. A.; McClerren, A. L.; Raetz, C. R., A formyltransferase required for polymyxin resistance in *Escherichia coli* and the modification of lipid A with 4-Amino-4-deoxy-L-arabinose. Identification and function oF UDP-4-deoxy-4-formamido-L-arabinose. *Journal of Biological Chemistry* **2005,** *280* (14), 14154-67.
136. Lujan, D. K.; Stanziale, J. A.; Mostafavi, A. Z.; Sharma, S.; Troutman, J. M., Chemoenzymatic synthesis of an isoprenoid phosphate tool for the analysis of complex bacterial oligosaccharide biosynthesis. *Carbohydrate Research* **2012,** *359*, 44-53.
137. Dodbele, S.; Martinez, C. D.; Troutman, J. M., Species differences in alternative substrate utilization by the antibacterial target undecaprenyl pyrophosphate synthase. *Biochemistry* **2014,** *53* (30), 5042-50.
138. Mostafavi, A. Z.; Lujan, D. K.; Erickson, K. M.; Martinez, C. D.; Troutman, J. M., Fluorescent probes for investigation of isoprenoid configuration and size discrimination by bactoprenol-utilizing enzymes. *Bioorganic & Medicinal Chemistry* **2013,** *21* (17), 5428-35.
139. Linton, D.; Dorrell, N.; Hitchen, P. G.; Amber, S.; Karlyshev, A. V.; Morris, H. R.; Dell, A.; Valvano, M. A.; Aebi, M.; Wren, B. W., Functional analysis of the *Campylobacter jejuni* N-linked protein glycosylation pathway. *Molecular Microbiology* **2005,** *55* (6), 1695-1703.
140. Patrick, S.; Reid, J. H.; Coffey, A., Capsulation of in vitro and in vivo grown *Bacteroides* species. *Journal of General Microbiology* **1986,** *132* (4), 1099-1109.
141. Champasa, K.; Longwell, S. A.; Eldridge, A. M.; Stemmler, E. A.; Dube, D. H., Targeted Identification of Glycosylated Proteins in the Gastric Pathogen *Helicobacter pylori*. *Molecular & Cellular Proteomics* **2013,** *12* (9), 2568-2586.
142. Moulton, K. D.; Adewale, A. P.; Carol, H. A.; Mikami, S. A.; Dube, D. H., Metabolic Glycan Labeling-Based Screen to Identify Bacterial Glycosylation Genes. *ACS Infectious Diseases* **2020,** *6* (12), 3247-3259.
143. Mahal, L. K.; Yarema, K. J.; Bertozzi, C. R., Engineering Chemical Reactivity on Cell Surfaces Through Oligosaccharide Biosynthesis. *Science* **1997,** *276* (5315), 1125-1128.
144. Geva-Zatorsky, N.; Alvarez, D.; Hudak, J. E.; Reading, N. C.; Erturk-Hasdemir, D.; Dasgupta, S.; von Andrian, U. H.; Kasper, D. L., In vivo imaging and tracking of host–microbiota interactions via metabolic labeling of gut anaerobic bacteria. *Nature Medicine* **2015,** *21* (9), 1091-1100.
145. Koenigs, M. B.; Dube, D. H., Metabolic profiling of Helicobacter pylori glycosylation. *The FASEB Journal* **2009,** *23* (S1), 695.4-695.4.
146. Eddenden, A.; Dooda, M. K.; Morrison, Z. A.; Shankara Subramanian, A.; Howell, P. L.; Troutman, J. M.; Nitz, M., Metabolic usage and glycan destinations of GlcNAz in *E. coli*. *ACS Chemical Biology* **2024,** *19* (1), 69-80.
147. Mostafavi, A. Z.; Troutman, J. M., Biosynthetic Assembly of the Bacteroides fragilis Capsular Polysaccharide A Precursor Bactoprenyl Diphosphate-Linked Acetamido-4-amino-6-deoxygalactopyranose. *Biochemistry* **2013,** *52* (11), 1939-1949.

148. Williams, D. A.; Pradhan, K.; Paul, A.; Olin, I. R.; Tuck, O. T.; Moulton, K. D.; Kulkarni, S. S.; Dube, D. H., Metabolic inhibitors of bacterial glycan biosynthesis. *Chemical Science* **2020,** *11* (7), 1761-1774.
149. Morrison, Z. A.; Eddenden, A.; Subramanian, A. S.; Howell, P. L.; Nitz, M., Termination of Poly-N-acetylglucosamine (PNAG) Polymerization with N-Acetylglucosamine Analogues. *ACS Chemical Biology* **2022,** *17* (11), 3036-3046.
150. Navasa, N.; Rodríguez-Aparicio, L.; Martínez-Blanco, H.; Arcos, M.; Ferrero, M. Á., Temperature has reciprocal effects on colanic acid and polysialic acid biosynthesis in E. coli K92. *Applied Microbiology and Biotechnology* **2009,** *82* (4), 721-729.
151. Porter, N. T.; Canales, P.; Peterson, D. A.; Martens, E. C., A subset of polysaccharide capsules in the human symbiont *Bacteroides thetaiotaomicron* promote increased competitive fitness in the mouse gut. *Cell Host & Microbe* **2017,** *22* (4), 494-506.e8.
152. Sprecher, K. S.; Hug, I.; Nesper, J.; Potthoff, E.; Mahi, M.-A.; Sangermani, M.; Kaever, V.; Schwede, T.; Vorholt, J.; Jenal, U., Cohesive Properties of the *Caulobacter crescentus* Holdfast Adhesin Are Regulated by a Novel c-di-GMP Effector Protein. *mBio* **2017,** *8* (2), e00294-17.
153. Fiebig, A.; Herrou, J.; Fumeaux, C.; Radhakrishnan, S. K.; Viollier, P. H.; Crosson, S., A cell cycle and nutritional checkpoint controlling bacterial surface adhesion. *PLOS Genetics* **2014,** *10* (1), e1004101.
154. Herr, K. L.; Carey, A. M.; Heckman, T. I.; Chávez, J. L.; Johnson, C. N.; Harvey, E.; Gamroth, W. A.; Wulfing, B. S.; Van Kessel, R. A.; Marks, M. E., Exopolysaccharide production in *Caulobacter crescentus*: A resource allocation trade-off between protection and proliferation. *PLOS One* **2018,** *13* (1), e0190371.
155. Wacker, M.; Linton, D.; Hitchen, P. G.; Nita-Lazar, M.; Haslam, S. M.; North, S. J.; Panico, M.; Morris, H. R.; Dell, A.; Wren, B. W.; Aebi, M., N-linked glycosylation in *Campylobacter jejuni* and its functional transfer into *E. coli*. *Science* **2002,** *298* (5599), 1790-3.
156. Finsterer, J., Triggers of Guillain–Barré Syndrome: *Campylobacter jejuni* predominates. *International Journal of Molecular Sciences* **2022,** *23* (22), 14222.
157. Szymanski, C. M.; Yao, R.; Ewing, C. P.; Trust, T. J.; Guerry, P., Evidence for a system of general protein glycosylation in *Campylobacter jejuni*. *Molecular Microbiology* **1999,** *32* (5), 1022-1030.
158. Szymanski Christine, M.; Burr Donald, H.; Guerry, P., *Campylobacter* Protein Glycosylation Affects Host Cell Interactions. *Infection and Immunity* **2002,** *70* (4), 2242-2244.
159. Karlyshev, A. V.; Everest, P.; Linton, D.; Cawthraw, S.; Newell, D. G.; Wren, B. W., The *Campylobacter jejuni* general glycosylation system is important for attachment to human epithelial cells and in the colonization of chicks. *Microbiology* **2004,** *150* (6), 1957-1964.
160. Nita-Lazar, M.; Wacker, M.; Schegg, B.; Amber, S.; Aebi, M., The N-X-S/T consensus sequence is required but not sufficient for bacterial N-linked protein glycosylation. *Glycobiology* **2005,** *15* (4), 361-367.
161. Glover, K. J.; Weerapana, E.; Imperiali, B., In vitro assembly of the undecaprenylpyrophosphate-linked heptasaccharide for prokaryotic N-linked glycosylation. *Proceedings of the National Academy of Sciences* **2005,** *102* (40), 14255-14259.
162. Kowarik, M.; Young, N. M.; Numao, S.; Schulz, B. L.; Hug, I.; Callewaert, N.; Mills, D. C.; Watson, D. C.; Hernandez, M.; Kelly, J. F.; Wacker, M.; Aebi, M., Definition of the

bacterial N-glycosylation site consensus sequence. *The EMBO Journal* **2006,** *25* (9), 1957-1966-1966.
163. Kelly, J.; Jarrell, H.; Millar, L.; Tessier, L.; Fiori Laura, M.; Lau Peter, C.; Allan, B.; Szymanski Christine, M., Biosynthesis of the N-Linked Glycan in *Campylobacter jejuni* and Addition onto Protein through Block Transfer. *Journal of Bacteriology* **2006,** *188* (7), 2427-2434.
164. Young, N. M.; Brisson, J.-R.; Kelly, J.; Watson, D. C.; Tessier, L.; Lanthier, P. H.; Jarrell, H. C.; Cadotte, N.; St. Michael, F.; Aberg, E.; Szymanski, C. M., Structure of the N-Linked Glycan Present on Multiple Glycoproteins in the Gram-negative Bacterium, *Campylobacter jejuni* *. *Journal of Biological Chemistry* **2002,** *277* (45), 42530-42539.
165. Nothaft, H.; Perez-Muñoz, M. E.; Yang, T.; Murugan, A. V. M.; Miller, M.; Kolarich, D.; Plastow, G. S.; Walter, J.; Szymanski, C. M., Improving Chicken Responses to Glycoconjugate Vaccination Against *Campylobacter jejuni*. *Frontiers in Microbiology* **2021,** *12*.
166. Wacker, M.; Feldman, M. F.; Callewaert, N.; Kowarik, M.; Clarke, B. R.; Pohl, N. L.; Hernandez, M.; Vines, E. D.; Valvano, M. A.; Whitfield, C.; Aebi, M., Substrate specificity of bacterial oligosaccharyltransferase suggests a common transfer mechanism for the bacterial and eukaryotic systems. *Proceedings of the National Academy of Sciences* **2006,** *103* (18), 7088-7093.
167. Kay, E. J.; Yates, L. E.; Terra, V. S.; Cuccui, J.; Wren, B. W., Recombinant expression of *Streptococcus pneumoniae* capsular polysaccharides in *Escherichia coli*. *Open Biology* **2016,** *6* (4), 150243-150243.
168. Kay, E.; Cuccui, J.; Wren, B. W., Recent advances in the production of recombinant glycoconjugate vaccines. *npj Vaccines* **2019,** *4* (1), 16.
169. Herbert, J. A.; Kay, E. J.; Faustini, S. E.; Richter, A.; Abouelhadid, S.; Cuccui, J.; Wren, B.; Mitchell, T. J., Production and efficacy of a low-cost recombinant pneumococcal protein polysaccharide conjugate vaccine. *Vaccine* **2018,** *36* (26), 3809-3819.
170. Samaras, J. J.; Mauri, M.; Kay, E. J.; Wren, B. W.; Micheletti, M., Development of an automated platform for the optimal production of glycoconjugate vaccines expressed in *Escherichia coli*. *Microbial Cell Factories* **2021,** *20* (1), 104.
171. Kay, E. J.; Mauri, M.; Willcocks, S. J.; Scott, T. A.; Cuccui, J.; Wren, B. W., Engineering a suite of *E. coli* strains for enhanced expression of bacterial polysaccharides and glycoconjugate vaccines. *Microbial Cell Factories* **2022,** *21* (1), 66.
172. Passmore, I. J.; Faulds-Pain, A.; Abouelhadid, S.; Harrison, M. A.; Hall, C. L.; Hitchen, P.; Dell, A.; Heap, J. T.; Wren, B. W., A combinatorial DNA assembly approach to biosynthesis of N-linked glycans in E. coli. *Glycobiology* **2023,** *33* (2), 138-149.
173. Ma, Z.; Wang, P. G., RecET Direct Cloning of Polysaccharide Gene Cluster from Gram-Negative Bacteria. In *Bacterial Polysaccharides: Methods and Protocols*, Brockhausen, I., Ed. Springer New York: New York, NY, 2019; pp 15-23.
174. Marr, N.; Tirsoaga, A.; Blanot, D.; Fernandez, R.; Caroff, M., Glucosamine found as a substituent of both phosphate groups in *Bordetella* lipid A backbones: Role of a BvgAS-activated ArnT ortholog. *Journal of Bacteriology* **2008,** *190* (12), 4281.
175. Wang, X.; Ribeiro, A. A.; Guan, Z.; McGrath, S. C.; Cotter, R. J.; Raetz, C. R., Structure and biosynthesis of free lipid A molecules that replace lipopolysaccharide in *Francisella tularensis* subsp. *novicida*. *Biochemistry* **2006,** *45* (48), 14427-40.

176. Winfield, M. D.; Latifi, T.; Groisman, E. A., Transcriptional regulation of the 4-amino-4-deoxy-L-arabinose biosynthetic genes in *Yersinia pestis*. *Journal of Biological Chemistry* **2005,** *280* (15), 14765-14772.
177. Harris, T. L.; Worthington, R. J.; Hittle, L. E.; Zurawski, D. V.; Ernst, R. K.; Melander, C., Small molecule downregulation of PmrAB reverses lipid A modification and breaks colistin resistance. *ACS Chemical Biology* **2014,** *9* (1), 122-7.
178. Kline, T.; Trent, M. S.; Stead, C. M.; Lee, M. S.; Sousa, M. C.; Felise, H. B.; Nguyen, H. V.; Miller, S. I., Synthesis of and evaluation of lipid A modification by 4-substituted 4-deoxy arabinose analogs as potential inhibitors of bacterial polymyxin resistance. *Bioorganic & Medicinal Chemistry Letters* **2008,** *18* (4), 1507-1510.
179. Breazeale, S. D.; Ribeiro, A. A.; Raetz, C. R., Origin of lipid A species modified with 4-amino-4-deoxy-L-arabinose in polymyxin-resistant mutants of *Escherichia coli*. An aminotransferase (ArnB) that generates UDP-4-deoxyl-L-arabinose. *Journal of Biological Chemistry* **2003,** *278* (27), 24731-9.
180. Gatzeva-Topalova, P. Z.; May, A. P.; Sousa, M. C., Structure and mechanism of ArnA: conformational change implies ordered dehydrogenase mechanism in key enzyme for polymyxin resistance. *Structure* **2005,** *13* (6), 929-42.
181. Lee, M.; Sousa, M. C., Structural basis for substrate specificity in ArnB. A key enzyme in the polymyxin resistance pathway of Gram-negative bacteria. *Biochemistry* **2014,** *53* (4), 796-805.
182. Williams, G. J.; Breazeale, S. D.; Raetz, C. R.; Naismith, J. H., Structure and function of both domains of ArnA, a dual function decarboxylase and a formyltransferase, involved in 4-amino-4-deoxy-L-arabinose biosynthesis. *Journal of Biological Chemistry* **2005,** *280* (24), 23000-8.
183. Adak, T.; Morales, D. L.; Cook, A. J.; Grigg, J. C.; Murphy, M. E. P.; Tanner, M. E., ArnD is a deformylase involved in polymyxin resistance. *Chemical Communications* **2020,** *56* (50), 6830-6833.
184. Yan, A.; Guan, Z.; Raetz, C. R., An undecaprenyl phosphate-aminoarabinose flippase required for polymyxin resistance in Escherichia coli. *Journal of Biological Chemistry* **2007,** *282* (49), 36077-89.
185. Trent, M. S.; Ribeiro, A. A.; Lin, S.; Cotter, R. J.; Raetz, C. R., An inner membrane enzyme in *Salmonella* and *Escherichia coli* that transfers 4-amino-4-deoxy-L-arabinose to lipid A: induction on polymyxin-resistant mutants and role of a novel lipid-linked donor. *Journal of Biological Chemistry* **2001,** *276* (46), 43122-31.
186. Trent, M. S.; Ribeiro, A. A.; Doerrler, W. T.; Lin, S.; Cotter, R. J.; Raetz, C. R., Accumulation of a polyisoprene-linked amino sugar in polymyxin-resistant *Salmonella typhimurium* and *Escherichia coli*: structural characterization and transfer to lipid A in the periplasm. *Journal of Biological Chemistry* **2001,** *276* (46), 43132-44.
187. Mann, E.; Whitfield, C., A widespread three-component mechanism for the periplasmic modification of bacterial glycoconjugates. *Canadian Journal of Chemistry* **2016,** *94* (11), 883-893.
188. Rubin, E. J.; Herrera, C. M.; Crofts, A. A.; Trent, M. S., PmrD is required for modifications to *Escherichia coli* endotoxin that promote antimicrobial resistance. *Antimicrobial Agents and Chemotherapy* **2015,** *59* (4), 2051.

189. Groisman, E. A., The pleiotropic two-component regulatory system PhoP-PhoQ. *Journal of Bacteriology* **2001,** *183* (6), 1835-42.
190. Cannatelli, A.; Giani, T.; Aiezza, N.; Di Pilato, V.; Principe, L.; Luzzaro, F.; Galeotti, C. L.; Rossolini, G. M., An allelic variant of the PmrB sensor kinase responsible for colistin resistance in an *Escherichia coli* strain of clinical origin. *Scientific Reports* **2017,** *7* (1), 5071.
191. Wösten, M. M.; Kox, L. F.; Chamnongpol, S.; Soncini, F. C.; Groisman, E. A., A signal transduction system that responds to extracellular iron. *Cell* **2000,** *103* (1), 113-25.
192. Zhou, Z.; Lin, S.; Cotter, R. J.; Raetz, C. R., Lipid A modifications characteristic of *Salmonella* typhimurium are induced by NH4VO3 in *Escherichia coli* K12. Detection of 4-amino-4-deoxy-L-arabinose, phosphoethanolamine and palmitate. *Journal of Biological Chemistry* **1999,** *274* (26), 18503-14.
193. Hagiwara, D.; Yamashino, T.; Mizuno, T., A genome-wide view of the *Escherichia coli* BasS-BasR two-component system implicated in iron-responses. *Bioscience, Biotechnology & Biochemistry* **2004,** *68* (8), 1758-67.
194. Song, F.; Guan, Z.; Raetz, C. R., Biosynthesis of undecaprenyl phosphate-galactosamine and undecaprenyl phosphate-glucose in *Francisella novicida*. *Biochemistry* **2009,** *48* (6), 1173-82.
195. Guan, S.; Bastin, D. A.; Verma, N. K., Functional analysis of the O antigen glucosylation gene cluster of *Shigella flexneri* bacteriophage SfX. *Microbiology* **1999,** *145* (5), 1263-1273.
196. Bligh, E. G.; Dyer, W. J., A rapid method of total lipid extraction and purification. *Canadian Journal of Biochemistry and Physiology* **1959,** *37* (8), 911-917.
197. Henderson, J. C.; O'Brien, J. P.; Brodbelt, J. S.; Trent, M. S., Isolation and chemical characterization of lipid A from gram-negative bacteria. *Journal of Visualized Experiments* **2013,** (79), e50623.
198. Jeong, H.; Barbe, V.; Lee, C. H.; Vallenet, D.; Yu, D. S.; Choi, S. H.; Couloux, A.; Lee, S. W.; Yoon, S. H.; Cattolico, L.; Hur, C. G.; Park, H. S.; Ségurens, B.; Kim, S. C.; Oh, T. K.; Lenski, R. E.; Studier, F. W.; Daegelen, P.; Kim, J. F., Genome sequences of *Escherichia coli* B strains REL606 and BL21(DE3). *Journal of Molecular Biology* **2009,** *394* (4), 644-52.
199. Jansson, P. E.; Lindberg, A. A.; Lindberg, B.; Wollin, R., Structural studies on the hexose region of the core in lipopolysaccharides from Enterobacteriaceae. *European Journal of Biochemistry* **1981,** *115* (3), 571-7.
200. Bretscher, L. E.; Morrell, M. T.; Funk, A. L.; Klug, C. S., Purification and characterization of the L-Ara4N transferase protein ArnT from *Salmonella typhimurium*. *Protein Expression and Purification* **2006,** *46* (1), 33-9.
201. Petsch, D.; Anspach, F. B., Endotoxin removal from protein solutions. *Journal of Biotechnology* **2000,** *76* (2-3), 97-119.
202. Olagnon, C.; Monjaras Feria, J.; Grünwald-Gruber, C.; Blaukopf, M.; Valvano, M. A.; Kosma, P., Synthetic Phosphodiester-Linked 4-Amino-4-deoxy-l-arabinose Derivatives Demonstrate that ArnT is an Inverting Aminoarabinosyl Transferase. *Chembiochem* **2019,** *20* (23), 2936-2948.
203. Barr, K.; Rick, P. D., Biosynthesis of enterobacterial common antigen in *Escherichia coli*. In vitro synthesis of lipid-linked intermediates. *Journal of Biological Chemistry* **1987,** *262* (15), 7142-7150.

204. Cartee, R. T.; Forsee, W. T.; Bender, M. H.; Ambrose, K. D.; Yother, J., CpsE from type 2 *Streptococcus pneumoniae* catalyzes the reversible addition of glucose-1-phosphate to a polyprenyl phosphate acceptor, initiating type 2 capsule repeat unit formation. *Journal of Bacteriology* **2005,** *187* (21), 7425-33.
205. Osborn, M. J.; Tze-Yuen, R. Y., Biosynthesis of bacterial lipopolysaccharide. VII. Enzymatic formation of the first intermediate in biosynthesis of the O-antigen of *Salmonella typhimurium*. *Journal of Biological Chemistry* **1968,** *243* (19), 5145-52.
206. Gantt, R. W.; Peltier-Pain, P.; Singh, S.; Zhou, M.; Thorson, J. S., Broadening the scope of glycosyltransferase-catalyzed sugar nucleotide synthesis. *Proceedings of the National Academy of Sciences* **2013,** *110* (19), 7648.
207. Chng, S. S.; Gronenberg, L. S.; Kahne, D., Proteins required for lipopolysaccharide assembly in *Escherichia coli* form a transenvelope complex. *Biochemistry* **2010,** *49* (22), 4565-7.
208. Sherman, D. J.; Xie, R.; Taylor, R. J.; George, A. H.; Okuda, S.; Foster, P. J.; Needleman, D. J.; Kahne, D., Lipopolysaccharide is transported to the cell surface by a membrane-to-membrane protein bridge. *Science* **2018,** *359* (6377), 798-801.
209. Owens, T. W.; Taylor, R. J.; Pahil, K. S.; Bertani, B. R.; Ruiz, N.; Kruse, A. C.; Kahne, D., Structural basis of unidirectional export of lipopolysaccharide to the cell surface. *Nature* **2019,** *567* (7749), 550-553.
210. Paradis-Bleau, C.; Kritikos, G.; Orlova, K.; Typas, A.; Bernhardt, T. G., A genome-wide screen for bacterial envelope biogenesis mutants identifies a novel factor involved in cell wall precursor metabolism. *PLOS Genetics* **2014,** *10* (1), e1004056-e1004056.
211. Kahler, C. M.; Sarkar-Tyson, M.; Kibble, E. A.; Stubbs, K. A.; Vrielink, A., Enzyme targets for drug design of new anti-virulence therapeutics. *Current Opinion in Structural Biology* **2018,** *53*, 140-150.
212. Troutman, J. M.; Erickson, K. M.; Scott, P. M.; Hazel, J. M.; Martinez, C. D.; Dodbele, S., Tuning the production of variable length, fluorescent polyisoprenoids using surfactant-controlled enzymatic synthesis. *Biochemistry* **2015,** *54* (18), 2817-27.
213. Hankins, J. V.; Madsen, J. A.; Needham, B. D.; Brodbelt, J. S.; Trent, M. S., The Outer Membrane of Gram-Negative Bacteria: Lipid A Isolation and Characterization. In *Bacterial Cell Surfaces: Methods and Protocols*, Delcour, A. H., Ed. Humana Press: Totowa, NJ, 2013; pp 239-258.
214. Fomsgaard, A.; Freudenberg, M. A.; Galanos, C., Modification of the silver staining technique to detect lipopolysaccharide in polyacrylamide gels. *Journal of Clinical Microbiology* **1990,** *28* (12), 2627-2631.
215. Datsenko, K. A.; Wanner, B. L., One-step inactivation of chromosomal genes in *Escherichia coli* K-12 using PCR products. *Proceedings of the National Academy of Sciences* **2000,** *97* (12), 6640.
216. Moradali, M. F.; Rehm, B. H. A., Bacterial biopolymers: from pathogenesis to advanced materials. *Nature Reviews Microbiology* **2020,** *18* (4), 195-210.
217. Brubaker, J. O.; Li, Q.; Tzianabos, A. O.; Kasper, D. L.; Finberg, R. W., Mitogenic activity of purified capsular polysaccharide A from *Bacteroides fragilis*: Differential stimulatory effect on mouse and rat lymphocytes in vitro. *The Journal of Immunology* **1999,** *162* (4), 2235-2242.

218. Tzianabos, A. O.; Wang, J. Y.; Lee, J. C., Structural rationale for the modulation of abscess formation by *Staphylococcus aureus* capsular polysaccharides. *Proceedings of the National Academy of Sciences* **2001,** *98* (16), 9365-9370.
219. Kalka-Moll, W. M.; Tzianabos, A. O.; Bryant, P. W.; Niemeyer, M.; Ploegh, H. L.; Kasper, D. L., Zwitterionic polysaccharides stimulate T cells by MHC Class II-dependent interactions. *The Journal of Immunology* **2002,** *169* (11), 6149-6153.
220. De Silva, R. A.; Wang, Q.; Chidley, T.; Appulage, D. K.; Andreana, P. R., Immunological response from an entirely carbohydrate antigen: Design of synthetic vaccines based on Tn−PS A1 conjugates. *Journal of the American Chemical Society* **2009,** *131* (28), 9622-9623.
221. Ochoa-Repáraz, J.; Mielcarz, D. W.; Ditrio, L. E.; Burroughs, A. R.; Begum-Haque, S.; Dasgupta, S.; Kasper, D. L.; Kasper, L. H., Central nervous system demyelinating disease protection by the human commensal *Bacteroides fragilis* depends on polysaccharide A expression. *Journal of Immunology* **2010,** *185* (7), 4101-8.
222. Baumann, H.; Tzianabos, A. O.; Brisson, J. R.; Kasper, D. L.; Jennings, H. J., Structural elucidation of two capsular polysaccharides from one strain of *Bacteroides fragilis* using high-resolution NMR spectroscopy. *Biochemistry* **1992,** *31* (16), 4081-4089.
223. Wang, H.; Li, Z.; Jia, R.; Hou, Y.; Yin, J.; Bian, X.; Li, A.; Muller, R.; Stewart, A. F.; Fu, J.; Zhang, Y., RecET direct cloning and Redalphabeta recombineering of biosynthetic gene clusters, large operons or single genes for heterologous expression. *Nature Protocols* **2016,** *11* (7), 1175-90.
224. Wegmann, U.; Horn, N.; Carding Simon, R., Defining the *Bacteroides* Ribosomal Binding Site. *Applied and Environmental Microbiology* **2013,** *79* (6), 1980-1989.
225. Riegert, A. S.; Thoden, J. B.; Schoenhofen, I. C.; Watson, D. C.; Young, N. M.; Tipton, P. A.; Holden, H. M., Structural and biochemical investigation of PglF from *Campylobacter jejuni* reveals a new mechanism for a member of the short chain dehydrogenase/reductase superfamily. *Biochemistry* **2017,** *56* (45), 6030-6040.
226. Cunneen, M. M.; Liu, B.; Wang, L.; Reeves, P. R., Biosynthesis of UDP-GlcNAc, UndPP-GlcNAc and UDP-GlcNAcA involves three easily distinguished 4-epimerase enzymes, Gne, Gnu and GnaB. *PLOS One* **2013,** *8* (6), e67646.
227. Park, N. Y.; Lee, J. H.; Kim, M. W.; Jeong, H. G.; Lee, B. C.; Kim, T. S.; Choi, S. H., Identification of the *Vibrio vulnificus wbpP* gene and evaluation of its role in virulence. *Infection and Immunity* **2006,** *74* (1), 721-728.
228. Reid, A. J.; Erickson, K. M.; Hazel, J. M.; Lukose, V.; Troutman, J. M., Chemoenzymatic preparation of a *Campylobacter jejuni* lipid-linked heptasaccharide on an azide-linked polyisoprenoid. *ACS Omega* **2023,** *8* (17), 15790-15798.
229. Schoenhofen, I. C.; McNally, D. J.; Vinogradov, E.; Whitfield, D.; Young, N. M.; Dick, S.; Wakarchuk, W. W.; Brisson, J.-R.; Logan, S. M., Functional characterization of dehydratase/aminotransferase pairs from *Helicobacter* and *Campylobacter*: Enzymes distinguishing the pseudaminic acid and cacillosamine biosynthetic pathways. *Journal of Biological Chemistry* **2006,** *281* (2), 723-732.
230. Comstock, L. E.; Coyne, M. J.; Tzianabos, A. O.; Pantosti, A.; Onderdonk, A. B.; Kasper, D. L., Analysis of a capsular polysaccharide biosynthesis locus of *Bacteroides fragilis*. *Infection and Immunity* **1999,** *67* (7), 3525-3532.

231. Meredith, T. C.; Mamat, U.; Kaczynski, Z.; Lindner, B.; Holst, O.; Woodard, R. W., Modification of lipopolysaccharide with colanic acid (M-antigen) repeats in *Escherichia coli**. *Journal of Biological Chemistry* **2007,** *282* (11), 7790-7798.
232. Marolda, C. L.; Tatar, L. D.; Alaimo, C.; Aebi, M.; Valvano, M. A., Interplay of the Wzx translocase and the corresponding polymerase and chain length regulator proteins in the translocation and periplasmic assembly of lipopolysaccharide o antigen. *Journal of Bacteriology* **2006,** *188* (14), 5124-5135.
233. Maciejewska, A.; Kaszowska, M.; Jachymek, W.; Lugowski, C.; Lukasiewicz, J., Lipopolysaccharide-linked enterobacterial common antigen (ECA(LPS)) occurs in rough strains of *Escherichia coli* R1, R2, and R4. *International Journal of Molecular Sciences* **2020,** *21* (17), 6038.
234. Ruan, X.; Loyola, D. E.; Marolda, C. L.; Perez-Donoso, J. M.; Valvano, M. A., The WaaL O-antigen lipopolysaccharide ligase has features in common with metal ion-independent inverting glycosyltransferases*. *Glycobiology* **2012,** *22* (2), 288-299.
235. Abeyrathne, P. D.; Daniels, C.; Poon, K. K. H.; Matewish, M. J.; Lam, J. S., Functional characterization of WaaL, a ligase associated with linking O-antigen polysaccharide to the core of *Pseudomonas aeruginosa* lipopolysaccharide. *Journal of Bacteriology* **2005,** *187* (9), 3002-3012.
236. Liu, D.; Reeves, P. R., *Escherichia coli* K12 regains its O antigen. *Microbiology* **1994,** *140* (1), 49-57.
237. Kreisman, L. S. C.; Friedman, J. H.; Neaga, A.; Cobb, B. A., Structure and function relations with a T-cell-activating polysaccharide antigen using circular dichroism. *Glycobiology* **2007,** *17* (1), 46-55.
238. Merino, S.; Gonzalez, V.; Tomás, J. M., The first sugar of the repeat units is essential for the Wzy polymerase activity and elongation of the O-antigen lipopolysaccharide. *Future Microbiology* **2016,** *11* (7), 903-918.
239. Feldman, M. F.; Marolda, C. L.; Monteiro, M. A.; Perry, M. B.; Parodi, A. J.; Valvano, M. A., The activity of a putative polyisoprenol-linked sugar translocase (Wzx) involved in *Escherichia coli* O antigen assembly is independent of the chemical structure of the O repeat. *Journal of Biological Chemistry* **1999,** *274* (49), 35129-38.
240. Marolda, C. L.; Vicarioli, J.; Valvano, M. A., Wzx proteins involved in biosynthesis of O antigen function in association with the first sugar of the O-specific lipopolysaccharide subunit. *Microbiology* **2004,** *150* (Pt 12), 4095-105.
241. Danese, P. N.; Oliver, G. R.; Barr, K.; Bowman, G. D.; Rick, P. D.; Silhavy, T. J., Accumulation of the enterobacterial common antigen lipid II biosynthetic intermediate stimulates *degP* transcription in *Escherichia coli*. *Journal of Bacteriology* **1998,** *180* (22), 5875-5884.
242. Kay, E. J.; Dooda, M. K.; Bryant, J. C.; Reid, A. J.; Wren, B. W.; Troutman, J. M.; Jorgenson, M. A., Engineering *Escherichia coli* for increased Und-P availability leads to material improvements in glycan expression technology. *Microbial Cell Factories* **2024,** *23* (1), 72.
243. Ranjit, D. K.; Young, K. D., Colanic acid intermediates prevent de novo shape recovery of *Escherichia coli* spheroplasts, calling into question biological roles previously attributed to colanic acid. *Journal of Bacteriology* **2016,** *198* (8), 1230-40.
244. Poindexter, J. S., The caulobacters: ubiquitous unusual bacteria. *Microbiological Reviews* **1981,** *45* (1), 123-179.

245. Poindexter, J. S., Biological Properties and Classification of the Caulobacter Group. *Bacteriological Reviews* **1964,** *28* (3), 231-295.
246. Cole, J. L.; Hardy, G. G.; Bodenmiller, D.; Toh, E.; Hinz, A.; Brun, Y. V., The HfaB and HfaD adhesion proteins of *Caulobacter crescentus* are localized in the stalk. *Molecular Microbiology* **2003,** *49* (6), 1671-83.
247. Tsang, P. H.; Li, G.; Brun, Y. V.; Freund, L. B.; Tang, J. X., Adhesion of single bacterial cells in the micronewton range. *Proceedings of the National Academy of Sciences of the United States of America* **2006,** *103* (15), 5764-5768.
248. Hengge, R., Principles of c-di-GMP signalling in bacteria. *Nature Reviews Microbiology* **2009,** *7*, 263.
249. Hershey, D. M.; Fiebig, A.; Crosson, S., Flagellar perturbations activate adhesion through two distinct pathways in *Caulobacter crescentus*. *mBio* **2021,** *12* (1), e03266-20.
250. Merker, R. I.; Smit, J., Characterization of the adhesive holdfast of marine and freshwater caulobacters. *Applied and Environmental Microbiology* **1988,** *54* (8), 2078-85.
251. Li, G.; Smith, C. S.; Brun, Y. V.; Tang, J. X., The elastic properties of the *Caulobacter crescentus* adhesive holdfast are dependent on oligomers of N-acetylglucosamine. *Journal of Bacteriology* **2005,** *187* (1), 257-65.
252. Chepkwony, N. K.; Hardy, G. G.; Brun, Y. V., HfaE Is a component of the holdfast anchor complex that tethers the holdfast adhesin to the cell envelope. *Journal of Bacteriology* **2022,** *204* (11), e00273-22.
253. Lombard, V.; Golaconda Ramulu, H.; Drula, E.; Coutinho, P. M.; Henrissat, B., The carbohydrate-active enzymes database (CAZy) in 2013. *Nucleic Acids Research* **2014,** *42* (Database issue), D490-5.
254. Kurtz, H. D.; Smith, J., Analysis of a *Caulobacter crescentu*s gene cluster involved in attachment of the holdfast to the cell. *Journal of Bacteriology* **1992,** *174* (3), 687-694.
255. Wan, Z.; Brown, P. J.; Elliott, E. N.; Brun, Y. V., The adhesive and cohesive properties of a bacterial polysaccharide adhesin are modulated by a deacetylase. *Molecular Microbiology* **2013,** *88* (3), 486-500.
256. Caufrier, F.; Martinou, A.; Dupont, C.; Bouriotis, V., Carbohydrate esterase family 4 enzymes: substrate specificity. *Carbohydrate Research* **2003,** *338* (7), 687-92.
257. Liu, Q.; Hao, L.-f.; Chen, Y.; Liu, Z.-c.; Xing, W.-w.; Zhang, C.; Fu, W.-l.; Xu, D.-g., The screening and expression of polysaccharide deacetylase from *Caulobacter crescentus* and its function analysis. *Biotechnology and Applied Biochemistry* **2023,** *70* (2), 688-696.
258. Hardy, G. G.; Allen, R. C.; Toh, E.; Long, M.; Brown, P. J.; Cole-Tobian, J. L.; Brun, Y. V., A localized multimeric anchor attaches the *Caulobacter* holdfast to the cell pole. *Molecular Microbiology* **2010,** *76* (2), 409-27.
259. Wolucka, B. A.; McNeil, M. R.; de Hoffmann, E.; Chojnacki, T.; Brennan, P. J., Recognition of the lipid intermediate for arabinogalactan/arabinomannan biosynthesis and its relation to the mode of action of ethambutol on mycobacteria. *Journal of Biological Chemistry* **1994,** *269* (37), 23328-35.
260. Ishii, K.; Sagami, H.; Ogura, K., A novel prenyltransferase from *Paracoccus denitrificans*. *The Biochemical Journal* **1986,** *233(3)*, 773–777.
261. Contreras, I.; Shapiro, L.; Henry, S., Membrane phospholipid composition of *Caulobacter crescentus*. *Journal of Bacteriology* **1978,** *135* (3), 1130-1136.

262. Ogura, K.; Koyama, T., Enzymatic Aspects of Isoprenoid Chain Elongation. *Chemical Reviews* **1998,** *98* (4), 1263-1276.
263. Ko, T.-P.; Chen, Y.-K.; Robinson, H.; Tsai, P.-C.; Gao, Y.-G.; Chen, A. P. C.; Wang, A. H. J.; Liang, P.-H., Mechanism of Product Chain Length Determination and the Role of a Flexible Loop in Escherichia coli Undecaprenyl-pyrophosphate Synthase Catalysis *Journal of Biological Chemistry* **2001,** *276* (50), 47474-47482.
264. Allen, C. M., Jr.; Muth, J. D., Lipid activation of undecaprenyl pyrophosphate synthetase from *Lactobacillus plantarum*. *Biochemistry* **1977,** *16* (13), 2908-2915.
265. MacCain, W. J.; Kannan, S.; Jameel, D. Z.; Troutman, J. M.; Young, K. D., A defective undecaprenyl pyrophosphate synthase induces growth and morphological defects that are suppressed by mutations in the isoprenoid pathway of *Escherichia coli*. *Journal of Bacteriology* **2018,** *200* (18), 10.1128/jb.00255-18.
266. Pan, J.-J.; Yang, L.-W.; Liang, P.-H., Effect of site-directed mutagenesis of the conserved aspartate and glutamate on *E. coli* undecaprenyl pyrophosphate synthase catalysis. *Biochemistry* **2000,** *39* (45), 13856-13861.
267. Jumper, J.; Evans, R.; Pritzel, A.; Green, T.; Figurnov, M.; Ronneberger, O.; Tunyasuvunakool, K.; Bates, R.; Žídek, A.; Potapenko, A.; Bridgland, A.; Meyer, C.; Kohl, S. A. A.; Ballard, A. J.; Cowie, A.; Romera-Paredes, B.; Nikolov, S.; Jain, R.; Adler, J.; Back, T.; Petersen, S.; Reiman, D.; Clancy, E.; Zielinski, M.; Steinegger, M.; Pacholska, M.; Berghammer, T.; Bodenstein, S.; Silver, D.; Vinyals, O.; Senior, A. W.; Kavukcuoglu, K.; Kohli, P.; Hassabis, D., Highly accurate protein structure prediction with AlphaFold. *Nature* **2021,** *596* (7873), 583-589.
268. Fujikura, K.; Zhang, Y.-W.; Fujihashi, M.; Miki, K.; Koyama, T., Mutational analysis of allylic substrate binding aite of *Micrococcus luteus* B-P 26 undecaprenyl diphosphate synthase. *Biochemistry* **2003,** *42* (14), 4035-4041.
269. Chang, S. Y.; Ko, T. P.; Liang, P. H.; Wang, A. H., Catalytic mechanism revealed by the crystal structure of undecaprenyl pyrophosphate synthase in complex with sulfate, magnesium, and triton. *Journal of Biological Chemistry* **2003,** *278(31)*, 29298-29307.
270. Kellogg, B. A.; Poulter, C. D., Chain elongation in the isoprenoid biosynthetic pathway. *Current Opinion in Chemical Biology* **1997** *1(4)*, 570-578.
271. Tarshis, L. C.; Fau, P. P.; Fau, K. B.; Fau, S. J.; Poulter, C. D., Regulation of product chain length by isoprenyl diphosphate synthases. *Proceedings of the National Academy of Sciences* **1996,** (0027-8424 (Print)).
272. Kharel, Y.; Takahashi, S.; Yamashita, S.; Koyama, T., Manipulation of prenyl chain length determination mechanism of cis-prenyltransferases. *The FEBS Journal* **2006,** *273* (3), 647-657.
273. Wang, W.; Dong, C.; McNeil, M.; Kaur, D.; Mahapatra, S.; Crick, D. C.; Naismith, J. H., The Structural Basis of Chain Length Control in Rv1086. *Journal of Molecular Biology* **2008,** *381* (1), 129-140.
274. The UniProt, C., UniProt: the Universal Protein Knowledgebase in 2023. *Nucleic Acids Research* **2023,** *51* (D1), D523-D531.
275. Schulbach, M. C.; Mahapatra, S.; Macchia, M.; Barontini, S.; Papi, C.; Minutolo, F.; Bertini, S.; Brennan, P. J.; Crick, D. C., Purification, enzymatic characterization, and Inhibition of the *Z* Farnesyl Diphosphate Synthase from *Mycobacterium tuberculosis*. *Journal of Biological Chemistry* **2001,** *276* (15), 11624-11630.

276. Chang, S.-Y.; Ko, T.-P.; Chen, A. P. C.; Wang, A. H. J.; Liang, P.-H., Substrate binding mode and reaction mechanism of undecaprenyl pyrophosphate synthase deduced from crystallographic studies. *Protein Science* **2004,** *13* (4), 971-978.
277. Berne, C.; Ellison, C. K.; Agarwal, R.; Severin, G. B.; Fiebig, A.; Morton, R. I., 3rd; Waters, C. M.; Brun, Y. V., Feedback regulation of *Caulobacter crescentus* holdfast synthesis by flagellum assembly via the holdfast inhibitor HfiA. *Molecular microbiology* **2018,** *110* (2), 219-238.
278. Schrader, J. M.; Shapiro, L., Synchronization of *Caulobacter crescentus* for investigation of the bacterial cell cycle. *Journal of Visualized Experiments* **2015,** (98).
279. McLaughlin, M.; Hershey, D. M.; Reyes Ruiz, L. M.; Fiebig, A.; Crosson, S., A cryptic transcription factor regulates Caulobacter adhesin development. *PLOS Genetics* **2022,** *18* (10), e1010481.
280. Hallgren, J.; Tsirigos, K.; Pedersen, M. D.; Almagro Armenteros, J. J.; Marcatili, P.; Nielsen, H.; Krogh, A.; Winther, O., DeepTMHMM predicts alpha and beta transmembrane proteins using deep neural networks. bioRxiv: 2022.
281. Rick, P. D.; Hubbard, G. L.; Kitaoka, M.; Nagaki, H.; Kinoshita, T.; Dowd, S.; Simplaceanu, V.; Ho, C., Characterization of the lipid-carrier involved in the synthesis of enterobacterial common antigen (ECA) and identification of a novel phosphoglyceride in a mutant of *Salmonella typhimurium* defective in ECA synthesis. *Glycobiology* **1998,** *8* (6), 557-567.
282. Hug, I.; Deshpande, S.; Sprecher, K. S.; Pfohl, T.; Jenal, U., Second messenger–mediated tactile response by a bacterial rotary motor. *Science* **2017,** *358* (6362), 531-534.
283. Kawamura, T.; Ishimoto, N.; Ito, E., Enzymatic synthesis of uridine diphosphate N-acetyl-D-mannosaminuronic acid. *Journal of Biological Chemistry* **1979,** *254* (17), 8457-65.
284. Varadi, M.; Anyango, S.; Deshpande, M.; Nair, S.; Natassia, C.; Yordanova, G.; Yuan, D.; Stroe, O.; Wood, G.; Laydon, A.; Žídek, A.; Green, T.; Tunyasuvunakool, K.; Petersen, S.; Jumper, J.; Clancy, E.; Green, R.; Vora, A.; Lutfi, M.; Figurnov, M.; Cowie, A.; Hobbs, N.; Kohli, P.; Kleywegt, G.; Birney, E.; Hassabis, D.; Velankar, S., AlphaFold Protein Structure Database: massively expanding the structural coverage of protein-sequence space with high-accuracy models. *Nucleic Acids Research* **2021,** *50* (D1), D439-D444.
285. Varadi, M.; Bertoni, D.; Magana, P.; Paramval, U.; Pidruchna, I.; Radhakrishnan, M.; Tsenkov, M.; Nair, S.; Mirdita, M.; Yeo, J.; Kovalevskiy, O.; Tunyasuvunakool, K.; Laydon, A.; Žídek, A.; Tomlinson, H.; Hariharan, D.; Abrahamson, J.; Green, T.; Jumper, J.; Birney, E.; Steinegger, M.; Hassabis, D.; Velankar, S., AlphaFold Protein Structure Database in 2024: providing structure coverage for over 214 million protein sequences. *Nucleic Acids Research* **2023,** *52* (D1), D368-D375.
286. Lee, S.; Inzerillo, S.; Lee, G. Y.; Bosire, E. M.; Mahato, S. K.; Song, J., Glycan-mediated molecular interactions in bacterial pathogenesis. *Trends in Microbiology* **2022,** *30* (3), 254-267.
287. Comstock, L. E.; Kasper, D. L., Bacterial glycans: Key mediators of diverse host immune responses. *Cell* **2006,** *126* (5), 847-850.
288. Neff, C. P.; Rhodes, Matthew E.; Arnolds, Kathleen L.; Collins, Colm B.; Donnelly, J.; Nusbacher, N.; Jedlicka, P.; Schneider, Jennifer M.; McCarter, Martin D.; Shaffer, M.; Mazmanian, Sarkis K.; Palmer, Brent E.; Lozupone, Catherine A., Diverse intestinal bacteria

contain putative zwitterionic capsular polysaccharides with anti-inflammatory properties. *Cell Host & Microbe* **2016,** *20* (4), 535-547.
289. Krumm, S. A.; Doores, K. J., Targeting glycans on human pathogens for vaccine design. In *Vaccination Strategies Against Highly Variable Pathogens*, Hangartner, L.; Burton, D. R., Eds. Springer International Publishing: Cham, 2020; pp 129-163.
290. Fernández, L.; Gooderham, W. J.; Bains, M.; McPhee Joseph, B.; Wiegand, I.; Hancock Robert, E. W., Adaptive resistance to the "last hope" antibiotics polymyxin B and colistin in *Pseudomonas aeruginosa* is mediated by the novel two-component regulatory system ParR-ParS. *Antimicrobial Agents and Chemotherapy* **2010,** *54* (8), 3372-3382.
291. Troutman, J. M.; Sharma, S.; Erickson, K. M.; Martinez, C. D., Functional identification of a galactosyltransferase critical to *Bacteroides fragilis* Capsular Polysaccharide A biosynthesis. *Carbohydrate Research* **2014,** *395*, 19-28.
292. Pantosti, A.; Tzianabos, A. O.; Onderdonk, A. B.; Kasper, D. L., Immunochemical characterization of two surface polysaccharides of *Bacteroides fragilis*. *Infection and Immunity* **1991,** *59* (6), 2075.
293. Hegerle, N.; Bose, J.; Ramachandran, G.; Galen, J. E.; Levine, M. M.; Simon, R.; Tennant, S. M., Overexpression of O-polysaccharide chain length regulators in Gram-negative bacteria using the Wzx-/Wzy-dependent pathway enhances production of defined modal length O-polysaccharide polymers for use as haptens in glycoconjugate vaccines. *Journal of Applied Microbiology* **2018,** *125* (2), 575-585.
294. Kajimura, J.; Rahman, A.; Rick Paul, D., Assembly of cyclic enterobacterial common antigen in *Escherichia coli* K-12. *Journal of Bacteriology* **2005,** *187* (20), 6917-6927.
295. Patrick, S.; Houston, S.; Thacker, Z.; Blakely, G. W., Mutational analysis of genes implicated in LPS and capsular polysaccharide biosynthesis in the opportunistic pathogen *Bacteroides fragilis*. *Microbiology* **2009,** *155* (4), 1039-1049.
296. Torres-Cabassa, A. S.; Gottesman, S., Capsule synthesis in *Escherichia coli* K-12 is regulated by proteolysis. *Journal of Bacteriology* **1987,** *169* (3), 981-989.
297. Keenleyside, W. J.; Jayaratne, P.; MacLachlan, P. R.; Whitfield, C., The rcsA gene of *Escherichia coli* O9:K30:H12 is involved in the expression of the serotype-specific group I K (capsular) antigen. *Journal of Bacteriology* **1992,** *174* (1), 8-16.
298. Mitchell, A. M.; Srikumar, T.; Silhavy, T. J., Cyclic enterobacterial common antigen maintains the outer membrane permeability barrier of *Escherichia coli* in a manner controlled by YhdP. *mBio* **2018,** *9* (4).